

ASPECTS OF THE VOLUMETRIC AND
UNDRAINED BEHAVIOR OF
BOSTON BLUE CLAY

by

PHILIPPE H. FAYAD

Diplôme d'Ingénieur, St. Joseph University
Faculty of Engineering
(1984)

Submitted to the Department of Civil Engineering
on September 16, 1986 in partial fulfillment of the
requirements for the Degree of

MASTER OF SCIENCE
IN CIVIL ENGINEERING

at the

MASSACHUSETTS INSTITUTE OF TECHNOLOGY

September 1986

© Philippe H. Fayad 1986

The author hereby grants to M.I.T. permission to reproduce and
to distribute copies of this thesis document in whole or in part.

Signature of Author _____

Department of Civil Engineering
September 16, 1986

Certified by _____

Prof. Mohsen M. Baligh
Thesis Supervisor

Certified by _____

Dr. John T. Germaine
Thesis Supervisor

Accepted by _____

Prof. Ole S. Madsen
Chairman, Department Committee on Graduate Students

MASSACHUSETTS INSTITUTE
OF TECHNOLOGY

MAR 23 1987

LIBRARIES

ASPECTS OF THE VOLUMETRIC AND
UNDRAINED BEHAVIOR OF
BOSTON BLUE CLAY

by

PHILIPPE H. FAYAD

Submitted to the Department of Civil Engineering
on September 16, 1986 in partial fulfillment of the
requirements for the Degree of Master of Science in
Civil Engineering

ABSTRACT

This research investigates the volumetric and undrained shear behavior of resedimented Boston Blue Clay (BBC) at different overconsolidation ratios. Oedometer and triaxial compression and extension tests are conducted on anisotropically (K_0) consolidated samples and results are compared to existing data on BBC. A conceptual behavioral framework is developed for BBC which is then compared with the comprehensive data set on reconstituted Lower Cromer Till (LCT), a clay of similar low plasticity.

Special aspects of this research include: the effects of thixotropy and storage time after resedimentation on BBC behavior; the effects of consolidation stress ratio (K) on compressibility and on undrained behavior in triaxial compression vs extension and the effects of clay type. In addition, results of two unconventional triaxial tests are presented in order to investigate: 1) the drained and undrained behavior of BBC during and after consolidation at very low stress ratios following undrained shear failure and strain softening of the clay, and; 2) the undrained cyclic behavior of BBC at two levels of cyclic shearing.

Thesis Supervisor: Dr. Mohsen M. Baligh
Title: Professor of Civil Engineering

Thesis Supervisor: Dr. John T. Germaine
Title: Lecturer in Civil Engineering

ACKNOWLEDGEMENTS

The author wishes to acknowledge the following people:

Prof. Mohsen M. Baligh, for his intensive review of the technical and literary content of my thesis. His friendly academic advice and our non-technical discussions were always constructive.

Dr. John T. Germaine, without whom the testing program could not have been completed. The many hours of instruction and his infinite patience were remarkable. I am impressed by his capability of solving the most complex experimental problems.

Prof. Charles C. Ladd, who kindly reviewed parts of this document. The thorough reading and the many comments he provided were extremely helpful.

The numerous discussions on social behavior with Ronni Schwartz and her friendly support provided the extra energy often needed. I am also very grateful for the patient and accurate typing of my thesis.

Andrew Whittle, with whom a friendship developed throughout the long discussions we had. I will always recall his untiring will to help people out. His suggestions and comments on several parts of my thesis were of great assistance.

Gretchen Young, my laboratory mate with whom I shared the first (sometimes tragic) steps in the lab. I will never forget the long hours of agony preparing homework, exams and papers.

I would also like to acknowledge the closeness of my out-of-department friends, who contributed so much to my life around MIT. Wael Yared, my squash, Lobdell and 2:00-A.M. discussion-mate, whose friendship during the two years was very rewarding. Dynamic Rhea Kettaneh, whose endless availability and generosity was and will always be remembered. Fouad Tamer, the impetuous "president" whose constant obligingness was very much appreciated. Farid Kettaneh, who never missed a chance to help, and whose cooking abilities enabled me to survive Lobdell's food. They all efficiently contributed to the final production of this document.

John Salameh and Myriam Asselly who were so present in the darkest moments. Together with their respective families, they provided the warm support needed in this place.

Finally, special thanks go to my parents who gave me the opportunity to pursue my studies at MIT. Their love and support was a continuous source of encouragement.

TABLE OF CONTENTS

	<u>Page</u>
Title Page	1
Abstract	2
Acknowledgements	3
Table of Contents	4
List of Symbols	7
List of Tables	11
List of Figures	12
<u>CHAPTER 1: INTRODUCTION</u>	17
<u>CHAPTER 2: BACKGROUND ON BOSTON BLUE CLAY</u>	19
2.1 Introduction	19
2.2 Previous work on Boston Blue Clay	20
2.2.1 Bailey (1961)	20
2.2.2 Jackson (1963)	20
2.2.3 Ladd and Varallyay (1965)	20
2.2.4 Ladd and Luscher (1965)	21
2.2.5 Preston (1965), Braathen (1966)	22
2.2.6 Dickey, Ladd & Rixner (1968)	22
2.2.7 Kinner and Ladd (1970)	22
2.2.8 Ladd, Bovee, Edgers and Rixner (1971)	23
2.2.9 Ladd and Edgers (1972)	23
2.2.10 Germaine (1982)	24
2.2.11 Bensari (1984)	24
2.2.12 O'Neill (1985)	25
2.3 Boston Blue Clay	25

TABLE OF CONTENTS

	<u>Page</u>
<u>CHAPTER 3: TESTING PROCEDURES</u>	31
3.1 Introduction	31
3.2 Testing Procedure	32
3.2.1 Triaxial Apparatus	32
3.2.1.1 Set-up	32
3.2.1.2 Saturation	33
3.2.1.3 Consolidation	34
3.2.1.4 Special case of K_0 -consolidation	36
3.2.1.5 Shearing	37
3.2.2 Oedometer Apparatus	39
<u>CHAPTER 4: VOLUMETRIC BEHAVIOR OF BOSTON BLUE CLAY</u>	47
4.1 Test Results	47
4.1.1 Triaxial tests	47
4.1.2 Oedometer tests	50
4.2 Anisotropic vs Isotropic volumetric behavior of BBC	52
4.3 Effect of thixotropy	54
<u>CHAPTER 5: UNDRAINED BEHAVIOR</u>	73
5.1 Test Results	73
5.1.1 Isotropic test	73
5.1.2 Anisotropic compression tests	75
5.1.3 Anisotropic extension tests	79
5.2 Isotropic behavior of BBC	80
5.3 Anisotropic behavior	83
5.3.1 Compression	83
5.3.2 Extension	85

TABLE OF CONTENTS

	<u>Page</u>
5.3.3 Compression vs extension	87
5.4 Comparison of isotropically and Anisotropically consolidated samples	88
5.5 Concluding remarks	89
<u>CHAPTER 6: COMPARATIVE BEHAVIOR OF BBC AND LCT</u>	139
6.1 Basis and scope of comparison	139
6.2 Background on BBC and LCT	139
6.3 Volumetric behavior	141
6.4 Undrained behavior	143
6.4.1 Isotropic behavior	144
6.4.2 Anisotropic behavior	145
<u>CHAPTER 7: SPECIAL TESTS</u>	161
7.1 Test CK ₀ UCI	161
7.1.1 Volumetric behavior	162
7.1.2 Undrained behavior	163
7.2 Cyclic loading: Test CKU-Cyc-4	164
7.2.1 Procedure	164
7.2.2 Presentation of results	166
<u>CHAPTER 8: CONCLUSIONS AND RECOMMENDATIONS</u>	193
8.1 Conclusions	193
8.2 Recommendations	197
<u>REFERENCES</u>	199
<u>APPENDIX A: Resedimented BBC Batch Data</u>	208
<u>APPENDIX B: Miscellaneous Details of the Triaxial Test</u>	210
<u>APPENDIX C: Triaxial Test Data</u>	215
<u>APPENDIX D: Oedometer Test Data</u>	262

LIST OF SYMBOLS

Prefix Δ indicates a change

A prime over a stress indicates an effective stress

A subscript f indicates a final or failure condition

A subscript o indicates initial or in situ conditions

A subscript ult indicates end of test conditions.

GENERAL

BBC Resedimented Boston Blue Clay

LCT Reconstituted Lower Cromer Till

SD Standard Deviation

SHANSEP Stress History and Normalized Soil Engineering Properties

INDEX AND CLASSIFICATION PROPERTIES

e Void ratio

e_o Initial void ratio

G_s Specific gravity

LL Liquid Limit

PI Plasticity index

PL Plastic Limit

S Degree of saturation

w Water content

STRESSES, STRAINS, MODULI, AND STRENGTH PARAMETERS

A, A_f Skempton's pore pressure parameter A (at peak)

b $(\sigma_2 - \sigma_3) / (\sigma_1 - \sigma_3)$

B Skempton's pore pressure parameter $B = \Delta u / \Delta \sigma_c$

c, c' Intercept of Mohr-Coulomb failure envelope

E, E_{sec} Undrained secant Young's modulus

E_{50} E half way to failure

LIST OF SYMBOLS

G_1	Initial undrained shear modulus
K	σ'_h/σ'_v
K_0	Coefficient of earth pressure at rest
OCR	Overconsolidation ratio = $\sigma'_{vm}/\sigma'_{vc}$
p, p'	$1/2(\sigma_v + \sigma_h), 1/2(\sigma'_v + \sigma'_h)$
q	$1/2(\sigma_v - \sigma_h)$
q_{max}	$1/2(\sigma_1 - \sigma_3)_{max}$
s_u	Undrained shear strength
t_c	Consolidation time under last increment (days)
u	Pore water pressure
$\dot{\epsilon}$	Strain rate
ϵ_a, ϵ_v	Axial and volumetric strain
ϵ_{ap}	Peak axial strain
$\epsilon_{ar}, \epsilon_{vr}$	Axial and volumetric strain at reference (beginning of unloading)
$\sigma_1, \sigma_2, \sigma_3$	Principal stresses
σ_c	Cell pressure
σ'_h, σ'_v	Effective horizontal and vertical stresses
σ'_{oct}	Octahedral stress
σ'_s	Effective stress of a sample after actual sampling
ϕ, ϕ'	Slope of Mohr-Coulomb failure envelope
t_{cyc}	Cyclic period
t_s	Storage time
TYR	Thixotropic yield ratio

CONSOLIDATION PARAMETERS

c_v	Coefficient of consolidation
-------	------------------------------

LIST OF SYMBOLS

C_c	Virgin compression index = $-\Delta e / \Delta \log \bar{\sigma}_{vc}$
C_s	Swelling index
C_α	Rate of secondary compression = $\Delta \epsilon_v / \Delta \log t$
CR	Virgin compression ratio = $\Delta \epsilon_v / \Delta \log \sigma'_{vc}$
RR	Recompression Ratio
SR	Swelling Ratio
LIR	Load increment ratio
σ'_p	Preconsolidation pressure
σ'_{vc}	Vertical consolidation stress
σ'_{vo}	Initial vertical effective stress
σ'_{vm}	Maximum past pressure
σ'_c	Consolidation stress
σ'_o	Consolidation stress at beginning of unloading or reloading
ξ	Stress ratio = $\frac{\sigma'_c / \sigma'_o \text{ during recompression}}{\sigma'_o / \sigma'_c \text{ during swelling}}$
VCL	Virgin compression line

CONSOLIDATION AND STRENGTH TESTS

CIU	Isotropically consolidated-undrained shear test
CK ₀ U	K ₀ consolidated-undrained shear test
CK ₀ UC	CK ₀ U triaxial compression test
CK ₀ UE	CK ₀ U triaxial extension test
CRSC	Constant rate of strain consolidation test
DSS	Direct simple shear
NC	Normally consolidated
OC	Overconsolidated
OED	Oedometer test

LIST OF SYMBOLS

TC Triaxial compression

TE Triaxial extension

LIST OF TABLES

<u>TABLE</u>	<u>TITLE</u>	<u>PAGE</u>
2.1	Studies on Boston Blue Clay	27
2.2	Index Properties of the different batches	29
3.1	Summary of tests	40
3.2	Stress history	41
3.3	Rationale for names	42
4.1	Summary consolidation data from triaxial tests	56
4.2	Summary consolidation data from oedometer tests	57
4.3	Summary consolidation data for BBC	58
5.1	Summary of stress data for triaxial tests	91
5.2	Summary shear data for isotropically consolidated samples of BBC	92
5.3	Summary shear data for anisotropically consolidated samples of BBC	94
6.1	Mineralogy of BBC and LCT	149
6.2	Index Properties of BBC and LCT	150
7.1	Shear data at failure for $K=1$, 0.47 and 0.34	171
A-1	Summary of consolidation data for resedimented BBC	209

LIST OF PLATES

<u>PLATE</u>	<u>TITLE</u>	<u>PAGE</u>
7.1	Driving system with the pivot wheel, adjusting arm and mechanical counter	172
7.2	Air regulator wheel	173
7.3	Belloframe air jack with upper chamber connection	174

LIST OF FIGURES

<u>FIGURE</u>	<u>TITLE</u>	<u>PAGE</u>
2.1	Grain size distribution curves for different batches	30
3.1	Set-up of sample in the triaxial cell	43
3.2	Stress path for an increment of the anisotropic consolidation	44
3.3	Variation of K_0 upon reloading	45
3.4	a) MIT-oedometer device b) Oedometer trimming technique	46
4.1	Stress path during consolidation	60
4.2	Summary of the compression curves	61
4.3	Anisotropic vs. isotropic consolidation in CK_0U tests	62
4.4	Swelling in CK_0U tests	63
4.5	Axial vs volumetric strain for CK_0U tests	64
4.6	Compression curve in the oedometer tests	65
4.7	Overconsolidated volumetric behavior	66
4.8	Batch consolidation characteristics	67
4.9	Triaxial and oedometer consolidation characteristics for Batch 113	68
4.10	Isotropic vs anisotropic swelling behavior	69
4.11	Effect of thixotropy on preconsolidation pressure	70
4.12	Effect of thixotropy on K_0	71
4.13	Effect of thixotropy on the initial vertical effective stress	72
5.1	Stress path for CIUC8 test	95
5.2	Stress-strain for CIUC8 test	96
5.3	Obliquity-axial strain for CIUC8 test	97
5.4	Normalized modulus-axial strain for CIUC8 test	98

LIST OF FIGURES

<u>FIGURE</u>	<u>TITLE</u>	<u>PAGE</u>
5.5	Definition of Δq and Δq_{\max}	99
5.6	Stress path for CK_0UC tests	100
5.7	Stress-strain curves for CK_0UC tests (small strains)	101
5.8	Stress-strain curves for CK_0UC tests (large strains)	102
5.9	Stress-strain curves for CK_0UC tests (log scale)	103
5.10	Obliquity data for CK_0UC tests	104
5.11	Softening characteristics of CK_0UC tests	105
5.12	Obliquity vs OCR for CK_0UC tests	106
5.13	Variation of strains with OCR for CK_0UC tests	107
5.14	Variation of the pore pressure parameter at failure for CK_0UC tests	108
5.15	Normalized undrained modulus vs OCR	109
5.16	Normalized undrained modulus vs strain	110
5.17	Stress path for CK_0UE tests	111
5.18	Stress-strain curves for CK_0UE tests (small strains)	112
5.19	Stress-strain curves for CK_0UE tests (large strains)	113
5.20	Stress-strain curves for CK_0UE tests (log scale)	114
5.21	Obliquity vs. strain for CK_0UC tests	115
5.22	Stress paths for CIUC tests	116
5.23	Stress-strain curves for CIUC tests (NC)	117
5.24	Normalized undrained strength for CIUC (NC) tests	118
5.25	Stress-strain curves for CIUC tests	119
5.26	Normalized undrained strength vs OCR for CIUC tests	120
5.27	Stress paths for CK_0UC (NC) tests	121
5.28	Stress paths for CK_0UC tests	122

LIST OF FIGURES

<u>FIGURE</u>	<u>TITLE</u>	<u>PAGE</u>
5.29	Stress-strain curves for CK ₀ UC (NC) tests	123
5.30	Variation of undrained shear strength with OCR for CK ₀ UC tests	124
5.31	Stress paths for CK ₀ UE tests	125
5.32	Stress-strain curves for CK ₀ UE tests	126
5.33	Variation of the undrained strength ratio with OCR for CK ₀ UE tests	127
5.34	Variation of A _f with OCR for CK ₀ UE tests	128
5.35	Summary of undrained strength ratio with OCR	129
5.36	Summary of the variation of A _f with OCR	130
5.37	Summary of the variation of stiffness vs OCR ($\Delta q/\Delta q_{\max}=50\%$)	131
5.38	Stress paths for compression tests	132
5.39	Shear strength and normal stress at peak and ultimate conditions vs water contact for anisotropically consolidated samples	133
5.40	Peak undrained shear strength for isotropically and anisotropically consolidated samples	134
5.41	Relative increase in undrained strength ratio with OCR from anisotropically and isotropically consolidated samples (replot of data in Fig. 5.18)	135
5.42	Relative increase in undrained strength ratio with OCR for isotropically and anisotropically consolidated samples (log-log scale)	136
5.43	Variation in A _f vs OCR for isotropically and anisotropically consolidated samples	137
5.44	Variation of normalized undrained secant modulus with OCR for isotropically and anisotropically consolidated samples ($\Delta q/\Delta q_{\max}=50\%$)	138
6.1	Grain size distribution of BBC and LCT	151
6.2	Virgin compression curves of BBC and LCT	152

LIST OF FIGURES

<u>FIGURE</u>	<u>TITLE</u>	<u>PAGE</u>
6.3	Swelling curves of BBC and LCT	153
6.4	K_0 vs OCR (unloading) for BBC and LCT	154
6.5	Stress paths for CIUC tests on BBC and LCT	155
6.6	Stress-strain curves for CIUC tests on BBC and LCT	156
6.7	Normalized undrained strength for CIUC tests on BBC and LCT	157
6.8	Stress paths for CK_0UC tests on BBC and LCT	158
6.9	Stress-strain curves for CK_0UC tests on BBC and LCT	159
6.10	Normalized undrained strength for CK_0UC tests on BBC and LCT	160
7.1	Stress path for test CK_0UC1	175
7.2	Compression curves of test CK_0UC1	176
7.3	Normalized stress path for test CK_0UC1	177
7.4	Stress-strain curves of NC samples at different values of K	178
7.5	Obliquity-strain curves of NC samples at different values of K	179
7.6	Axial strains at peak vs stress ratio K for NC samples on BBC	180
7.7	Definition of stresses during cyclic loading	181
7.8	Stress paths for cyclic loading (CSR=40%)	182
7.9	Stress-strain curves for cyclic loading (CSR=40%)	183
7.10	Excess pore pressure vs strain for cyclic loading (CSR=40%)	184
7.11	Stress paths for cyclic loading (CSR=60%)	185
7.12	Stress-strain curves for cyclic loading (CSR=60%)	186
7.13	Excess pore pressure vs strain for cyclic loading (CSR=60%)	187

LIST OF FIGURES

<u>FIGURE</u>	<u>TITLE</u>	<u>PAGE</u>
7.14	Minimum and maximum axial strain during cyclic loading (CSR=60%)	188
7.15	Minimum and maximum pore pressure during cyclic loading (CSR=60%)	189
7.16	Applied shear stress for low number of cycles (CSR=60%)	190
7.17	Axial strain response for low number of cycles (CSR=60%)	191
7.18	Pore pressure response for low number of cycles (CSR=60%)	192
7.19	Applied shear stress for N=1,8,20,25,30 and 35 (CSR=60%)	193
7.20	Axial strain response for N=1,8,20,25,30 and 35 (CSR=60%)	194
7.21	Pore pressure response for N=1,8,20,25,30 and 35 (CSR=60%)	195

CHAPTER 1

INTRODUCTION

The development of computer programs to predict the response of soil masses under stress requires generalized models of soil behavior involving a comprehensive set of constitutive equations. Realistic soil behavioral models must be based on experimental data.

The Modified Cam-Clay (MCC; Roscoe and Burland, 1968) was the first generalized model which provided an elegant framework for describing the basic behavior of clays after isotropic consolidation and sheared in triaxial tests. At MIT, Kavvasdas (1982) extended the MCC to incorporate the stress-strain-strength anisotropy and the strain softening exhibited by anisotropically consolidated clays during undrained shearing. Whittle (1987) further extended Kavvasdas's MIT-E1 model to achieve more realistic predictions of the undrained behavior of overconsolidated clays during monotonic as well as cyclic shearing.

The main aim of this thesis is to establish an experimental framework for the behavior of resedimented Boston Blue Clay (BBC) in the overconsolidated range. This is achieved by first compiling and analyzing the available test data on BBC and then complementing these data by additional triaxial and oedometer tests. Results of monotonic and cyclic triaxial shear tests are then compared with existing data on BBC and on another low plasticity clay, Lower Cromer Till (LCT).

Chapter 2 briefly describes available data on BBC by summarizing the index properties of the resedimented clay, describing the various experimental studies conducted at MIT on resedimented BBC since 1961 and highlighting their achievements and their weaknesses.

The testing procedures adopted for this experimental program are detailed and discussed in Chapter 3. Chapters 4 and 5 present the data of the testing program and compare them to the relevant data reported in the various studies. Chapter 4 deals with the isotropic and anisotropic (K_0) consolidation characteristics, whereas Chapter 5 focuses on the undrained behavior of isotropically and anisotropically (K_0) consolidated samples.

Chapter 6 compares the behavior of BBC to another clay of similar low plasticity, Lower Cromer Till (LCT) (Gens, 1982; Hight, 1983).

Chapter 7 presents results of two "special" tests after describing the testing procedures and the relevant data. The first test was performed to confirm some of the conclusions of Chapters 4 and 5 and extend the results to conditions of very low consolidation stress ratio. The second test evaluated the undrained cyclic behavior of overconsolidated BBC in triaxial shearing.

Chapter 8 presents the main conclusions of this study and provides recommendations for further research.

CHAPTER 2

BACKGROUND ON BOSTON BLUE CLAY

2.1 Introduction

Boston Blue Clay has been historically chosen by MIT researchers to study clay behavior because of the availability of this soil and the existence of thick deposits underlying the Boston Basin. The initial researchers used the natural, undisturbed soil. As the volume of experimental work increased, so did the demand for large and uniform quantities of clay. Remolded, resedimented clay was developed as an economic alternative to the natural, undisturbed soil in order to meet that demand.

Techniques to prepare such soils improved over the years, but still conform to the same underlying concept. The process begins with the consolidation of a dilute slurry of soil in a cylindrical container to a moderate pressure. The resulting cake is then trimmed to samples of the desired shape (Appendix A). The unused soil is carefully wrapped with cellophane paper and coated with several layers of wax before being stored in the humid room.

At MIT, the first researchers requiring this resedimentation process modeled the behavior of footings on clay, using 9.5 in. diameter by 4.5 in. high consolidometers. Wissa (1961) developed the extrusion technique, allowing smaller samples to be trimmed to the desired size with a minimum amount of disturbance. The inability to produce fully saturated batches was a major problem faced by these researchers. Germaine (1982) succeeded in producing a uniform saturated clay. In this thesis, the term "old" batch will refer to the 1960-era batches. The term "new" batch will designate a batch consolidated following specifications in Germaine, 1982.

2.2 Previous work on Boston Blue Clay

Much research has been conducted since 1961 on Boston Blue Clay. The most important is summarized in chronological order in Table 2.1. The batch used and the index properties, if reported, are presented in Table 2.2. Results of only a few of the investigations summarized in Table 2.1 have been selected for comparison with those found by the author. Reference to these investigations will be made when dealing with specific points of soil behavior in the succeeding chapters. The following presents, very briefly, the different research projects and assesses the quality of the results.

2.2.1 Bailey (1961)

Isotropically consolidated undrained triaxial compression tests were run on NC and OC samples to investigate the effects of salt on the shear strength of Boston Blue Clay. Two values of pore fluid salt concentration were analyzed. The shear strength did not change by varying the salt concentration, providing the same consolidation pressure was applied. However, if two samples of different salt concentration were compared at the same water content, a higher shear strength was observed for the higher salt concentration.

2.2.2 Jackson (1963)

"The purpose of this thesis was to obtain triaxial stress-strain data, both drained and undrained, and under a variety of stress systems...". Normally consolidated samples were tested, and efforts to produce good K_0 -consolidated data were unsuccessful.

2.2.3 Ladd and Varallyay (1965)

This study investigated the effects of stress system variables on the

undrained shear behavior of saturated clays. The variables included: the effects of anisotropic consolidation; perfect sampling; the intermediate principal stress; and rotation of principal planes during shear. The report presented the results from consolidated undrained triaxial tests on normally consolidated resedimented Boston Blue Clay.

This study covered a wide range of normally consolidated tests and the results led to consistent trends. However, some intrinsic factors of the clay studied make broader comparisons difficult. The plasticity index is about half of that attributed to BBC, implying significant differences in the undrained behavior (see discussion in Chapter 5). The initial water content has also been affected by this lower plasticity index, leading to dramatic differences in the position of the virgin compression line (see discussion in Chap. 4). Also, a very small number of load increments was used during anisotropic consolidation (typically 3 increments). This large load increment ratio may well be the cause of the observed scatter in the reported compression curves.

2.2.4 Ladd and Luscher (1965)

This report is part of the MIT campus foundation evaluation program called FERMIT (Foundation Evaluation and Research-MIT). One-dimensional consolidation (oedometer) tests, unconfined compression, unconsolidated-undrained triaxial compression, and consolidated-undrained triaxial compression and extension tests were run on undisturbed natural Boston Blue Clay. The results of this report will not be incorporated in this thesis because the intact soil does not provide the uniformity and the control achieved in the batches.

2.2.5 Preston (1965), Braathen (1966)

Both investigators examined the effects of sample disturbance on the behavior of resedimented Boston Blue Clay during undrained shear. It was found that "the 'perfect sampling' s_u could be estimated on the basis of strength reduction versus overconsolidation ratio using the ratio of the perfect sampling effective stress to the preshear effective stress."

The difference between the two studies is not very clear, since the same tests comprised the data bases and the same problem was investigated.

However, Braathen checked the data and reevaluated the tests. Corrections were probably made to the initial geometric measurements and to the computed area of samples during undrained shear.

2.2.6 Dickey, Ladd and Rixner (1968)

The testing program covered by this study was primarily for the purpose of evaluating the performance of a prototype plane strain device designed by J. Dickey (1967). The results were compared to triaxial tests run on the same material (resedimented BBC). They concluded that "the applied stress system does change the stress and deformation properties of a soil," the reasons for which could not be explained by the observed data.

2.2.7 Kinner and Ladd (1970)

This study compared the predicted and observed load-settlement behavior of a strip footing during undrained shear. The observed undrained load-deformation and bearing capacity data were obtained from model footing tests on resedimented BBC consolidated one-dimensionally and tested at overconsolidation ratios of 1, 2 and 4. The theoretical predictions of bearing capacity utilized a "bi-linearly elastic finite element program,

FEAST-3." The input parameters for this program were derived from consolidated-undrained (CU) shear tests of the following type: triaxial compression with $K=1$ and K_0 condition; K_0 -consolidated plane strain active and passive tests; and K_0 -consolidated direct-simple shear tests.

The tabulated consolidation data for the different batches will prove very useful as they complement the same type of data obtained by Germaine (1982) (see Chap. 4).

2.2.8 Ladd, Bovee, Edgers and Rixner (1971)

The plane strain device developed by Dickey and further modified by Bovee (Bovee and Ladd, 1970) was used in the research. The investigators presented data from consolidated-undrained active and passive tests on K_0 -consolidated samples of resedimented BBC at overconsolidation ratios of 1, 2 and 4.

The active tests were reported to yield "reliable" data, and compared very well with $\overline{CK_0U}$ triaxial compression tests. The passive tests were judged unreliable because of necking and "friction" in the apparatus. Also, consolidation data were very scattered and did not provide a reasonable compression curve.

2.2.9 Ladd and Edgers (1972)

The results of consolidated-undrained direct-simple shear tests on seven normally consolidated clays were presented. Comparisons with undrained data from triaxial compression and extension and plane strain active and passive tests are also provided for several clays.

The available consolidation data will not be used, since no indication of the initial water content or void ratio is given. Those parameters are in fact difficult to measure for this type of apparatus.

2.2.10 Germaine (1982)

In this research, the Directional Shear Cell (DSC) device developed at the University College of London was modified to enable K_0 -consolidated-undrained testing of soft clays with pore pressure measurements, and hence measure cross-anisotropic stress-strain-strength parameters. Resedimented Boston Blue Clay was tested and an elaborate system was fabricated to produce uniform saturated samples. The uniformity of the clay was verified "using water content data, x-ray diffraction and visual observation. Pore pressure response (B values) from special triaxial tests and measurements of the phase quantities show the material to be fully saturated". The realization of uniform saturated batches was a major achievement since the earlier generation of batches depended on the operators' skill and experience (e.g., see the water content data in Table 2.2).

The DSC data was compared to triaxial and direct-simple shear tests reconsolidated to the vertical effective stress corresponding to the last load increment in the batches. Those data will not be used in this thesis, since the preconsolidation pressure was later shown to be affected by thixotropy. The overconsolidation ratios are therefore unknown.

2.2.11 Bensari (1984)

Undrained and drained triaxial tests were run on resedimented BBC to investigate and establish the yield envelope for BBC. The yield stress during undrained shear was evaluated from the Casagrande and the strain energy methods. For the undrained tests, the yield stress was "estimated from a 'sharp change' in the slope of shear stress vs. axial strain." However, the highly non-linear undrained behavior of the clay, particularly at higher overconsolidation ratios, precludes the use of this approach (see Chapter 5).

The results that will be used were obtained from the tests run on normally consolidated samples which were consolidated beyond their preconsolidation pressure. The overconsolidated tests used the recompression procedure, with samples consolidated to the vertical effective stress corresponding to the last load increment in the batch. The overconsolidation ratio is unknown since thixotropy affected the value of the preconsolidation pressure.

2.2.12 O'Neill (1985)

An extensive testing program was undertaken to measure the undrained stress-strain-strength (inherent) anisotropy of resedimented BBC, using the Directional Shear Cell (DSC). Also, since the material exhibited significant thixotropic effects such as increased measured preconsolidation pressures and increased shear strength, a quantitative correction was developed. The results of a series of consolidated undrained triaxial compression and extension tests were used to quantify the corrections for application to the recompression DSC test results.

2.3 Boston Blue Clay

Boston Blue Clay is an illitic marine clay deposited in the Boston Basin from approximately 14,000 to 12,000 years B.C. (Kenney, 1964). The glacial retreat submerged the area by marine brackish waters, and the subsequent deposition was controlled to a great extent by both sea level and crustal movements.

Index properties and grain size distribution curves for the various listed investigations are presented in Table 2.2 and Fig. 2.1, respectively. The "old" batches are seen to have more scattered properties. The plasticity index (PI), for example, varies from 13% (Ladd

and Varallyay, 1965) to 25% (Braathen, 1966). This variation is related mainly to the determination of the Liquid Limit (LL), whereas a fairly constant Plastic Limit (PL) is reported for all batches. As expected, these variations are directly related to the water content measurements, independent of the maximum consolidation stress in the batch.

Surprisingly, the grain size distribution of Ladd and Varallyay's S6 batch is identical to Braathen's S1 batch, for which the water content values are dramatically different. The effects of these differences on the undrained behavior are not easy to quantify, but will be recalled when needed. On the other hand, the volumetric behavior will be particularly affected since a difference of 10% in the water content is very large and approximately represents the variation observed during the consolidation of a sample to a vertical effective stress of 4 kg/cm^2 (see Chap. 4 for further details).

Although fewer measurements have been made on the "new" batches, consistent values of the plasticity index and water content have been observed. The average index properties of Boston Blue Clay can be summarized as follows:

Specific Gravity	$G_s =$	2.77 ± 0.02
Liquid Limit (%)	$LL =$	42 ± 3
Plastic Limit (%)	$PL =$	21 ± 2
Plasticity Index (%)	$PI =$	21 ± 3

and for the "new" batches

Water Content (%)	$w =$	$41 \pm 2.$
-------------------	-------	-------------

Year	Source	TRIAXIAL					PLANE STRAIN			SS	MIS	Reference			
		UU	CI		CK		CA		Cyc	CI	CA		CA		
			U	D	U	D	U	D	UD	U	D		U	D	UD
	CE	CE	CE	CE	CE	CE	CE		CE	CE	CE	CE			
61	R														Bailey
63	R														Jackson
65	I														Ladd & Lusher
65	R														Ladd & Varallyay
65	R														Preston
66	R														Braathen
68	R														Dickey et al
70	R														Kinner & Ladd
71	R														Ladd et al
72	R														Ladd & Edgers
82	R														Germaine
84	R														Bensari
85	R														O'Neill
85	R														Lutz
86	R														This Thesis

Table 2.1 Studies on Boston Blue Clay



Tests carried out on samples at several OCR's



Tests carried out at OCR = 1



Tests carried out at one OCR value (OCR \neq 1)

CI	Isotropically Consolidated Samples
cA	Anisotropically Consolidated Samples
cK	K-consolidated samples
U	Undrained tests
D	Drained tests
C	Compression tests
E	Extension tests
SS	Simple shear tests
LL	Liquid limit
PI	Plasticity index
R	Samples reconstituted in the laboratory
I	Undisturbed samples

Table 2.2 (cont.)

TABLE 2.2 INDEX PROPERTIES OF THE DIFFERENT BATCHES

Source (Batch)	σ_{vm} (ksc)	G_B	w %	LL %	PL %	PI %	clay fraction <2 μ %	Salt g/l	Reference		
MIT 1139	1.5	2.77		30.0	17.5	12.5	40	2-3	Bailey (1961)		
MIT 1139	1.5	2.77		34.7	17.7	17.0	40	35			
				36.2		19.5			Jackson, (1963)		
S4	1.5		30	32.6	19.5	13.1			Ladd and		
S5	1.5	2.78	31.2	33.3	20.4	12.9	25	16.8	Varallyay,		
S6	1.5		30.3	32.8	20.3	12.5		16.0	(1965)		
	1.5	2.77	32	45	22	23		16	Ladd, R.S., (1965)		
S1	1.5	2.77	42.0	45.6	23.4	22.2		24	Braathan, (1966)		
S2	1.5	2.77	41.5	45.4	23.1	22.3		22	and		
			38.5	42.7	23.9	18.8		16	Preston, (1965)		
	1.5		34.4	43.5		19.6			Dickey, et al (1968)		
PS, DSS											
100	↑ 1.5 ↓	↑ Ave. 2.788 ↓		43.5	19.6	23.9	.478		Kinner and Ladd, (1970)		
150			34.1	43.5	19.6	23.9					
200				38.1	17.8	20.3	.391	~8			
300				35.9	39.7	21.6	18.1	~10			
400				36.7	39.4	21.3	18.1	.351		~10	
800					41.5	19.5	22.0	.460		16	
900					41.2	18.7	22.5	.42		16	
1000					37.3	41.1	19.5	22.6		.39	16
1100					43.4	42.0	20.6	21.4			16
1200					38.1	40.2	18.6	21.6		.45	16
Model test											
101						40.7	19.6	21.1		.406	
104				40.3	19.6	20.7					
107				41.3	19.6	21.7					
200				42.3	18.5	23.8	.458				
400				39.8	18.9	20.9	.445				
160	-		34.4	38.1	17.8	20.3		~8	Ladd et al, (1971)		
1300	1.5	2.788	35.6	42.1	22.1	20.0		16			
1500	1.5		37	43.8	20.6	23.2		16			
105	1.0	2.75	40.5	47.6	23.3	24.3		16	Bensari (1984)		
109	1.0		42.2								
110	1.0		41.0								
111	1.0	2.75	40.3	47.1	24.9	22.2		16			
Powder		2.779		41.8	21.6	20.2		~9	O'Neil (1985)		
103	1.0	2.782						16	$t_B = 36d.$		
105	1.0	2.766		40.2	22.0	18.2		16	$t_B = 366d.$		
	1.0			41.6	21.0	20.6			$t_B = 1150d.$		
111	1.0			41.5	25.3	16.2		16	$t_B = 250d.$		
	1.0			42.4	21.6	20.8			$t_B = 470d.$		
112	1.0			40.8	20.6	20.2		16	$t_B = 151d.$		

CHAPTER 3
TESTING PROCEDURES

3.1 Introduction

Nine triaxial and four oedometer consolidation tests were run on Resedimented Boston Blue Clay (BBC), from a batch prepared according to the procedure outlined in Appendix 1. Samples were stored after preparation* in the humid room until testing in order to prevent changes in water content.

Tables 3.1 and 3.2 highlight the steps followed for the triaxial and oedometer tests respectively. The number (or name) given to the tests follows the rationale described in Table 3.3. The following describes the triaxial test program.

1) The eight anisotropically consolidated undrained triaxial tests were performed as follow:.

- CK₀UC2, CK₀UC4, CK₀UC8 were sheared in compression well beyond peak strength, from overconsolidation ratios of 2, 4 and 8, respectively, then sheared in extension;
- CK₀UE2, CK₀UE4, CK₀UE8 were sheared in extension well beyond peak strength, from overconsolidation ratios of 2, 4 and 8, respectively;
- CK₀UC1 is a special test performed on a normally consolidated sample to quantify strain softening;
- CK₀U-Cyc-4 is a stress controlled cyclic test run at an overconsolidation ratio of 4.

2) One isotropically consolidated undrained triaxial compression test was performed, CIUC8 and sheared at a nominal OCR value of 8.

* Preparation involved consecutive layers of cellophane, wax and aluminum foil.

The following describes the oedometer test program.

1) Four oedometer tests were also performed.

- OED5, OED27, OED133 correspond to tests run at different OCRs to investigate the effect of OCR on volumetric behavior. The steps followed are presented in Table 3.2.
- OEDR1 is a test run on a completely remolded sample at the water content of batch.

As can be noted from Table 3.1, the triaxial samples were all consolidated to a vertical stress level of 4 kg/cm^2 (except for CK₀UC1B, see discussion in Chap. 7). This was done to minimize the effects of sampling disturbance and thixotropy, i.e., they were consolidated to stress levels much larger than 1.5 times the maximum past pressure as recommended by Ladd and Foott (1974). The oedometer tests were also rebounded from a vertical stress of 4 kg/cm^2 , as can be seen in Table 3.2, to various OCRs.

3.2 Testing Procedure

3.2.1 Triaxial Apparatus

A detailed description of the MIT triaxial cell and testing procedure is given by Ayan (1985). Only the main points will be highlighted in the following and divided into four distinct phases: set-up, saturation of the sample, consolidation, undrained shearing.

3.2.1.1 Set-up:

Two days before a test is scheduled to be run, leaks and compliance of the system are checked. The compliance is the volume change recorded in the burettes when the back pressure is increased from 0 to 2 kg/cm^2 with all connections completed to the triaxial cells. Air is removed by pressurizing the system several times, and flushing water through the

connections. The final compliance reached a negligible value of 0 to 0.02 cm³ in all tests. No further checks were made during the tests.

Specimens are trimmed down using a wire saw, from larger blocks stored in the humid room. The ends are cut parallel using a split mould. The sample is then weighed and slid between the top and bottom caps of the cell. Porous stones and filter paper are provided at each end, and filter strips* 1/4" wide are added to the outside of the sample to increase the rate of consolidation and equilibration of pore pressure during shear. Care was taken to connect the filter strips to the porous stones by sliding them behind the rubber sleeve that covers the porous stones, for leakage prevention. Two prophylactics were used as sample membranes and rolled upwards over the sample, they are then sealed in place with rubber O-rings (see Fig. 3.1).

The diameter is then measured using an optical device and the height of the sample checked. The cell is finally tightly locked, deaired and distilled water is added to fill the cell and a pressure equal to or larger than the assumed initial effective stress is applied. Drainage lines are kept closed, and pore pressure is monitored; if negative pore pressures develop the cell pressure is raised, with the piston locked, and left overnight for equilibration. The sampling effective stress, σ'_s is taken as the difference between the applied total stress and the measured pore pressure.

3.2.1.2 Saturation

From previous experience with resedimented Boston Blue Clay, the pore water pressure should be raised to 2 kg/cm² (\approx 200kPa) to achieve

* 8 vertical for samples sheared in compression, 6 spiral for samples sheared in extension.

saturation. The value of 2 kg/cm^2 is arbitrary and probably much higher than the required saturation pressure for this particular manufacturing process (Germaine, 1982), but is used as a standard procedure for resedimented Boston Blue Clay.

In order to reach the value of 2 kg/cm^2 and yet keep the effective stress constant, the stresses are raised by very small increments (0.15 to 0.25 kg/cm^2). The drainage valves being closed, the total stress is increased and the change of pore pressure monitored with time. The B-value ($\Delta u/\Delta \sigma_c$) (see Appendix 2) is calculated 30 seconds after the application of the total stress. A quick response of the pore pressure together with a high B value (more than 97%) indicate a saturated sample. The drainage valves are then opened to the backpressure which has been previously raised to the desired value. The process is continued until a back pressure of 2 kg/cm^2 is applied to the pore fluid.

3.2.1.3 Consolidation

The consolidation procedure depends on the stress path. In the case of isotropic consolidation, increments of total stress are applied with a Load Increment Ratio of 1 (LIR=1). As a result of a consolidation increment, greater water content is found at the center, and the sample has a soft core surrounded by a relatively stiff shell (Atkinson et al., 1985). These non-uniformities can amount to significant disturbances if the load increments used are large. Also the large steps cannot be used in case of anisotropic consolidation because of the induced shear stress component.

The total (ABC) and effective (AB'C'C) stress paths followed during consolidation for each increment are illustrated in Fig. 3.2. An isotropic stress state ($\Delta \sigma_3$) is initially applied (path AB), and pore pressures are

allowed to dissipate for about 30 seconds (path AB'). The deviatoric stress ($\Delta\sigma_1 - \Delta\sigma_3$) is then rapidly applied resulting in an undrained shear (B'C'). The pore pressures are then allowed to dissipate fully (C'C). The exact shape and position of the effective stress path depends on the element of soil considered in the sample. The closer it is to a draining boundary, the more pore pressure dissipation will occur and the further to the right will path B'C' be shifted. The amplitude of the larger acceptable load increments is not well known and depends on the proximity of the failure envelope. The latter factor is generally important at small effective stresses, since the effective stress path B'C' will be dangerously close to the failure envelope. Steps are generally chosen so as to increase the vertical effective stress by 20%. A combination of the amplitude of the load increment, and of the time allowed before the application of the deviatoric stress, is therefore necessary in order to minimize non-homogeneities and get a better control of the stress path.

For Boston Blue Clay, the time to reach end of primary consolidation is about 4 to 5 hours in triaxial samples having top and bottom drainage as well as radial drainage provided by filter strips. Loads are therefore left for approximately eight hours. A 24-hour period is commonly allowed for the last consolidation stress increment prior to shearing and the last consolidation stress increment prior to unloading. This is done to standardize results and remove relative effects of secondary compression and aging.

Volume and area measurements are made as detailed below:

- 1) External measurement of the vertical displacement represents the real displacement of the soil. No correction is made to account for the deformation of the different components such as the piston, filter papers

or porous stones. This does not lead to a significant error because of the low stiffness of Boston Blue Clay as compared to the different components in the system.

2) Volume changes are measured through a double burette with a blue silicon oil interface. Leaks and compliance of the system are checked at the beginning of the test. It is therefore assumed that during consolidation the change in volume read on the burette corresponds exactly to the volume of water flowing in or out of the cell. (Soil grains are assumed to be incompressible compared to the soil skeleton).

3) The area is computed assuming that the sample deforms as a right cylinder (Appendix 2). Knowing the change of height and the change of volume, the corrected area A is thus related to the original area A_0 by the following equation:

$$A = A_0 \frac{1 - \frac{\Delta V}{V_0}}{1 - \frac{\Delta L}{L_0}}$$

A period of 30 minutes is allowed at the end of consolidation with the drainage lines closed to check eventual leaks while allowing one full cycle of secondary consolidation. The pore pressure is monitored with time to detect possible leaks and other undesirable effects. Only small changes due to undrained creep and temperature effects were recorded.

3.2.1.4 Special case of K_0 -consolidation

In this research most of the samples are consolidated with no lateral strain (i.e., under K_0 conditions). This constraint is time-consuming and very difficult to achieve because of the need for small load increments. The first test was run to find the K_0 value which was then used for all other tests. Three distinctive steps were followed during consolidation.

1) Recompression, in which the sample is loaded from an overconsolidated stage to the normally consolidated range. A trial and error technique was used for the first test and a curve fitting for the following tests. The relationship between K_0 and OCR was developed from the preceding tests and adjusted for the subsequent test results. The average of this relationship is traced in Fig. 3.3. A precise estimation of the preconsolidation pressure (σ'_p) should be made in order to make good use of this plot.

2) Consolidation in the normally consolidated range is not a problem as it has been well established that K_0 is relatively constant (Bishop, 1958; R.S. Ladd, 1965). Also, empirical correlations have been derived for K_0 as function of the friction angle and the plasticity index.

3) Swelling or unloading path followed Schmidt's (1966) empirical equation

$$\frac{K_0(OC)}{K_0(NC)} = OCR^m \quad (3.1)$$

when m has been arbitrarily selected as 0.4. Many empirical correlations based on the friction angle and on the plasticity index have been also developed.

The main emphasis in this research was to reproduce the same consolidation stress path and reach ultimately the same stress point on the normally consolidated line. The paths therefore followed a constant stress ratio K , equal to the value of K_0 found from test CK₀UC1.

3.2.1.5 Shearing

All undrained static (monotonic) tests were run under displacement (or strain) controlled conditions at about 0.5% axial strain per hour (0.0067 mm/min). Previous experience with resedimented Boston Blue Clay has proved

that this rate is low enough to allow full pore pressure equilibration. In both compression and extension tests, shearing was continued until the piston reached its limit of travel, or until the formation of a clear neck that made subsequent results at higher strain levels dubious. The compression tests involved a second shearing phase in which the direction of shearing was reversed when the piston reached its limit of travel. This undrained extension phase was continued for the full stroke of the piston.

Test CK₀UC1 involved a different procedure as it was sheared to 1% strain, then consolidated to a higher vertical stress ($\sigma'_v=6 \text{ kg/cm}^2$) at constant obliquity ($K=0.34$) and sheared undrained to failure. The cyclic test was run stress-controlled using a double acting bellofram air jack to drive the piston (see Chapter 7).

A Hewlett-Packard central data acquisition system was used to monitor the tests during consolidation and shearing. Values of input voltage, vertical displacement, cell pressure or backpressure, axial load and pore pressure were stored on 5-1/2 inch flexible discs. The data were then retrieved from the discs and reduced by programs, taking into account different corrections (see Appendix 2). The reduced data were transferred to an IBM PC, where most of the plots were done using the Lotus 1-2-3 program.

When shearing was completed, the piston was locked, the height measured, the water emptied from the cell, and the sample removed. Excess water was wiped off and the sample weighed with the membranes to prevent evaporation. The diameter was then measured with an optical device after removing the membranes and filter strips. Sketches of the failed sample are drawn in Appendix 3, depicting the final shape, the dimensions and failure planes (if any).

3.2.2 Oedometer Apparatus

The consolidation tests were run at approximately the same storage time ($t_s=4-6$ days). The usual testing procedures for the oedometer tests described by Lambe (1951) and Germaine (1985) were followed. Fig. 3.4a illustrates the design used. Some points that deserve mention are;

- trimming was done in the humid room by pushing a cutting shoe in the soil and trimming the excess soil ahead of the ring with a spatula. Fig. 3.4b shows the trimming technique used.
- the porous stones were boiled prior to testing. Saturated filter papers were used between the soil and the stones. The apparatus was levelled before adding weight to compensate for the different tare weights. A load of one pound was then put on the top cap as a seating load to ensure adequate contacts. The zero dial reading was taken.
- In order to prevent swelling, the samples were flooded only after they had begun to consolidate.
- the compliances of the system were measured at the beginning of the test by performing the test on a steel block. The measured displacements were then corrected to eliminate the effects of the compliance of the system for each stress level.

Three consolidation tests were performed on resedimented samples rebounded to different OCRs, and one test was done on a thoroughly remolded sample. Remolding was done at constant water content. A chunk of clay was cut from the batch, and placed in a rubber bag which was connected to a vacuum pump. The bag was then banged on the table several times and the soil reworked while molding it to keep a fairly square shape. Once removed the soil was trimmed in the usual manner.

Table 3-1 Summary Of Tests

Test #	t_g (2) (days)	σ'_s (ksc)	Consolidation				Preshear K	Shear 1			Shear 2(1)		
			Loading		Unloading			Mode of Fail.	ult ϵ (%)	ult q (ksc)	Mode of Fail.	ult ϵ (%)	ult q (ksc)
			K (NC)	σ'_{vm} (ksc)	σ'_{vc} (ksc)	OCR							
A) CK ₀ UC1	10	0.11	0.47	4.08	4.08	0.47	0.47	C	1.158	1.106			
B) CK ₀ UC2	22	0.17	0.47	4.09	2.00	0.63	0.34	C	0.947	1.92			
CK ₀ UC4	36	0.22	0.47	4.10	1.01	0.82	2.05	C	14.98	.840	E	-10.6	
CK ₀ UC8	44	0.25	0.47	4.10	0.51	1.10	4.06	C	12.9	.847	E	-16.5	
CK ₀ UE2	55	0.15	0.47	4.01	2.00	0.63	8.04	E	-20.3	-0.506			
CK ₀ UE4	164	0.34	0.47	3.98	1.00	0.83	2.01	E	-13.4	-0.556			
CK ₀ UE8	164	0.35	0.47	4.00	0.49	1.07	3.99	E	-15.4	-0.658			
CK ₀ UC-Cyc-4	164	0.35	0.47	4.00	1.00	0.82	8.16	Cyclic					
CIUC8	35	0.15	1	4.04	0.54	0.88	7.5	C	19.2	0.844			

(1) Shear 2: direction of shearing was reversed at the end of Shear 1

(2) $t_g=t_r-t_c-5$ (O'Neill, 1985, p. 73): t_r =date on which samples were reconsolidated to 0.25 ksc in the lab
 t_c =date on which final batch consolidation stress of $\sigma'_{vc}=0.25$ ksc was applied, i.e., Oct. 7, 1985

(3) Strains are referenced at the beginning of the Shear 2 phase

TABLE 3.2 STRESS HISTORY

Test #	t _s (days)	Stress History																						
		Increment #																						
		1	2	3	4	5	6	7	8	9	10	11	12	13	14	15	16	17	18	19	20	21		
OED 5	4	0.125	0.25	0.5	1	2	4					1.2	1.8	2.7	4	8	16							
								2.7	2	1.2	(5) 0.8							8	4	2	(32) 0.5			
OED 27	6	0.125	0.25	0.5	1	2	4				(27) 0.15	0.35	0.8	1.3	2	4	8							
								2	0.8	0.35								16				(32) 0.5		
OED 133	6	0.125	0.25	0.5	1	2	4				(133) 0.03	0.125	0.4	1.5	4	8	16							
								1.5	0.4	0.125											8	4	2	(36) 0.5
OEDR I		0.12	0.22	0.4	0.78	1.5	3	6	105	18	30													
												15	8	4	2	1	(60) 0.5							

Note: * Numbers represent σ_v in kg/cm²
 * Numbers in brackets represent time of consolidation in hours

Triaxial

1 st letter	2 nd letter	3 rd letter	4 th letter	Digits
σ_c	TYPE of CONSOLIDATION	DRAINAGE	SHEAR MODE	O C R
Unconfined	I (K=1)	Undrained	Compression	
Consolidated	K _o (K=K _o) A (K≠1) (K≠K _o)	Drained	Extension Cyclic	

Oedometer

OED x Oedometer run at OCR x

OEDR x " " " " on

remolded clay

Table 3.3 Rationale for names

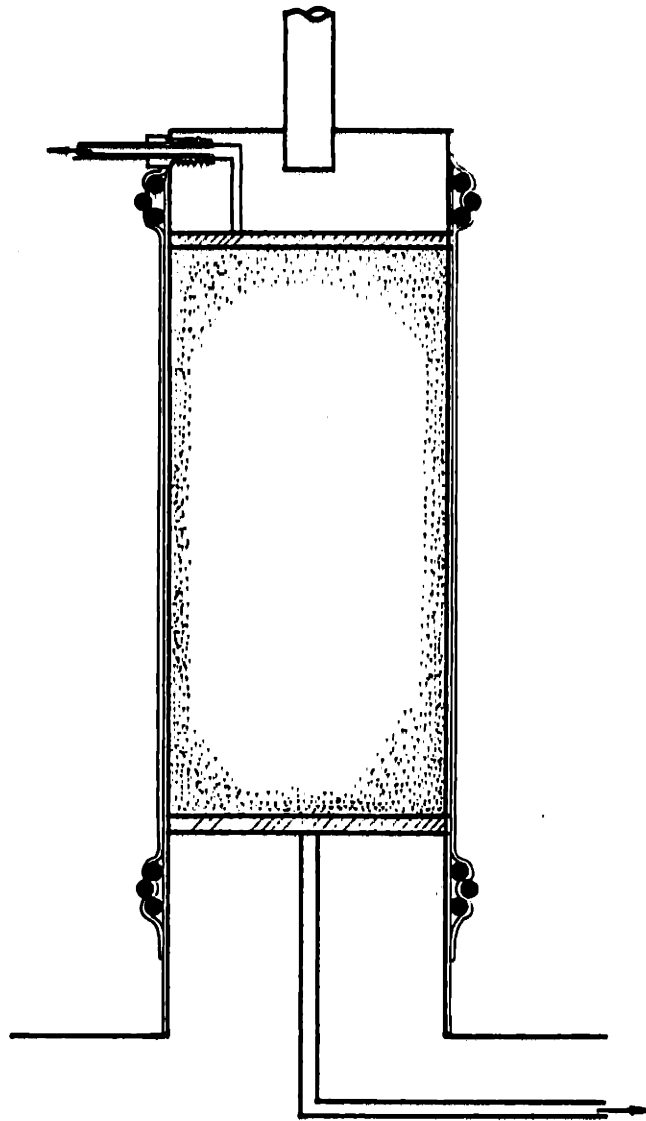


Figure 3.1 Set-up of sample in the triaxial cell

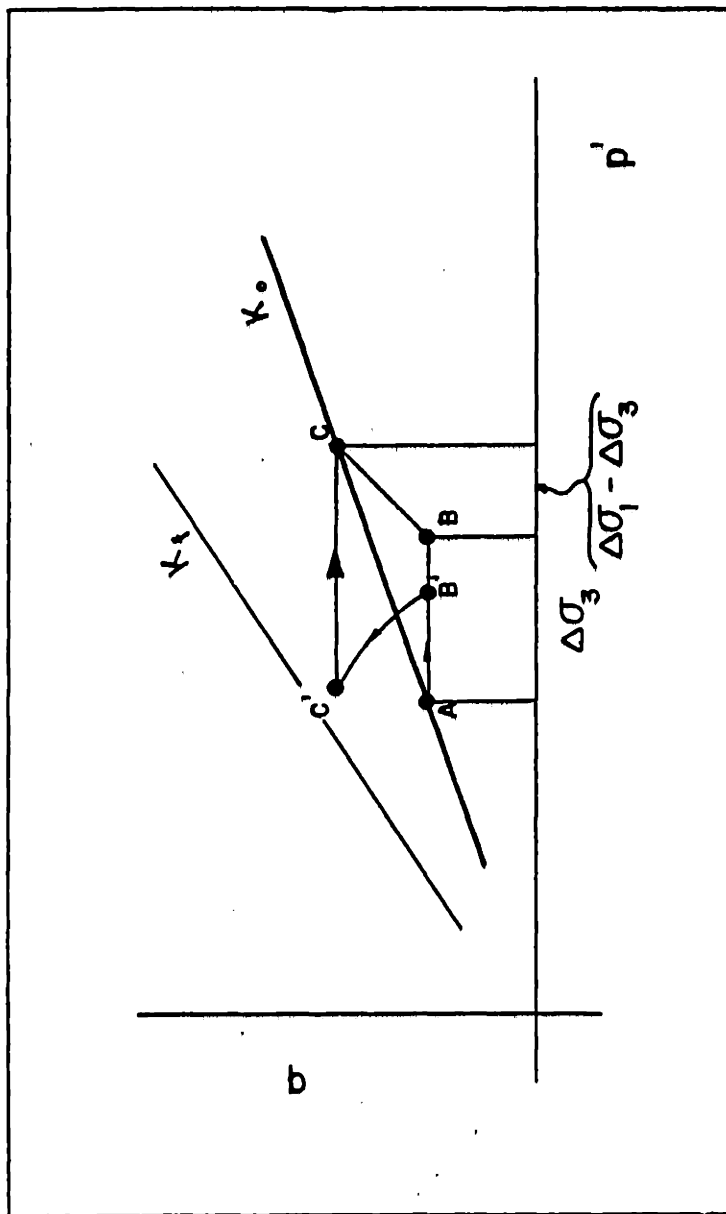


Figure 3.2 Stress path for an increment of the anisotropic consolidation

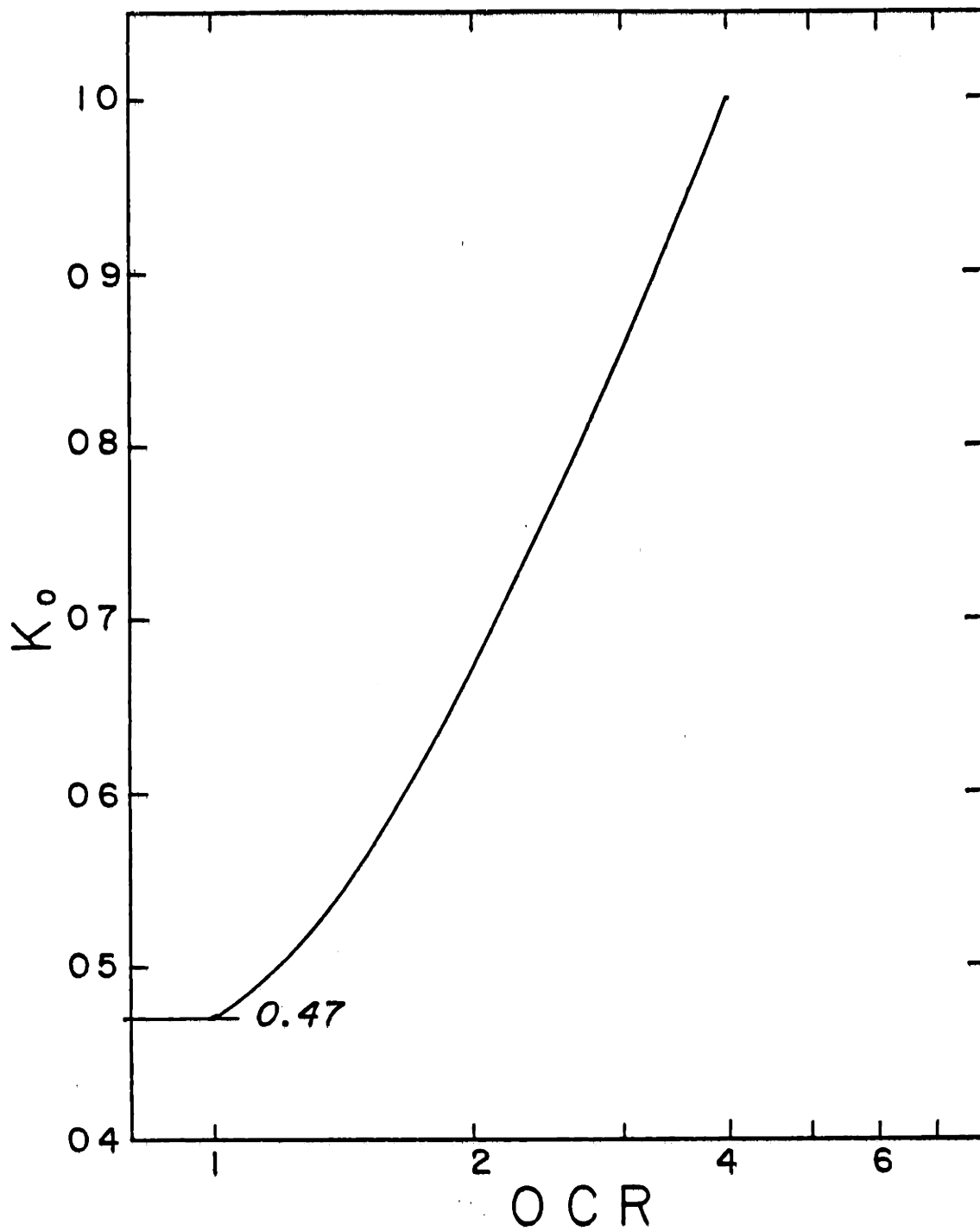
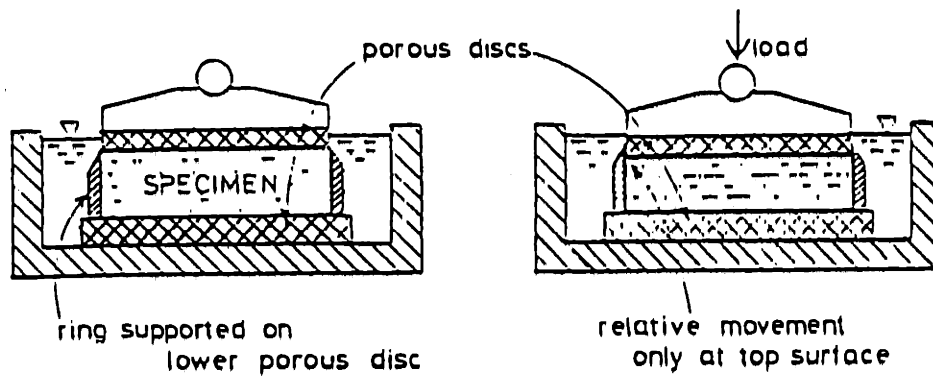
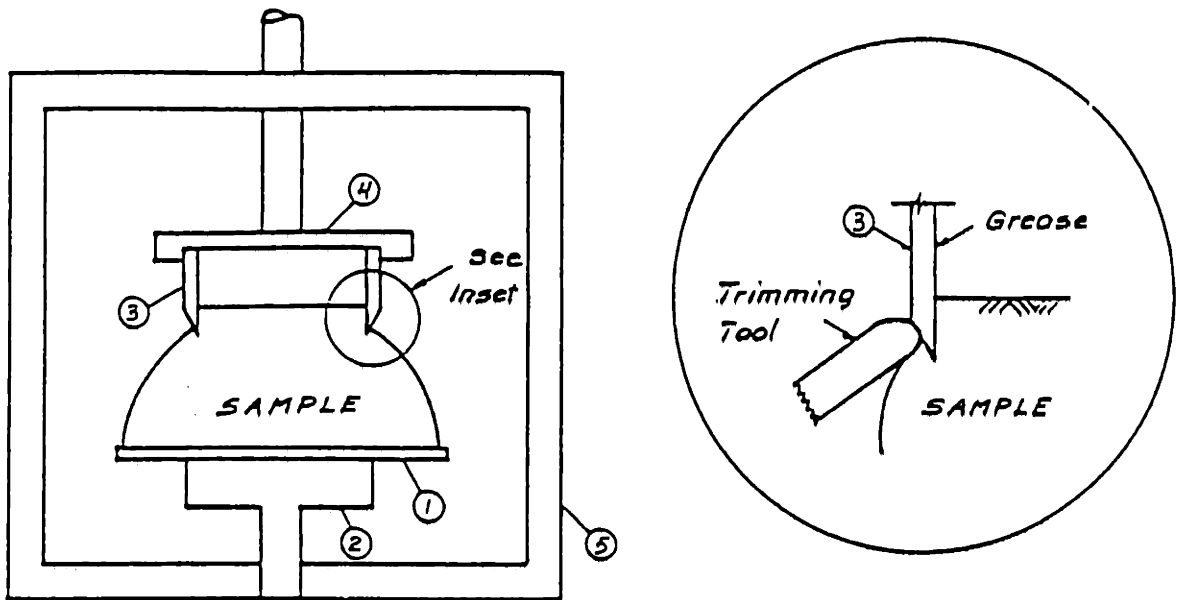


Figure 3.3 Variation of K_o upon reloading



a



b

- 1 - Glass Plate
- 2 - Rotating Base
- 3 - Cutting Ring
- 4 - Ring Clamp
- 5 - Alignment Frame

Figure 3.4 a) MIT-oedometer device
b) Oedometer trimming technique

CHAPTER 4

VOLUMETRIC BEHAVIOR OF BOSTON BLUE CLAY

4.1 Test Results4.1.1 Triaxial tests

Triaxial consolidation tests were conducted according to procedures described in Chapter 3 and results are summarized in Tables 3.1 and 4.1. The relevant data for each test are presented in Appendix C.

The average effective stress path followed during anisotropic consolidation is shown in Fig. 4.1 where the different steps are marked. The sample starts from an isotropic state (Point A) at which the initial effective stress (σ'_s) is measured and kept constant during saturation. From this overconsolidated isotropic stage, the sample is K_0 -consolidated to Point B, which corresponds to the yield stress or the preconsolidation pressure of the sample. Consolidation progresses along BC at a constant stress ratio corresponding to virgin compression up to a vertical effective stress of 4 kg/cm². Path CD is the unload or swelling path, where the variation in the stress ratio can be observed.

Figure 4.2 shows the volumetric behavior observed during anisotropic consolidation in the triaxial tests CK₀UC1, CK₀UC2, CK₀UC4, CK₀UC8, CK₀UE2, CK₀UE4, CK₀UE8 and CK₀U-Cyc-4. The individual curves are also drawn in Appendix 3, in terms of the volumetric and axial strains versus the vertical effective stress. The small load increments used during the anisotropic consolidation should be noted. In those figures, the end of increment rather than the usual end of primary* points is plotted.

* The determination of the end of primary, from displacement-log time (or Casagrande) curve, was not possible to obtain because the small increments used resulted in type III curves (Ladd, 1985)

The scatter observed in Fig. 4.2 can be reduced if we take into consideration the storage time effect. This topic will be discussed later in this chapter, but one can already notice that the three lower curves of Fig. 4.2 correspond to tests CK₀UE4, CK₀UE8 and CK₀U-Cyc-4, all run at a later stage of this research. Furthermore, the unusual broken shape observed for the compression curves, best seen in Appendix C, is probably due to the friction created by the piston.* It should be noted that the symbols in Fig. 4.2 only highlight the path and do not represent the data, because of their large number.

Fig. 4.3 compares the anisotropic average curve derived from Fig. 4.2 to the isotropic curve obtained for test CIUC8. The following can be noted:

1) The compression ratio (CR) of the virgin compression line (VCL) is similar for both types of consolidation.

$$CR = 0.162 \pm 0.009 \text{ SD}$$

2) The isotropic VCL is below the anisotropic VCL.

3) The similarity between the swelling lines is striking. Their upward curvature suggests an increasing swelling ratio (SR) with OCR.

A more complete description of the compressibility in the overconsolidated state is presented in Fig. 4.4, where the stress conditions are described by the stress ratio ξ , proposed by Azzouz and Baligh (1984), and defined as:

* The cells used in these experiments have stationary ball bearings sealed with a rolling diaphragm, with the force in the loading piston measured outside the cell. The broken shape of the curves is therefore a consequence of the stick-slip phenomenon described by Owen and Campbell (1967) especially since the applied increments are very small. The friction in the piston builds up with additional loads until the friction reaches a maximum value, after which the piston slides down suddenly.

$$\xi = \sigma'_c / \sigma'_o \quad \text{during recompression}$$

$$\xi = \sigma'_o / \sigma'_c \quad \text{during swelling} = \text{OCR}$$

where:

σ'_c = consolidation stress

σ'_o = consolidation stress at the beginning of unloading or reloading
(= OCR during swelling)

Since only swelling is involved in the triaxial consolidation tests, this definition of the stress ratio, ξ , is equivalent to the widely used "OCR" notation. However, ξ has been introduced in order to be consistent with the further results for oedometer tests.

It is observed that the compressibility changes significantly with the stress ratio ξ . Typical values of SR are:

<u>ξ</u>	<u>SR</u>
2	0.007
4	0.009
8	0.011

The two bands given in Fig. 4.4 represent the two stages at which the tests were run. It is interesting to observe a stiffer response as storage time increases. The distinction between the "early" and "late" tests, as quoted in Fig. 4.4, represents the effect of thixotropy. The "early" tests correspond to storage times varying between 22 and 55 days, while the 3 "late" tests correspond to the same storage time of 164 days.

The absence of lateral strains during K_0 -consolidation can be checked by comparing the axial strains, ϵ_a , with the volumetric strains, ϵ_v , with respect to the initial state in Fig. 4.5. It is seen that test CK₀UC1 follows the $\epsilon_a = \epsilon_v$ line corresponding to no lateral strain fairly well, and hence ascertains that the value $K_0 = 0.47$ imposed in all tests is reasonable. The tests plotting above this line indicate larger volumetric than axial

strain which means that horizontal strains developed, suggesting, therefore, that the stress ratio used ($K = 0.47$) was lower than the one required for the K_0 condition. It is also interesting to note how the tests run at a later stage, i.e., CK₀UE4, CK₀UE8, and CK₀U-Cyc-4 are grouped together below the critical line. A higher K would have therefore been needed to ensure the K_0 condition.

4.1.2 Oedometer tests

The results of the incremental 1-D oedometer tests are summarized in Table 4.2 and the corresponding data are found in Appendix D.

The consolidation histories used are seen in Fig. 4.6, where the consolidation curves for the three undisturbed (OED5, 27 and 133) and remolded (OEDR1) tests run are displayed. The anisotropic consolidation results of test CK₀UC2 are also shown for comparison. The following observations can be made:

- 1) The results obtained from the three undisturbed oedometers are very consistent and average CR equal to 0.145 ± 0.005 SD*.
- 2) The CR measured for the undisturbed oedometer tests is similar to the values measured in CK₀U tests (see also Fig. 4.2).
- 3) The relative positions of the compression curves can be compared in terms of volumetric strains only if the initial water content is identical for the materials involved. In this case, the water content data for the oedometer tests have not been measured reliably. However, since they have all been trimmed from the same batch, it can be assumed that the initial state of the sample is the same. Therefore, the different positions observed can be correlated to storage time, t_g . The oedometer

* A reading error may be the cause of the smaller strains reached in test OED5 after the unload-reload cycle.

having been consolidated at $t_s = 5 \pm 1$ days, an increasing storage time would shift the compression curves to the right, as illustrated in Fig. 4.6. This trend has been traced in Fig. 4.11 from O'Neill (1985), where the increase in preconsolidation pressure, σ'_p , is drawn as a function of the storage time, t_s .

4) The remolded sample develops larger volumetric strains, and does not show any consistent yield point. This suggests that the disturbance created by remolding destroys the inherent structure.

The overconsolidated behavior is plotted in Fig. 4.7, where the stress conditions are described by the stress ratio ξ defined previously. The range obtained from the triaxial tests is shaded. A few observations can be made:

1) The behavior is highly nonlinear, as the swelling ratio, SR, or the recompression ratio, RR, varies with the stress ratio, ξ . A stiffer response corresponds to lower values of ξ .

2) There is a large scatter in the data which may be attributable to the problems of measuring accuracy. At small ξ values (i.e., immediately at load reversals), the behavior is very stiff giving rise to small strains which are of comparable magnitude to the measuring precision. At larger ξ values, such as $\xi = 32$, for U16 ($\sigma'_{o} = 16 \text{ kg/cm}^2$), the swelling ratio, SR, varies by 20%. At the same ξ value there is a 40% difference between U4 and U16 (corresponding to $\sigma'_{o} = 4$ and 16 kg/cm^2 respectively). This suggests that there is some dependence of the swelling behavior on σ'_{o} . It is a surprising result as it indicates non-normalizeable behavior. However, measurement errors may be associated with side-friction in the oedometer ring, which could account for the differences observed and may also give rise to the increase in scatter of the data observed at high ξ values.

3) A difference is observed in the unloading and reloading curves for BBC, even at small ξ values. This differs from the findings of Azzouz et al. (1984) for Empire Clays, where reloading and unloading curves obtained from CRSC tests were found to coincide up to ξ values of about 10 (Whittle, pers. comm.).

4) For completeness, the swelling behavior measured in CK_{0UC} tests are also shown in Fig. 4.7. Good agreement is found between the triaxial and the oedometer results described above.

4.2 Anisotropic versus Isotropic Volumetric Behavior of BBC

For the range of stresses considered, the slope of the virgin compression line (VCL) is expected to be unique for a given soil when plotted in terms of the void ratio, e . For resedimented Boston Blue Clay, this slope is given by $C_c = CR / (1 + e_0)$ where values of the compression ratio, CR, are summarized in Table 4.3 and typically give:

$$CR = 0.153 \pm 0.020 \text{ SD} \quad (\text{avg. of 38 tests})$$

The hypothesis of uniqueness of slope cannot be validated for Boston Blue Clay, the number of isotropic tests being very limited and the results often dubious*. However, the few reported compression ratios (CR), for isotropic consolidation, tend to confirm this hypothesis, their range of scatter falling in the anisotropic range.

The available consolidation data are in terms of the void ratio, e , in Figs. 4.8 and 4.9. Fig. 4.8 summarizes batch consolidation data while Fig. 4.9 presents consolidation data from triaxial and oedometer tests.

* Preston (1965) ran series of isotropic and anisotropic triaxial tests for which the phase relationships derived for each test do not agree. This increases the difficulty in exploiting the data since the reliability of parameters is unknown. Ladd and Varallyay (1965) consolidated tests at different stress ratios, but their water contents are too low and very few increments were used during consolidation.

The relative position of the isotropic and anisotropic virgin compression line has generated a certain amount of controversy. Most of the disagreement appears to center on the hypothesis attributed to Rutledge (ref. by Gens, 1982) which states that the water content after consolidation is a function of the vertical consolidation stress (σ'_{vc}) only and is independent of the type of consolidation (isotropic, anisotropic). Broms and Ratnam (1963), and Lee and Morrison (1970) reported results confirming this hypothesis. Henkel and Sowa (1963) reported that the relationship between water content and the mean consolidation stress (σ'_{oct}) was "almost" identical for the isotropic and the K_0 consolidation. However, other investigators such as Ladd (1965), Donaghe and Townsend (1978), Khera and Krizek (1967), Gens (1982) and Mitachi and Kitago (1976), reported studies that contradict the Rutledge hypothesis. The reported experimental results show a decreasing water content trend with decreasing stress ratio at a constant mean consolidation stress. Akai and Adachi (1965) attributed this trend to the "dilatancy exerted by the increase in the deviator stress," i.e., the more shear is present in the sample, the more water will be driven out. Moreover, although they found results supporting the Rutledge hypothesis, Henkel and Sowa (1963) described their own experimental results as "the fact that the water content and σ'_{oct} lines for both types of consolidation almost coincide must be regarded as fortuitous."

Also, the results obtained here do not follow the Rutledge hypothesis, but the scatter involved in the anisotropic tests and the single isotropic test used to establish the comparison prevents us from drawing a definite conclusion.

The comparison between the swelling lines for both types of

consolidation is presented in Fig. 4.10. The consolidation stresses have been normalized by the maximum consolidation stress. If mean stresses are considered, a unique swelling line is found for both isotropic and anisotropic consolidation. The same behavior has been found by Amerasinghe and Parry (1975) and Gens (1982).

4.3 Effect of Thixotropy

A large part of the observed scatter in BBC data presented above can be attributed to thixotropy, defined as "an isothermal, reversible, time dependent process occurring under conditions of constant composition and volume whereby a material stiffens while at rest and softens or liquifies upon remolding" (Mitchell, 1976, quoted in O'Neill, 1985). Resedimented Boston Blue Clay proved to be very sensitive to thixotropy through an extensive laboratory testing program described by O'Neill (1985).

One of the major effects of thixotropy on this material is the variation in the measured preconsolidation stress, σ'_p (Fig. 4.11). Most of the data presented in (O'Neill, 1985) for which the trend has been quantified, are based on oedometer tests. The Thixotropic Yield Ratio, TYR*, is shown to increase steadily and reach a value of 1.35 after 100 days of storage. It was also observed that the increase in the preconsolidation pressure was not accompanied by a change in the slope of the virgin compression line.

The triaxial tests run as part of the present study were consolidated anisotropically, with a same value of the stress ratio K for the virgin range. At the time the tests were run, it was assumed that the value of $K_0=0.47$ adopted for this research was not affected by thixotropy. When

* TYR = $\frac{\text{maximum consolidation stress @ } t=t_g \text{ in the cell}}{\text{maximum consolidation stress of the batch}}$

plotted as a function of vertical effective stress, the consolidation curves are expected to shift to the right with increasing storage time t_s . However, the opposite trend was observed, with an increase in the value of K_0 being the only possible cause.

In order to show this trend, the tests are divided in two parts: those run at an "early" stage, for which $t_s=30 \pm 20$ days, and those run at a "later" stage for which $t_s=164$ days. Fig. 4.11 from O'Neill (1985) would predict a 25% increase in the preconsolidation pressure for the "later" tests, as compared to the "earlier" ones. Fig. 4.12 illustrates the results of test CK_0UC4 and CK_0UE4 as representative of their age category. The shift to the left is very clear. Fig. 4.5 also shows that test CK_0UE4 dilated significantly compared to CK_0UC4 . Both phenomena (shift of the VCL to the left and dilation) that characterized the "later" test, are synonymous with an increase in the value of K_0 as storage time t_s increases. Unfortunately, the available data on Boston Blue Clay do not provide the information necessary to quantify this trend.

Another noteworthy point is the increase in the initial effective stress σ'_s with storage time t_s . The initial effective stress is equal to the pore pressure measured under conditions of zero total stress. The data measured from the triaxial test immediately after the set-up procedure are presented in Fig. 4.13. The observed increase in σ'_s reaches a value of 0.35 kg/cm^2 for 164 days, whereas the last consolidation increment in the batch was at 0.25 kg/cm^2 . Those results are in agreement with Day's (1954) investigation, in which the pore water pressure was continuously monitored with a tensiometer. O'Neill's (1985) data from DSC and triaxial samples show considerable scatter associated with this trend.

Table 4-1 Summary Consolidation Data from Triaxial Tests

Batch 113
G_s=2.78

t_c=24 hours
K₀=0.47

Test #	Initial		@ σ'vm					Preshear				Δε _v Δlog σ'v		Remarks
	w _o (1)	e _o (S _o)	w (%)	ε _a (%)	$\frac{\Delta e}{1+e_0}$	σ'vm (ksc)	wf (%)	$\frac{\Delta e}{1+e_0}$	σ'vc (ksc)	K	CR	RR(2)		
CK ₀ UC1	43.8	1.218 (100)	35.7	0.096	0.101	4.08	S	A	M	E	0.155	--	Initial area not measured	
CK ₀ UC2	35.7	1.185 (104)	32.8	0.086	0.099	6.04	S	A	M	E	0.170	0.007	Second shear (see Chap.7) K=0.34 Dry weight not reliable	
CK ₀ UC4	42.4	1.193 (99)	34.8	0.087	0.097	4.10	34.9	0.096	2.00	0.63	0.172	0.010	Swelling stress path wrong (See App. C)	
CK ₀ UC8	43.7	1.207 (101)	34.7	0.095	0.097	4.10	35.6	0.086	0.51	1.10	0.171	0.010	Dry weight not reliable	
CK ₀ UE2	43.7	1.185 (102)	35.8	0.088	0.101	4.01	36.5	0.098	2.00	0.63	0.153	0.007		
CK ₀ UE4	43.2	1.199 (100)	35.3	0.115	0.102	3.98	35.7	0.097	1.00	0.83	0.152	0.008		
CK ₀ UE8	43.2	1.188 (101)	34.7	0.118	0.103	4.00	35.5	0.093	0.49	1.07	0.172	0.012		
CK ₀ U- Cyc-4	43.6	1.209 (100)	34.8	0.108	0.102	4.00	35.2	0.097	1.00	0.82	0.157	0.071		
CIUC8	43.5	1.191 (101.5)	32.1	0.028	0.128	4.04	34.0	0.104	0.54	0.88	0.153	0.019	Performed by students K=1	

(1) w_o based on sample

(2) Calculated between σ'vm and σ'vc

Table 4-2 Summary Consolidation Oedometer Tests

TEST	t_s (days)	w_l (%)	$\sigma'_{p'}$		$\Delta\epsilon/\Delta\log\sigma'$				C_v (NC) $\times 10^{-3}$ cm^2/sec	$C_{\alpha\epsilon}$ (NC)	$\frac{C_{\alpha}}{CR}$	Remarks (Quality)
			$\sigma'_{p'}$ (ksc)	ϵ (%)	CR	RR	SR					
OED5	4	41.2	1.02	3.3	0.128 (± 0.034)	0.008	0.009	6.97	0.443	3.46	(Fair)	
OED27	6	?	1.1 \pm 0.1	3.4	0.143 (0.018)	0.011	3.3				(Fair)	
OED133	6	42.7	1.35	3.5	0.152	0.010	4.6				(Poor)	
OEDR1	-	34.2	?			0.020					Batch 108 remolded	

Table 4.3a SUMMARY CONSOLIDATION DATA FOR BBC

Test #	Initial		θ σ'_{vm}		w %	Final		$\Delta e_v / \Delta \log \sigma'_v$			Batch #	Reference + Remarks	
	w _i %	e _i	w %	e		σ'_{vm} (ksc)	w %	ef	σ'_{vc} (ksc)	CR			RR
CIU-P1	42.0	1.20	31.6	0.87	6	32	Same	3	0.170		0.019	Preston (1965) • G _s not defined • e values dubious • K ₀ =0.5	
CIU-P2	42.1	1.16	31.3		6	32.7	0.88	1.5	0.145		0.019		
CIU-P3	41.7	1.18	30.9		6	33.0	0.90	0.75	0.150		0.022		
CIU-P4	42.5	1.17	31.4		6		0.90		0.145				
CIU-Cyc-EP9	42.6	1.20	31.1	0.86	6		Same		0.150				
CIU-Cyc-EP10	42.4	1.19	31.1	0.87	6		Same		0.149				
CK ₀ J-Cyc-P14	42.8	1.27	33.8	0.93	6		Same		0.168				
CK ₀ J-Cyc-P15	42.9	1.18	33.3	0.95	6		Same		0.156				
CK ₀ J-Cyc-P16	41.5	1.19	32.2	0.90	6		Same		0.166				
CK ₀ UU-P7	42.1	1.17	32.7	0.90	6		Same		0.152				
CK ₀ JU-P8	42.3	1.18	32.9	0.92	6		Same		0.150				
CK ₀ -CIU-P11	42.8	1.25	33.0	0.98	6	35.4	0.978	0.25	0.144		0.016		
CK ₀ -CIU-P12	42.6	1.25	33.4	0.952	6	34.4	0.985	0.75	0.151		0.012		
CK ₀ -CIU-P13	42.8	1.26	33.2	0.983	6	34.0	0.999	1.50	0.171				
CIU-RMG-P14	41.4	1.15	31.5	0.873	6		Same						
Batch 100	96.0		33.7	0.938	2		Same		(0.48)			100	Kinner & Ladd (1970) • Compressibility ratios in terms of void ratio
Batch 101	97.4		33.6	0.935	2		Same		(0.398)			101	
Batch 102	98.9		33.1	0.921	2		Same		(0.385)			102	
Batch 103	93.9		34.1	0.944	2		Same		(0.417)			103	
Batch 104	96.6		34.2	0.957	2		Same		(0.393)			104	
Batch 105	94.4		38.3	1.060	1		Same		(0.384)			105	
Batch 106	98.6		37.0	1.027	1		Same		(0.383)			106	
Batch 107	102.3		31.1	0.868	3.4		Same		(0.365)			107	
Batch 108	98.8		32.1	0.893	3.4		Same		(0.357)			108	
Batch 200	99.7				3.4	32.5	0.901	1.7	(0.368)	(0.018)	(0.029)	200	
Batch 201	98.8				3.4	32.5	0.901	1.7	(0.364)	(0.033)	(0.033)	201	
Batch 400	96.4				3.4	32.1	0.889	0.85	(0.357)	(0.024)	(0.035)	400	
Batch 401	97.3				3.4	32.1	0.888	0.84	(0.388)	(0.024)	(0.036)	401	
Batch 402	99.3				3.4	32.3	0.898	0.85				402	

Table 4.3 b SUMMARY CONSOLIDATION DATA FOR BBC

Test #	Initial		e σ'_{vm}				Final			$\Delta \epsilon_v / \Delta \log \sigma'_v$			Reference + Remarks	Batch #
	w _i %	e _i	w %	e	σ'_{vm} (ksc)	w %	ef	σ'_{vc} (ksc)	CR	RR	SR			
CIUC-2	31.4	.925	25.4	0.704	4		Same						S=94%	S5
CIUC-1	30.4	.893	23.5	0.655	6		Same						S=94%	S5
CIUC-3	31.5	.925	23.0	0.641	8		Same						S=95%	S5
CIUC-1	30.1	.885	24.6	0.683	4		Same						S=95%	S5
CIUC-2	30.9	.908	23.8	0.659	4		Same						S=94%	S6
CIUC-3	29.0	.870	21.6	0.606	6		Same						S=94%	S6
CK ₀ UC-1	31.2	.910	25.9	0.720	4.1		Same						S=95%, K ₀ =0.53	S5
CK ₀ UC-2	29.7	.860	23.3	0.648	6.1		Same						S=96%, K ₀ =0.54	S6
CK ₀ URE-4	30.5	.875	26.0	0.726	4		Same						S=97%, K ₀ =0.54	S6
CK ₀ URE-5	30.8	.883	23.1	0.644	6		Same						S=97%, K ₀ =0.54	S6
CK ₀ U(A)-2	33.6	.985	30.1	0.835	3.6		Same						Dickey et al. (1968)	
CK ₀ U(P)-1	34.7	1.012	27.1	0.794	4.5		Same		0.145 0.176				. Plane Strain Cell	
Batch 100	56.3	1.570	35.8	0.997	2	36.0	1.003	0.5	0.131		0.005			100
Batch 101	101.2	2.788	40.2	1.120	1	40.7	1.132	0.25	0.110		0.007			101
Batch 102	99.9	2.786	39.0	1.088	1	39.8	1.108	0.25	0.102		0.005		Germaine (1982)	102
Batch 103	97.6	2.722	39.7	1.106	1	40.1	1.119	0.25	0.150		0.006			103
Batch 104	97.1	2.665	39.1	1.072	1	39.6	1.087	0.25	0.114		0.008			104
CK ₀ UC(NC)	40.8		(5.3)		2.4		Same		0.114					110
CK ₀ UE(NC)	41.1		5.6		2.1		Same		0.120					110
CIUC(NC)	41.9		(12.1)	0.923	3.0		Same		0.152					109
CK ₀ 1/K ₀ UC(NC)	42.2		(6.6)		2.1		Same		0.16					109

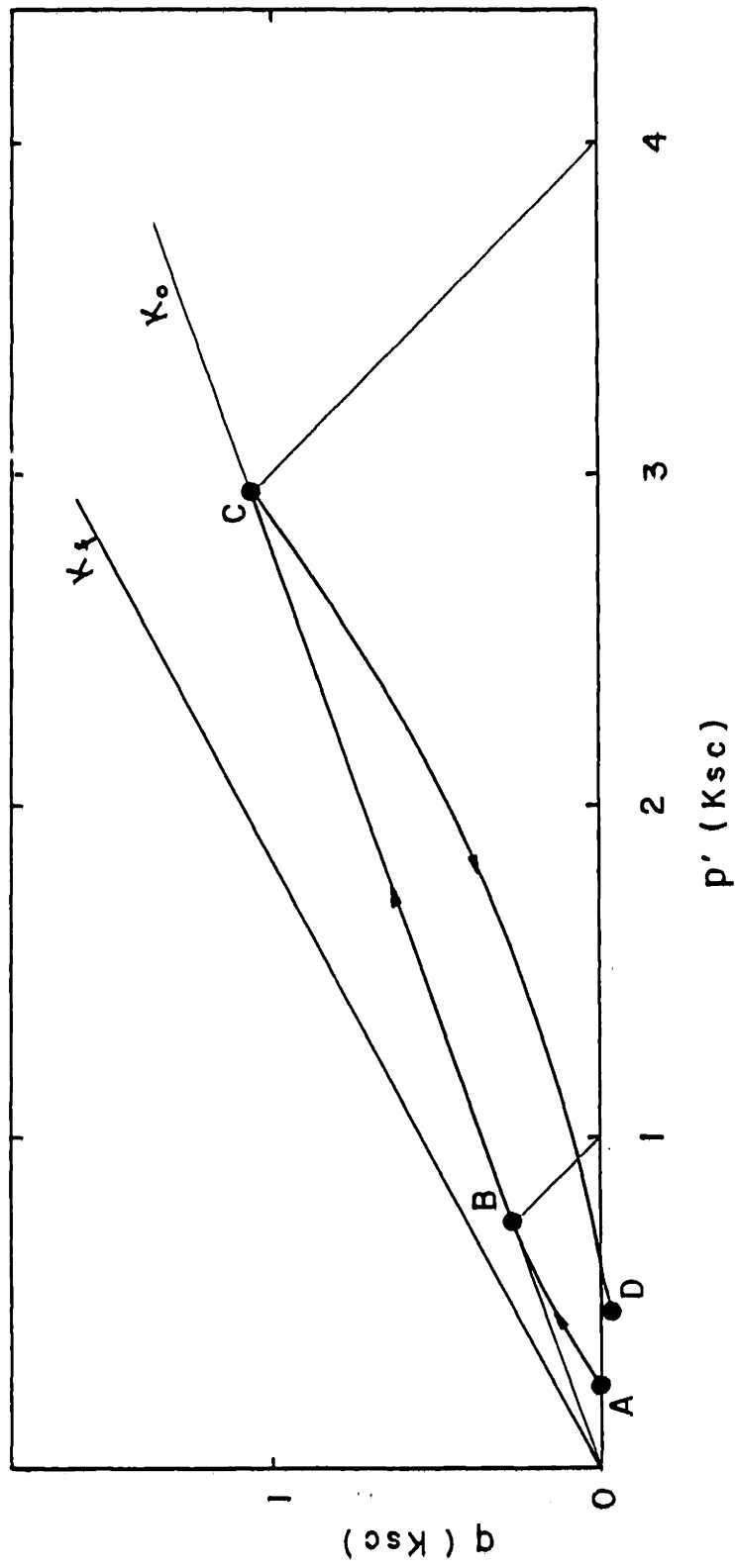


Figure 4.1 Stress path during consolidation

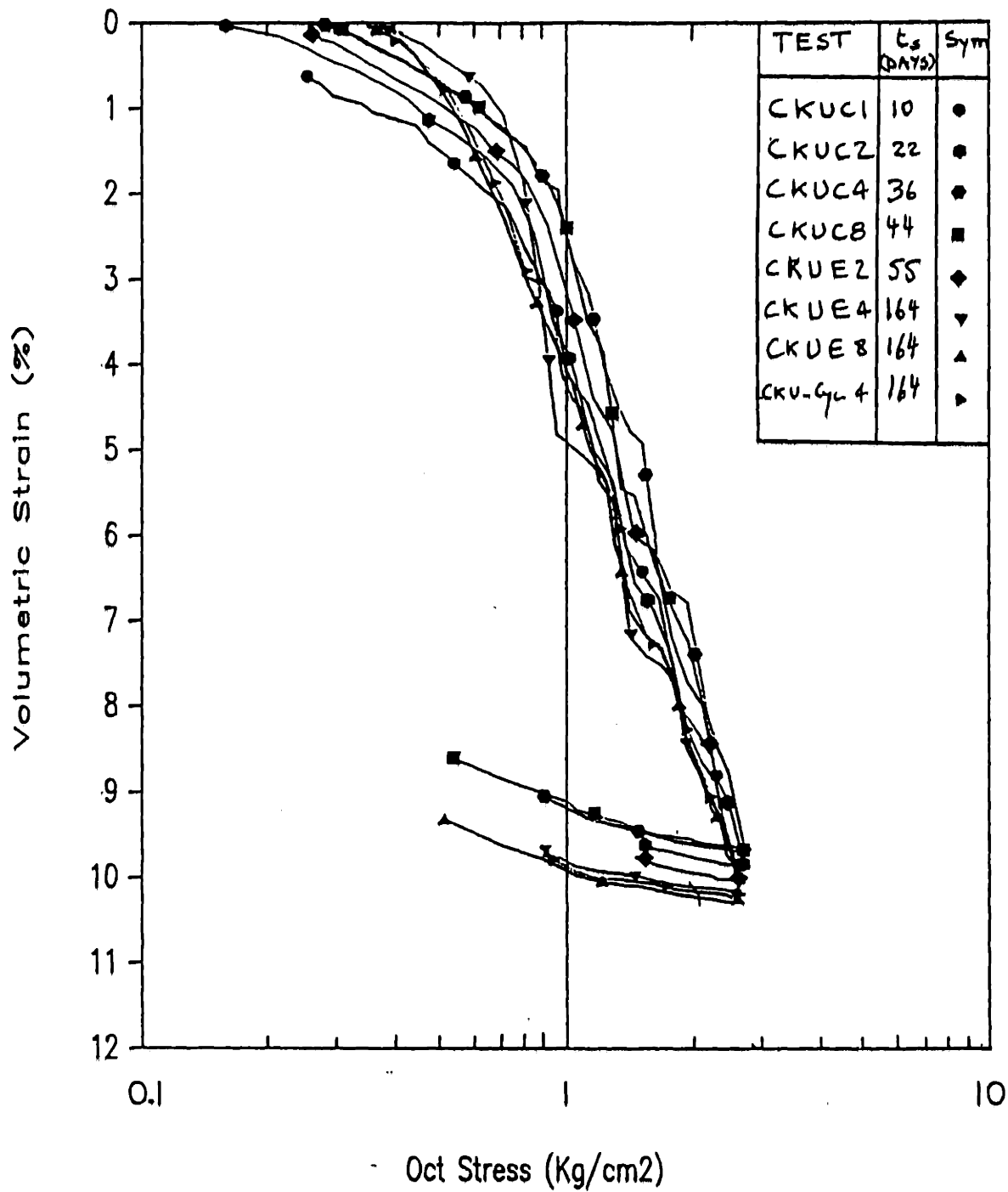


Figure 4.2 Summary of the compression curves

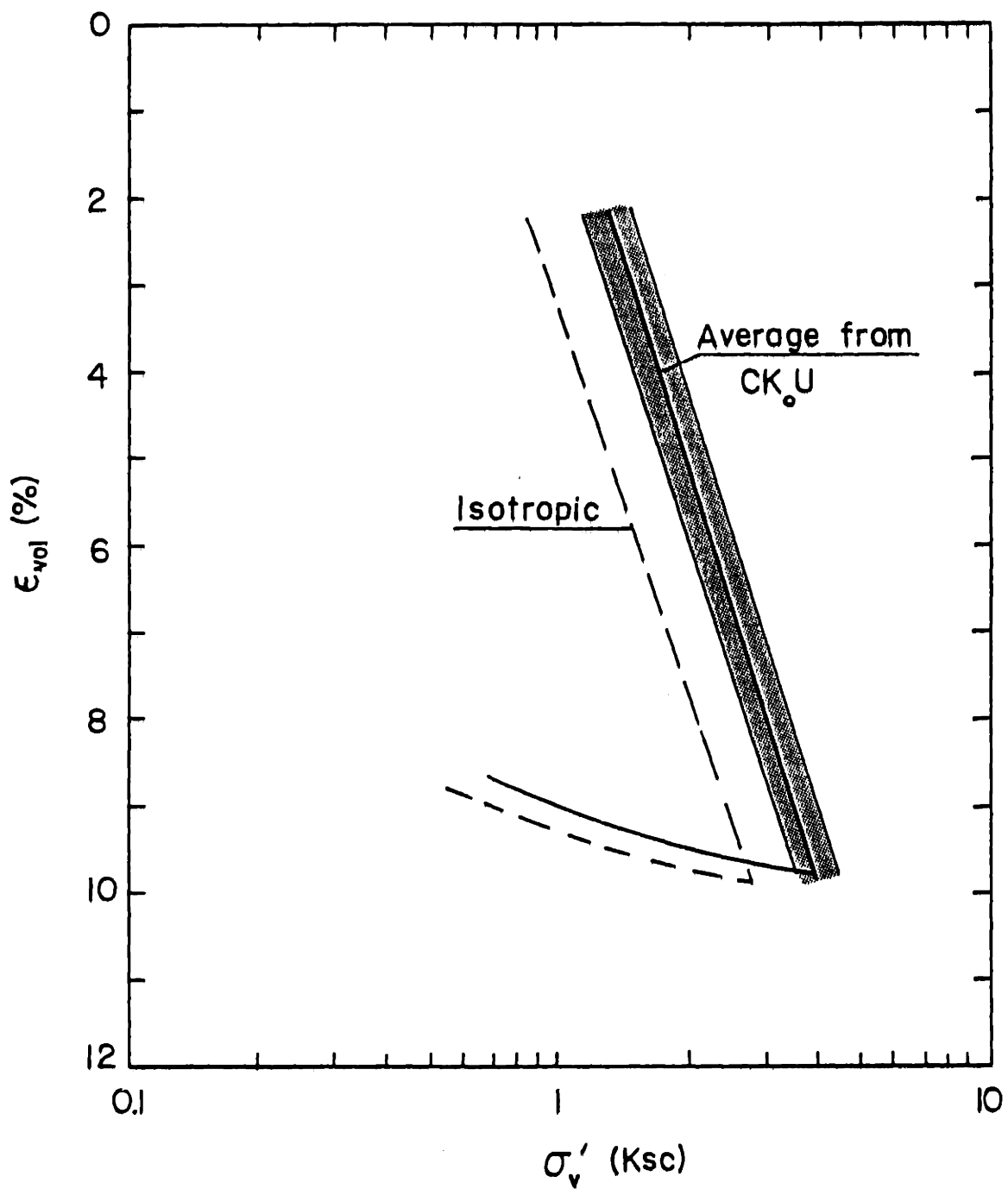


Figure 4.3 Anisotropic vs. isotropic consolidation in CK_0U tests

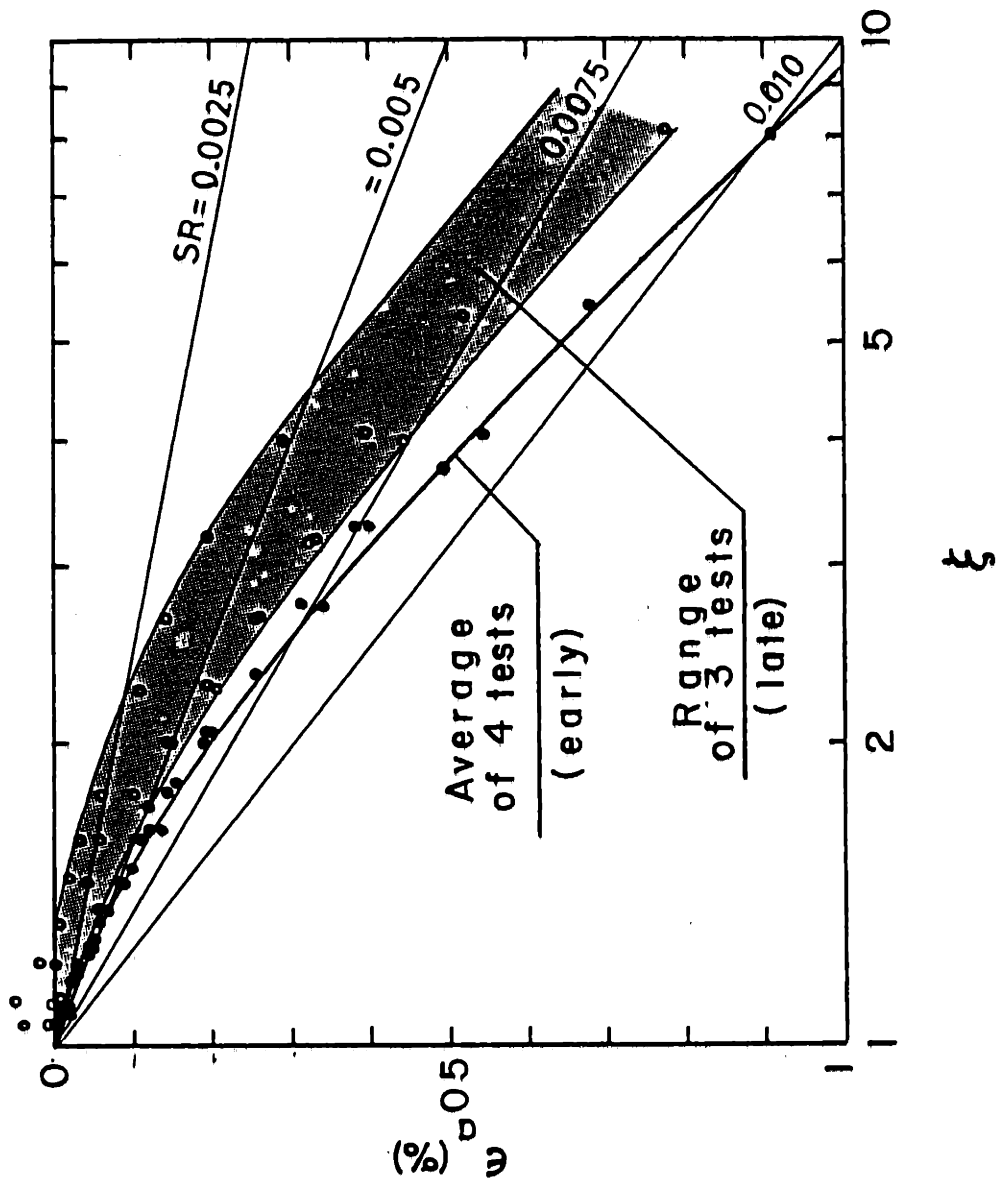


Figure 4.4 Swelling in CK₀U tests

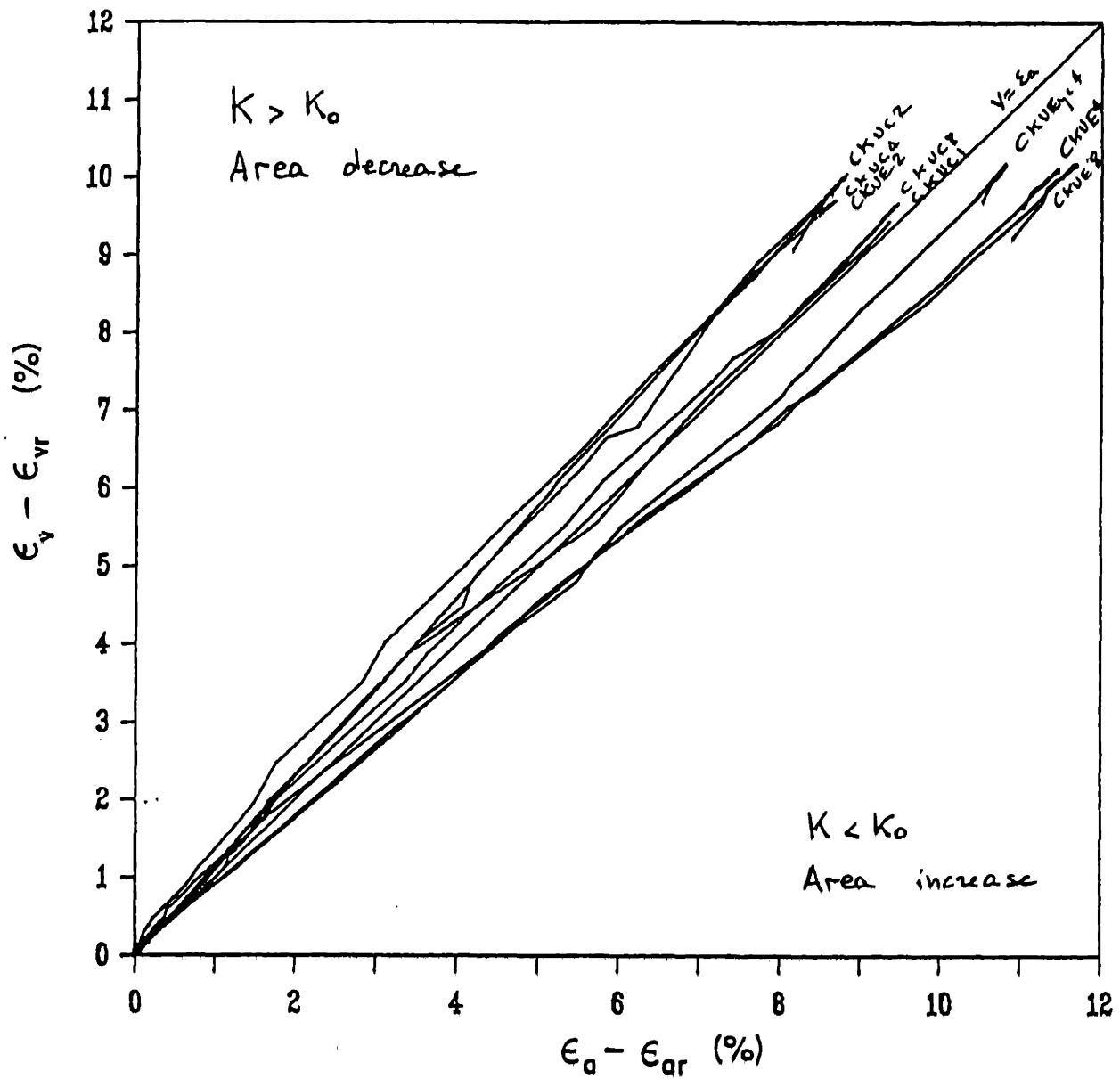


Figure 4.5 Axial vs volumetric strain for CK₀U tests

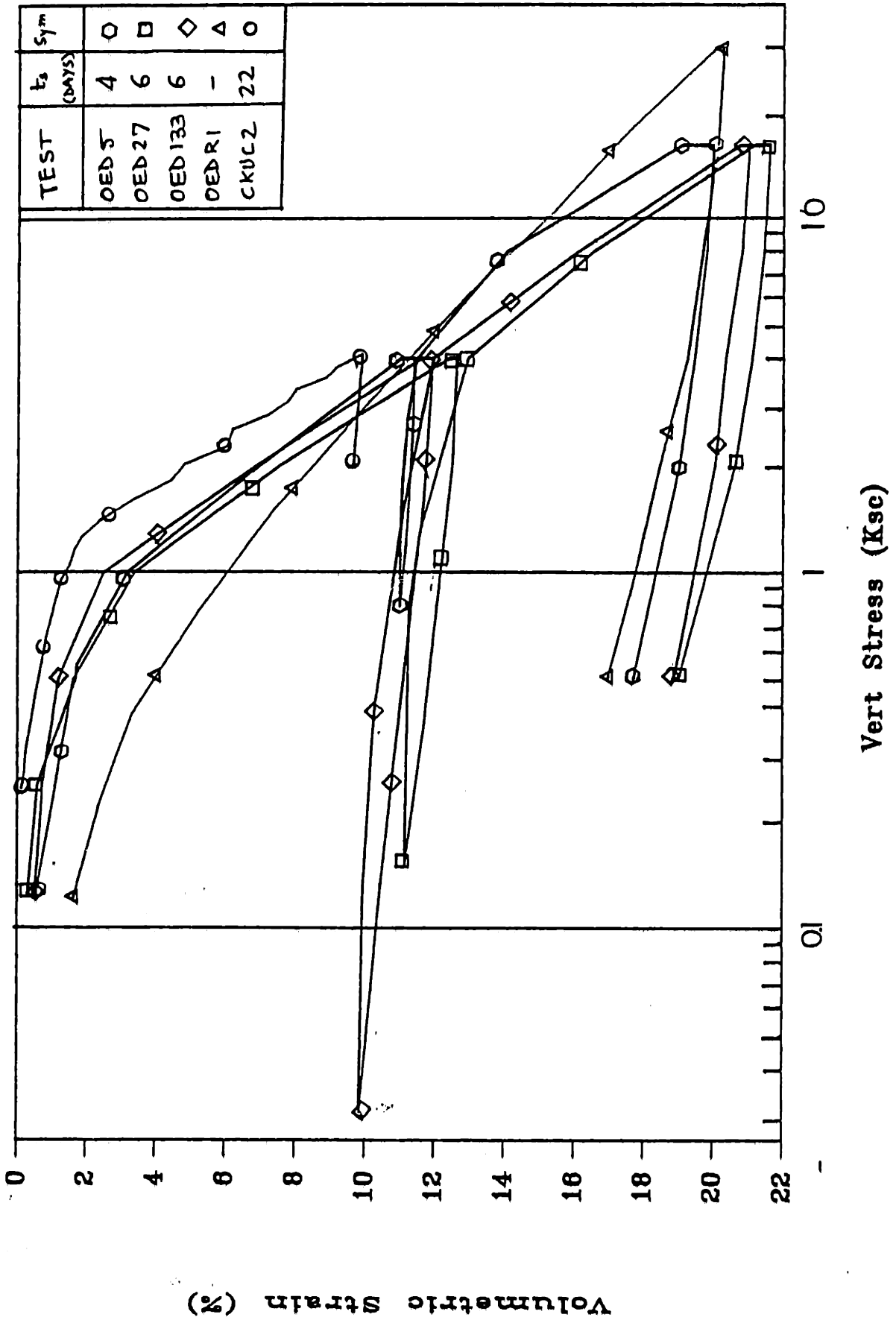


Figure 4.6 Compression curve in the oedometer tests

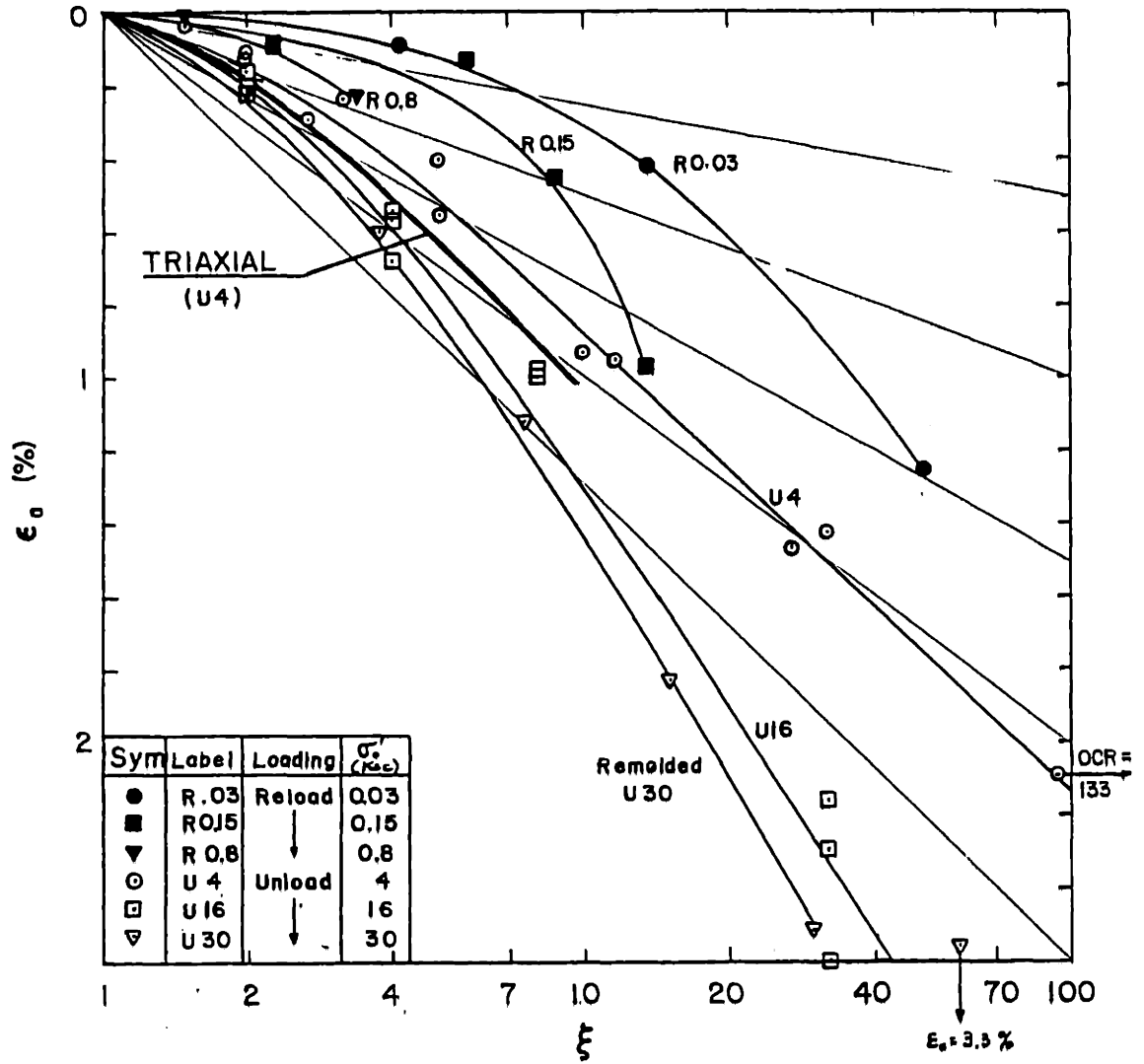


Figure 4.7 Overconsolidated volumetric behavior

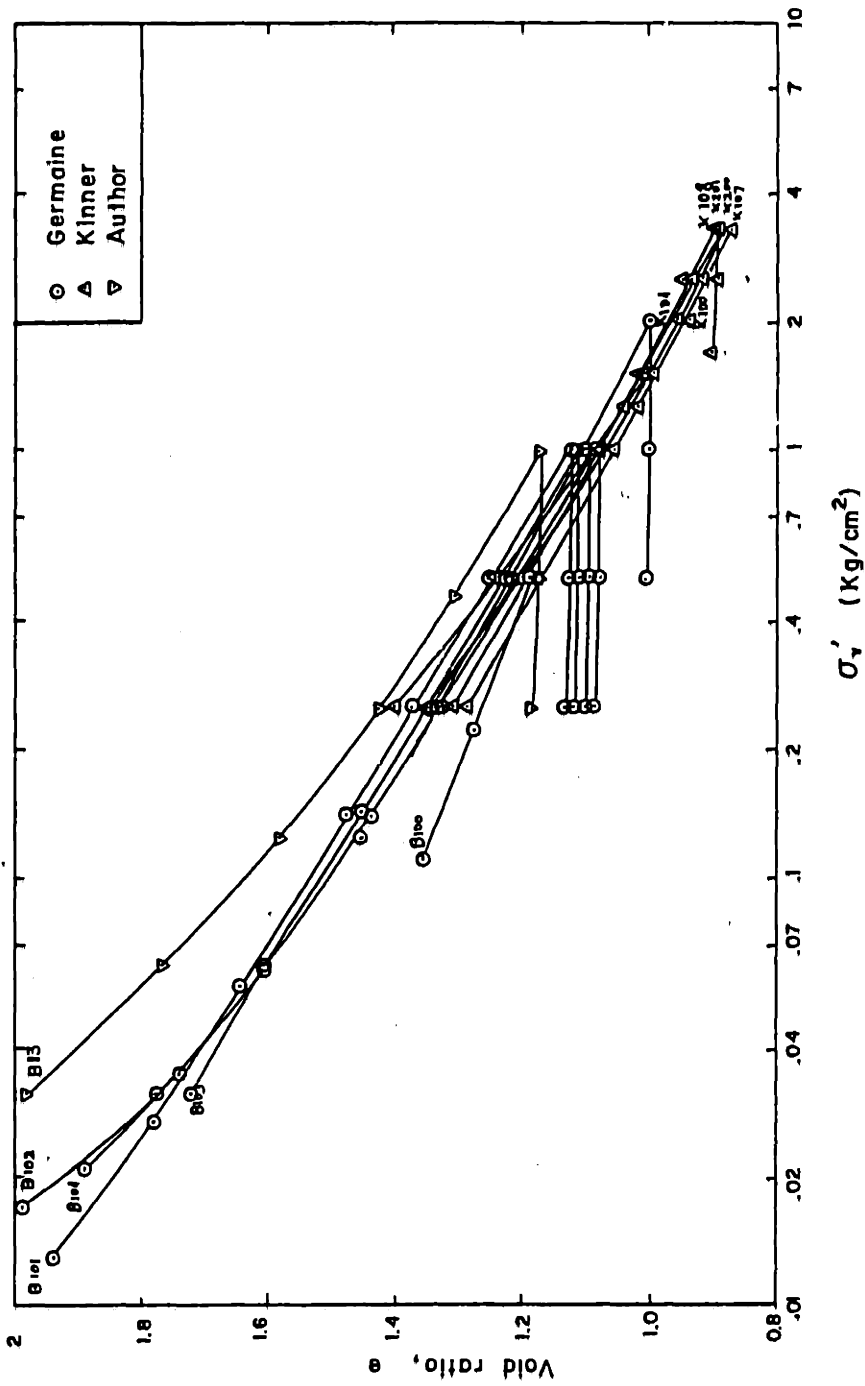


Figure 4.8 Batch consolidation characteristics

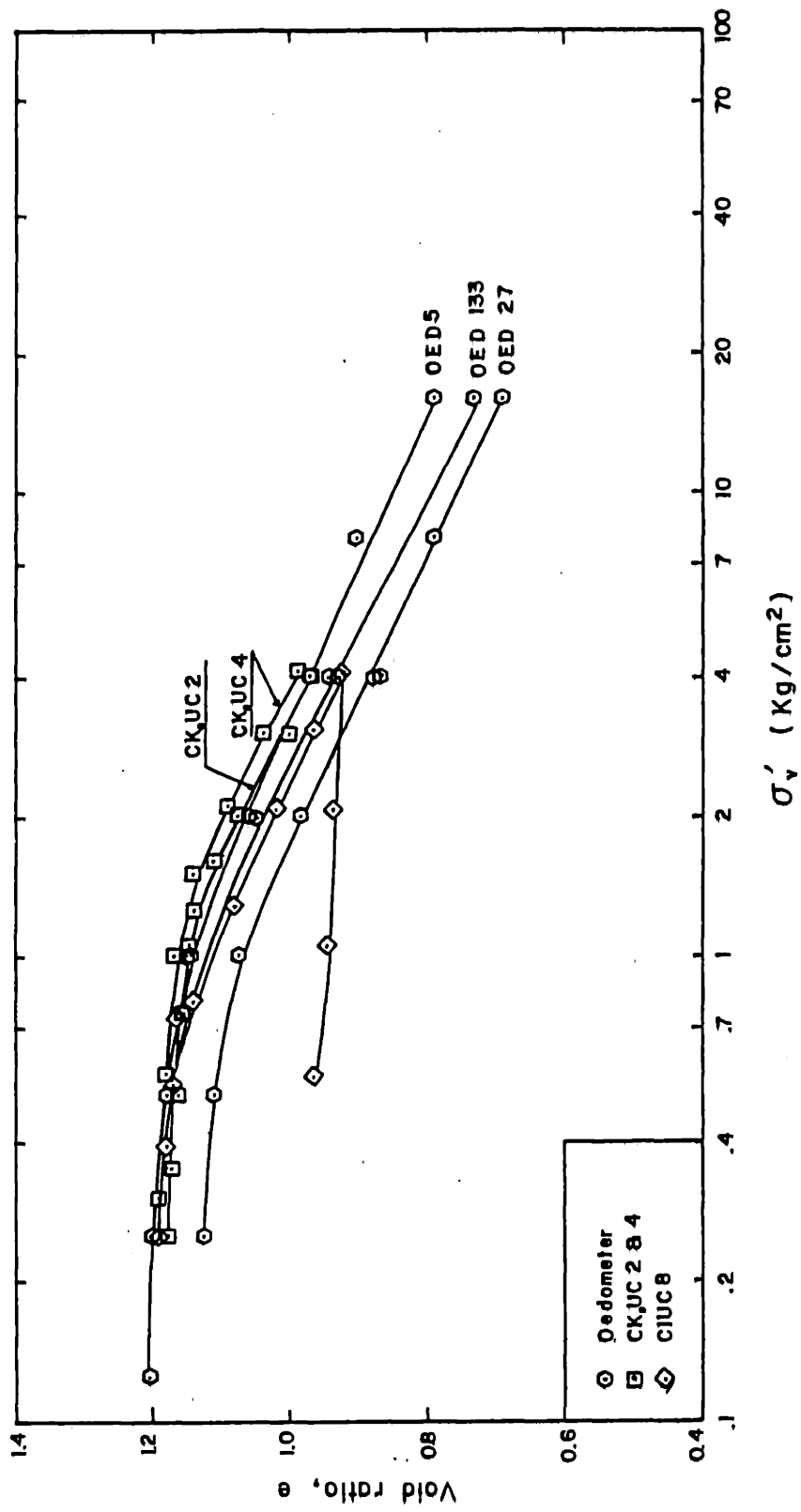


Figure 4.9 Triaxial and oedometer consolidation characteristics for Batch 113

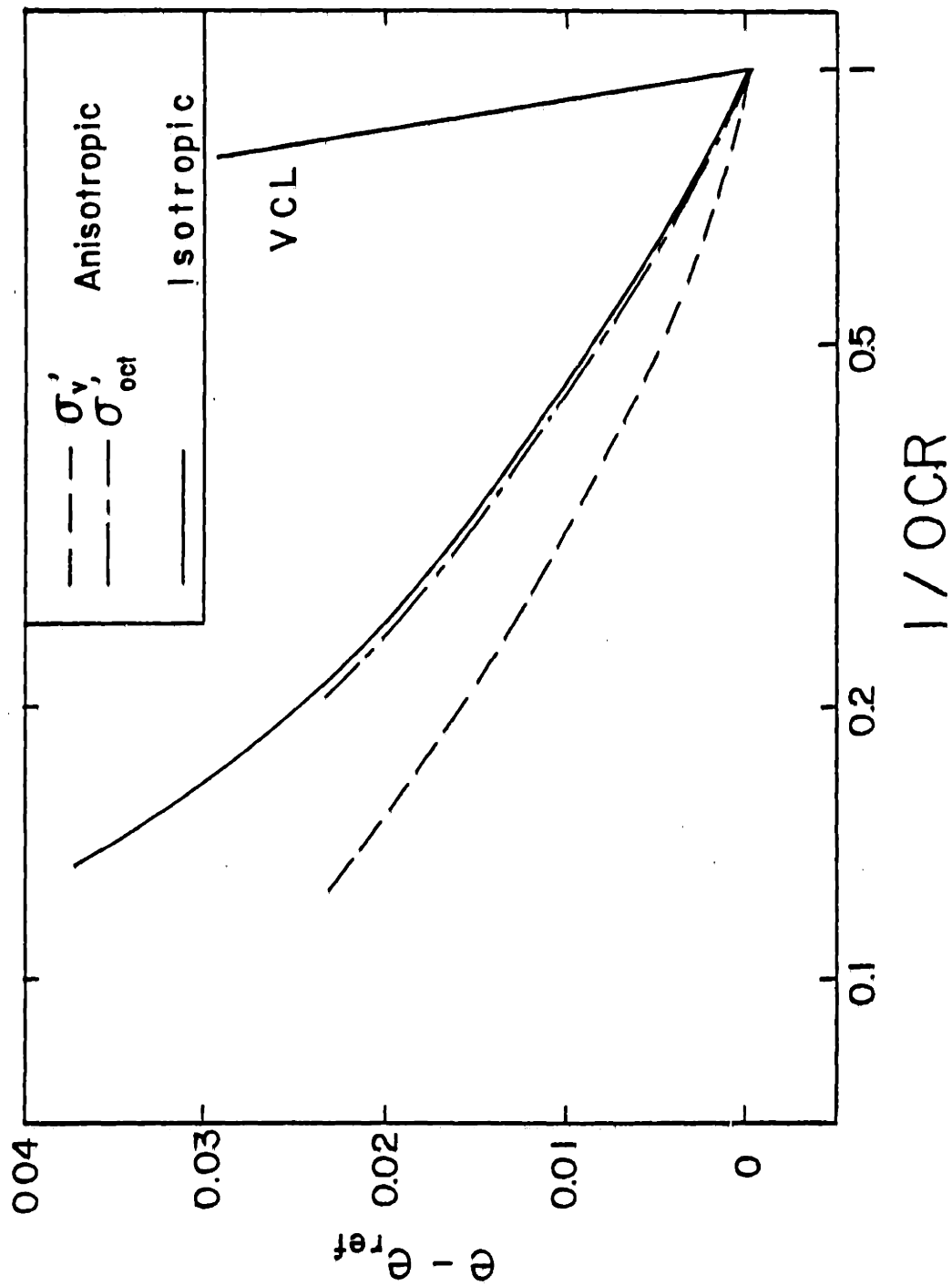


Figure 4.10 Isotropic vs anisotropic swelling behavior

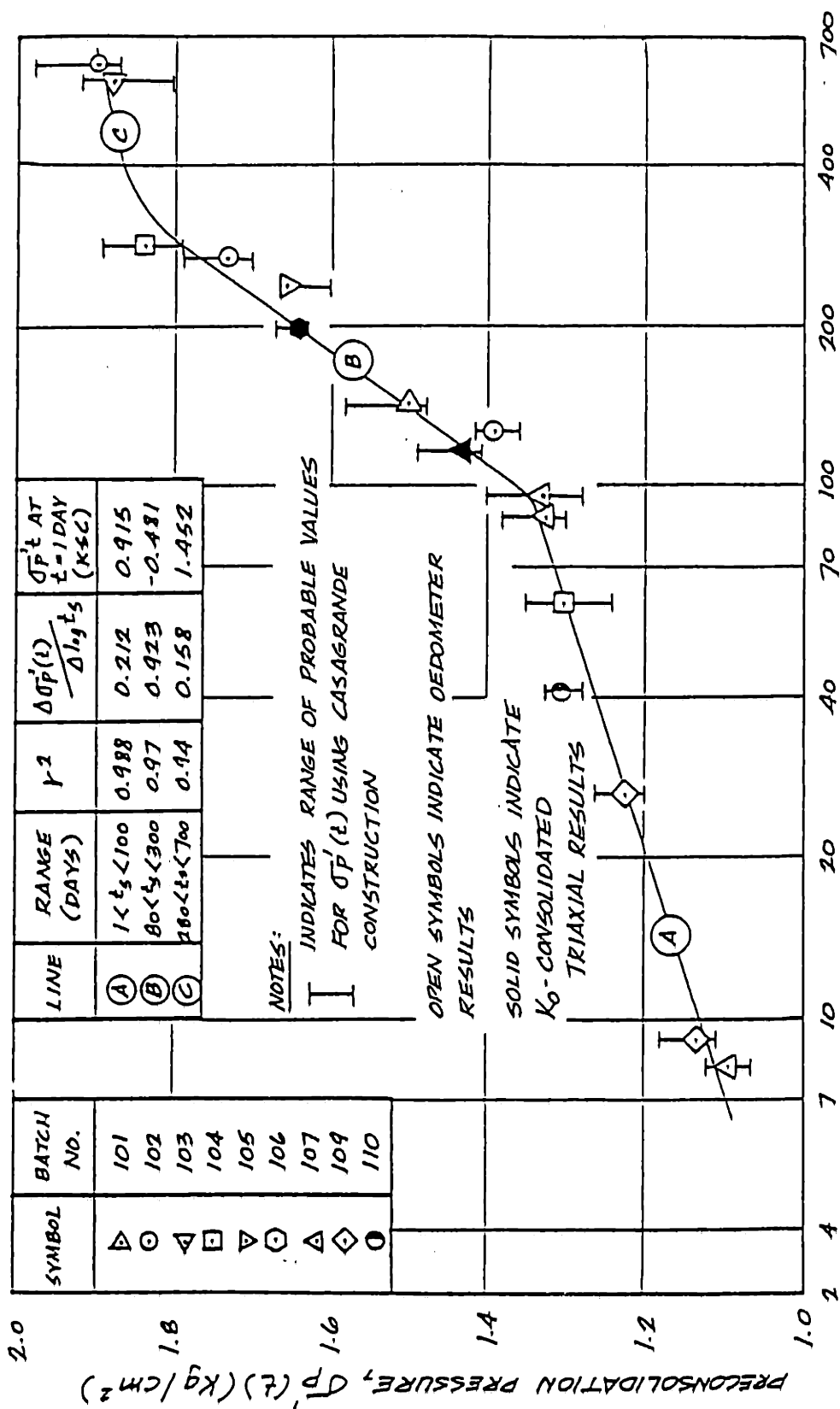


Figure 4.11 Effect of thixotropy on preconsolidation pressure (from O'Neil, 1985)

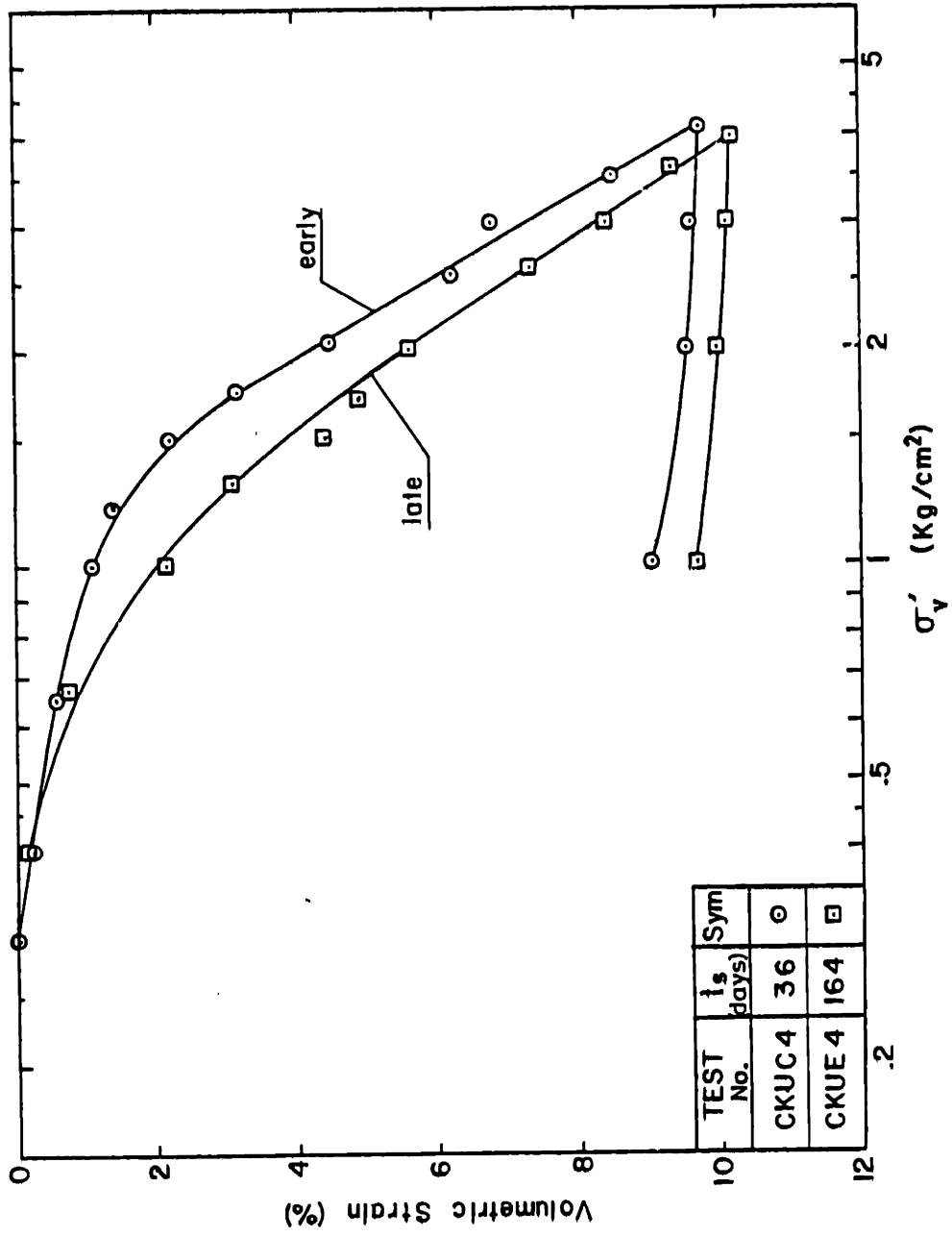


Figure 4.12 Effect of thixotropy on K_0

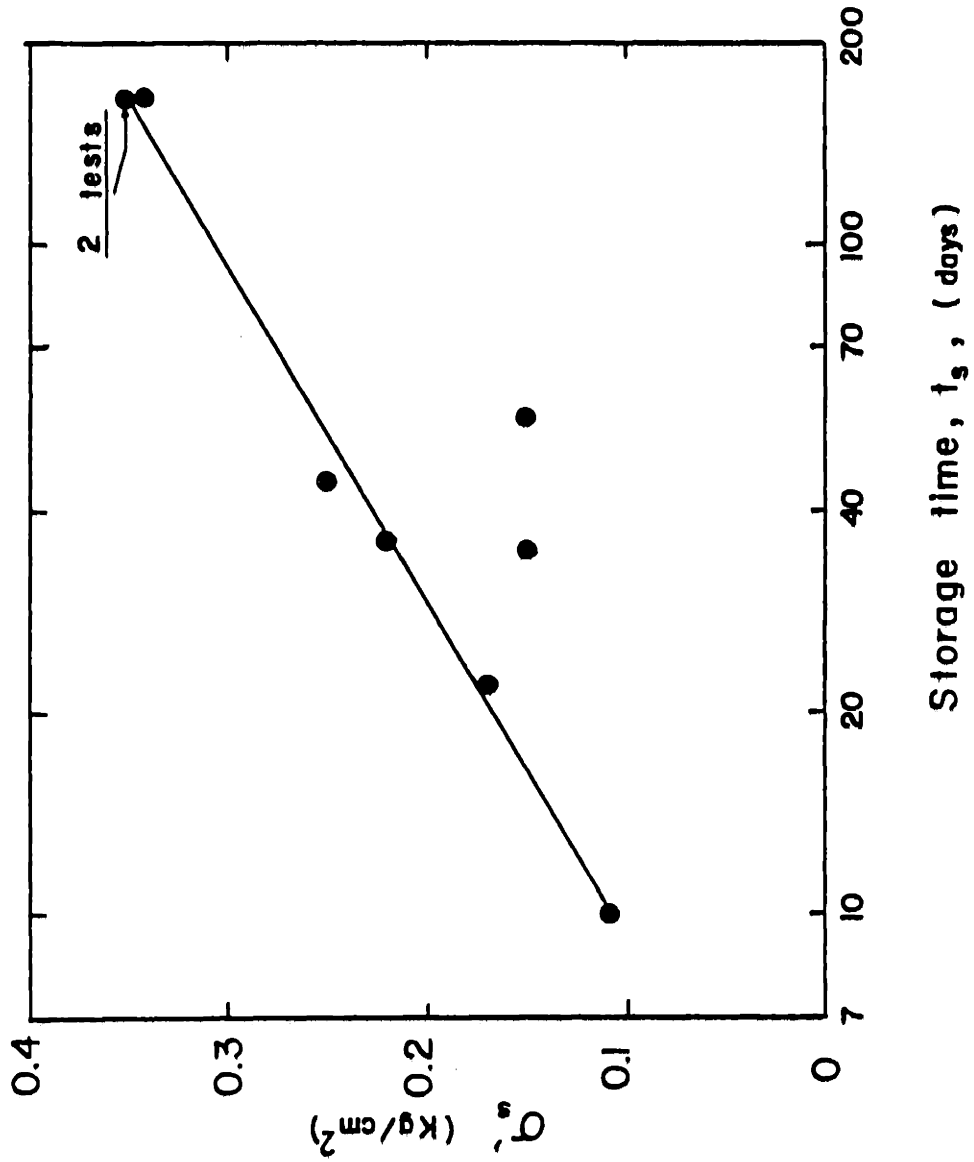


Figure 4.13 Effect of thixotropy on the initial vertical effective stress

CHAPTER 5

UNDRAINED BEHAVIOR

5.1 Test Results

The undrained behavior of resedimented Boston Blue Clay (BBC) has been determined from triaxial compression and extension tests on samples K_0 -consolidated at OCR's of 1, 2, 4 and 8 and on one isotropically consolidated compression test at an OCR of 8. Results are presented in Table 5.1 and the detailed data can be found in Appendix 3. All samples involved reconsolidation to a vertical effective stress, $\sigma'_{vm}=4 \text{ kg/cm}^2$, in excess of at least 1.5 times the preconsolidation pressure, σ'_p of the cakes. This was done in order to reduce uncertainties due to σ'_p , achieve good control of the stress history, and comply with the SHANSEP* methodology developed at MIT (Ladd and Foott, 1974). The high σ'_{vm} was chosen to remove the effects of thixotropy associated with the extended duration of the experimental program. Samples were all sheared in an undrained mode at a constant rate of 0.5% per hour (0.0067 mm/min) considered adequate for sufficient equilibration of excess pore pressures in triaxial samples of BBC. This rate was computed from a theoretical formulation proposed by Gibson and presented by Bishop and Henkel (1962), where 95% equalization of pore pressure would be achieved at a strain increment of 0.25% (Azzouz and Baligh, 1984). The time factor selected, T_{95} was 0.34, based on judgement and experience of soil behavior. The coefficient of consolidation, c_v , was taken to be $3.10^{-3} \text{ cm}^2/\text{sec}$.

5.1.1 Isotropic Test

Only one isotropically consolidated triaxial test was performed, and

* SHANSEP is an acronym for Stress History and Normalized Soil Engineering Properties.

results are shown in Figs. 5.1 through 5.4. In this test the sample was consolidated to a standard vertical effective stress of $\sigma'_{vm}=4 \text{ kg/cm}^2$ as in all tests, and rebound to an OCR of 8.

The effective stress path of the sample during undrained shear is shown in Fig. 5.1, where $q = \frac{\sigma'_v - \sigma'_h}{2}$ and $p' = \frac{\sigma'_v + \sigma'_h}{2}$. At small strains the sample exhibits virtually the same behavior as a linearly elastic isotropic material with a 1:3 slope in the p' - q plot. However, closer examination of Fig. 5.1 indicates a slight tendency of the sample to contract at very small strain levels as evidenced by the positive shear-induced pore pressures. The linear elastic behavior of the sample at small strains can also be observed in the stress-strain curve in Fig. 5.2. At large strains, the sample reaches its peak resistance at an axial strain of 11.5%, indicated by an arrow in Fig. 5.2, followed by a slight reduction in strength. Fig. 5.3 shows the obliquity during the test as expressed by the stress ratio (q/p'). Clearly, the maximum obliquity is reached very early in the test (at an axial strain of 1%), and remains fairly steady at an average value of 0.56. This behavior is consistent with the effective stress path in Fig. 5.1 indicating that the sample follows the failure envelope with a friction angle, $\phi'=34^\circ$. The normalized secant modulus, E/s_u , is plotted in Fig. 5.4 vs. $\log \epsilon_a$, where ϵ_a is the axial strain. The two points A and B in Fig. 5.4 correspond to stress levels $\Delta q/\Delta q_{max}=0.25$ and 0.5, respectively. Δq and Δq_{max} are defined in Fig. 5.5 for values of the stress ratio K larger or smaller than 1. Clearly, the soil stiffness decreases significantly (by a factor of 10) between point A and B. This is a characteristic behavior of highly overconsolidated clays.

5.1.2 Anisotropic Compression tests

Results of compression tests on K_0 -consolidated samples are plotted in Fig. 5.6 through 5.10 for tests CK_0UC1^* , CK_0UC2 , CK_0UC4 , CK_0UC8 . The detailed data can be found in Appendix C.

The effective stress paths are summarized in Fig. 5.6. The stress path of the normally consolidated sample initially deviates to the right then bends over to the left after peak. This behavior is typical of the normally consolidated samples, when the post peak behavior is very stable, i.e. failure zones rather than line failures develop after peak (Lade et al., 1985).

At high OCRs the stress path bends to the right indicating a tendency to dilate. The same trend was observed for the isotropic test $CIUC8$ in Fig. 5.1. The effective stress paths also exhibit a sudden collapse for the overconsolidated samples. This collapse, which manifests itself as a loop in Test CK_0UC2 and as a sudden regression in tests CK_0UC4 and CK_0UC8 could be attributed to the development of failure planes. This behavior is typical of tests run with frictional ends where the samples are not able to reach the critical state point (Rowe et al, 1964). Jardine et al. (1984) claim that the loops are caused by pore pressure measurement errors and Gens (1982) associates them with rate of shear (see also the discussion in Chapter 6 of this thesis).

Strain contours are also drawn in Fig. 5.6. The shaded area shows the zone where strains less than 0.01% were measured. This strain level is considered to represent the limit of measurement precision of the MIT triaxial cells. Burland and Symes (1980) developed internal strain

* Only the first shear will be discussed. For a full presentation of test $CKUC1$, see Chapter 7.

measurement gauges that bring down the measurement precision to 0.001%.

The equal strain contours are slightly concave upwards, but tend to be parallel to the K_0 swelling path and are spaced approximately logarithmically. Similar observations have been made by Parry and Nadarajah (1973), Gens (1982), and Hight et al. (1985). Moreover, the normally consolidated test does not conform to this picture.

In terms of effective stress parameters at peak, Fig. 5.6 yields the following values for the friction angle (ϕ'), and the cohesion (c'):

	ϕ'	c' (kg/cm ²)
NC	26	0
OC	33	0.1

Fig. 5.7 shows the stress-strain data in $q-\epsilon_a$ form for the initial part of the tests, whereas Fig. 5.8 presents the same data up to an axial strain of 14%. The early portion of the stress-strain curves is important since the behavior is non-linear and most of the changes appear at small strains. At large strains the deviator stress does not change very much although a small reduction can still be noticed, but a constant slope (further illustrated in Fig. 5.11) can be seen. Fig. 5.9 shows the same data presented on a semi-logarithmic format. This type of plot emphasizes again the nonlinearity of the early portion of the stress-strain curve. Finally, Fig. 5.10 shows the stress-ratio vs. axial strain for small strains.

A substantial undrained brittleness is observed in the stress-strain curves for the normally and lightly overconsolidated samples. A very well defined peak is noticed followed by a decrease in the deviator stress with increasing strain. This undrained brittleness is a function of OCR as it

decreases with increasing overconsolidation.

The post peak stress-strain relationship of BBC is illustrated in Fig. 5.11 by plotting $(q_{\max}-q)$ vs $(\epsilon_a-\epsilon_{ap})$ where q_{\max} and ϵ_{ap} are the values of the shear stress, q , and the axial strain, ϵ_a , at peak resistance, respectively. The post peak behavior falls in two zones: 1) an initial softening function of OCR; 2) a constant slope starting from a strain of 2%. The limitations of this way of representing the post-peak softening behavior are related to the occurrence of failure planes in the sample. This is especially crucial for high OCR's where the occurrence of failure planes or slip surfaces is expected*. Nevertheless, the trend observed is consistent and is felt to be a good representation of the brittleness susceptibility of a clay. On the other hand, whereas this representation applies better to small OCR's because of their higher brittleness, the obliquity (q/p') is more suitable for high OCR's. Fig. 5.10 illustrates this trend since a highly overconsolidated sample exhibits a better defined peak.

Concentrating on the obliquity values for the ultimate state, as measured at the end of the test in Fig. 5.12, one can observe that they align fairly well on the $q=0.555 p'$ line, which corresponds to an effective friction angle, ϕ'_u , of 33.7° . The ultimate state of test CK₀UC1 (OCR=1) has not been reached because shearing was stopped very early (see Chapter 7 for a full description of the test). The stress ratios for the peak points show a monotonic increase with OCR. The peak friction angle, ϕ'_p , is therefore an increasing function of OCR:

* Although failure planes were observed for all of the overconsolidated samples, their first appearance in the test was not recorded.

OCR	ϕ'_p	ϕ'_u
1	26°	28.7°
2	32.8°	33.6°
4	33.8°	33.4°
8	36.4°	34.4°

The peak axial strains (ϵ_{ap}) are shown versus OCR in Fig. 5.13 where an expected increasing trend is seen with increasing OCR. This plot also highlights the range of strain at which the samples fail. Two orders of magnitude separate the normally consolidated sample (0.07%) from the most highly overconsolidated sample CK₀UC8 (3%). But one should keep in mind the uncertainty related to the definition of ϵ_{ap} for high OCR's (OCR=8 in this case), since the stress-strain curve is much flatter. It is also interesting to notice that, for overconsolidated samples, the maximum obliquity is reached much earlier than peak resistance.

The variation of the pore pressure parameter at failure, A_f , with OCR presented in Fig. 5.14, shows the expected reduction in value as OCR increases.

The soil stiffness depends on OCR (Fig. 5.15) and the strain level (Fig. 5.16). Fig. 5.15 presents the values of the stiffness normalized by the shear strength E/S_u versus OCR at different stress levels, $\Delta q/\Delta q_{max}$, whereas Fig. 5.16 presents a more global picture of E/S_u plotted versus axial strain for all four tests. Contours of stress levels, $\Delta q/\Delta q_{max}$, have been superimposed, and it is clear that test CK₀UC1 does not conform to the same trends.

It is important to realize at this point that for normally and lightly overconsolidated samples, the stiffness is subject to experimental error, the strain level involved being of the same order of magnitude as the

measuring precision.

The variation of stiffness can also be seen in Fig. 5.6 where the distance between the lines of same strain level are readily noticeable. Higher values of stiffness involve larger distances for a same strain increment.

5.1.3 Anisotropic Extension Tests

The results of the extension tests are plotted in Figs. 5.17 through 5.21 for tests CK₀UE2, CK₀UE4 and CK₀UE8. The detailed data can be found in Appendix 3.

The effective stress paths have been drawn in Fig. 5.17, where a common intersection point is apparent. However, it is very plausible that this point has no physical meaning in terms of soil behavior.

Necking was noticed in all three tests run, but the time at which they necked could not be exactly determined because the tests were run overnight and the neck was already well formed in the morning. Test CK₀UE8 is seen to develop very high negative pore pressures, which can be attributed to either an experimental problem or to a failure plane which developed very early in test.

Strain contours are also drawn on this figure and the shaded area, where the strains are less than 0.01%, represents again the zone of uncertainty.

The loops observed for tests CK₀UE2 and CK₀UE4 are a consequence of necking. The computed stress, using a cylindrical area correction, would result in values much lower than the one existing in the sample, because of the large area reduction in the neck.

Figs. 5.18 and 5.19 show the stress strain curves up to 0.8% and 12% strain respectively. Surprisingly, the behavior at large strains

indicates the same ultimate strength $q_{ult} = -0.6 \pm 0.05 \text{ kg/cm}^2$. Moreover, the deviator stress becomes the same for all three tests as early as 1% strain. Fig. 5.20 presents the same type of data on a semi-logarithmic scale. Figs. 5.18 and 5.20, which emphasize the behavior at small strains, do not show any significant trend. There is, also, no sign of undrained brittleness as the deviator stress increases consistently (in absolute value) with increasing strain. At very large strains, the observed softening is a direct consequence of necking and hence does not represent real behavior of the soil.

Fig. 5.21 shows the obliquity-axial strain data and indicates that, at small strains, overconsolidation increases obliquity. This trend is however reversed at large strains. The three curves intersect at the same point which corresponds to the one noticed in the effective stress path (Fig. 5.17).

5.2 Isotropic Behavior of BBC

The isotropic behavior of Boston Blue Clay will be discussed in light of the different investigations presented in Table 5.2. This table includes the initial and final water contents, preshear consolidation stress, OCR and shear data. The time allowed for the last increment, t_c , the batch number, the strain rate during shear and the B parameter, if less than 97%, have been added, when available. The test number seen in the tables corresponds to the one used in the original reference.

The table is divided in four sections, each section representing a reference. These are: Ladd and Varallyay (1965), Braathen (1966), Bailey (1961) and Bensari (1984), whose studies have been summarized in Chapter 2.

The only extension tests available are for normally consolidated BBC

run by Ladd and Varallyay (1965). The following discussion will therefore be based on the compression tests reported by the above mentioned four works. The CIUC data are summarized in Figs. 5.22 through 5.26.

The effective stress paths in Fig. 5.22 are normalized by the maximum consolidation pressure, σ'_{vm} . The scatter observed in the early part of the normally consolidated stress paths is due to different pore pressure responses, which may be explained by the variation in the values of the plasticity index. The higher shear-induced pore pressure exhibited in Ladd and Varallyay's tests can be correlated to the lower clay fraction in the sample as illustrated by the grain size curve in Fig. 2.2. This can, in turn, be related to the significantly lower plasticity index (13%) measured as compared to the typical value of 24% attributed to BBC. However, the undrained strengths of the samples do not seem to be affected by the initial development of pore pressures, as their range of values is very small. On the other hand, the overconsolidated behavior measured by Braathen (1966) is consistent* and agrees very well with test CIUC8 (at an OCR=8). The difference in friction angle at peak strength and at maximum obliquity is small. For the normally consolidated samples, the friction angle is the same for both states and averages about 33°. For overconsolidated samples, $\phi'=35^\circ$ at peak and maximum obliquity.

Ladd and Varallyay's (1965) friction angle at peak was not considered, since the axial strains at peak were smaller than Braathen's (1966) and Bensari's (1984). This increased brittleness was expected because of the

* Test CIUC-P2 of Braathen (1966) is reported to have had a cap seating problem.

lower plasticity index of the samples tested. On the other hand, the stress-strain curves plotted in Fig. 5.23 show a very slight softening, suggesting that the strains measured at peak may well be tainted with error and do not represent therefore peak condition.

The few normally consolidated tests plotted in Fig. 5.23 show a very consistent trend in their effective stress paths. This is not the case for the normalized undrained strength (s_u/σ'_{vc}) for all the available tests. Fig. 5.24 illustrates this scatter. No consistent trends could be established between s_u/σ'_{vc} and the index properties of the clay, nor its pore fluid salt concentration, nor batch preparation. However, a decrease in the ratio with increasing σ'_{vc} can be seen. On the other hand, a consistent increase in s_u/σ'_{vc} with increasing t_c was noted (Fig. 5.25) by Kinner and Ladd (1970). They replotted the same data in such a way as to highlight the effect of t_c (t_c is the time allowed for secondary compression after the last consolidation increment).

An estimate of the quality of the test appears also on Fig. 5.24 where the closed symbols represent a "good" quality test. The "bad" tests are the cyclic ones reported by Braathen for which the first compression cycle was reported in Table 5.2, and Bailey's (1961), for which the batching procedure did not seem to produce uniform, saturated samples.

The average strength ratio calculated from the so-called "good" normally consolidated tests is found to be:

$$\frac{s_u}{\sigma'_{vc}} = 0.286 \pm 0.016 \text{ SD} \quad (\text{Ave of 5 tests})$$

The stress strain curves for overconsolidated samples based on Braathen's (1966) and the author's tests are shown in Fig. 5.25. Compared to normally consolidated samples, the behavior of overconsolidated samples is characterized by:

1) a lower stiffness at smaller strains, i.e., the slope of the stress-strain curves is smaller.

2) an increased axial strain at failure.

3) an increased undrained strength, s_u .

4) an increased obliquity and decrease in the pore pressure parameter, A .

The undrained strength has been normalized by the vertical effective stress, σ'_{vc} , and plotted versus OCR in Fig. 5.26. Bailey's overconsolidated results have also been shown but are erratic and do not fit in Braathen's curve. Furthermore, they will not be considered since they have been judged unreliable.

5.3 Anisotropic Behavior

5.3.1 Compression

The results of the anisotropic tests are found in Table 5.3, organized in the same manner as Table 5.2. The same investigators quoted in section 5.2 will be part of this discussion except for Bailey (1961). These are Ladd and Varallyay (1965), Braathen (1966) and Bensari (1984) who ran normally consolidated tests only. Lutz investigated sampling effects by shearing anisotropically consolidated samples, until an axial strain of 1%. Lutz's six available tests were all normally consolidated, and only one of them was sheared until a strain of 3%. There has been no evidence of overconsolidated tests run according to the SHANSEP procedure (Ladd and Foott, 1974) followed in this research*.

The effective stress paths in Fig. 5.27 are normalized by the maximum consolidation stress, σ'_{vm} . At first glance, the figure reveals some

* Recompression type tests were run by Germaine (1982), Bensari (1984) and O'Neill (1985). They consolidated the samples isotropically to a vertical stress equal to a quarter of the estimated preconsolidation pressure, σ'_p . OCR=4 was chosen because the value of K_0 during unloading was assumed to be around 1.

scatter problems due to Bensari's (1984) and Braathen's (1966) tests. The lower strength measured by Bensari can be explained by the fact that the test was run at 0.27% axial strain per hour and hence at a rate four times slower than Ladd and Varallyay's (1% strain per hour). The increase in strength with strain rate is well established (Richardson and Whitman, 1963). Surprisingly however, the author's normally consolidated test run at a rate of 0.5% strain per hour compares very well with Ladd and Varallyay's. This agreement can be due to compensating factors since the author's test was consolidated along a lower stress ratio path, $K_0=0.47$ versus $K_0=0.53$. On the other hand Braathen's \overline{CK}_0U -Cyc-P14 test gives a much higher strength ($s_u/\sigma'_{vc}=0.364$). Braathen's reported tests were all cyclically loaded, the first compression cycle being presented. The shape of their effective stress paths and the strengths generated could well be linked to testing procedures. On the other hand, Lutz (1985) tests have been stopped at 1% strain; up to that limit, these tests are highly consistent. The effective stress paths are replotted in Fig. 5.28 by showing both Ladd and Varallyay's tests, Lutz's SPTRI-6 which was the only one sheared beyond 3% and the author's. The author's overconsolidated tests are added to illustrate the failure envelope.

For the normally consolidated tests, the variation in the friction angle between the peak and the maximum obliquity condition is in the order of 8° . The tests lead to an average peak friction angle of $\phi'_p=26^\circ$ and a maximum (or ultimate) obliquity one of $\phi'_u=33^\circ$.

It is interesting to note at this point the brittleness of \overline{CK}_0UC1 run by the author, plotted in Fig. 5.29. The axial strain mobilized at peak is

about two times smaller than Lutz's or Ladd and Varallyay's (0.07% vs 0.135%), and the sharp increase in the pore pressure parameter A compared to the other tests indicates the high degree of instability accompanying the anisotropic consolidation.

The normalized strengths (s_u/σ'_{vc}) are averaged and give

$$\frac{s_u}{\sigma'_{vc}} = 0.320 \pm 0.010 \text{ SD} \quad (\text{Ave of 13 tests})$$

The overconsolidated undrained strength ratios are plotted versus OCR in Fig. 5.30, where a similar trend is observed for the isotropically consolidated samples. A discussion of the undrained behavior of the overconsolidated samples has been already presented in section 5.1.2 and will not be repeated here, since no other similar data exists for comparison.

5.3.2 Extension

Available extension tests on anisotropically consolidated samples were run by Ladd and Varallyay (1965) and Bensari (1984) on normally consolidated samples, whereas OCR values of 2, 4 and 8 were also considered in this research. The standard strain rate of shearing was 0.5% strain per hour except for Ladd and Varallyay's who used a rate of 1% strain per hour.

The results of those studies are summarized in the effective stress path space of Fig. 5.31 and in the stress-strain curves presented in Fig. 5.3.2. The normally consolidated tests, although involving some scatter, provide a limit beyond which an undrained effective stress path cannot exist. Test CK₀UE8 violates this rule very clearly and development of negative pore pressures are such that the stress path extends to the right of the normally consolidated tests without variation in the shearing

resistance. The negative pore pressure reaches a value of about 2 to 3 times the maximum shear strength of the sample. Therefore, considering the possibility of an experimental mishap, and based on the preceding observations, test CK₀UE8 appears to be unreliable and will be disregarded.

It is well known that a sample of clay sheared in extension involves a weak link structure because "the tendency to dilate during shear aggravates initial nonuniformities of density" (Lade et al., 1985). A "line failure" will develop very easily in the test and will mask the real behavior of the soil. This "line failure" is generally followed by the progressive formation of a "neck." Once the neck is apparent, computations of stresses and strains are questionable and results should be discarded. For this reason it is important to detect neck formation during the test. The dots in the effective stress paths of Fig. 5.31 correspond to necking observed by Ladd and Varallyay's tests. In spite of necking, an increase in shear resistance takes place in their tests leading to a very high value of the friction angle at peak, $\phi'_p = 37.8 \pm 1.6$.

It is worthwhile to note that with the choice of failure envelope, $\phi' = 31^\circ$ in Fig. 5.31, the various paths seem to converge toward a common point on this line. This implies the existence of a critical state point (Whittle, pers. com.) for BBC in extension.

The normalized undrained strength, s_u/σ'_{vc} , and the pore pressure parameter at failure, A_f , are plotted in Figs. 5.33 and 5.34 respectively. The dashed part of the curves corresponds to the unreliable results of tests CK₀UE8. The parameters (A_f and s_u/σ'_{vc}) plotted correspond to the point of intersection of the test in consideration and the assumed failure line traced in Fig. 5.31.

5.3.3 Compression vs. Extension

For isotropically consolidated samples, the variation in the intermediate principal effective stress as expressed by the coefficient b^* and the inherent anisotropy account for the difference between compression and extension. This, however, must be compounded with the effect of the stress induced anisotropy in the case of anisotropically consolidated samples. References to the isotropically consolidated samples will be recalled for comparative purposes, whenever the separation of the effect of the two blocks of variables is possible.

The value of the friction angle ϕ'^{**} , observed in extension on CKUE samples, $\phi'=38^\circ$, is significantly higher than that observed at the ultimate state in compression tests ($\phi'=33^\circ$) on a normally consolidated sample. This difference (here 5°) was noticed by other investigators on various clays with various relationships: 7.2° on Spestone Kaolin (Parry and Nadarajah, 1973), 1.6° on Lower Cromer Till (Gens, 1982), 2.1° on Hokkaido clay (Mitachi and Kitago, 1980), 2.5° on Marine clay (Koutsoftas, 1981), 0° on Drammen clay (Anderson et al., 1980), and 11° on AGS clay (Koutsoftas and Ladd, 1985).

The undrained strength ratio, s_u/σ'_{vc} , is plotted versus OCR in Fig. 5.35, where results of the isotropic tests have been superimposed. A significant increase in strength is observed when comparing compression to extension. This variation seems to be mainly related to the change in the value of b , since the undrained strengths of the isotropic tests are very close to the anisotropic ones. The curves showing the pore pressure

* $b = \frac{\sigma_2 - \sigma_3}{\sigma_1 - \sigma_3}$	compression	$\sigma_2 = \sigma_3$; $b = 0$
	extension	$\sigma_2 = \sigma_1$; $b = 1$

** The friction angle quoted for extension tests corresponds to the time at which "necking" is detected, or to the maximum deviator stress, if the time to peak is not recorded.

parameter at failure, A_f , are drawn for reference in Fig. 5.36. A_f is seen to be lower for compression and decreases with OCR. The same trend was observed by Parry and Nadarajah (1973), Gens (1982), Koutsoftas (1981), and Koutsoftas and Ladd (1985).

The stiffness in terms of E/s_u is plotted versus OCR in Fig. 5.37, at a stress level, $\Delta q/\Delta q_{max}$, of 50%. The samples in compression are seen to be very much stiffer than in extension for CK_{OU} tests and do not follow the same pattern.

5.4 COMPARISON OF ISOTROPICALLY AND ANISOTROPICALLY CONSOLIDATED SAMPLES

This discussion is limited to the compression tests, since it is the only complete series covering the overconsolidated domain.

The effective stress paths summarized in Fig. 5.38, for the isotropic and anisotropic cases, show the same friction angle when peak conditions are considered. A comparison based on the ultimate conditions as recommended by Gens (1982), may not be appropriate in this case, since the development of failure planes is very likely to occur, negating the uniformity of the sample at large strains. The use of frictionless ends is imperative, if ultimate conditions are to be considered. Fig. 5.39 demonstrates the inadequacy of the ultimate state where the undrained shear strength at the peak and ultimate states have been plotted versus water content. No consistent trend is detected for the ultimate strength for either the isotropically or the anisotropically consolidated samples.

The peak undrained strengths are compared in Fig. 5.40, plotted versus the vertical consolidation stress, σ'_{vc} . From the figure it is obvious that the undrained strength, s_u , of the OC clay is much higher than that of the NC clay at the same consolidation pressure, σ'_{vc} , the difference being larger for the isotropically consolidated samples. The strength data have

been normalized by the corresponding normally consolidated strength and plotted versus OCR in Fig. 5.41. A marked similarity in the shape of the curves is found between isotropically and anisotropically consolidated samples. When the data are plotted on a log-log scale, as in Fig. 5.42, they fall along a straight line. The expression describing the curve in Fig. 5.41 is therefore of the form,

$$\frac{(s_u/\sigma'_{vc})(OC)}{(s_u/\sigma'_{vc})(NC)} = OCR^m$$

where m is the slope of the line in Fig. 5.42. An average value of 0.79 is found for m , in agreement with Ladd and Edgers' (1972) data from CK_{OU} Direct-Simple-Shear tests. The increase in undrained strength with OCR is primarily correlated with the sharp decrease in the pore pressure parameter at peak, A_f , as illustrated by the data in Fig. 5.43.

The normalized stiffness, E/σ'_{vc} , is shown in Fig. 5.44 versus OCR at a stress level ($\Delta q/\Delta q_{max}$) of 50%. The same type of behavior has been observed when comparing compression to extension data, a much higher stiffness for anisotropically consolidated samples and a different variation with OCR being observed.

5.5 Concluding Remarks

Although CIUE tests on overconsolidated BBC are not available, available data enable important conclusions to be drawn with regards to the undrained behavior of Boston Blue Clay. Compared to triaxial extension shearing, results of undrained compression tests on anisotropically consolidated samples show the following:

- 1) The ultimate friction angle is decreased by 5° for NC samples, the exact difference being more difficult to measure for OC samples,
- 2) The undrained strength almost doubled,

- 3) The excess pore pressure is much lower for small OCR's. This decrease is believed to be the main factor that causes the increase in strength, and
- 4) The stress-strain modulus ($\Delta q/\Delta q_{\max}=50\%$) is substantially increased, and a different pattern of variation is observed with OCR.

On the other hand, comparing results of anisotropically consolidated tests with isotropically consolidated tests during undrained compression shearing, anisotropic consolidation has the following effects:

- 1) Maintains the same effective stress envelope for peak conditions (except for OCR=1), whereas the ultimate state is altered by the occurrence of failure planes.
- 2) Increases the undrained shear strength by 12% for all OCR's. The normalized strength is consistent, and is not affected by the consolidation mode, (best seen in Fig. 5.41)
- 3) Decreases the pore pressure parameter at failure, A_f , substantially. The difference is more accentuated at small OCR's.
- 4) Decreases the peak axial strain by an amount difficult to estimate because of the flatness of the stress strain curves.
- 5) A direct consequence is the large increase in stiffness. The pattern of variation with OCR is also different.

Table 5.1

SUMMARY OF SHEAR DATA FOR TRIAXIAL TESTS

Test #	Water Content		Preshear		Fail mode	At maximum q				At maximum obliquity				$\frac{E_u(50)}{q_f}$	$\frac{G_f}{\sigma'_{vc}}$	R _f	
	Initial %	Final %	σ'_p (ksc)	σ'_{vc} (ksc)		K	ϵ_a %	$\frac{q}{\sigma'_{vc}}$	$\frac{p'}{\sigma'_{vc}}$	ϕ'	A_p	ϵ_a %	$\frac{q}{\sigma'_{vc}}$				$\frac{p'}{\sigma'_{vc}}$
CK ₀ UC1	43.8	35.7	4.08	4.0	0.47	C	0.066	0.334	0.740	25.9	0.321						
	35.7	32.8	6.04	6.2	0.34	C	0.053	0.365	0.667	32.6	0.040				136.6		
CK ₀ UC2	44.5	34.9	4.09	2.00	0.63	C	0.265	0.623	1.148	32.9	0.238	0.165	0.599	33.6	1516.3	52.5	1.62
						E	4.167	-0.198	0.224	-61.8	1.539	S A H E					
CK ₀ UC4	42.5	35.3	4.10	1.01	0.82	C	1.064	1.049	1.878	33.9	0.018	0.417	0.936	36.0	743.3	233	1.22
						E	-3.715	-0.445	0.621	-45.7	0.596	S A H E					
CK ₀ UC8	43.7	35.6	4.10	0.51	1.10	C	2.970	1.749	2.939	36.5	-0.053	0.597	1.312	40.8	399.6	3764	1.09
						E	-3.585	-0.916	0.984	-68.5	0.094	S A H E					
CK ₀ UE2	43.7	36.5	4.01	2.00	0.63	E	-10.803	-0.312	0.333	-69.3	0.463	-10.143	-0.308	-71.8	-699.7	134	1.05
CK ₀ UE4	43.2	35.7	3.98	1.00	0.83	E	-8.994	-0.623	1.033	-37.1	-0.084	-7.744	-0.611	-39.4	-235.9	84.5	.997
CK ₀ UE8	43.2	35.5	4.00	0.49	1.07	E	-10.091	-1.367	3.257	-24.6	-1.662	-4.728	-1.082	-29.2	-69.1	66.3	.909
CIUC8	41.2	34.0	4.04	0.54	0.88	C	11.517	1.650	2.907	34.6	-0.22	6.908	1.583	35.2	246.6	363	.995

Table 5.2 o

SUMMARY SHEAR
ISOTROPICALLY CONSOLIDATED SAMPLES

Test #	(1) t_c (days)	Water Content (%)		Consolidation		at $(\sigma_1 - \sigma_3)_{max}$						at $(\sigma_1 / \sigma_3)_{max}$				Batch	Remarks: + Investigators + Strain Rate (2)
		Initial	Final	σ'_{vc} k _{sc}	OCR	ϵ %	$\frac{q}{\sigma'_{vc}}$	$\frac{p'}{\sigma'_{vc}}$	Δf	$\phi' p$	$\frac{\epsilon}{\lambda}$	$\frac{q}{\sigma'_{vc}}$	$\frac{p'}{\sigma'_{vc}}$	$\frac{p'}{\sigma'_{vc}}$	ϕ'		
CIUC-1	3	30.40	23.45	6	1	3.5	0.263	0.541	1.37	29.0	10.1	0.250	0.455	33.3	Ladd and Varallyay (1965) neck @ 6.4Z		
CIUC-2	4	31.40	25.40	4	1	2.8	0.308	0.645	1.08	28.5	10.7	0.289	0.521	33.6			
CIUC-3	3	31.50	23.0	8	1	3.8	0.287	0.557	1.27	31.0	10.4	0.280	0.503	34.0			
CIUC-2	23	30.90	23.75	4	1	1.0	0.264	0.579	1.30	27.1	6.1	0.256	0.399	40.0			
CIUC-3	6	29.00	21.60	6	1	7.7	0.235	0.367	1.85	39.9	7.7	0.235	0.367	39.9			
CIUC-1	3	42.00	31.6	6	1	9.54	0.283	0.523	1.35	32.7	NOT REACHED	REACHED	REACHED	SI/S2		Preston (1965) Braathen (1966) $\epsilon = 0.012$ mm/min 1st cycle compression	
CIUC-2	2	42.1	32.0	2.9	2	13.8	0.483	0.901	0.67	32.4	NOT REACHED	REACHED	REACHED	SI/S2			
CIUC-3	2	41.7	32.7	1.5	4	9.08	0.899	1.554	0.20	25.3	9.08	0.899	1.554	35.3			
CIUC-4	2	42.5	33.0	7.4	8	14.0	1.595	2.676	-0.34	26.6	14.0	1.595	2.676	36.6			
CIUC-2	NA	38.5	30.0	6	1	4.45	0.331	0.624	1.07	32.0	NOT REACHED	REACHED	REACHED	S3			
CIUC-Cyc-E-P9	2	42.6	31.1	6	1	3.04	0.340	0.658	1.00	31.1	3.04	0.340	0.658	31.1			
CIUC-Cyc-E-P10	2	42.4	31.1	6	1	1.78	0.324	0.697	0.97	27.7	1.78	0.324	0.697	27.7			
CIUC-Cyc-E-P20	NA	38.4	30.7	6	1	3.60	0.308	0.588	1.17	31.5	3.60	0.308	0.588	31.5			
CIUC	NA	41.9	31.3	3	1	14.0	0.288	0.527	1.32	33.1	11.6	0.286	0.521	33.3	Bensari (1984) $0.5Z/hr, t_c = 196$ days		
W-1	5	26.9	20.6	6	1	2.10	0.293	0.725	0.97	23.9	8.4	0.280	0.567	29.6	Bailey (1961) B? $\epsilon = 0.015$ mm/min B? $\epsilon = 0.013$ mm/min B? $\epsilon = 0.015$ mm/min B? $\epsilon = 0.015$ mm/min		
W-2	6	25.4	22.2	3	1	2.10	0.337	0.793	0.81	25.1	8.3	0.300	0.623	28.8			
W-3	4	25.3	20.5	6	1	2.4	0.297	0.722	0.97	24.3	7.4	0.297	0.625	28.3			
W-4	3	25.6	23.6	2	1	1.4	0.330	0.825	0.77	23.6	7.3	0.275	0.560	29.4			
W-5	4	26.0	22.0	4	1	1.9	0.283	0.708	1.02	23.5	8.6	0.265	0.533	29.8			
W-7	46	24.8	22.03	3	1	1.9	0.393	0.870	0.66	26.9	6.7	0.367	0.737	29.9			
W-8	2	25.7	22.3	3	1	2.6	0.347	0.770	0.83	26.8	5.7	0.347	0.710	29.2			
W-9	5	25.1	22.03	4	1	2.2	0.252	0.710	0.99	24.8	6.5	0.293	0.603	29.0			
W-10	3	25.1	21.7	1	6	7.3	1.080	2.150	-0.33	30.2	7.3	1.080	2.150	30.2			
W-11	4	25.2	22.6	0.5	12	4.3	1.480	2.840	-1.22	31.4	3.8	1.440	2.740	31.7			
W-12	3	25.1	22.9	0.25	24	10.0	2.00	3.920	-0.23	30.7	1.9	1.280	2.320	33.5			

Table 5.2 b

SUMMARY SHEAR
ISOTROPICALLY CONSOLIDATED SAMPLES

Test #	(1) t_c (days)	Water Content (%)		Consolidation σ'_{vc} ksc	OCR	at $(\sigma_1 - \sigma_3)_{max}$				at $(\sigma_1 / \sigma_3)_{max}$				Batch	Remarks: + Investigators + Strain Rate (2)
		Initial	Final			ϵ %	$\frac{q}{\sigma'_{vc}}$	$\frac{p'}{\sigma'_{vc}}$	A_f	$\phi' p$	ϵ %	$\frac{q}{\sigma'_{vc}}$	$\frac{p'}{\sigma'_{vc}}$		
S-1	7	28.60	25.8	2	1	1.8	0.355	0.800	0.78	26.3	7.0	0.350	0.660		Bailey (1961) B-96Z B-86Z B-68Z
S-2	4	29.00	23.9	4	1	2.2	0.303	0.678	1.03	26.5	8.3	0.300	0.563		
S-3	2	28.10	22.9	6	1	2.1	0.293	0.688	1.04	25.1	8.0	0.300	0.582		
S-4	3	28.40	25.1	3	1	2.5	0.337	0.723	0.91	27.7	7.4	0.333	0.647		
S-5	3	28.80	24.25	1	6	10.5	1.120	2.180	-0.027	27.3	10.5	1.120	2.180		
S-6	2	29.0	24.6	0.5	12	9.0	1.780	3.280	-0.14	32.9	2.1	1.220	2.180		
S-8	2	29.1	23.9	1	6	7.8	1.120	2.120	-0.022	31.9	7.8	1.120	2.120		
S-9	6	29.3	25.0	3	1	2.1	0.313	0.697	0.99	26.7	8.0	0.310	0.587		
S-10	46	29.2	24.6	3	1	1.9	0.337	0.743	0.88	26.9	8.0	0.327	0.613		

(1) t_c - time allowed for secondary compression under the last load increment (days)

(2) $\dot{\epsilon}$ - strain rates, unless otherwise noted, are:
Ladd and Varallyay (1965) 1%/hr \cong 0.013 mm/min
Branthen (66), Preston (65) 1%/hr \cong 0.013 mm/min
Bailey (61) 0.7%/hr \cong 0.009 mm/min

(3) t_s - storage time (days)

(4) B = $\Delta u / \Delta \sigma_v$ Skempton parameter, noted if less than 97%

4

1

1

Table 5.3

SUMMARY SHEAR DATA FOR ANISOTROPICALLY CONSOLIDATED SAMPLES OF BBC

Test #	t_c (1) (days)	Water Content		Consolidation σ'_{vc} (kN/c)	$\bar{\alpha}$	at $(\sigma_1 - \sigma_3)_{max}$						at $(\sigma'_1 / \sigma'_3)_{max}$			Batch	Remarks: + Investigators + Strain Rate (2)	
		Initial	Final			ϵ %	$\frac{q}{\sigma'_{vc}}$	$\frac{p'}{\sigma'_{vc}}$	A_f	ϕ'	ϵ %	$\frac{q}{\sigma'_{vc}}$	$\frac{p'}{\sigma'_{vc}}$	ϕ'			
CK ₀ UC-1	6	31.2	25.9	4	.53	1	0.3	0.329	0.742	0.62	26.4	9.2	0.224	0.420	32.3	Ladd and Varallyay	
CK ₀ UC-3	8	29.7	23.3	6	.54	1	0.3	0.328	0.761	0.54	25.5	6.4	0.237	0.412	35.1		
CK ₀ URE-4	6	30.5	26.0	4	.54	1	10.0	0.165	0.260	1.14	39.4	9.7	0.163	0.255	39.6		
CK ₀ URE-5	4	30.8	23.1	6	.54	1	10.0	0.143	0.243	1.21	36.0	10.0	0.143	0.243	36.0	neck @ $\epsilon=6\%$ neck @ $\epsilon=7.2\%$	
CK ₀ U-Cyc-EP14	2	42.8	33.8	5.5	.5	1	0.37	0.364	0.778	0.53	27.9	NOT REACHED	NOT REACHED	NOT REACHED	SI/S2		Braathen (1966) Preston (1965) 1st cycle compression
CK ₀ U-Cyc-EP15	2	42.9	33.5	6	.5	1	0.43	0.322	0.699	0.85	27.4	NOT REACHED	NOT REACHED	NOT REACHED	SI/S2		
CK ₀ U-Cyc-EP16	2	41.5	32.1	6	.5	1	0.35	0.334	0.723	0.67	27.5	NOT REACHED	NOT REACHED	NOT REACHED	SI/S2		
CK ₀ U-P8	2	42.3	32.9	6	.5	1	0.44	0.328	0.690	0.62	28.4	NOT REACHED	NOT REACHED	NOT REACHED	SI/S2		
CK ₀ UC(NC)	NA	40.8	35.4	2.4	.55	1	0.2	0.290	0.720	0.90	23.7	12.6	0.261	0.476	33.3	110 110	$\epsilon=0.27\%/hr$ $t_g=30$ days(3) $t_g=52$ days Bensari (1984)
CK ₀ UE(NC)	NA	41.1	35.9	2.1	.51	1											
CK ₀ U(C)-1	NA	NA	NA	4		1	.38	0.315	0.719	0.75	26.0	NOT REACHED	NOT REACHED	NOT REACHED		Dickey et al. (1968)	
SPTRI-1	NA	NA	NA	4		1	.109	0.321	0.738	0.52	25.8					Lutz (1985)	
SPTRI-2	NA	NA	NA	3		1	.273	0.320	0.728	0.61	26.1						
SPTRI-3	NA	NA	NA	3		1	.135	0.322	0.749	0.45	25.5						
SPTRI-4A	NA	NA	NA	3		1	.127	0.318	0.712	0.76	26.5						
SPTRI-5A	NA	NA	NA	3		1	.103	0.320	0.717	0.69	26.5						
SPTRI-6	NA	NA	NA	3		1	.226	0.314	0.712	0.75	26.2						

(1) t_c -time allowed for secondary compression under the last load increment (days)(2) $\dot{\epsilon}$ strain rates, unless otherwise noted, are:Ladd and Varallyay (1965) 1Z/hr \equiv 0.013 mm/minBraathen (66), Preston (65) 1Z/hr \equiv 0.013 mm/minBensari (84), Lutz (85) 0.5Z/hr \equiv 0.007 mm/minDickey et al. (1968) 1Z/hr \equiv 0.013 mm/min(3) t_g -storage time (days)

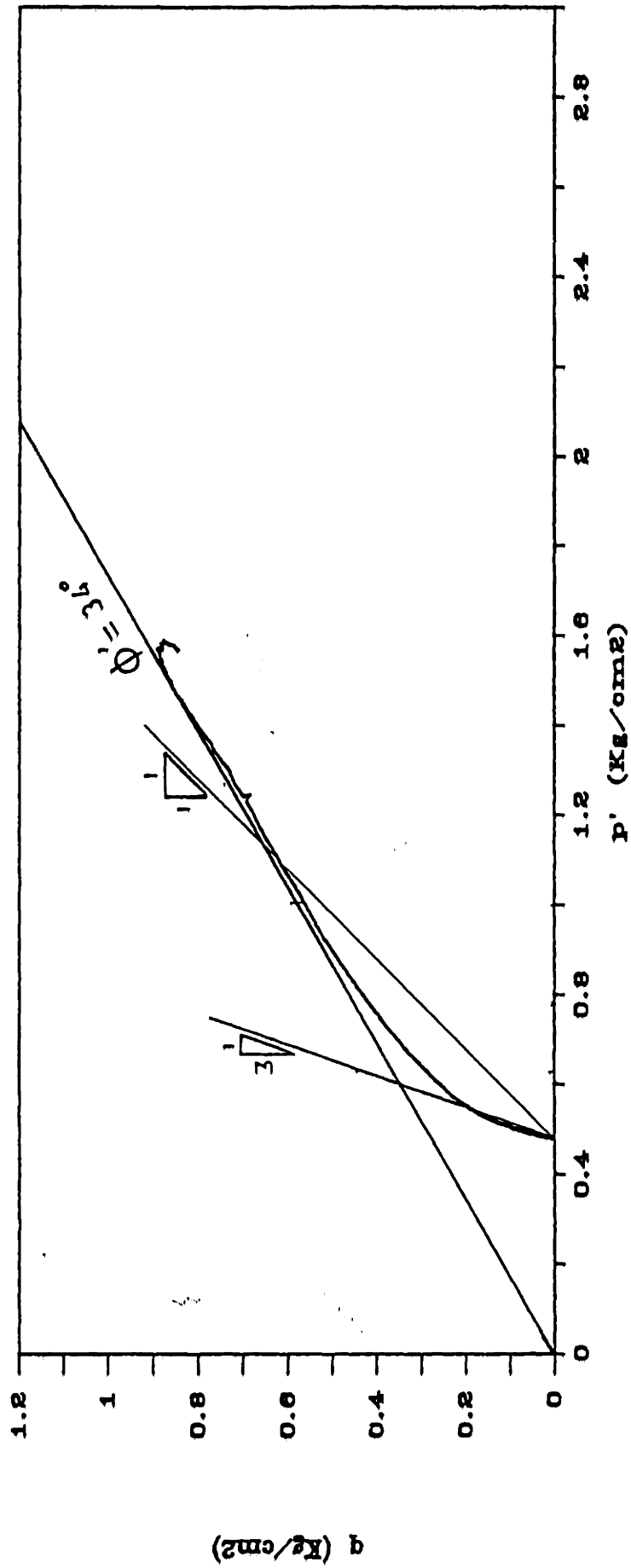


Figure 5.1 Stress path for CIUC8 test

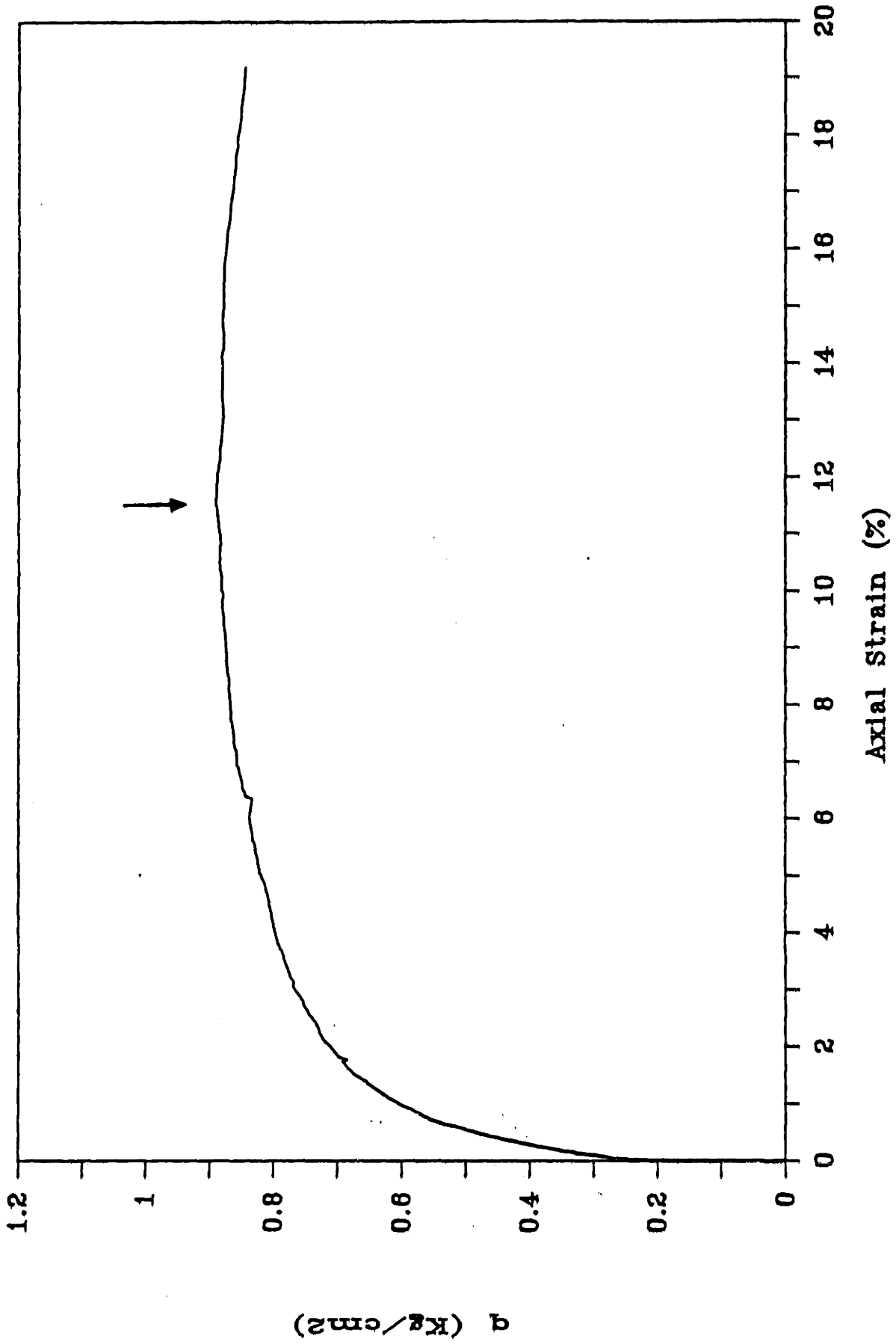


Figure 5.2 Stress-strain for CIUC8 test

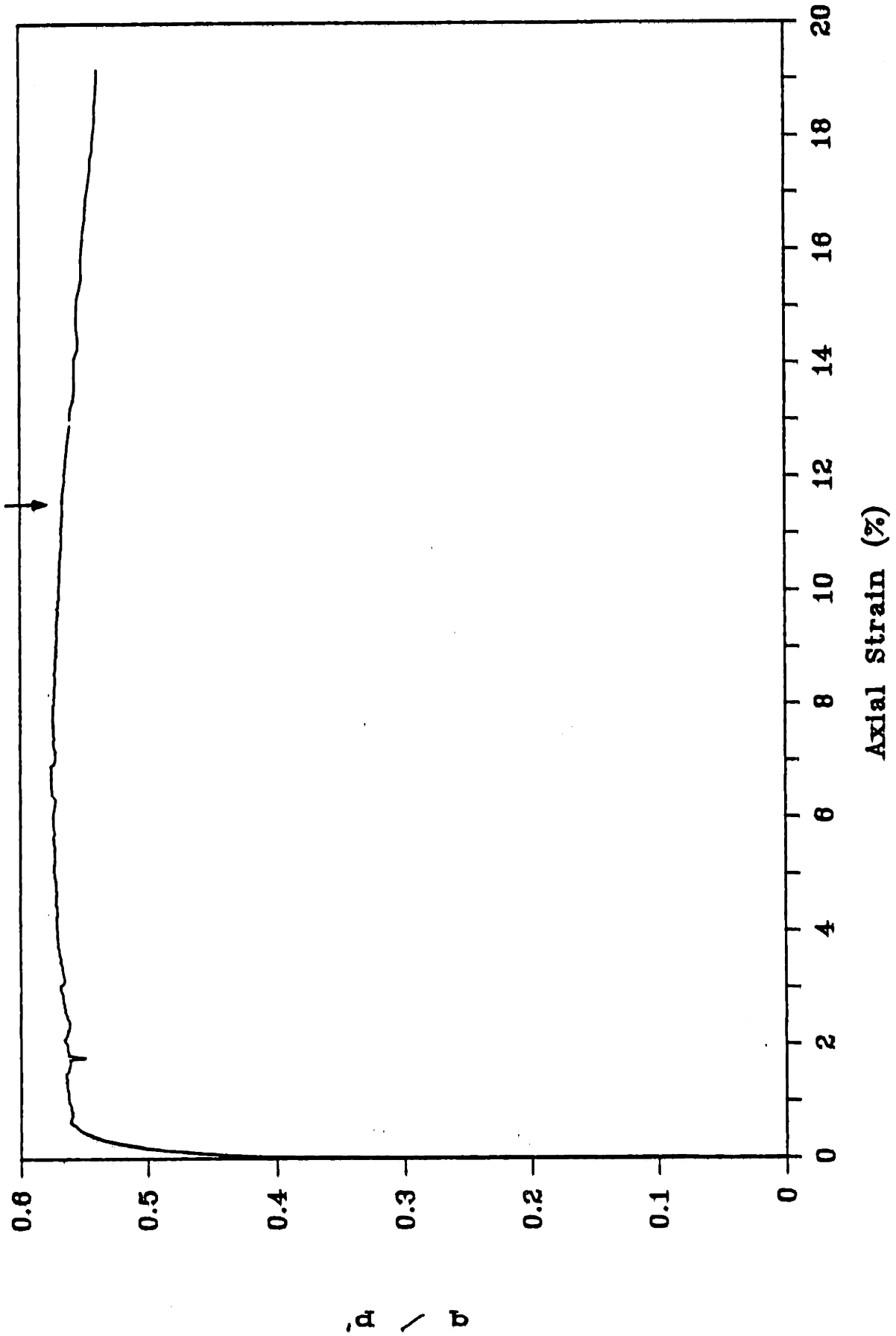


Figure 5.3 Oblliquity-axial strain for CIUC8 test

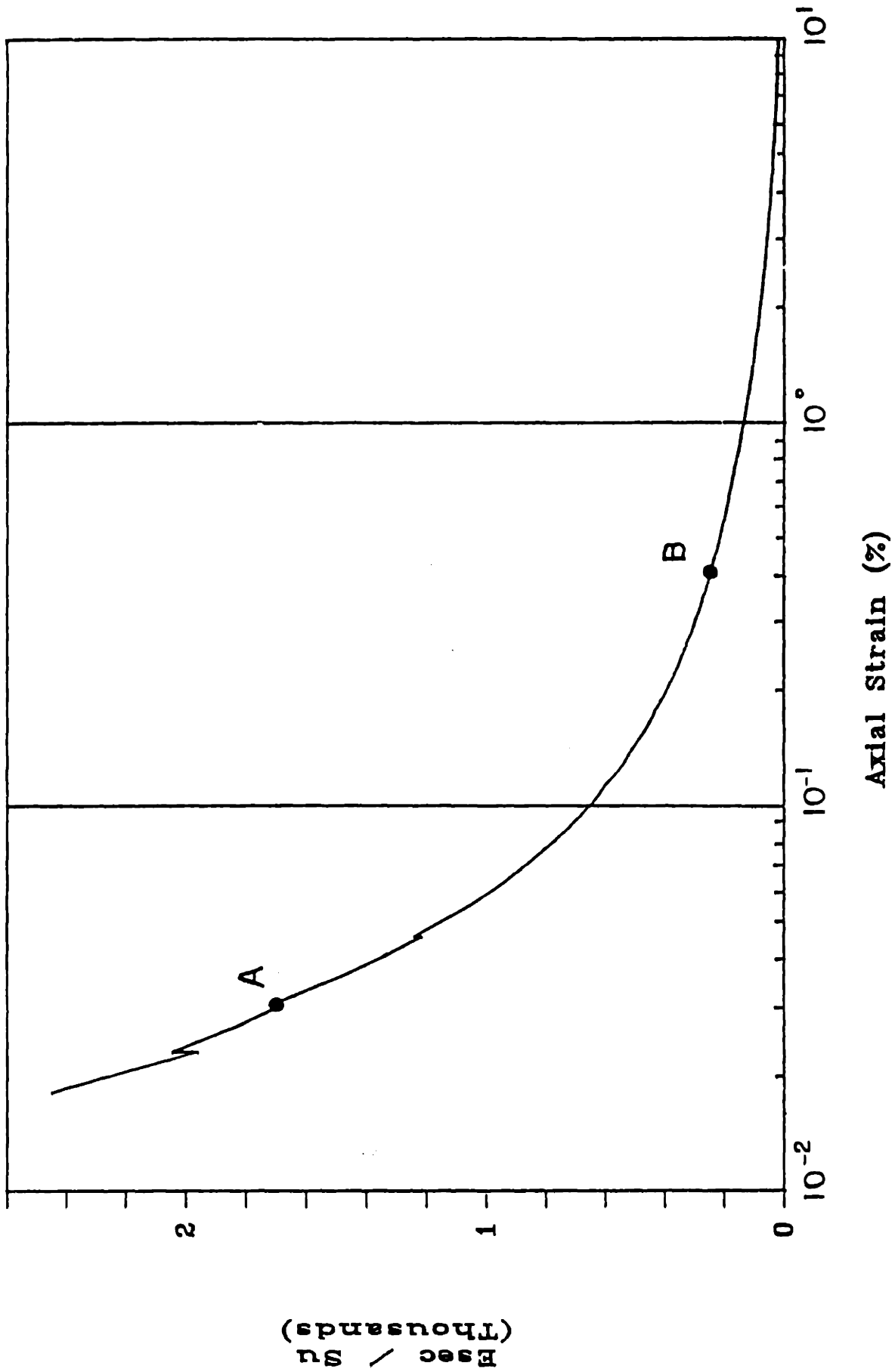


Figure 5.4 Normalized modulus-axial strain for CIUC8 test

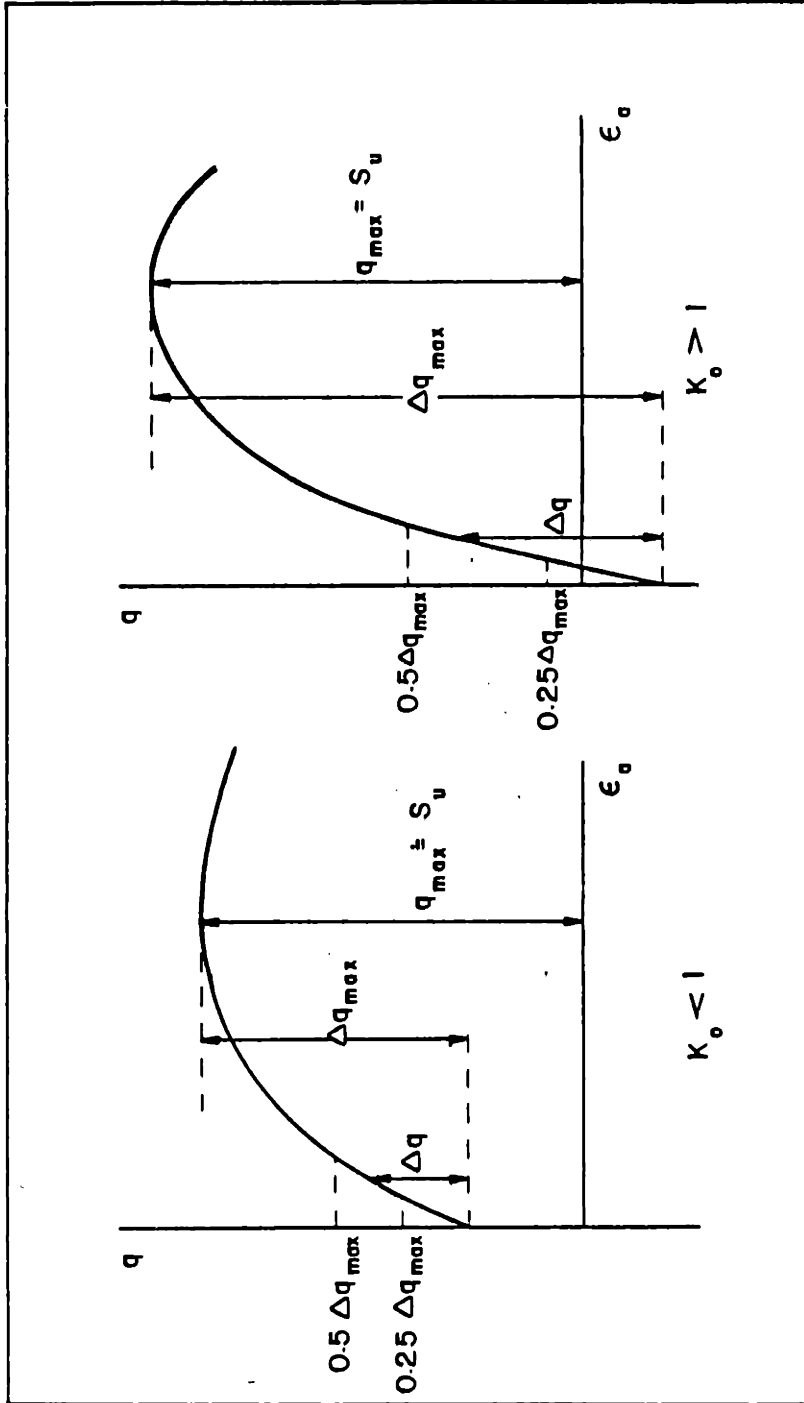


Figure 5.5 Definition of Δq and Δq_{max}

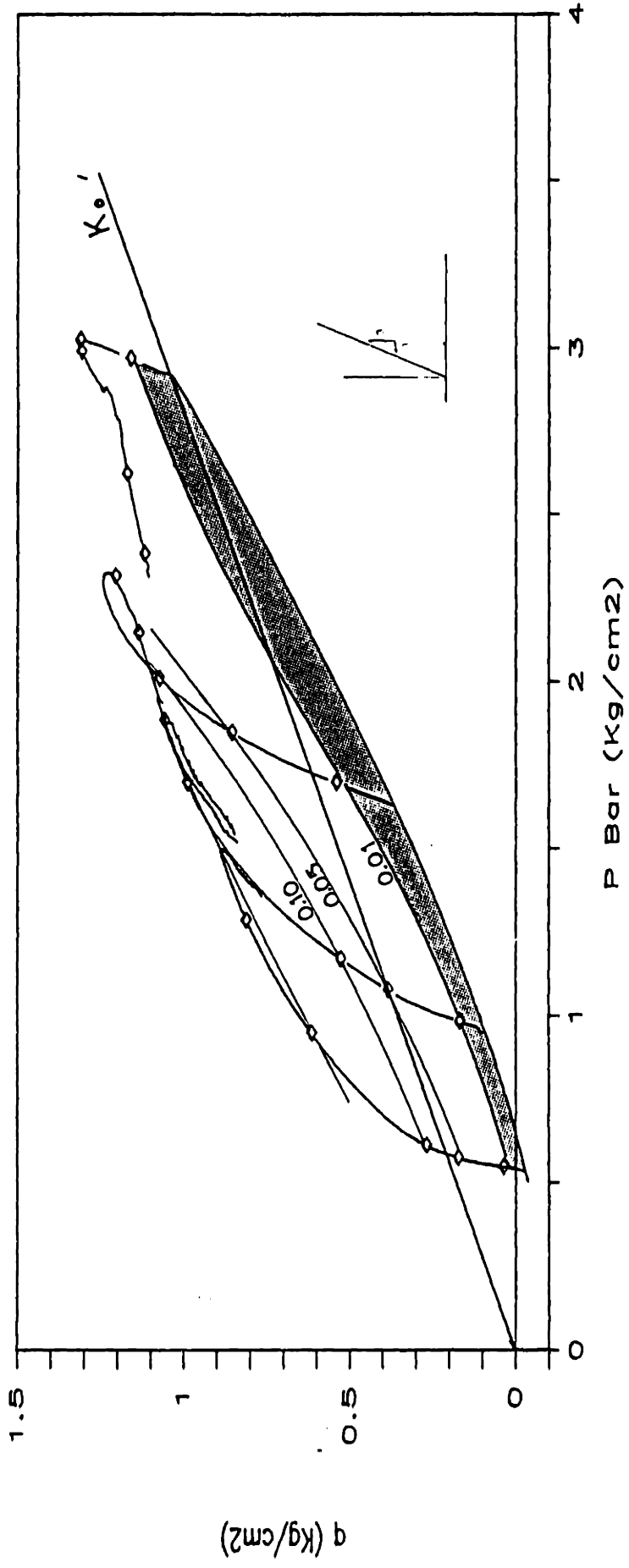


Figure 5.6 Stress path for CK₀UC tests

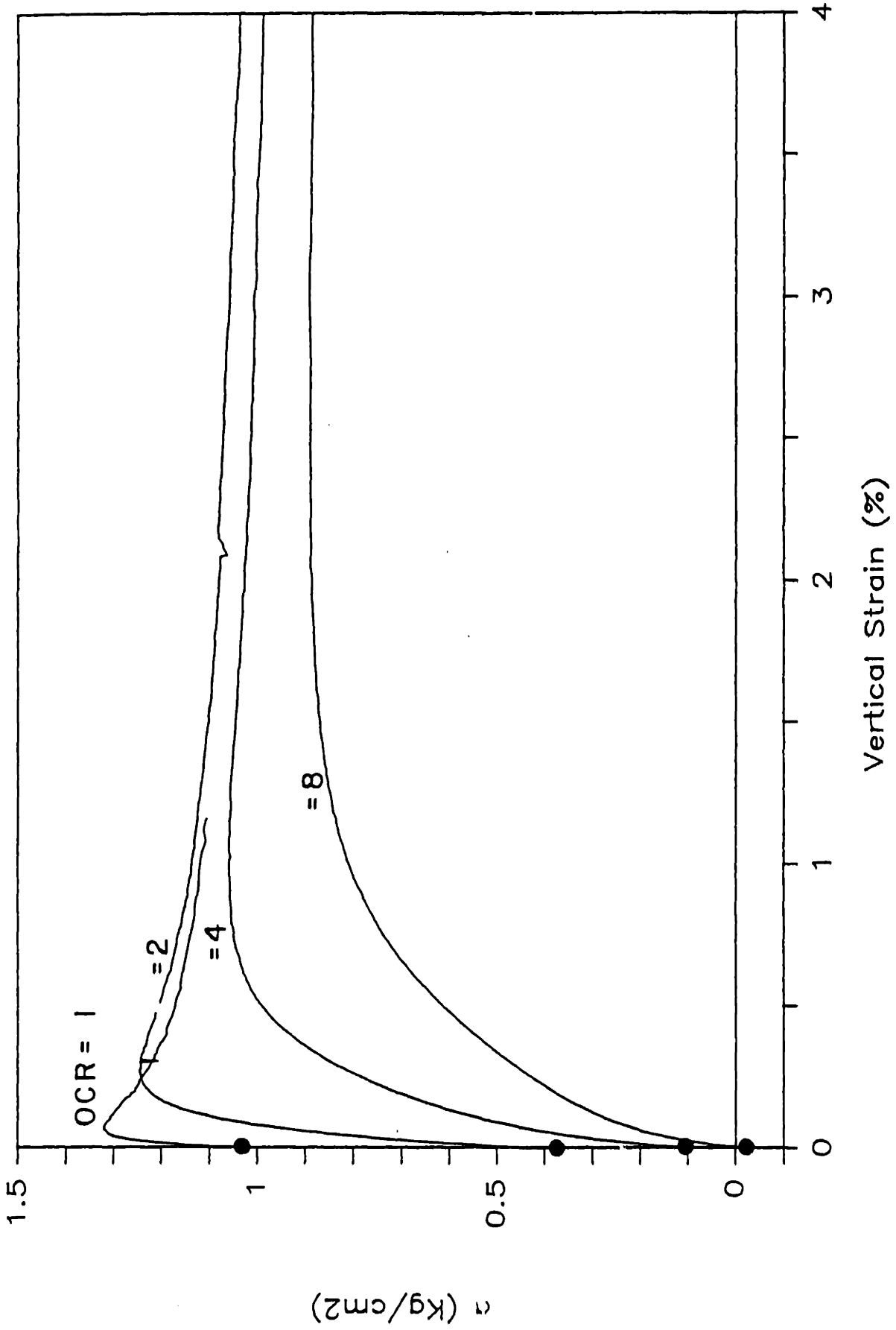


Figure 5.7 Stress-strain curves for CK₀JC tests (small strains)

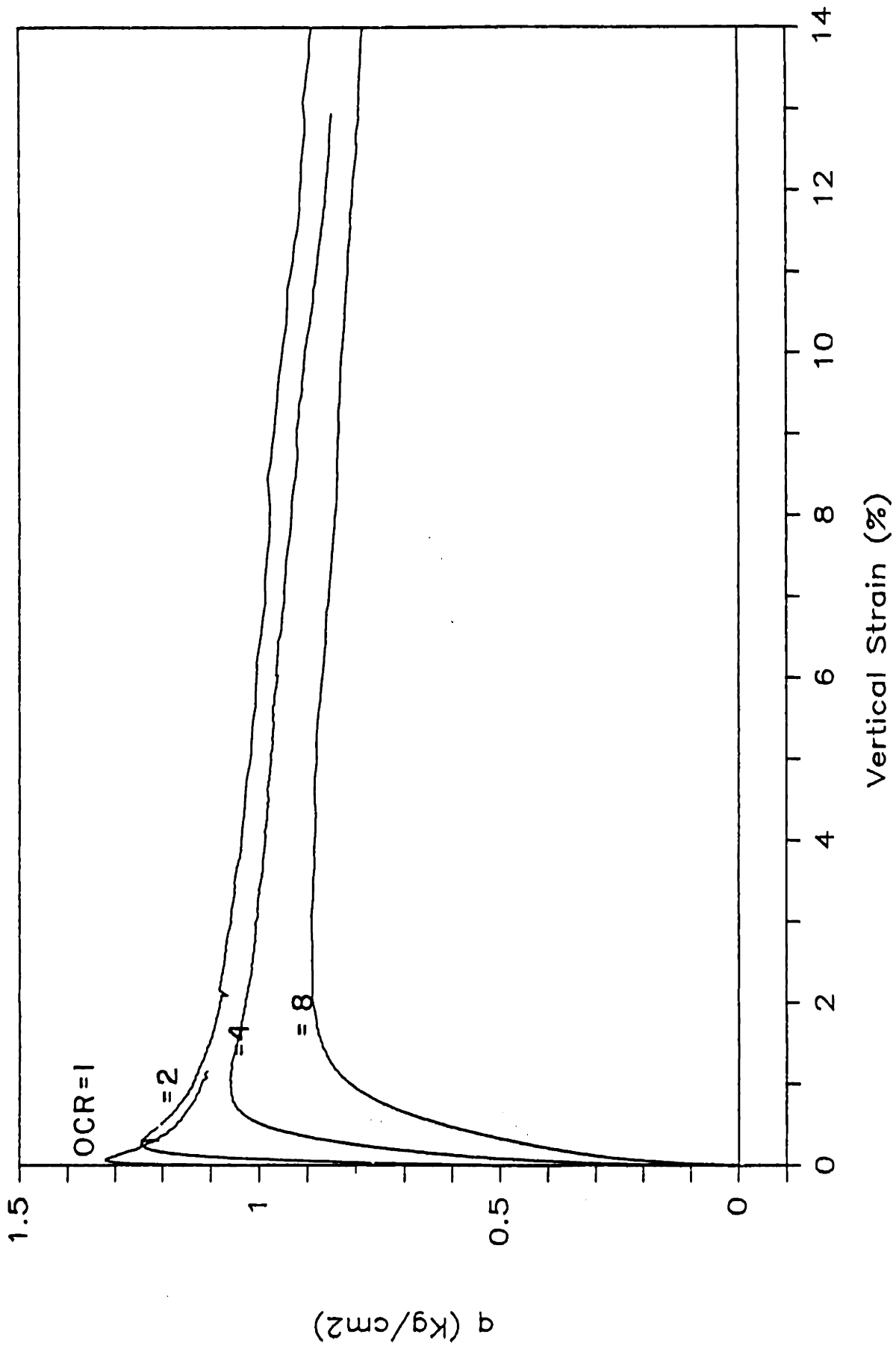


Figure 5.8 Stress-strain curves for CK₀UC tests (large strains)

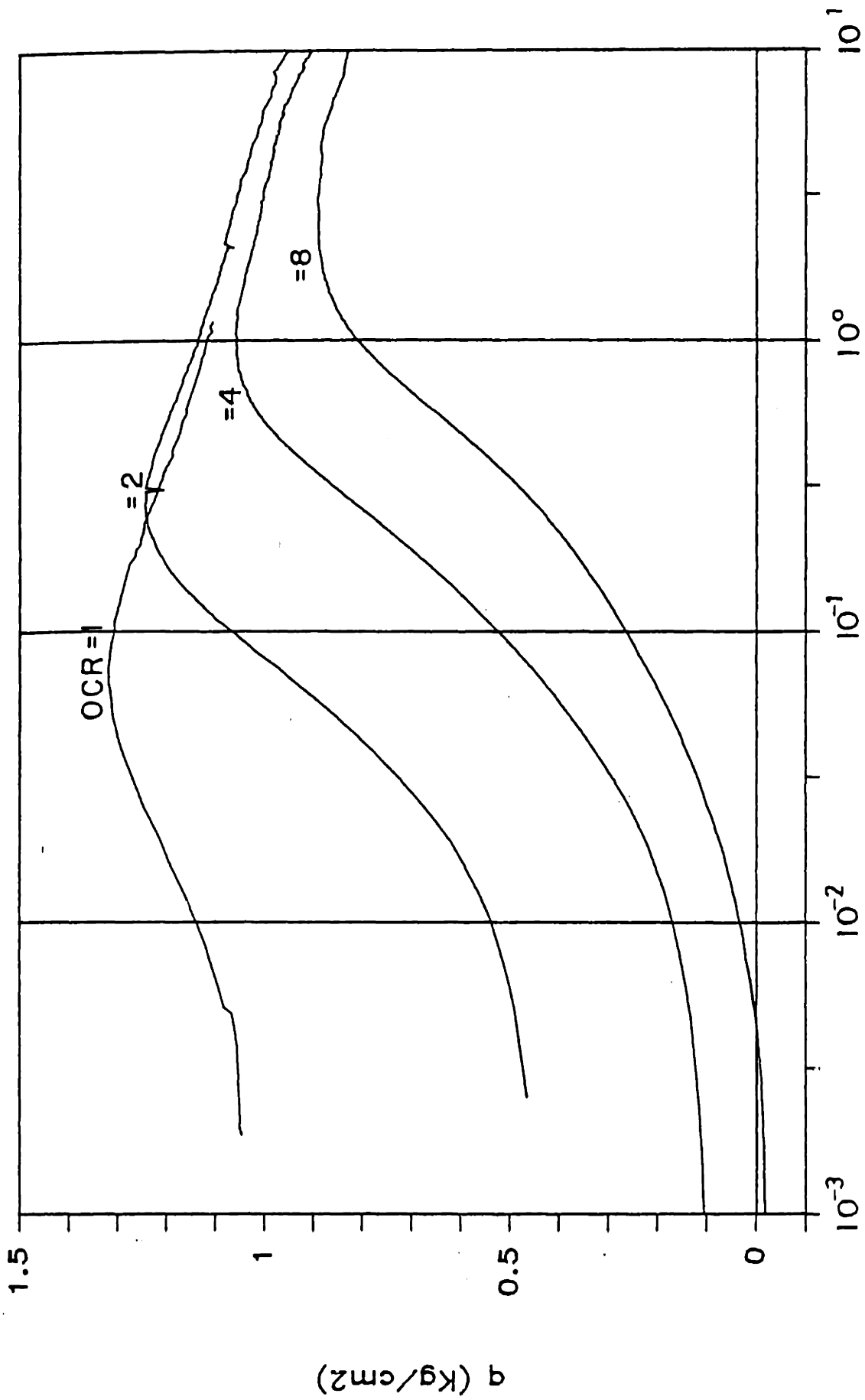


Figure 5.9 Stress-strain curves for CK₀UC tests (log scale)

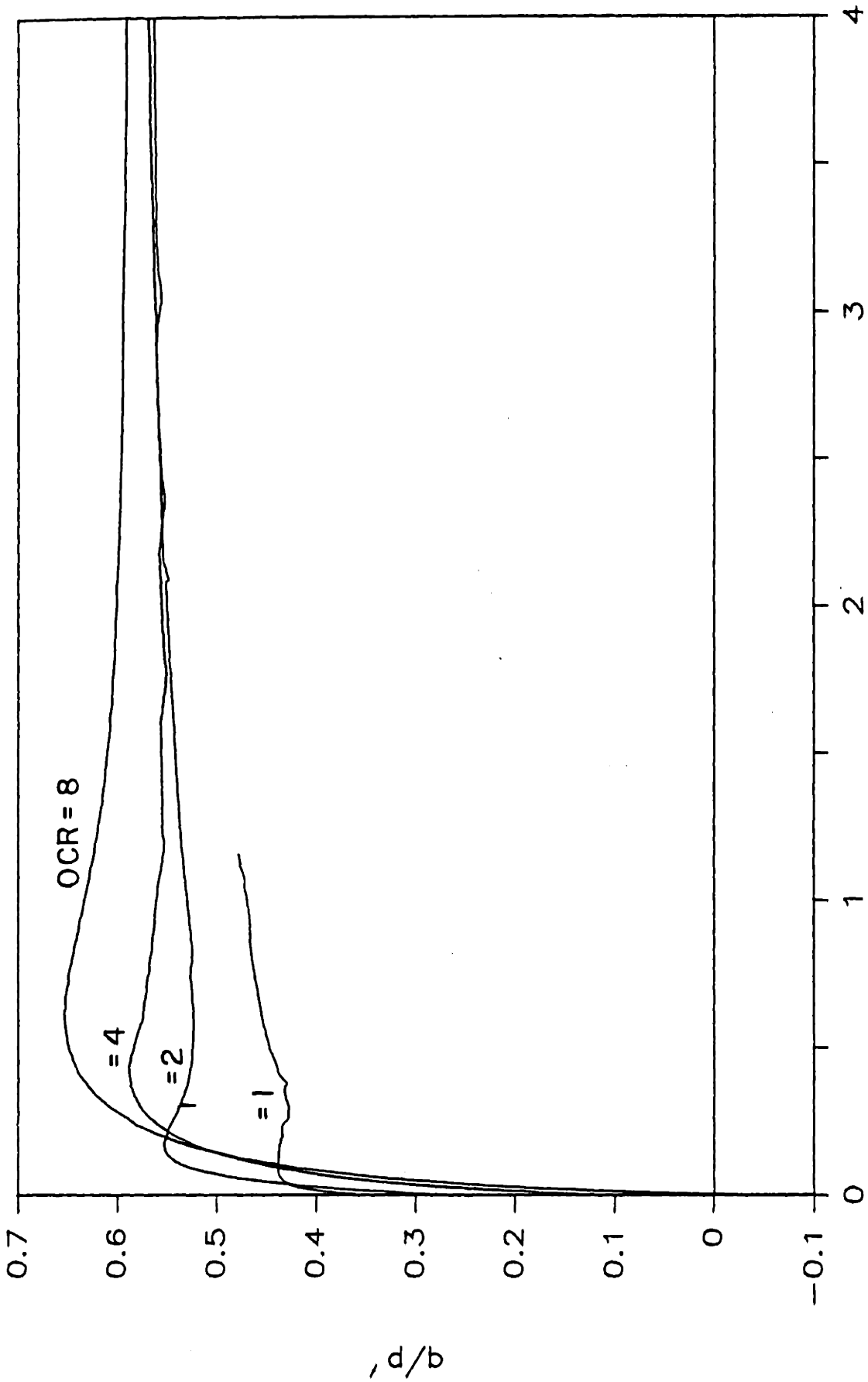
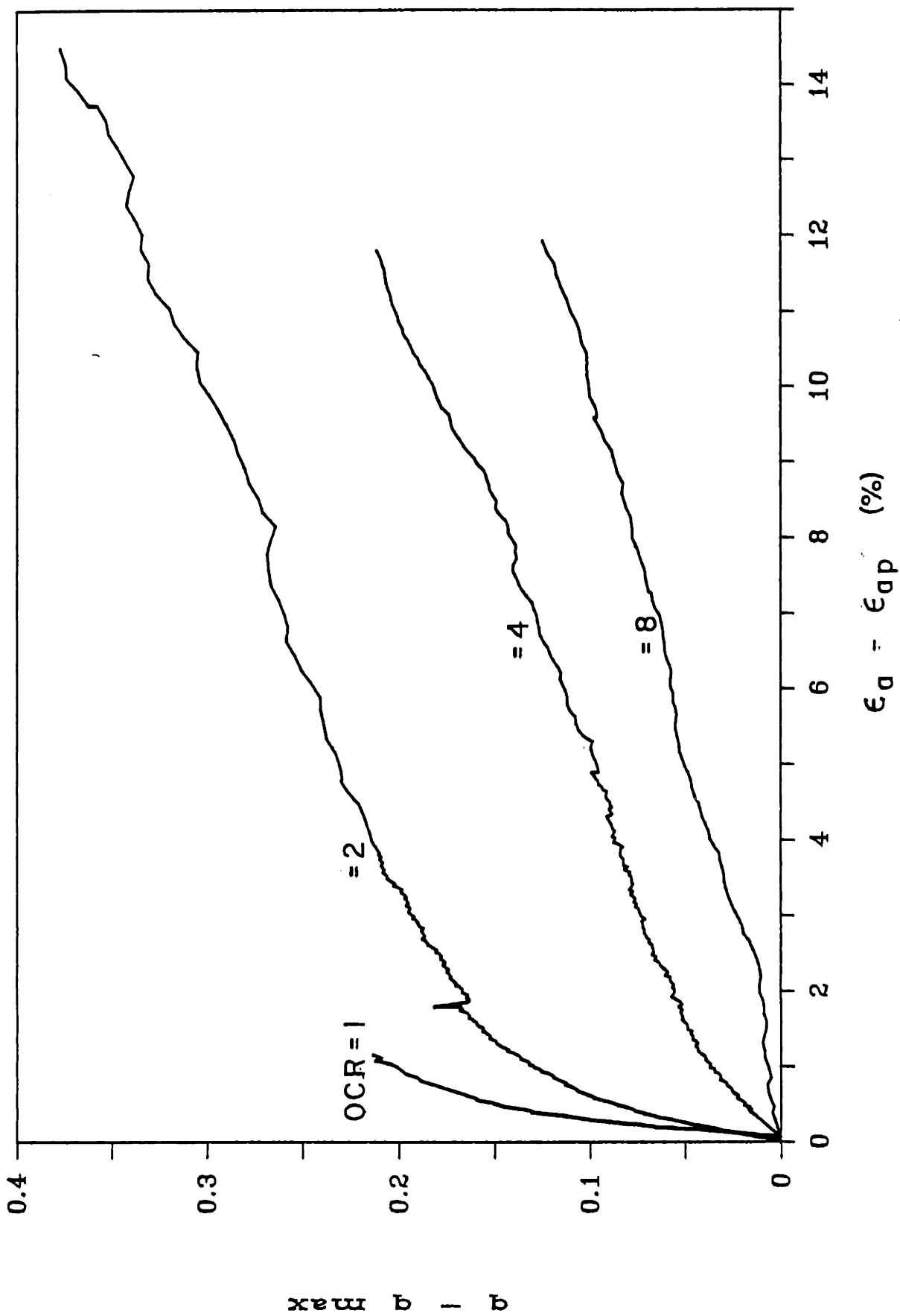


Figure 5.10 Oblivious data for CK₀UC tests

Figure 5.11 Softening characteristics of CK₀UC tests

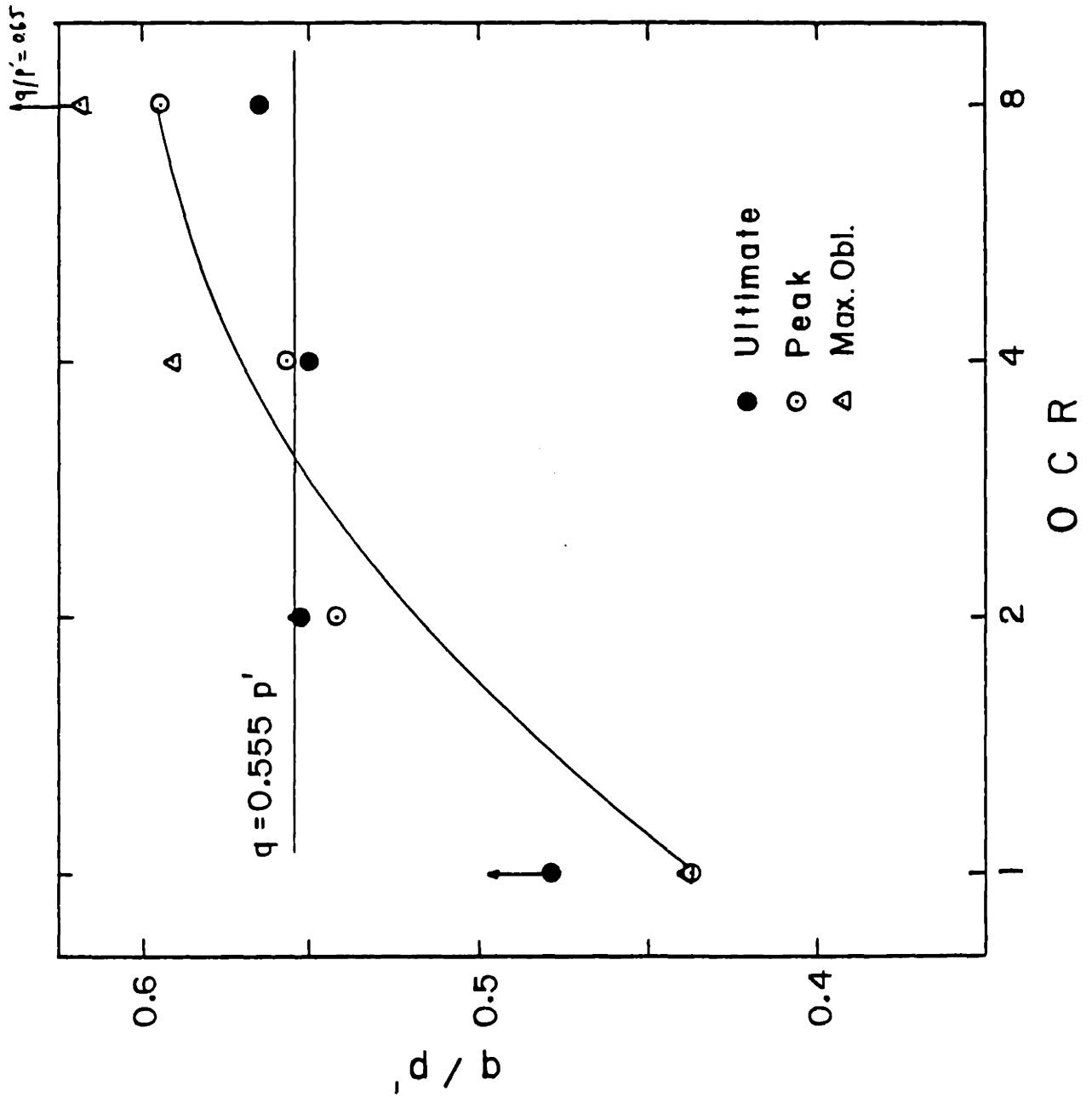


Figure 5.12 Obliquity vs OCR for CK₀UC tests

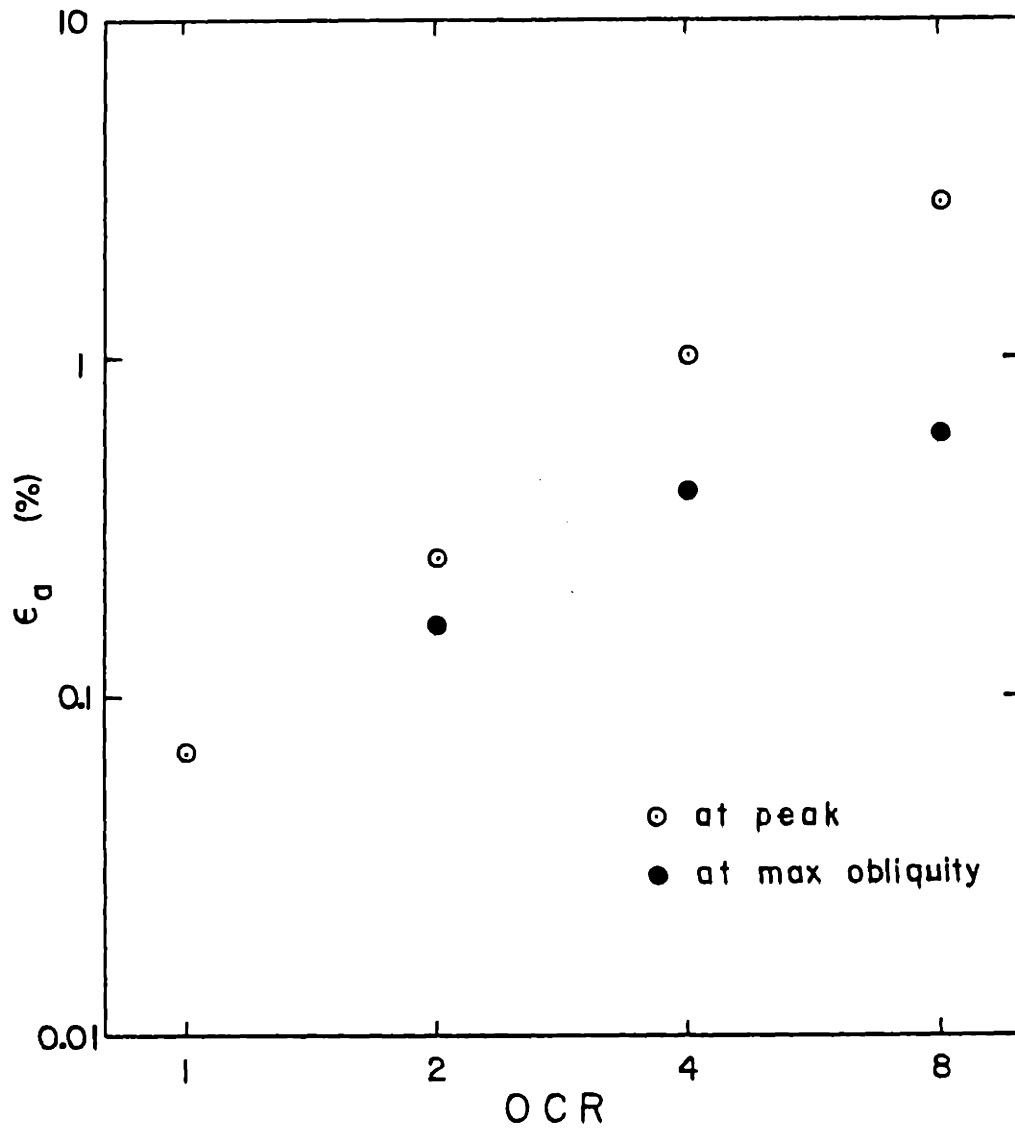


Figure 5.13 Variation of strains with OCR for CK_0UC tests

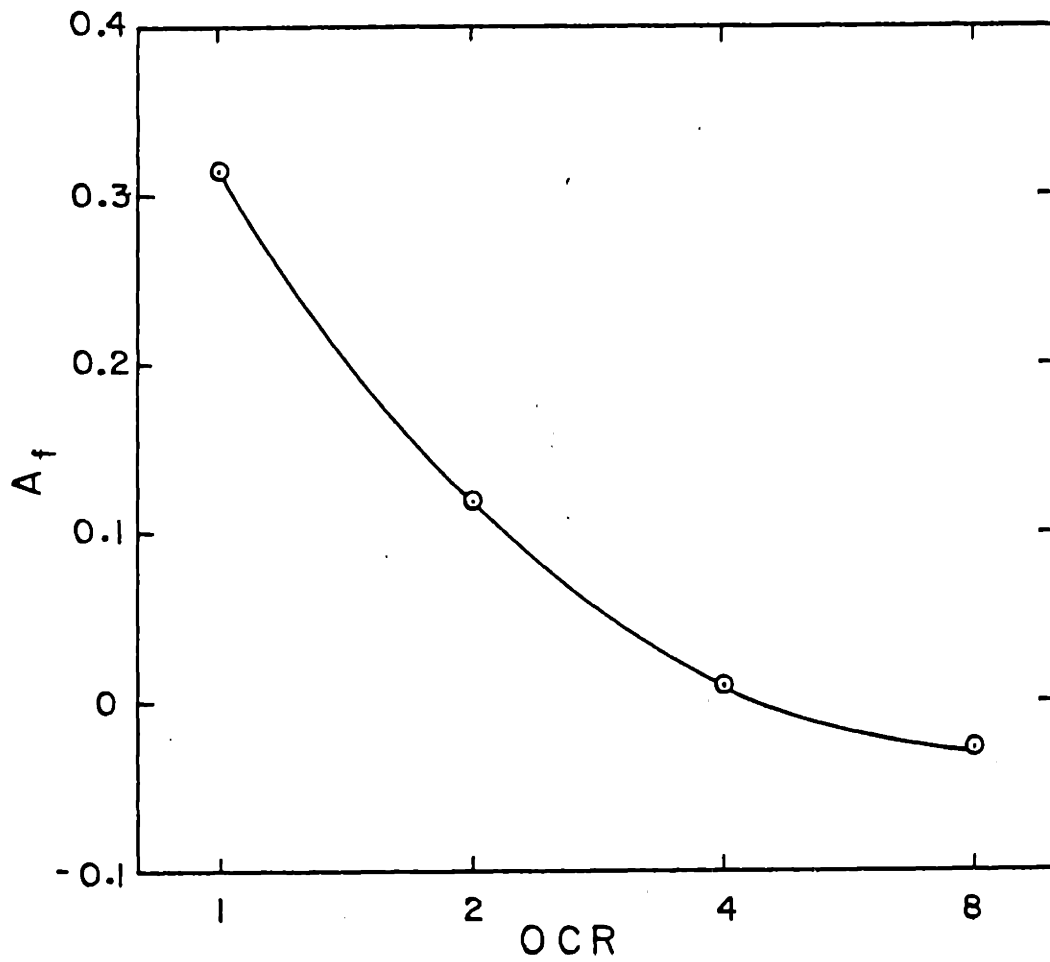


Figure 5.14 Variation of pore pressure parameter at failure for CK_0UC tests

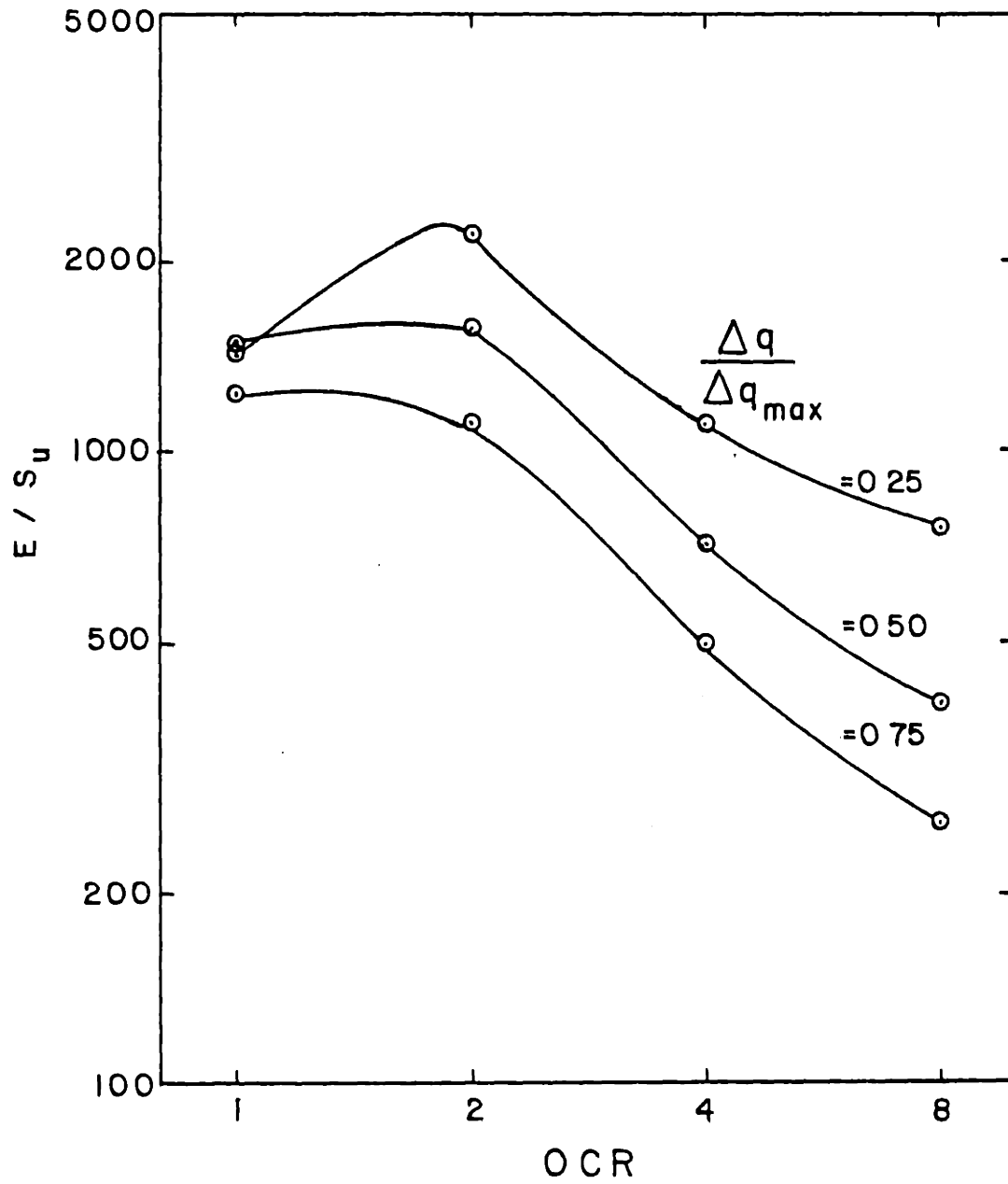


Figure 5.15 Normalized undrained modulus vs OCR

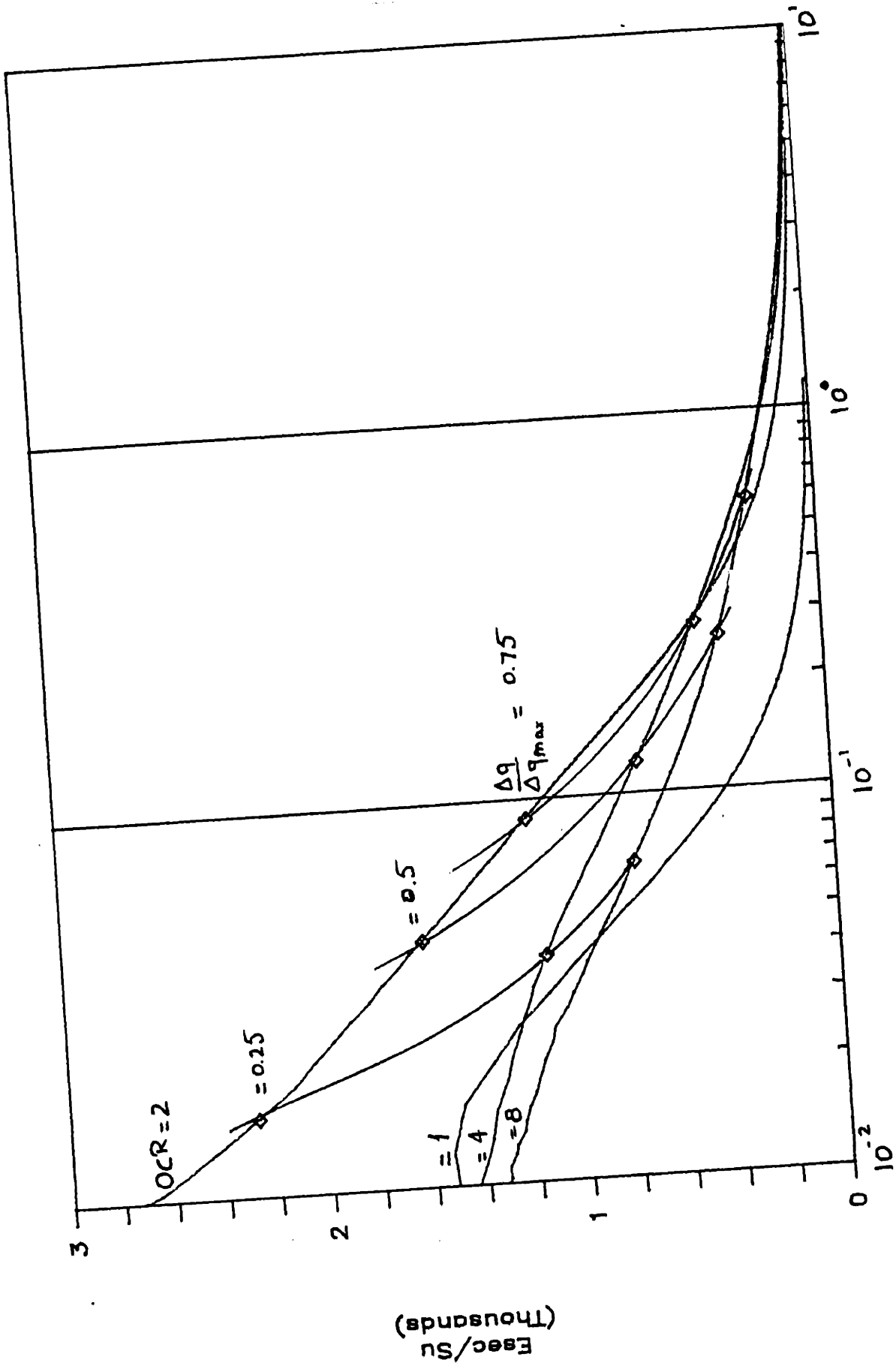


Figure 5.16 Normalized undrained modulus vs strain
Vert Strain (%)

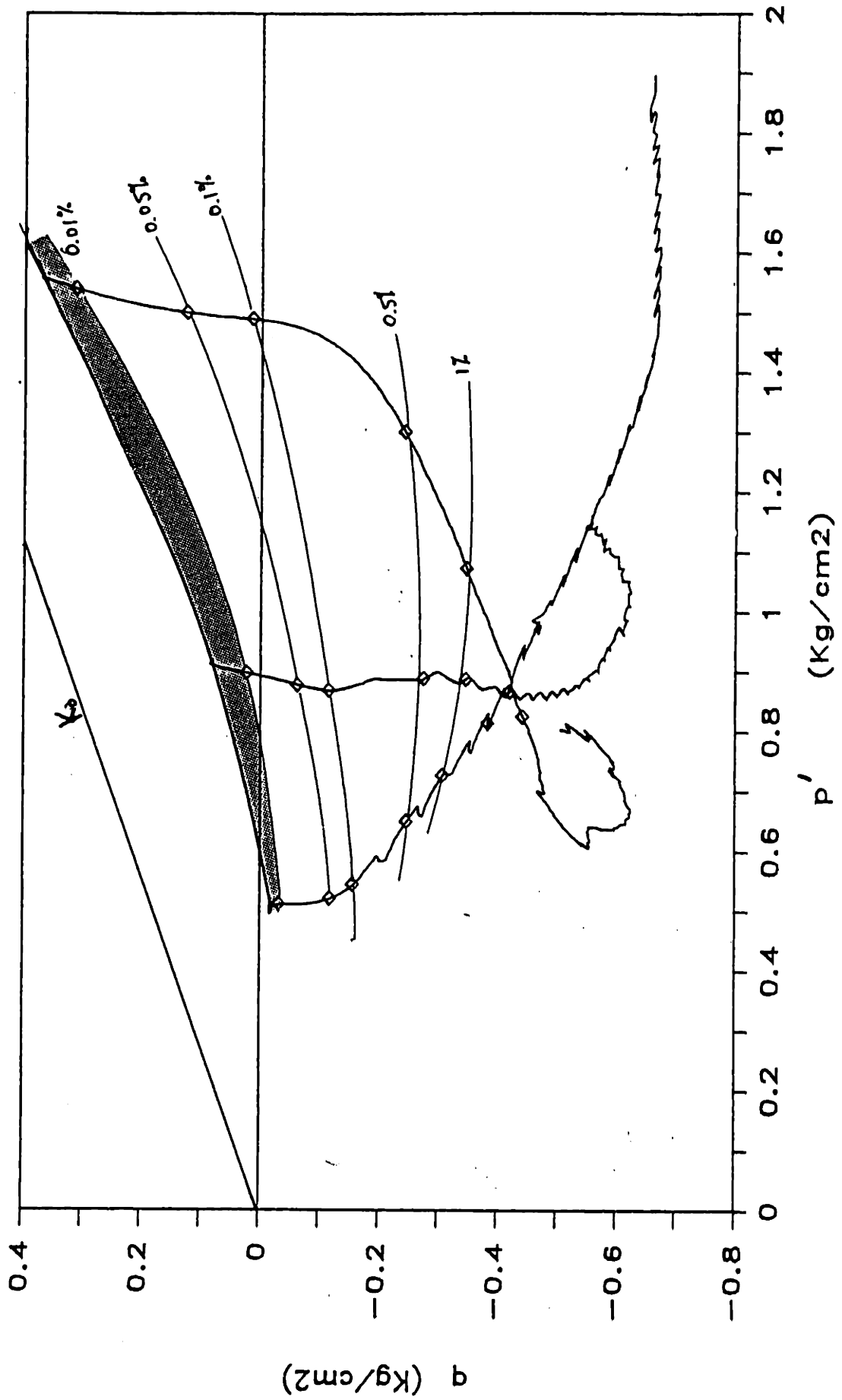


Figure 5.17 Stress path for CK₀UE tests

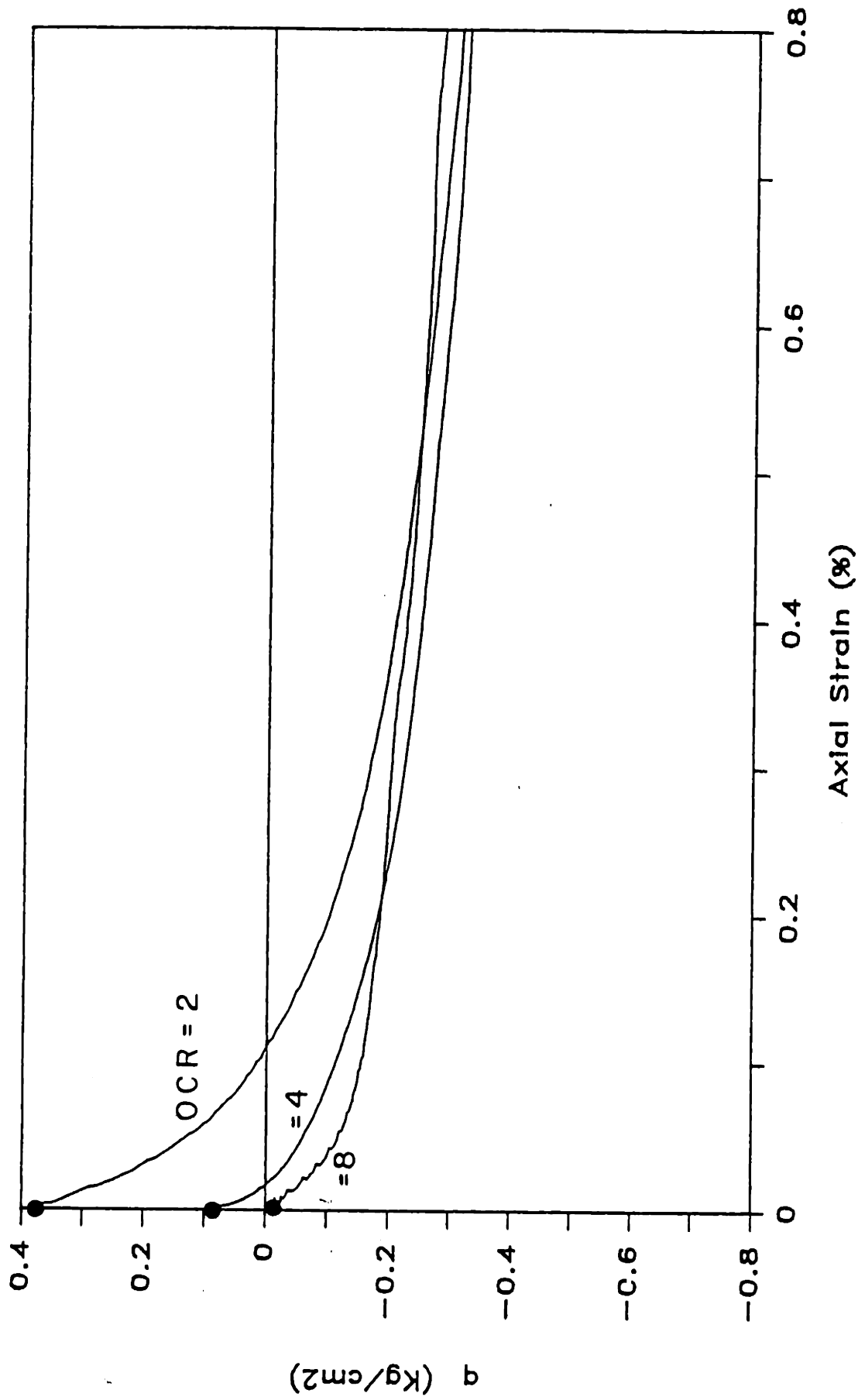


Figure 5.18 Stress-strain curves for CK₀JE tests (small strains)

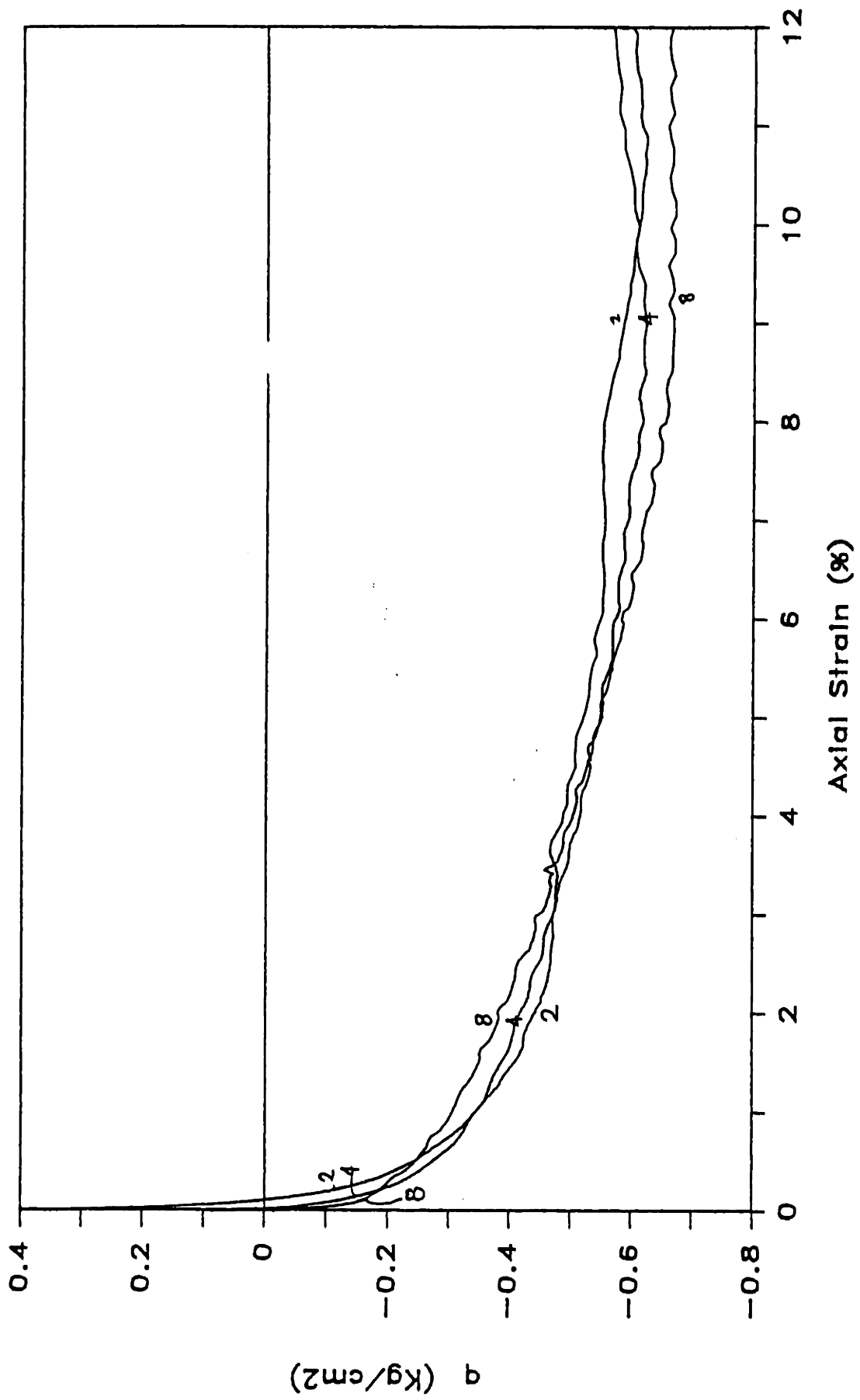
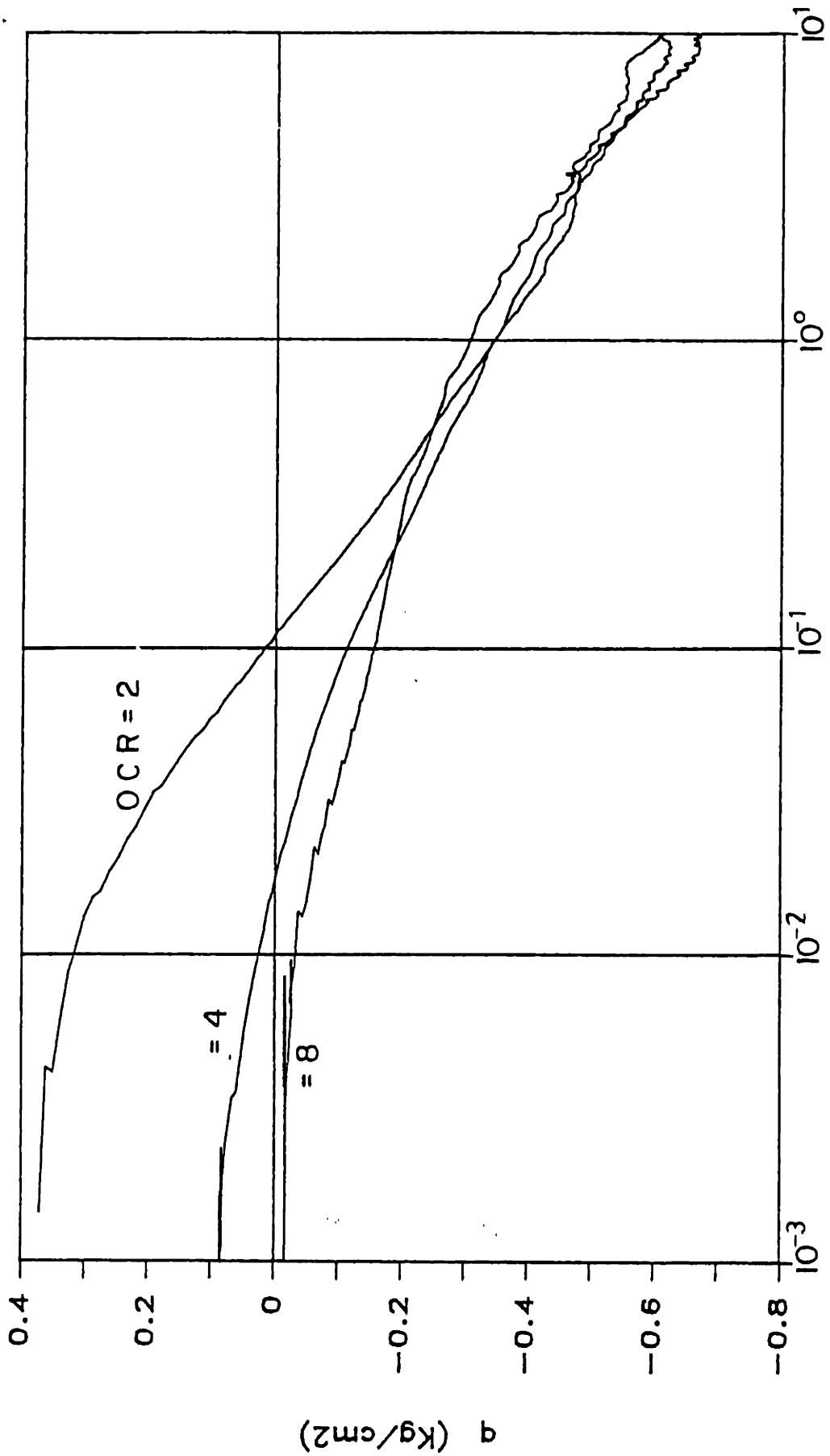


Figure 5.19 Stress-strain curves for CK₀UE tests (large strains)



Axial Strain (%)

Figure 5.20 Stress-strain curves for CK₀JE tests (log scale)

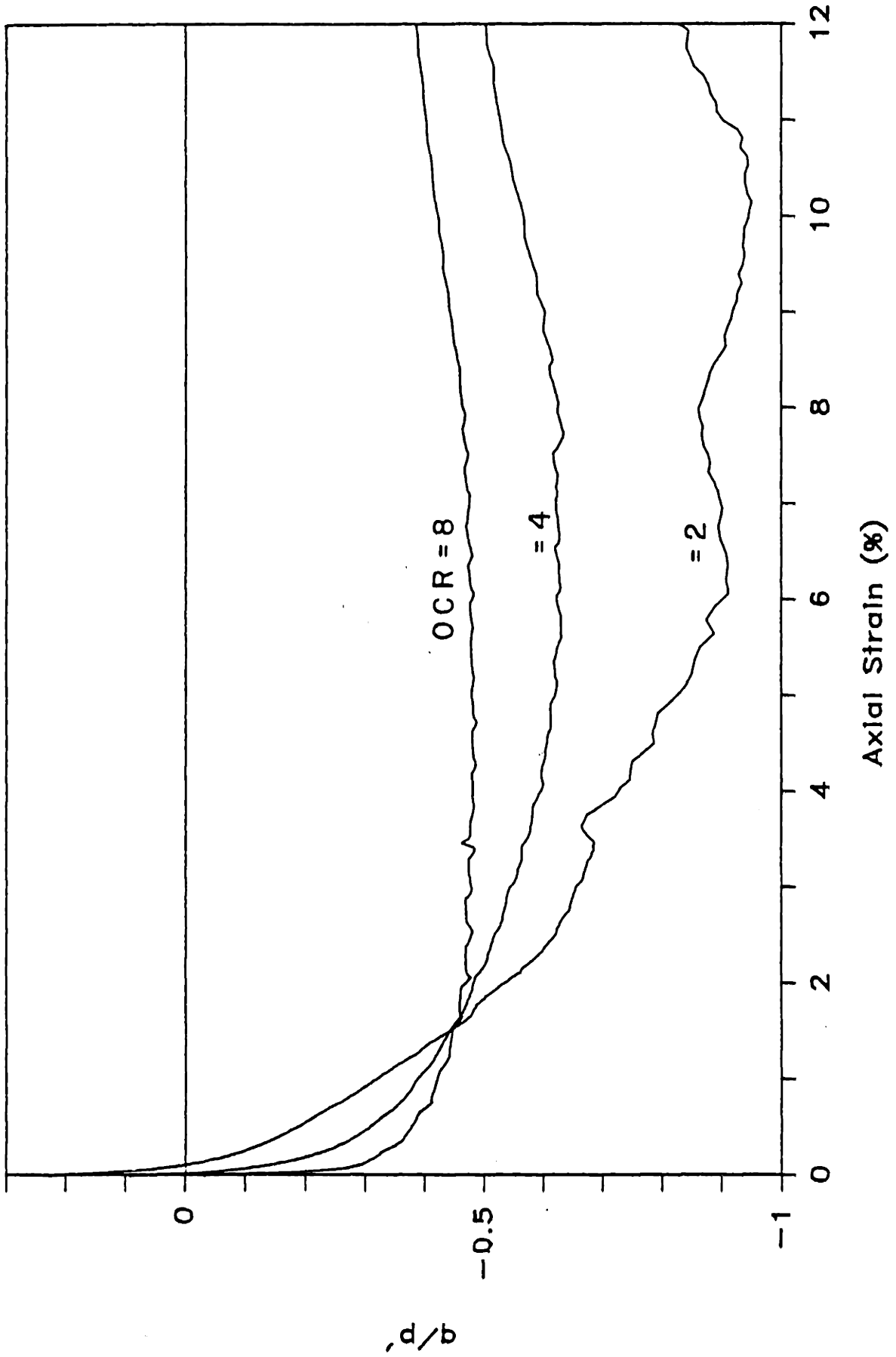


Figure 5.21 Obliquity data vs. strain for CK₀JE tests

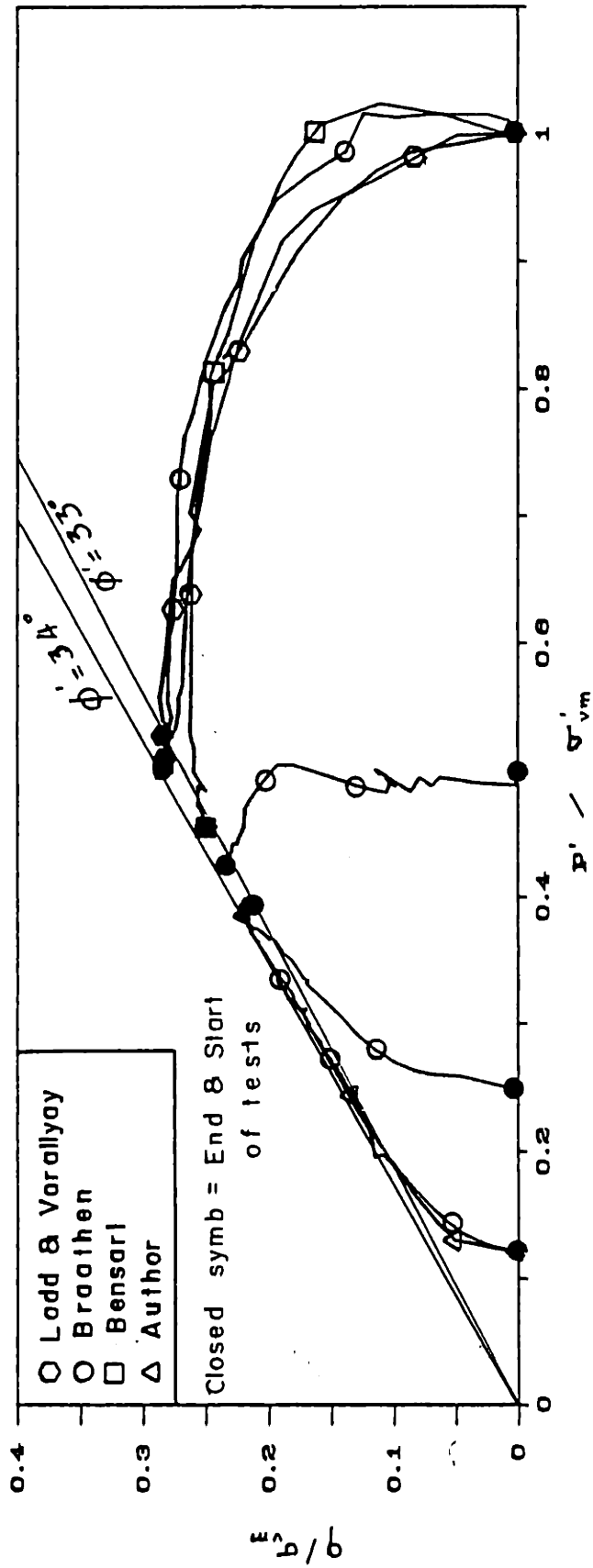


Figure 5.22 Stress paths for CIUC tests

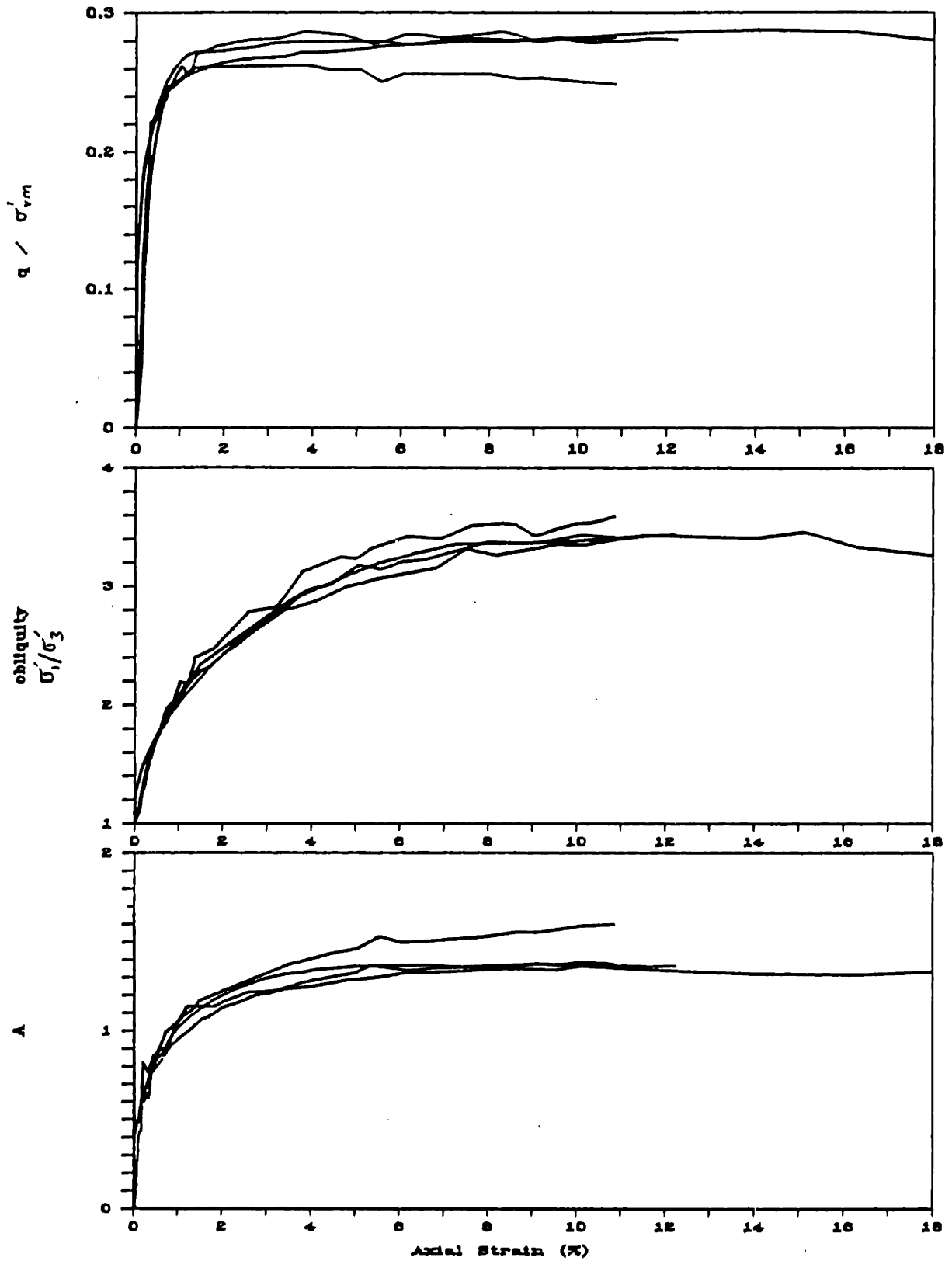


Figure 5.23 Stress-strain curves for CIUC tests (NC)

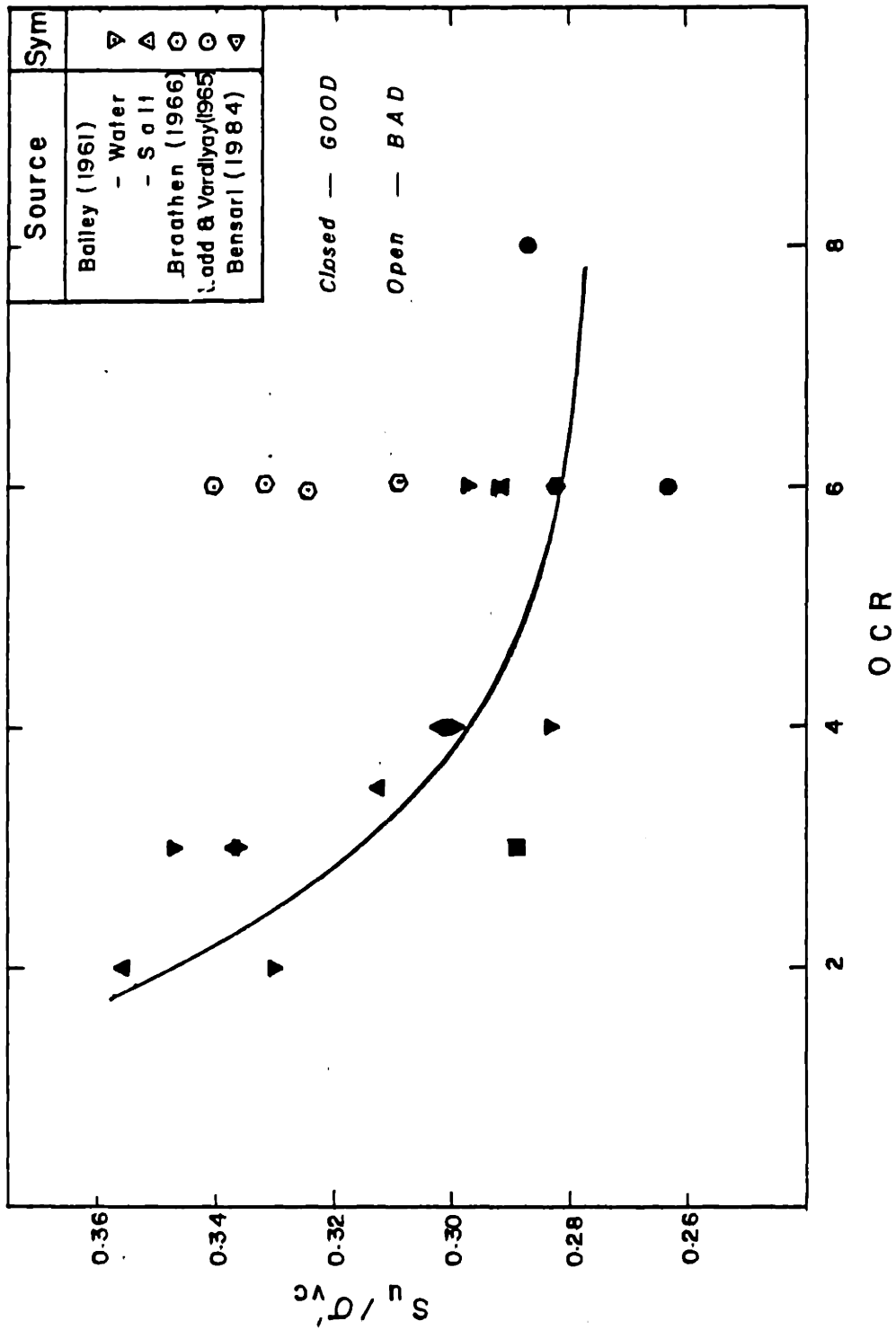


Figure 5.24 Normalized undrained strength for CIUC (NC) tests

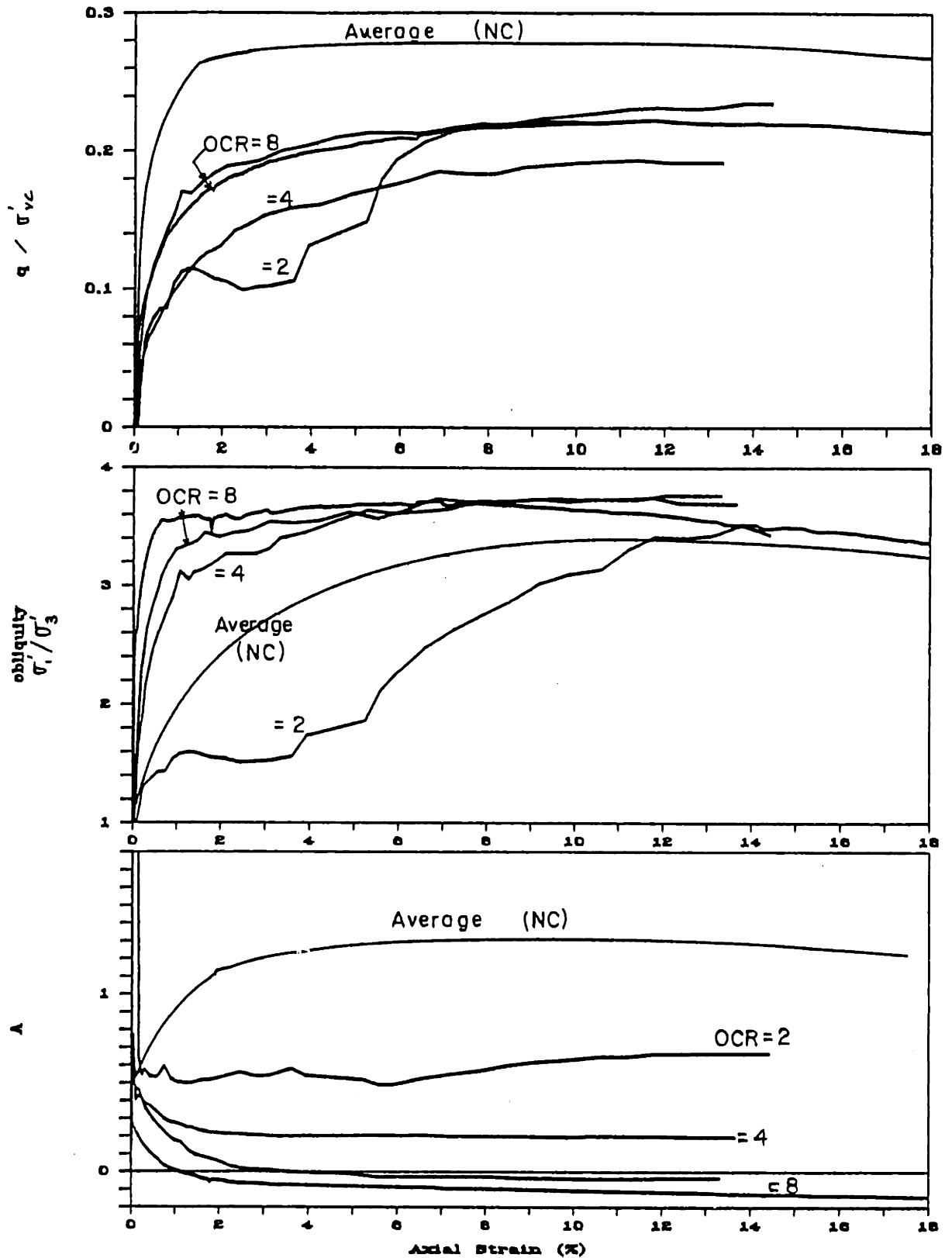


Figure 5.25 Stress-strain curves for CIUC tests

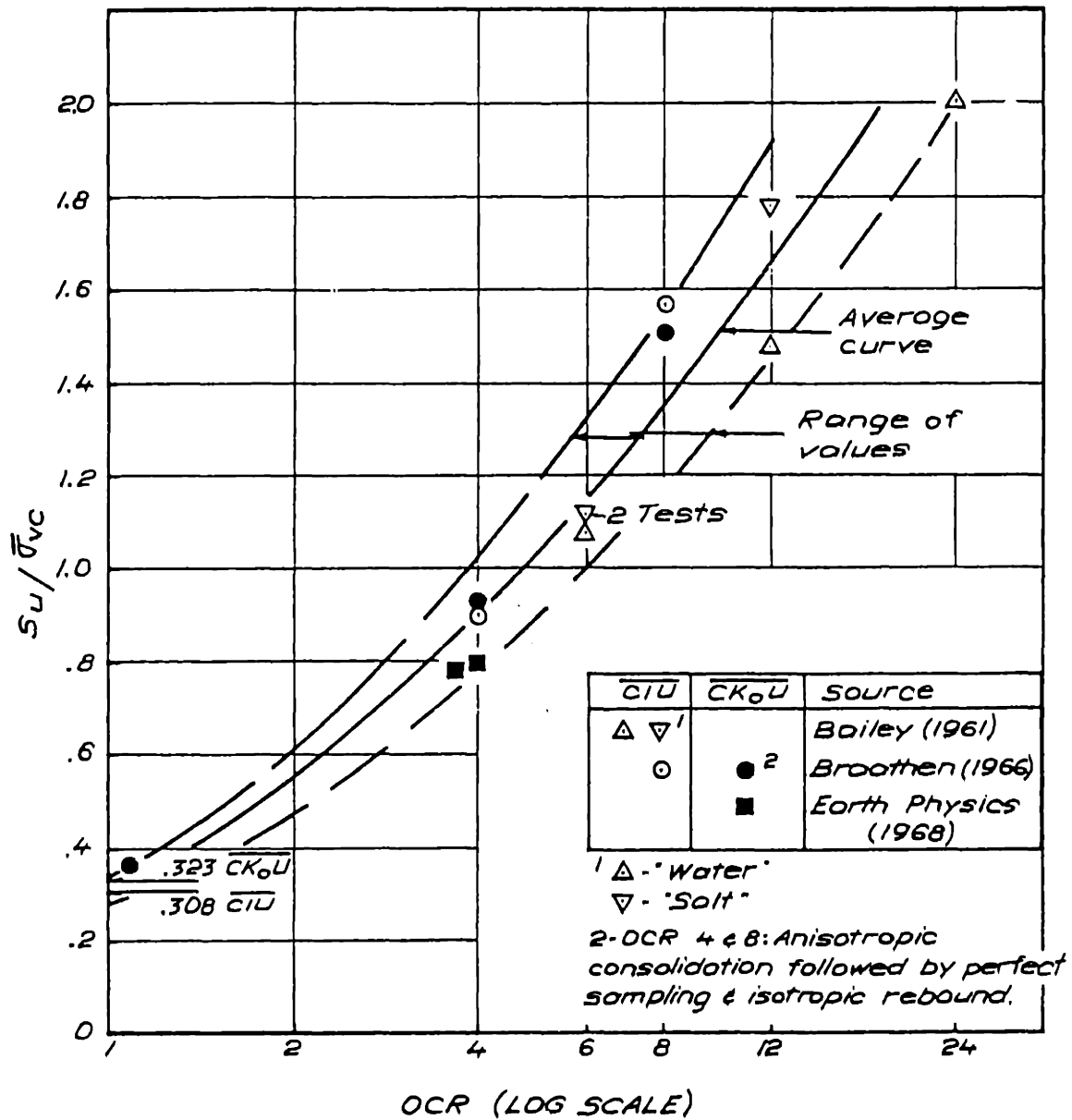


Figure 5.26 Normalized undrained strength vs OCR for CIUC tests

(from Kinner and Ladd, 1970)

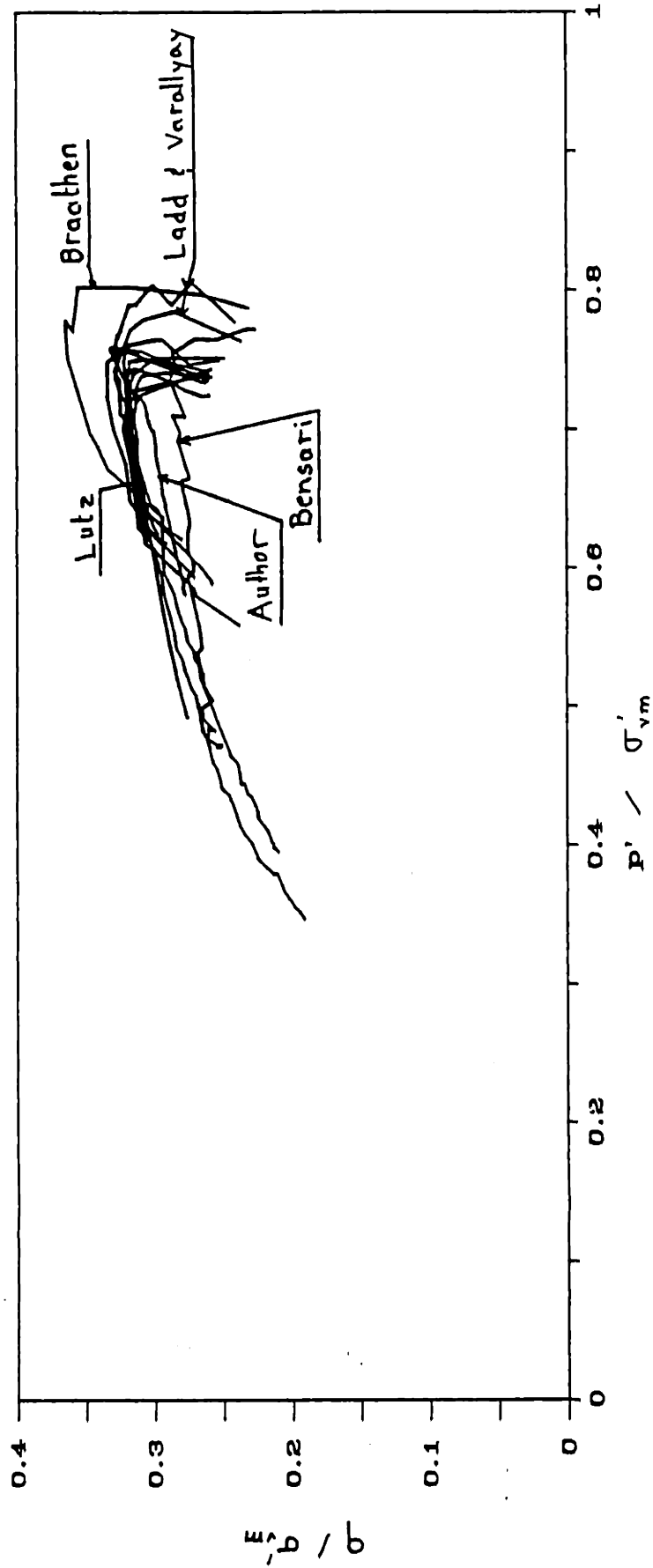


Figure 5.27 Stress paths for CK₀JC (NC) tests

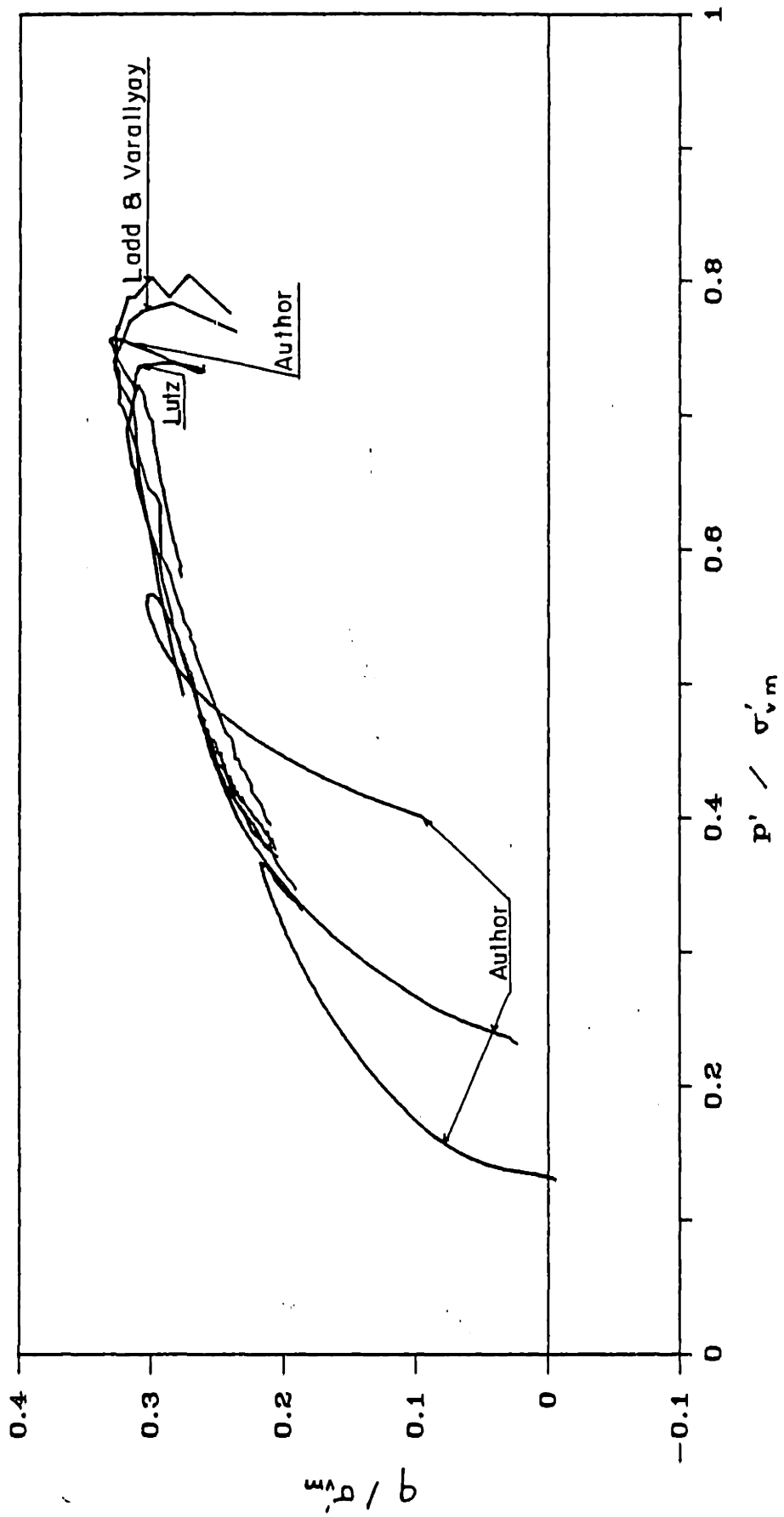


Figure 5.28 Stress paths for CK₀UC tests

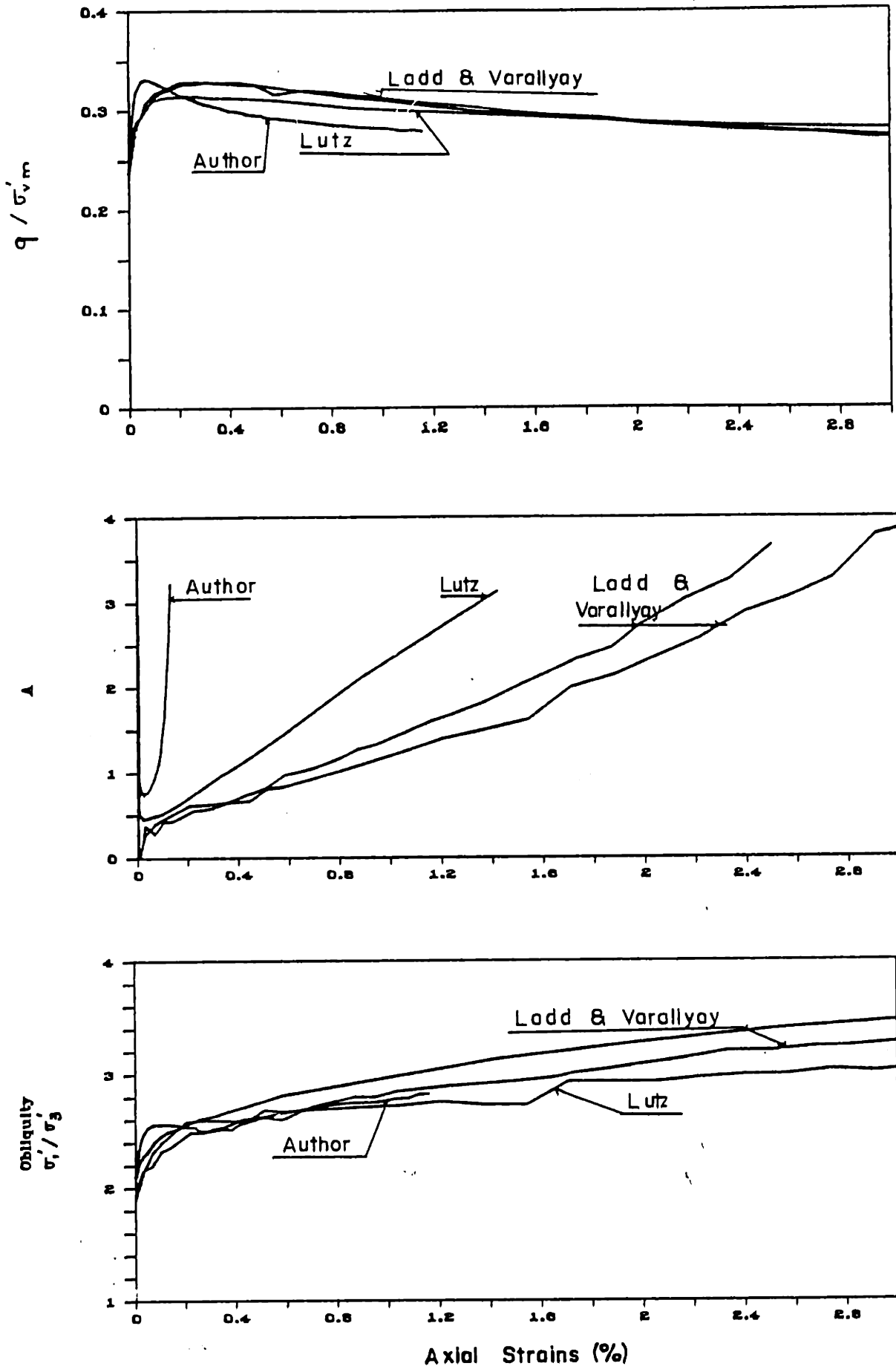


Figure 5.29 Stress-strain curves for CK₀UC (NC) tests

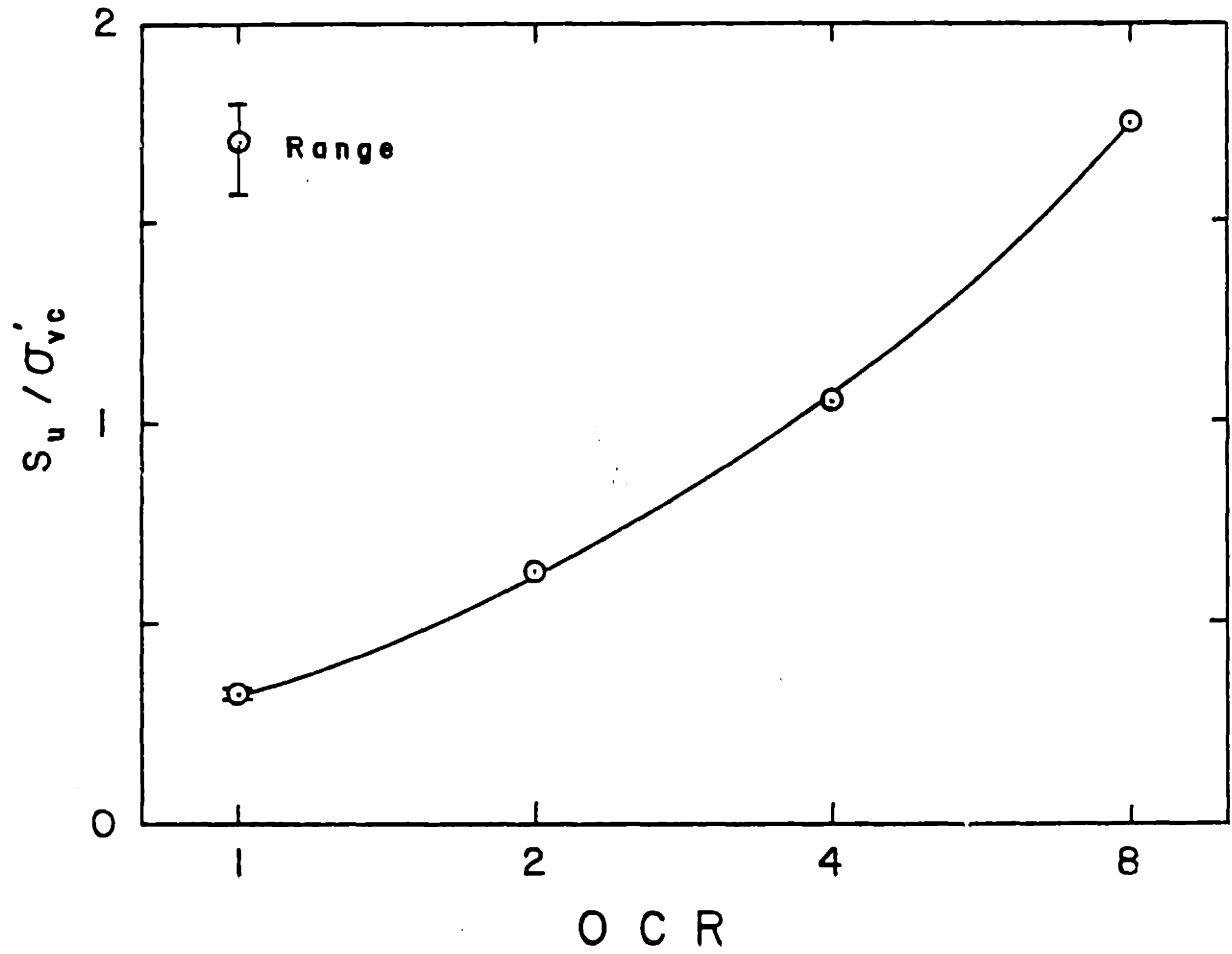


Figure 5.30 Variation of undrained shear strength with OCR for CK_0UC tests

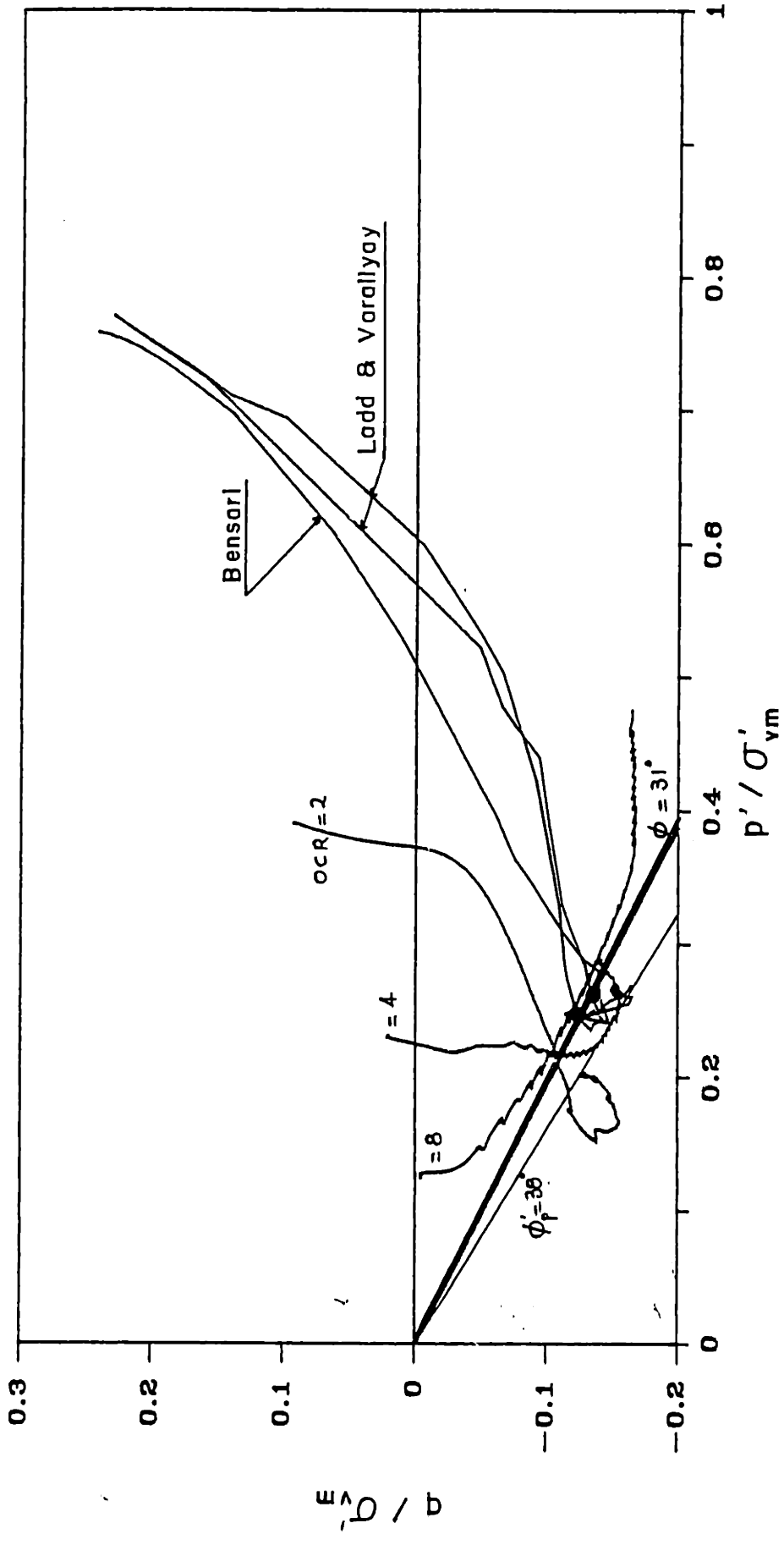


Figure 5.31 Stress paths for CK₀UE tests

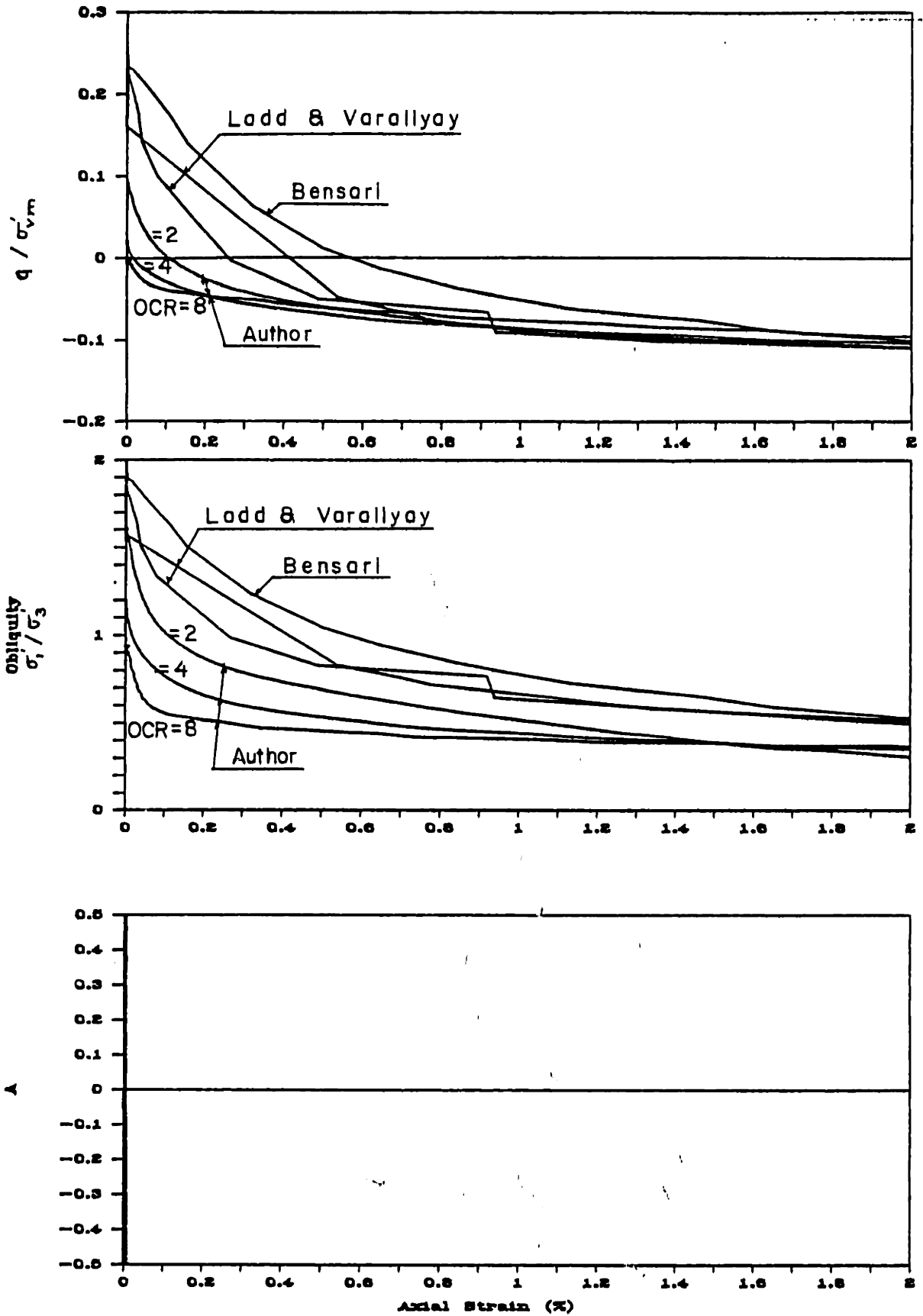


Figure 5.32 Stress-strain curves for CK_0UE tests

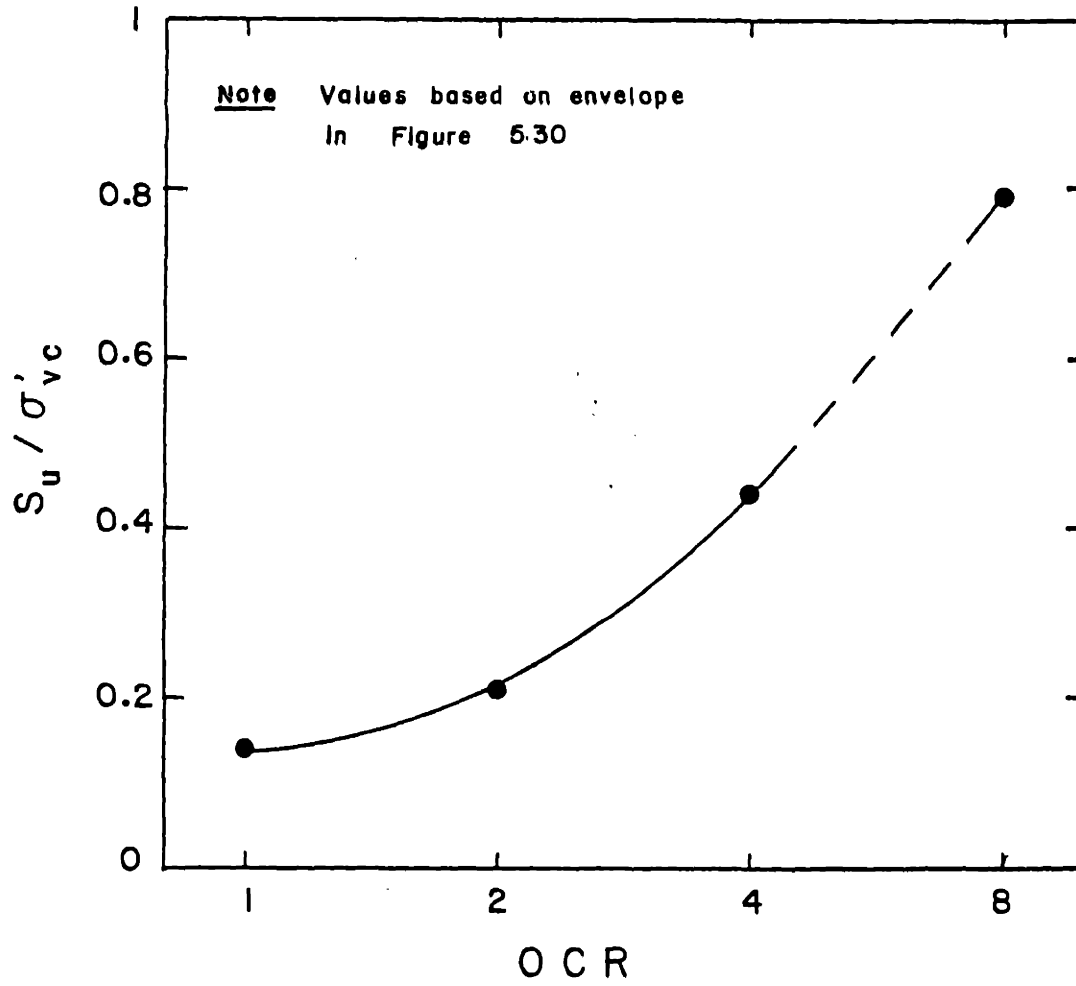


Figure 5.33 Variation of the undrained strength ratio with OCR for CK₀UE tests

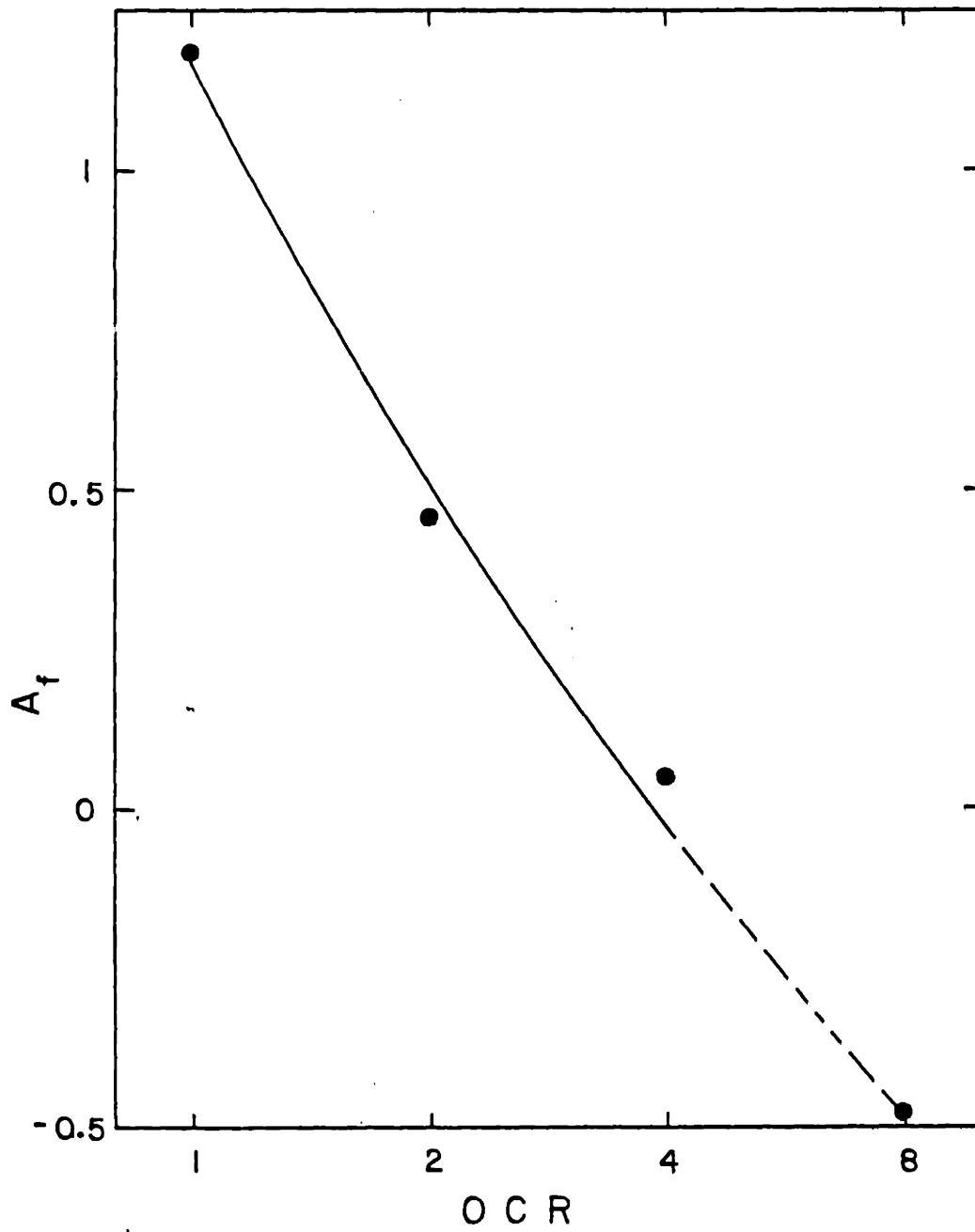


Figure 5.34 Variation of A_f with OCR for CK_oUE tests

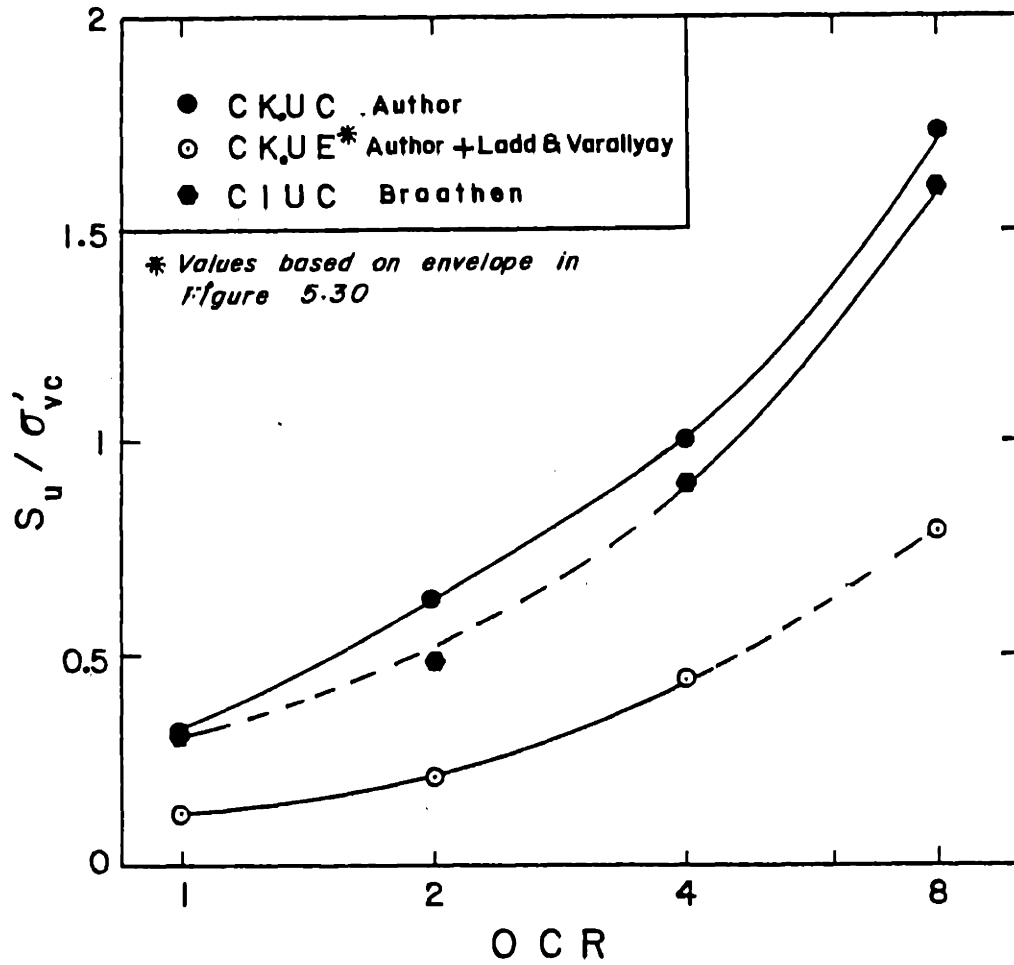


Figure 5.35 Summary of undrained strength ratio with OCR

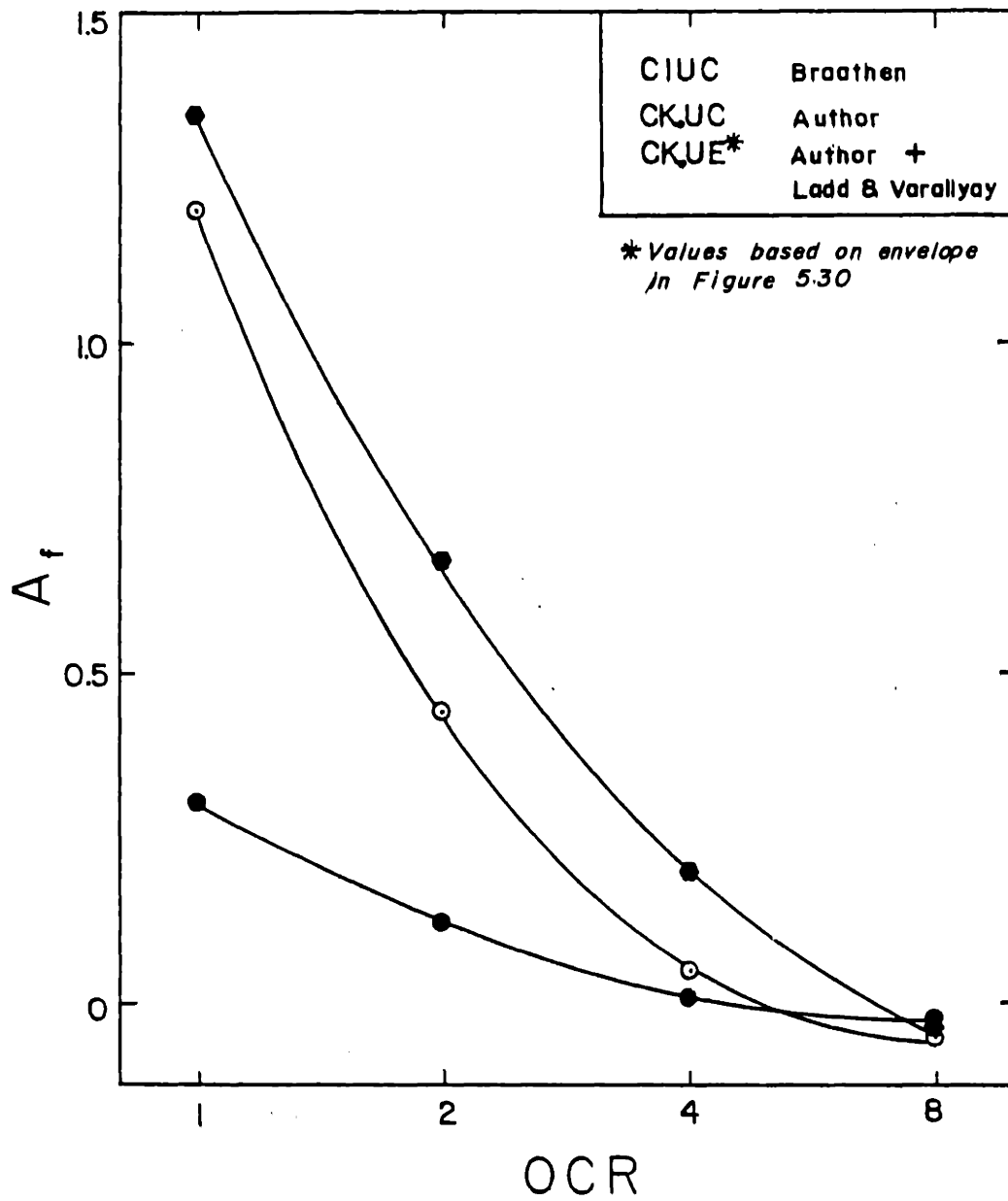


Figure 5.36 Summary of the variation of A_f with OCR

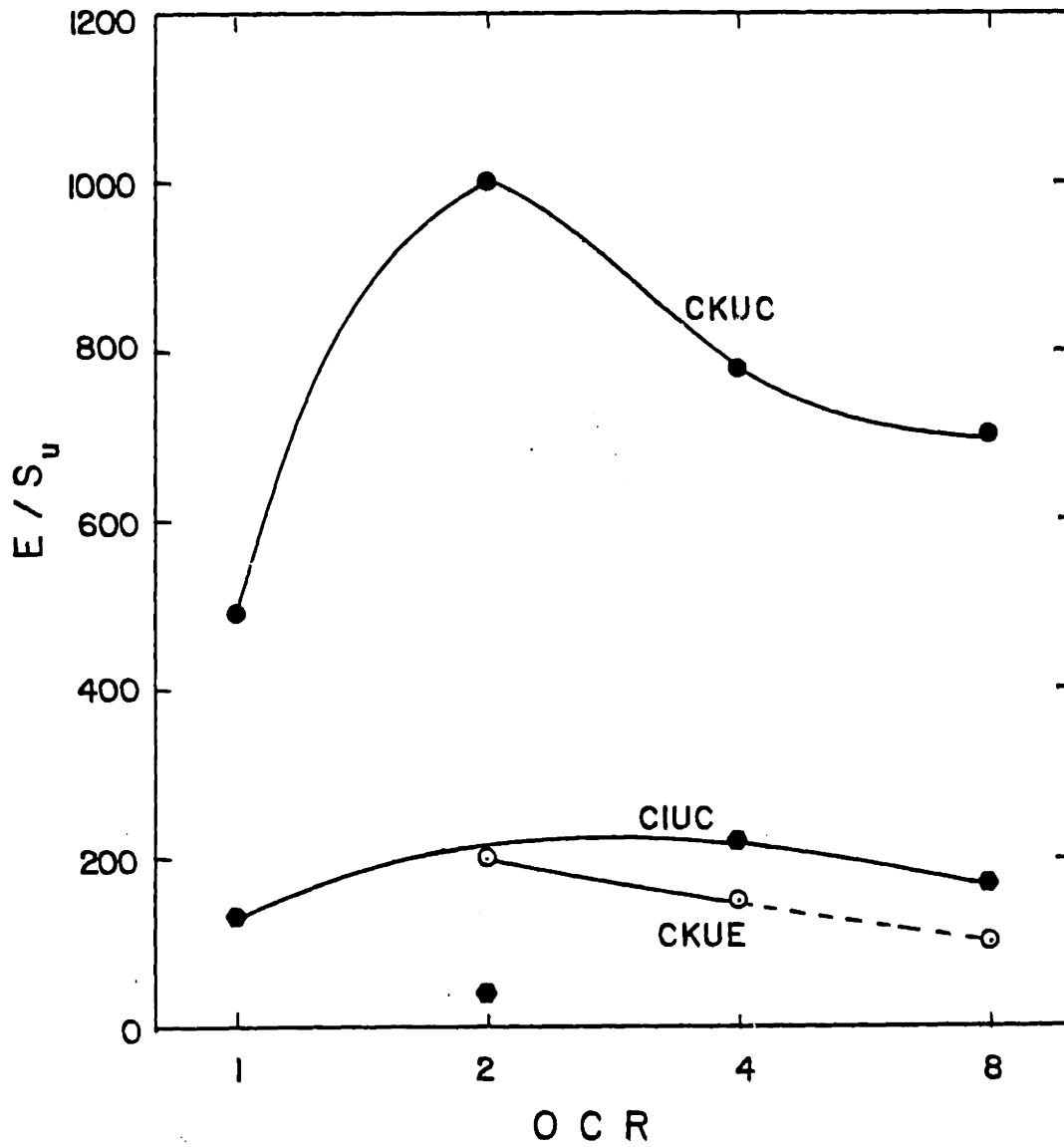


Figure 5.37 Summary of the variation of stiffness vs OCR ($\Delta q/\Delta q_{\max}=50\%$)

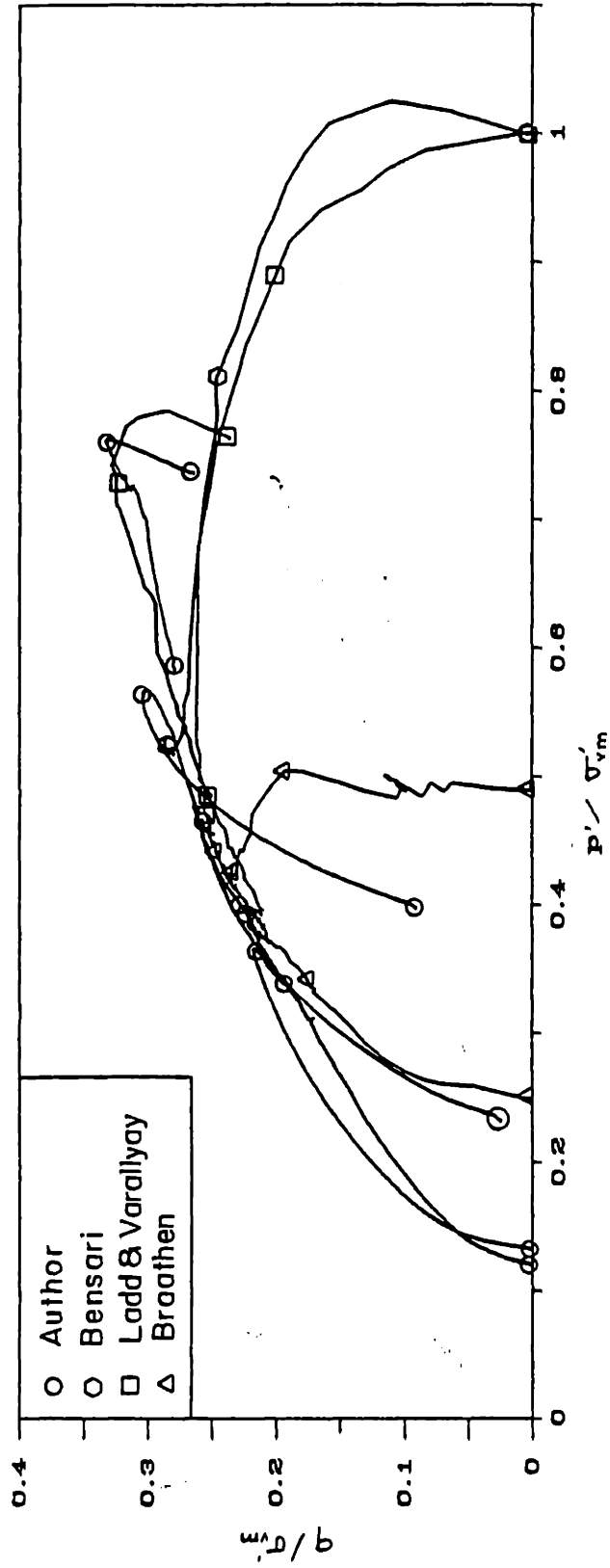


Figure 5.38 Stress paths for compression tests

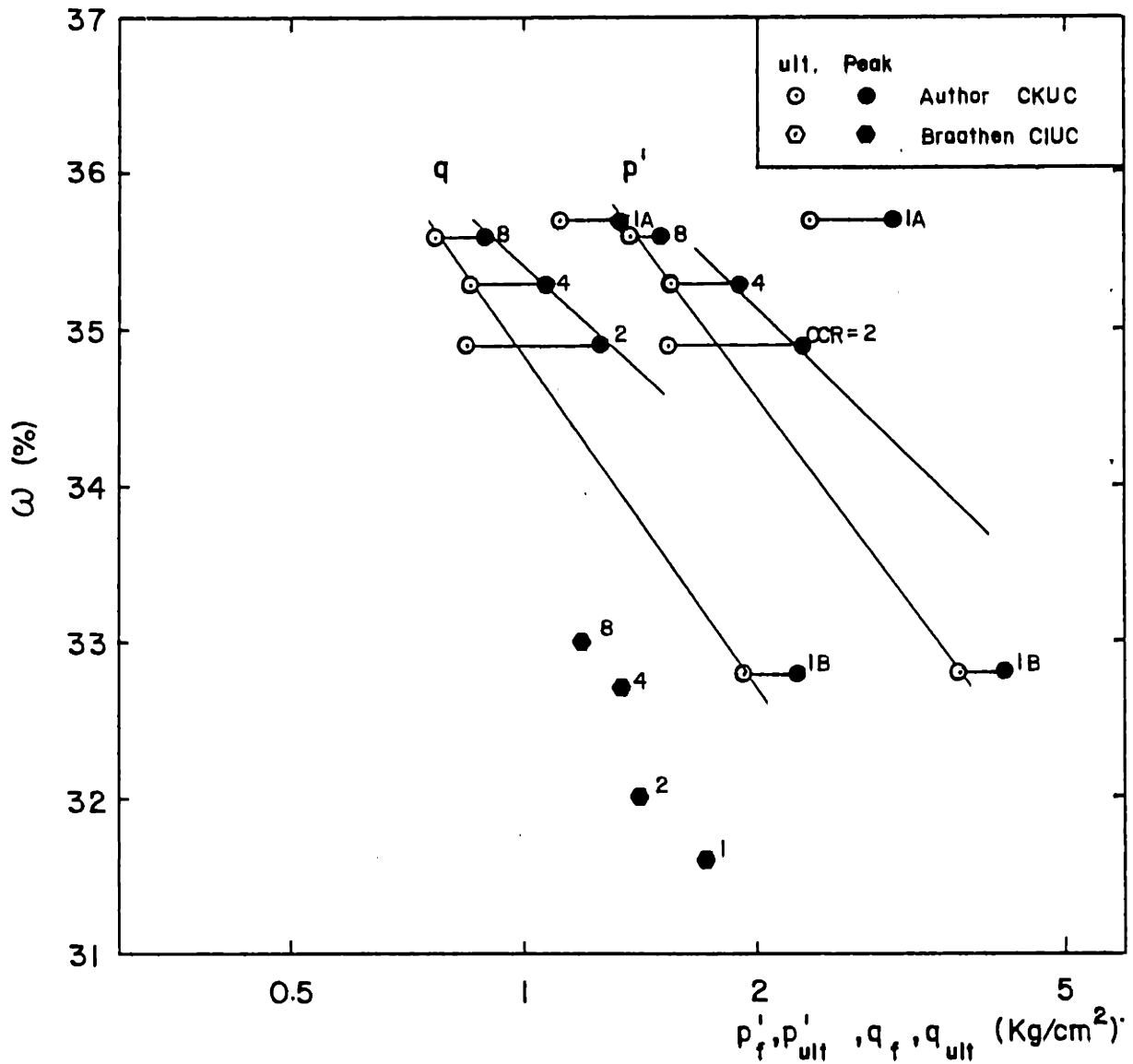


Figure 5.39 Shear strength and normal stress at peak and ultimate conditions vs water contact for anisotropically consolidated samples

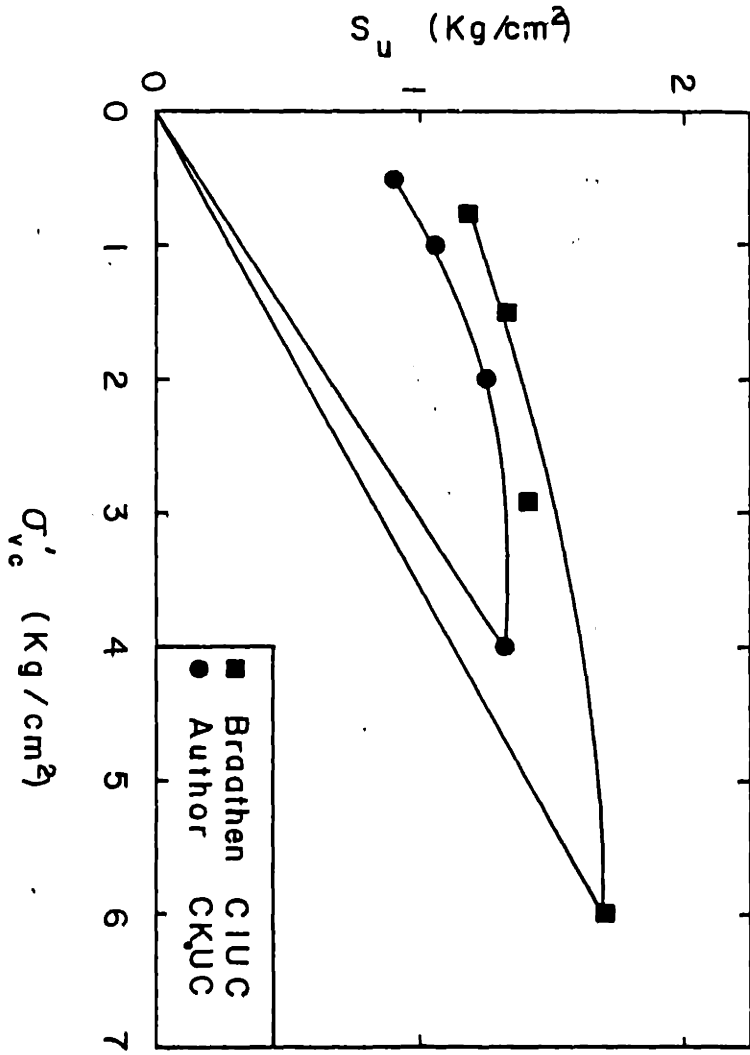


Figure 5.40 Peak undrained shear strength for isotropically and anisotropically consolidated samples

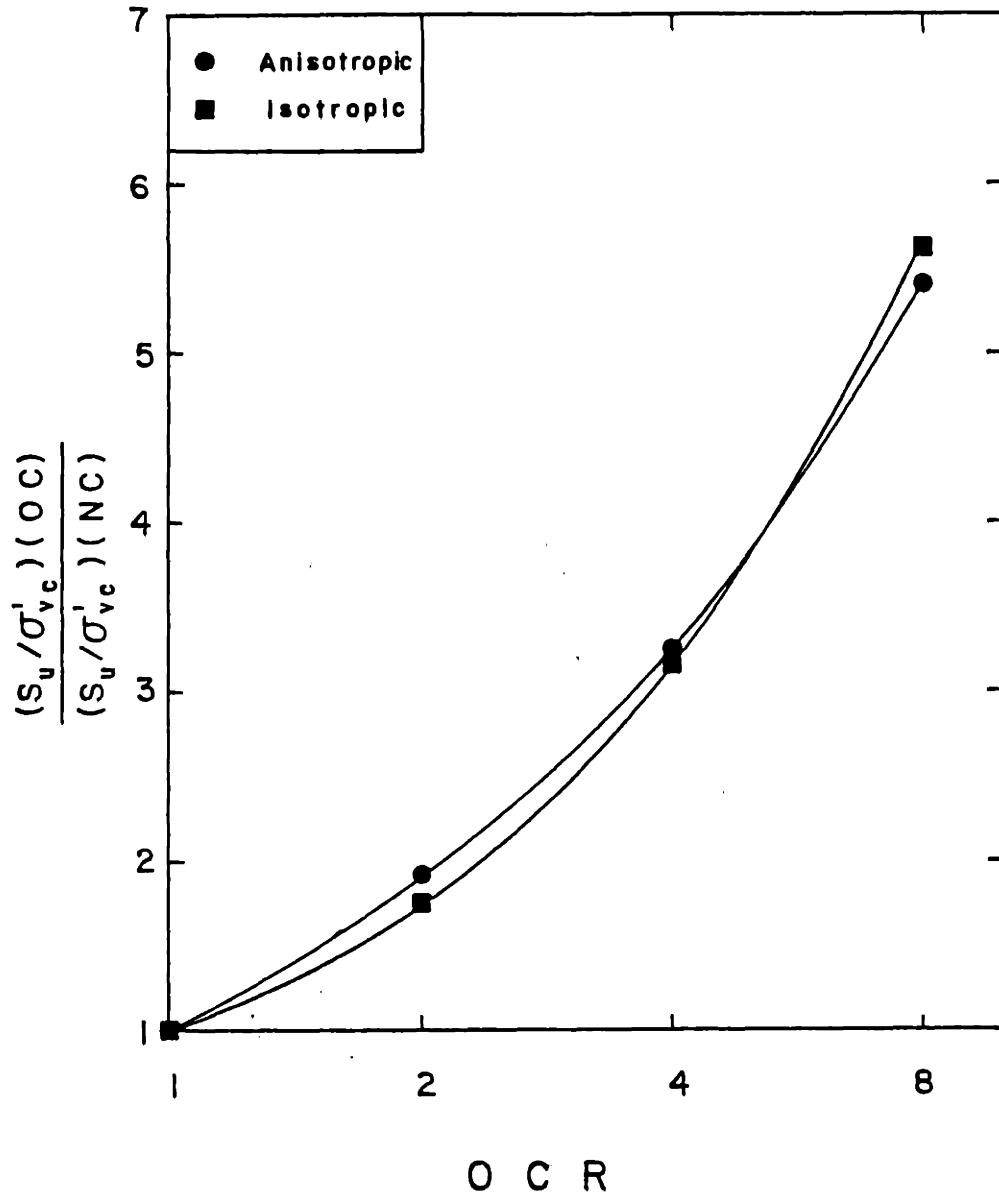


Figure 5.41 Relative increase in undrained strength ratio with OCR from anisotropically and isotropically consolidated samples (replot of data in Fig. 5.18)

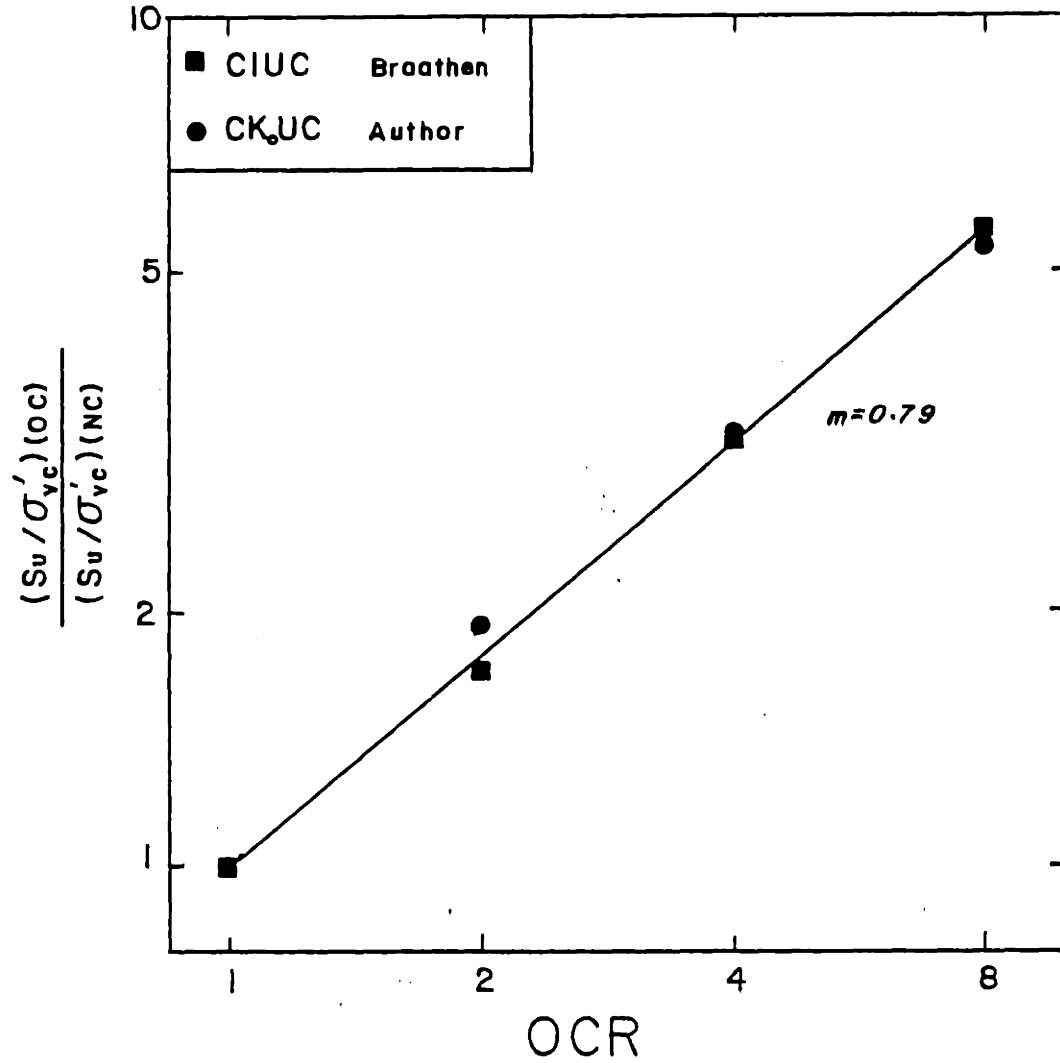


Figure 5.42 Relative increase in undrained strength ratio with OCR for isotropically and anisotropically consolidated samples (log-log scale)

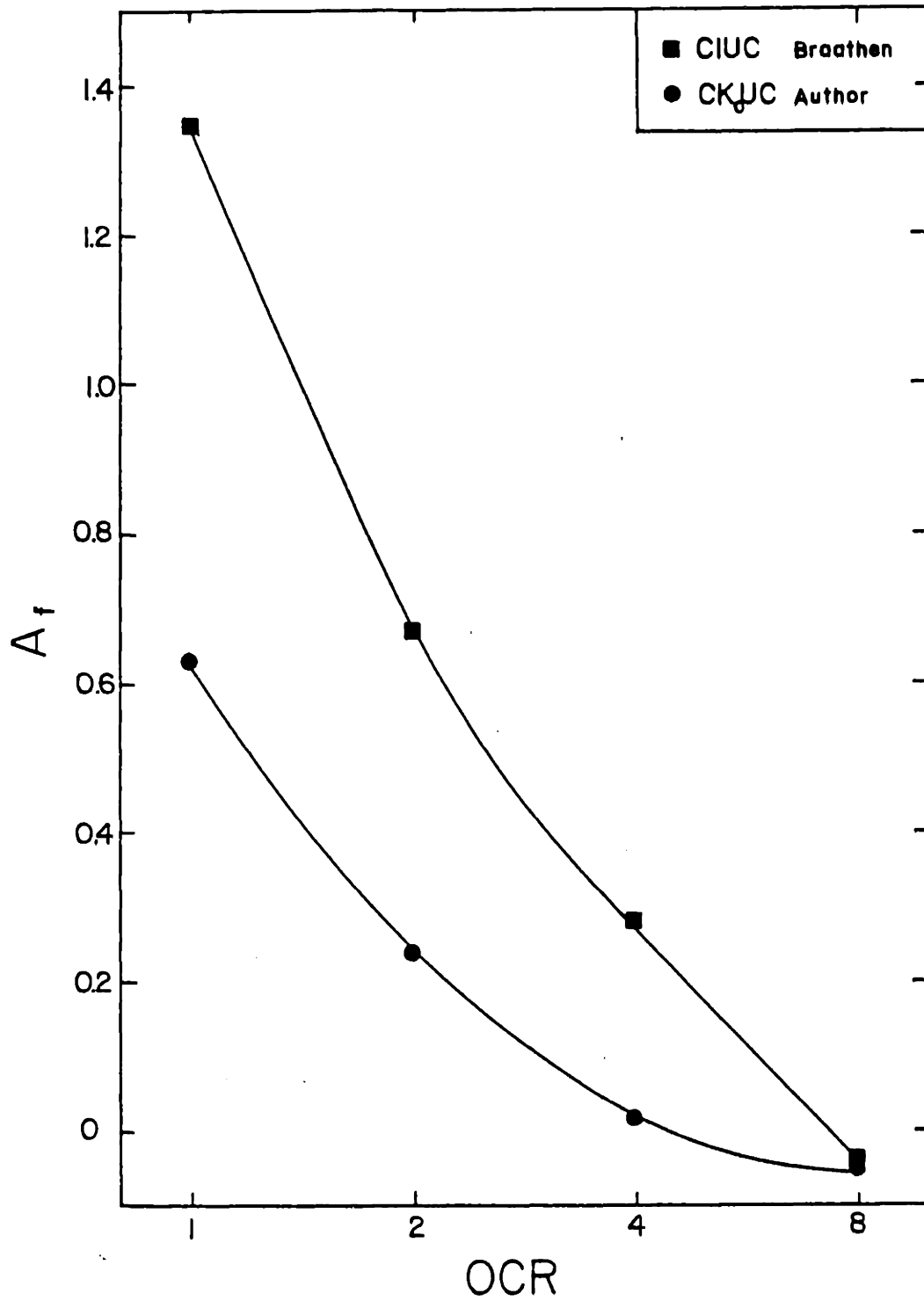


Figure 5.43 Variation in A_f vs OCR for isotropically and anisotropically consolidated samples

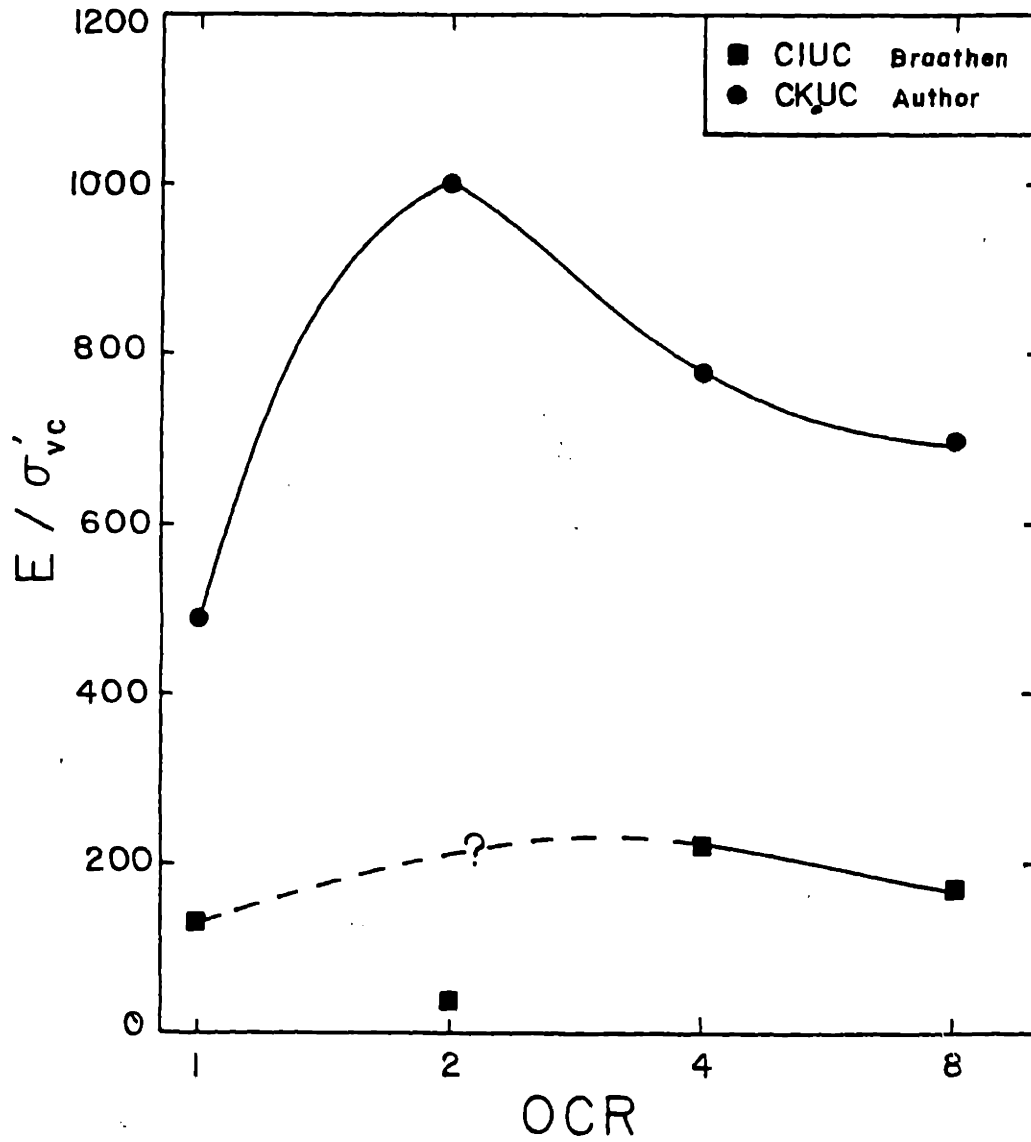


Figure 5.44 Variation of normalized undrained secant modulus with OCR for isotropically and anisotropically consolidated samples ($\Delta q / \Delta q_{max} = 50\%$)

CHAPTER 6

COMPARATIVE BEHAVIOR OF BBC AND LCT

6.1 Basis and Scope of Comparison

Chapters 4 and 5 present and discuss consolidation and undrained characteristics of resedimented Boston Blue Clay (BBC*). A conceptual framework based on experimental data compiled since 1961 (see Chapter 2 for a brief overview) is suggested. Although the guidelines sketched in these chapters are representative only of BBC, it would be interesting to apply the results to a global framework for soil behavior.

This chapter compares the behavior of resedimented Boston Blue Clay (BBC*) to reconstituted Lower Cromer Till (LCT). LCT has been chosen because of the comprehensive available data on this clay obtained from an exhaustive testing program conducted by Gens (1982) and Hight (1983). Moreover, the index properties and testing procedures of both clays are very similar, providing a solid basis for comparison.

6.2 Background on BBC and LCT

The large variability of natural Boston Blue Clay and Lower Cromer Till and the large amount of soil needed for research required the use of resedimented (or reconstituted) samples. The soils were initially sieved**, discarding the larger diameter fractions. The approximate mineralogy of both clays is compared in Table 6.1. Both clays have a high quartz concentration, with illite dominant in the clay fraction. The salt concentration is different, but its effect on the undrained behavior of BBC is negligible (Bailey, 1961). The average index properties and grain size

* BBC refers to resedimented Boston Blue Clay unless otherwise noted. The same is true for reconstituted Lower Cromer Till (LCT).

**A #40 sieve (0.4 mm) was used for BBC whereas LCT discarded the grains larger than the #10 sieve (2 mm).

distributions for both clays are presented in Table 6.2 and Fig. 6.1, respectively. The large proportion of silt in LCT is largely responsible for the lower plasticity and, to a lesser degree, of cementation.

The preparation of BBC samples was discussed in previous sections with details in Germaine (1982). The method followed for LCT samples was generally similar, except for the following. During mixing and sedimentation no vacuum was applied, and no further saturation check seems to have been done. The values of $B (= \Delta u / \Delta \sigma_v)$ were determined, and in order "to standardize the measurements, the pore pressure observed 10 minutes after the pressure application was used for the calculation of the parameter. In all cases, the measured values of B were higher than 0.97" (Gens, 1982). The 10 minute interval reported is significantly higher than the standard 15 to 30 second interval used at MIT for the measurement of the B value. Lateral drainage was provided by means of four spiral filter strips when only lubricated ends were used. Filter strips were unnecessary when porous stones were employed, since the permeability was high enough to ensure rapid dissipation of pore pressures. In addition to these differences, three sample preparation methods were used: 1) Type A samples, consolidated anisotropically in a large oedometer (229 mm diameter); 2) type I samples, consolidated isotropically in a large triaxial cell (6 in.=152 mm diameter), and; 3) type SS samples, consolidated in the standard triaxial cell (1.5 in.=38 mm diameter) from a slurry condition. This last method had the advantage of avoiding disturbances due to sampling but lacked good control of the sample geometry.

The above differences in testing and sampling procedures of BBC vs LCT are believed to be insignificant and should not affect the undrained

behavior of the two clays.

6.3 Volumetric Behavior

Thixotropy and its effects on compression curves for BBC have been discussed in Chap. 4. The preconsolidation pressure, $'_p$, and the value of K_0 increased with storage time. The effect on $'_p$ was measured by O'Neill (1985) and the trend for K_0 was estimated on the basis of measurements during anisotropic consolidation. LCT showed no trend with storage time, probably due to short storage duration. A maximum storage period of 2 months was reported by Gens (1982).

Although BBC showed significant sensitivity to thixotropy, these effects are not included in the following discussion.

The isotropic and anisotropic (K_0) consolidation behavior of BBC and LCT is summarized in Figs. 6.2 and 6.3 for the virgin compression and swelling ranges, respectively. The following should be noted:

1) The lower plasticity of LCT explains its lower compressibility, C_c , which is about two times smaller than for BBC (0.152 vs. 0.334). These values of C_c are in reasonable agreement with existing empirical correlations with the plasticity index.

C_c	Meas.	Wroth*	Mayne**	Remarks
BBC	0.334	0.278	0.333	PI=20%, $G_s=2.70$
LCT	0.152	0.172	0.283	PI=13%, $G_s=2.65$

2) The position of the virgin compression line (VCL) depends on the initial water content (or the initial void ratio).

$$* C_c = \frac{G_s \cdot PI}{2}$$

$$** C_c = (PI + 26) / 138$$

3) Neither material has a unique $e\text{-log}\sigma'_v$ or $e\text{-log}\sigma'_{oct}$ relationship with respect to the type of consolidation. The scatter produced from triaxial tests on BBC is large, but the average value plots to the left of the $K=1$ VCL, as does LCT data. This scatter has been discussed in previous sections and is a combination of thixotropy and experimental limitations.

The average compression curve of the oedometer tests OED-1 and OED-6* (O'Neill, 1985) plotted in Fig. 6.2 are identical to the triaxial curves of LCT. OED-1 and OED-6 have been chosen because of their short storage times (7-8 days), for which the effects of thixotropy are believed to be limited.

4) The swelling lines are non-linear in both cases, concave upwards. The higher compressibility and plasticity of BBC result in greater elastic response.

In order to illustrate the differences in behavior of anisotropically consolidated samples of BBC and LCT, the particular case of K_0 -consolidation was considered. K_0 was found to be equal to 0.47 for BBC and 0.5 for LCT in the normally consolidated range. These values compare fairly well to Jaky's (1948) expression, $K_0=1-\sin\phi'$ and to the revised formulation by Mayne and Kulhawy (1982), $K_0=1-0.987 \sin\phi'$:

Soil	ϕ'	K_0		
		Meas.	Jaky	M.& K.
BBC	33	0.47	0.45 ⁵	0.46
LCT	30	0.50	0.5	0.51

* OED-1 and OED-6 are extracted from Fig. 3.6 in O'Neill (1985). An initial void ratio $e_0=1.19$ and a K_0 value of 0.47 were assumed in order to draw the average curves in terms of vertical and mean stress as functions of the void ratio.

The determination of K_0 on unloading was more difficult due to the stiff response of low plasticity clays. The strains measured were of the same order of magnitude as the sensitivity and the stability of the measuring equipment. An empirical relation was therefore used for BBC (Schmidt, 1966); interpolation from varying unloading paths (Andrawes and El-Sohby, 1973) set the value of K_0 for LCT. The relationship between K_0 and OCR for the unloading paths is shown in Fig. 6.4.

6.4 Undrained Behavior

The similarities and differences in the undrained behavior of Boston Blue Clay and Lower Cromer Till are based on results of triaxial tests. The following overconsolidation ratios were selected: 1, 2, 4 and 8 for BBC; and 1, 2, 4 and 7 (or 10) for LCT. The strain rates during shear were approximately the same: 0.0067 mm/min for BBC and 0.006 mm/min for LCT.

Since both soils were prepared in a controlled environment, samples of the same soil at the same OCR should show an identical behavior, when normalized by the consolidation pressure, σ'_{vc} . This normalization hypothesis has been carefully checked by Gens (1982) on LCT, and further confirmed by the test results. The available results for BBC have been discussed in sections 5.2 and 5.3, and show the validity of the normalization hypothesis despite the scatter observed. This concept is the basis of the SHANSEP procedure (Ladd and Foott, 1974) followed by the author and implies that the effective stress paths and the stress-strain curves, when normalized by σ'_{vc} , should be uniquely related to OCR for a given clay. For good control of OCR, samples should be consolidated beyond the preconsolidation pressure, σ'_p , in order to recover the normally consolidated behavior. Gens (1982) found that it was necessary to

consolidate the samples to a stress of at least $1.875 \sigma'_p$ for isotropic consolidation, and $1.75 \sigma'_p$ for anisotropic consolidation to achieve full reconsolidation.

In addition, the uniqueness of the relationship between water content (or void ratio) and undrained shear stress has been carefully examined for LCT. A similar behavior applies to BBC (Chapter 5), although scattered. Water content, rather than void ratio, will be used in the following discussion.

6.4.1 Isotropic Behavior

The isotropic behavior of LCT will be drawn from the ICI series of Gens (1982). These tests were run for the specific purpose of checking the normalization hypothesis. "Because a substantial number of tests had to be carried out...the consolidation stage was carried out in one step" (Gens, 1982). This procedure had the effect of increasing the volume change during consolidation, resulting in a lower preshear water content.

The effective stress paths and the stress-strain curves, normalized by the maximum consolidation stress, are compared in Figs. 6.5 and 6.6, respectively. Although following the same trends, the behavior of the two clays is quite different. The effective stress envelope at ultimate stress is seen to be lower for LCT, but the normalized undrained strengths, s_u/σ'_{vc} , plotted in Fig. 6.7, are slightly higher. Both observations are a direct consequence of the difference in pore pressure development during undrained shear. LCT develops higher pore pressure than BBC for the normally consolidated samples, where shearing induces positive pore pressures and the sample tends to compress. At high OCR, LCT samples tend to expand more than BBC. These differences are illustrated in Fig. 6.5,

where the LCT samples are more structurally deformable in the corresponding stress environment. This behavior can be explained on the microscopic level. The scale and volume of the granular particles in LCT are much larger than in BBC, resulting in lower interparticle forces. Hight (1983) uses an idealized model for LCT in which a "granular framework" has its sand grains connected by "clay bridges", and where the void space is infilled by a "clay matrix". This complex structure gives rise to inhomogeneities in the rate of equalization of pore pressure. This rate is determined by factors such as: the coefficient of consolidation c_v , the pore pressure gradients and the dimensions of the clay bridges. Because BBC contains silt particles, the same framework would not be applicable. Nevertheless, bonding forces generated by the thickness of the double layers in BBC exhibit the same type of features, although less pronounced than LCT. This, coupled with the overall finer matrix of BBC, results in larger viscous effects and less particle reorientation.

On the other hand, the stress-strain relationships are quite similar for both clays, as seen in Fig. 6.6. The small strain region is not well defined for LCT because of the uncertainty associated with data digitization.

The extension mode of failure investigated by Gens (1982) does not have its counterpart for BBC, since the available tests on LCT have been run at a slower rate (0.0005 mm/min) with frictionless ends.

6.4.2 Anisotropic Behavior

The compression behavior only will be compared because different strain rates were used in extension tests. A standard rate of 0.0005 mm/min was generally employed, with frictionless ends for most tests run by

Gens (1982). The faster rates were used only to check the normalization hypothesis, discussed earlier. Moreover, Gens showed that variations in strain rates affected the stress paths before and immediately after peak, with ultimate conditions remaining quite similar. The comparisons to faster tests will therefore involve a great deal of uncertainty. However, Gens's extension tests will be presented very briefly at the end of this section.

The tests run by the author will be compared to the test series AC1 run by Gens (1982). The samples of LCT were anisotropically consolidated to a common maximum consolidation stress ($\sigma'_{vm}=3.5$ ksc, $K_0=0.5$) and swelled to varying values of OCR (1, 1.5, 2, 4 and 7). The effective stress paths and the stress-strain curves are normalized by the maximum consolidation stress, σ'_{vm} in Fig. 6.8 and 6.9 respectively. The normalized undrained strength, δ_u/σ'_{vc} , are plotted in Fig. 6.10.

Although the effective stress paths are not identical, both clays appear to exhibit a very similar behavior.

1) The development and equilibration of the shear-induced pore pressure is a function of OCR as discussed in Chap. 5. LCT exhibits more rounded stress paths, suggesting that the pore pressure dissipation is more gradual. This is particularly observed before samples reach their peak strength.

2) The effective stress envelope and the strengths mobilized are lower in the case of LCT. However, the deviator stress difference at peak, Δq_{max} , is identical in the two clays. The lower strength of LCT can therefore be directly correlated to a lower initial deviator stress, since its consolidation stress ratio (K_0) is higher for all OCR's.

3) The characteristic loop observed in test CK₀UC2 on BBC also occurs for LCT at OCR's of 1.5 and 2. For a better understanding of this feature,

Gens ran undrained tests at a slower rate (0.0005 mm/min) on samples consolidated to the same OCR. He found that the shape of the effective stress path is dependent on the rate of shearing and the differences occur before and immediately after peak. The loops observed at the lightly overconsolidated sample disappeared at the slower rate accompanied by a decrease in the undrained shear strengths. Another possible explanation for the loops is provided in Chapter 7, where the normally consolidated test CKUC1 is studied in detail. A loop may form as a result of a lower consolidation stress ratio K .

4) At high OCR's, the samples of BBC were observed to "collapse," as a result of the sudden reversal of the effective stress paths. This is not observed for LCT, as continuous hardening is seen for the test at an OCR of 7.

5) The ultimate stresses (defined by the value of the shear stress at an axial strain of 20%) for LCT are dependent only on the water content (Gens, 1982). This behavior is not observed for BBC, probably because of failure plane development at large strains.

6) The significant undrained brittleness observed on the K_0 -consolidated BBC samples is more apparent than for the LCT samples. The lower value of K_0 used for BBC may be the cause of the increase in brittleness susceptibility.

Since both clays show similar trends for anisotropically consolidated samples sheared in an undrained compression mode, the same type of agreement may be expected for extension tests. The comparison between compression and extension tests made by Gens on samples anisotropically consolidated at the slower strain rate of 0.0005 mm/min shows that, compared to extension, undrained compression shearing:

1) decreases the value of the effective stress friction angle, ϕ' , measured at the ultimate state. Same trends are noted for other clays with various differences (see discussion in section 5.3.3).

2) significantly increases the undrained shear strength.

3) significantly increases the value of stiffness, measured at a stress level $\Delta q/\Delta q_{\max}=50\%$, by almost a factor of 10.

MINERAL/SUBSTANCE	% by volume
Quartz	≈ 15-20
Chlorite	≈ 5
Illite	≈ 30-45
Iron Oxides	≈ 1.5-3
Organic Matter	< 1

Table 6.1a Mineralogy of Resedimented BBC (Mitchell, 1956 quoted by Germaine, 1982)

Mineralogy

<u>Whole rock</u>	Major (>30%) :	quartz
	Minor (10-30%) :	calcite, feldspar, clay minerals
	Trace (<10%) :	mica (muscovite type)
<u>Clay fraction</u>	Major (>30%) :	calcite, illite
	Minor (10-30%) :	smectite, kaolin, chlorite
	Trace (<10%) :	quartz, feldspar

Pore water chemistry

Cl ⁻	0.66	g/l
Na	0.4	g/l
K	20.28	mg/l
Ca	40.56	mg/l
Mg	233.22	mg/l
SO ₄ ⁻²	0	

Carbonate content 4 - 8%

Table 6.1b Mineralogy of Reconstituted LCT (Gens, 1982)

Table 6.1 Mineralogy of BBC and LCT.

Parameter	BBC	LCT
Classification (US)	CL	CL-ML
G_S	2.78	2.65
LL	42.0	25.0
PL	21.0	13.0
PI	21.0	12.0
$C_C = \frac{\Delta e}{\Delta \log \sigma'_v}$	0.368	0.157
$C_S = \frac{\Delta e}{\Delta \log \sigma'_s}$ (1 cycle)	0.027	0.013

Table 6.2 - Index Properties of BBC and LCT

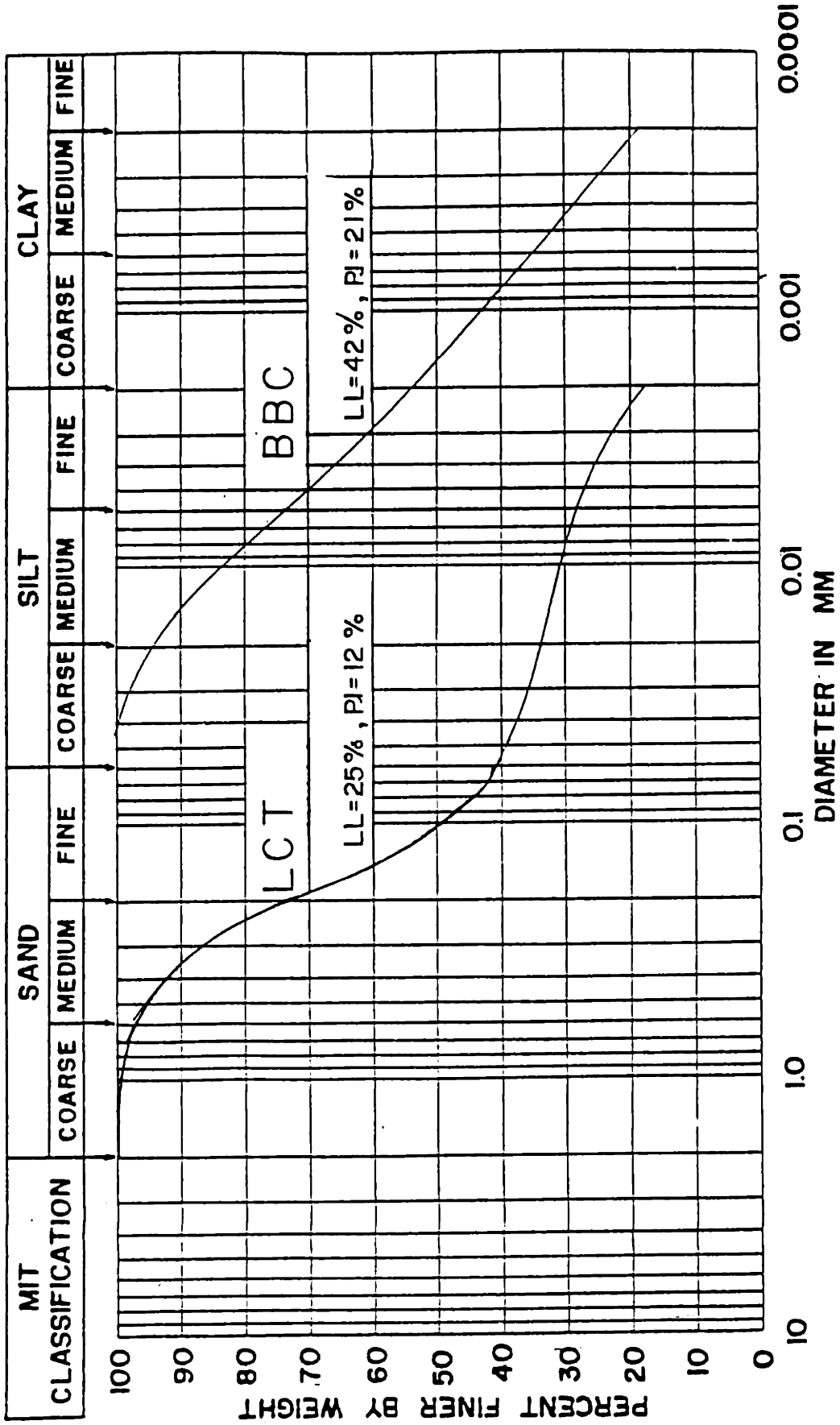


Figure 6.1 Grain size distribution of BBC and LCT

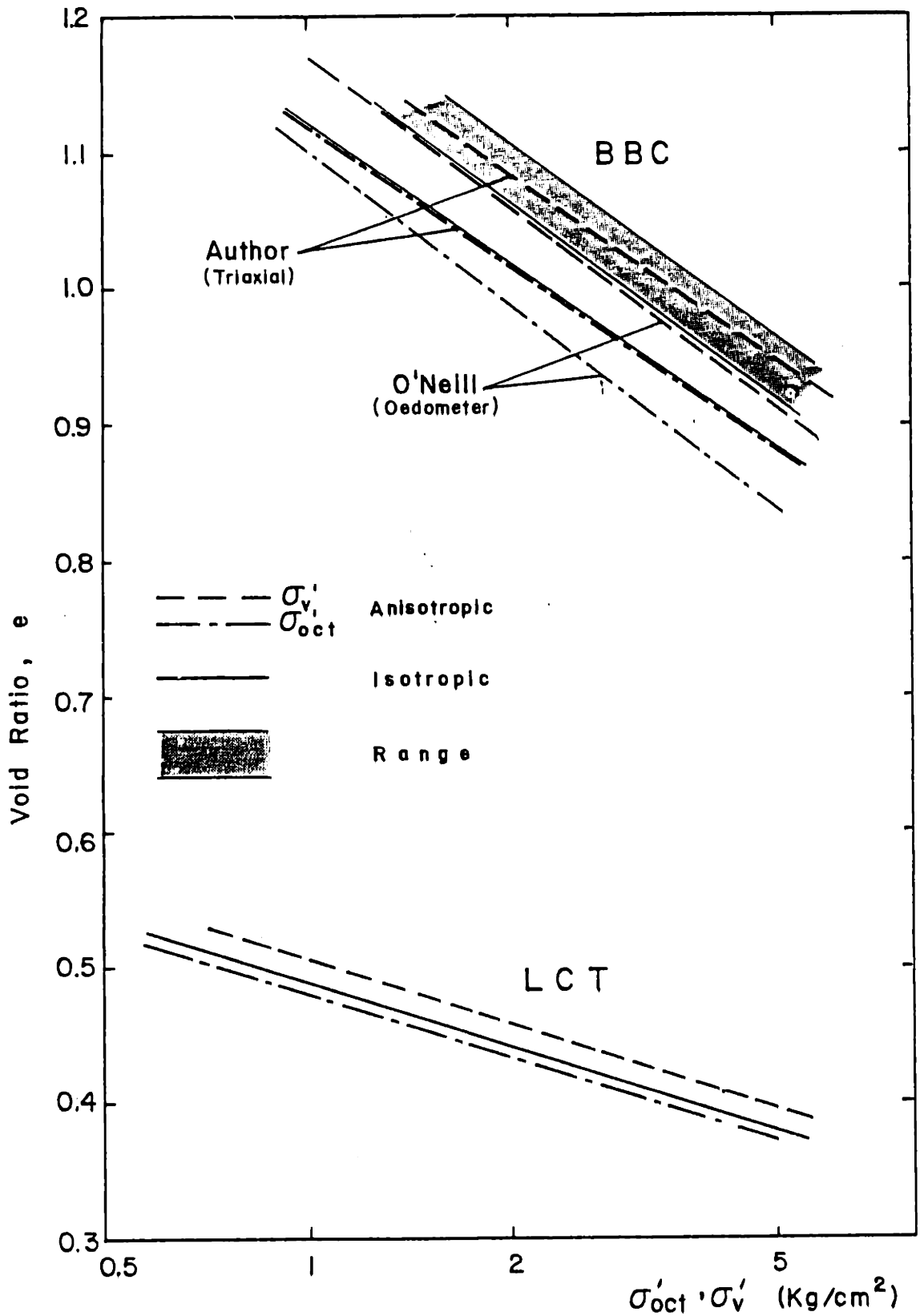


Figure 6.2 Virgin compression curves of BBC and LCT

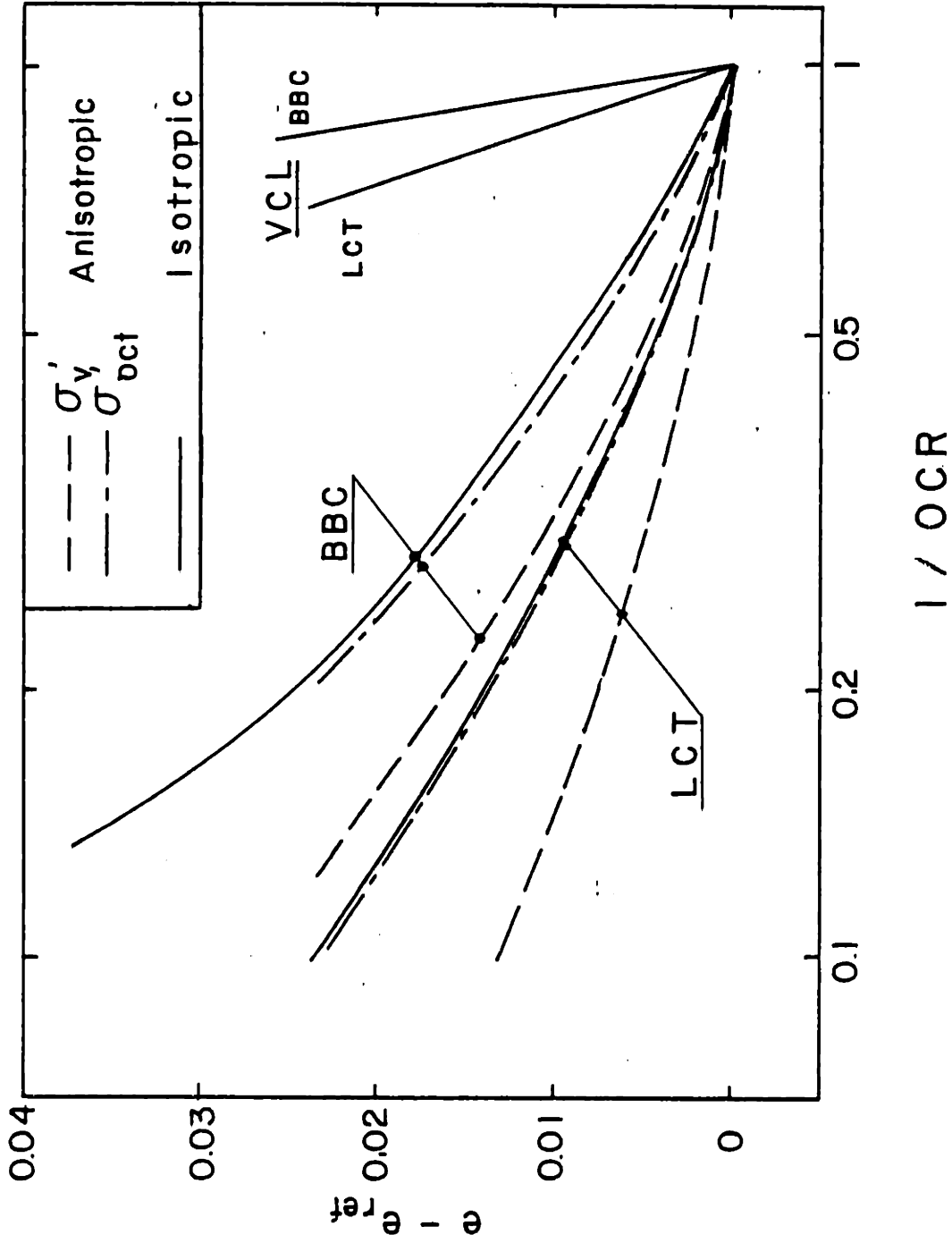


Figure 6.3 Swelling curves of BBC and LCT

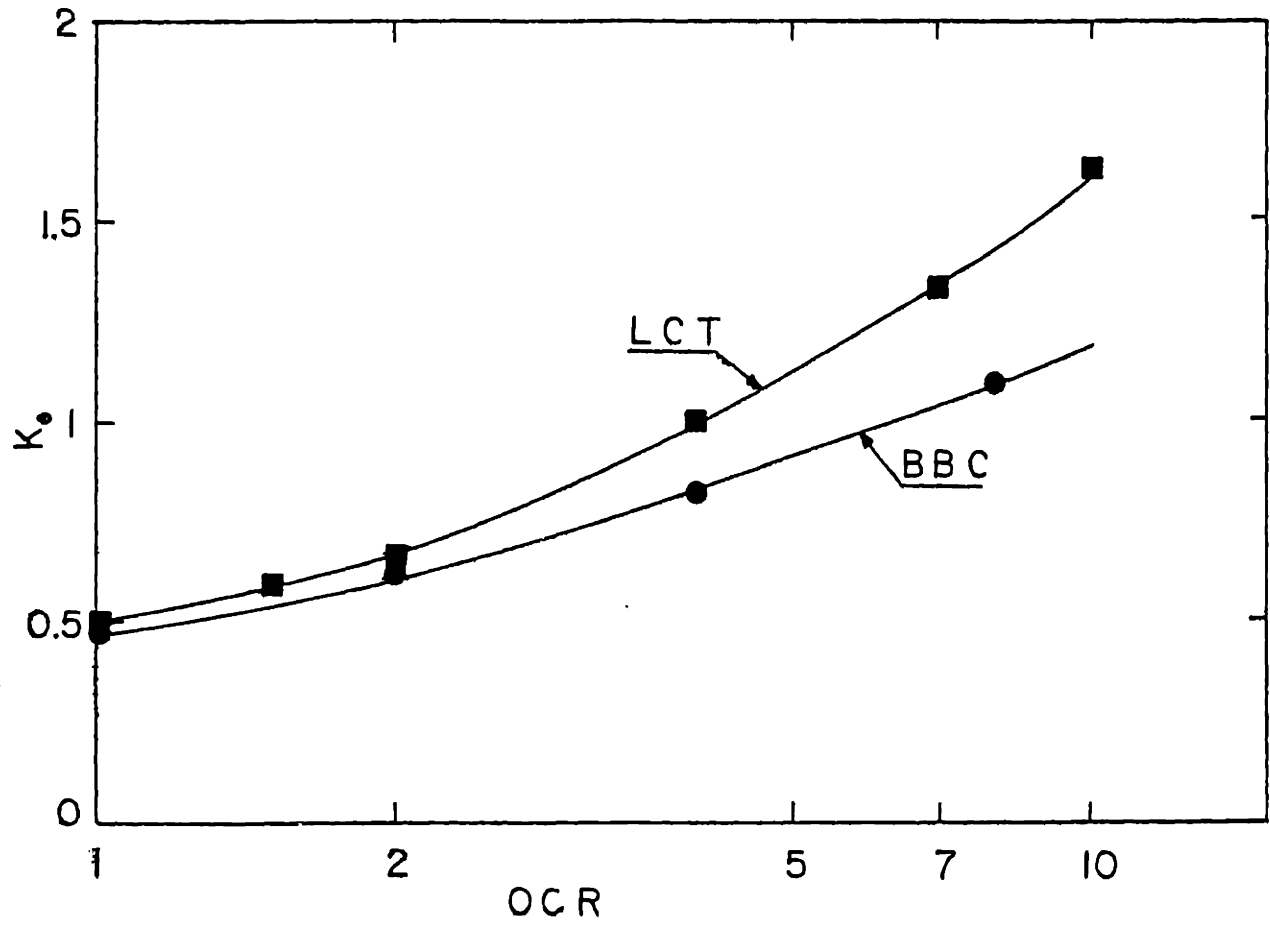


Figure 6.4 K_0 vs OCR (unloading) for BBC and LCT

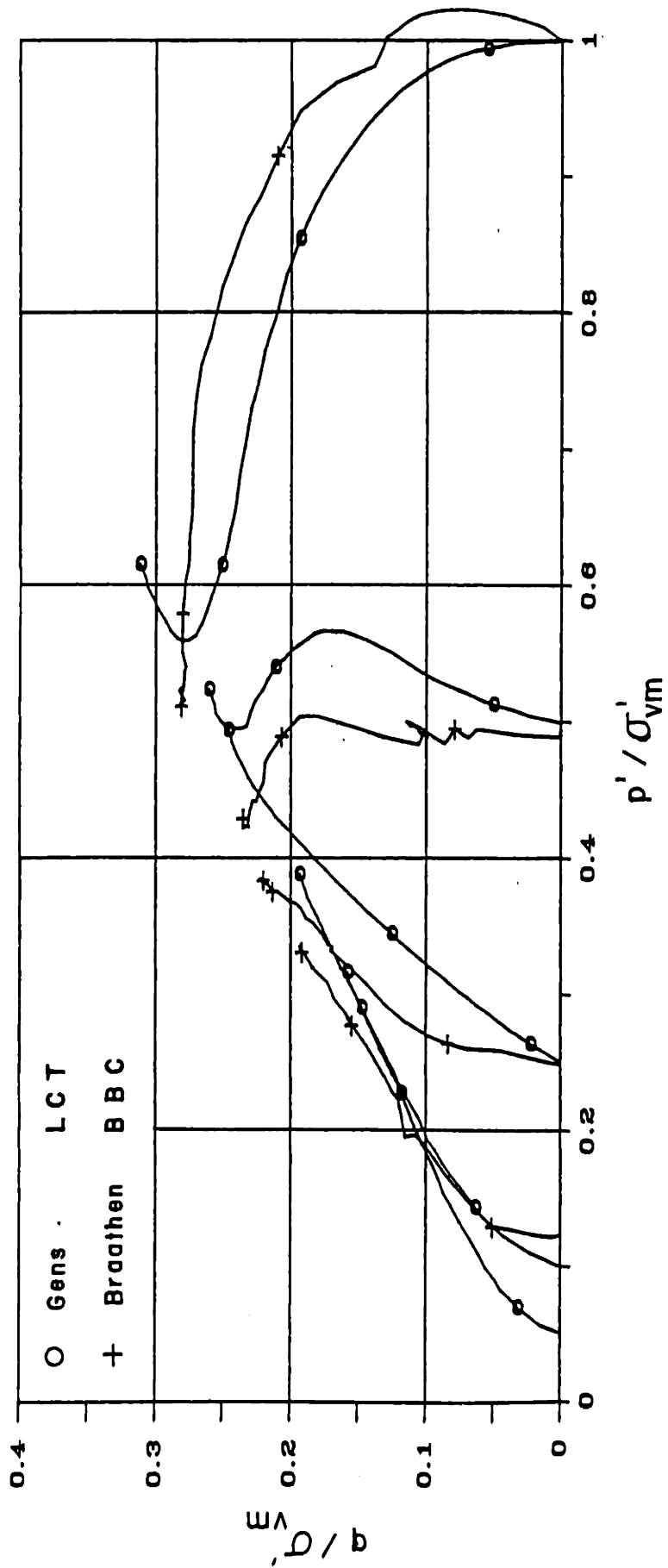


Figure 6.5 Stress paths for CIUC tests on BBC and LCT

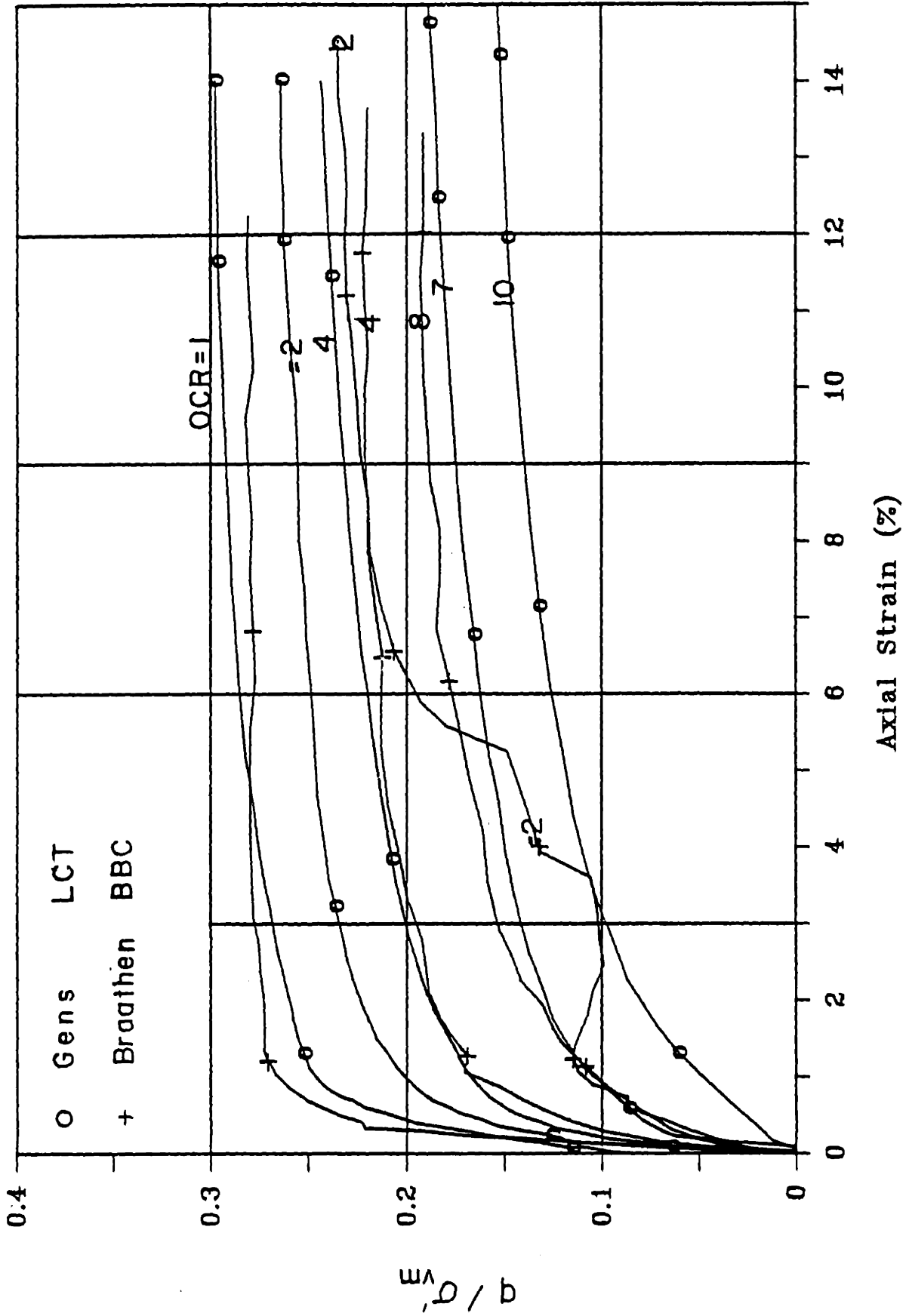


Figure 6.6 Stress-strain curves for CIUC tests on BBC and LCT

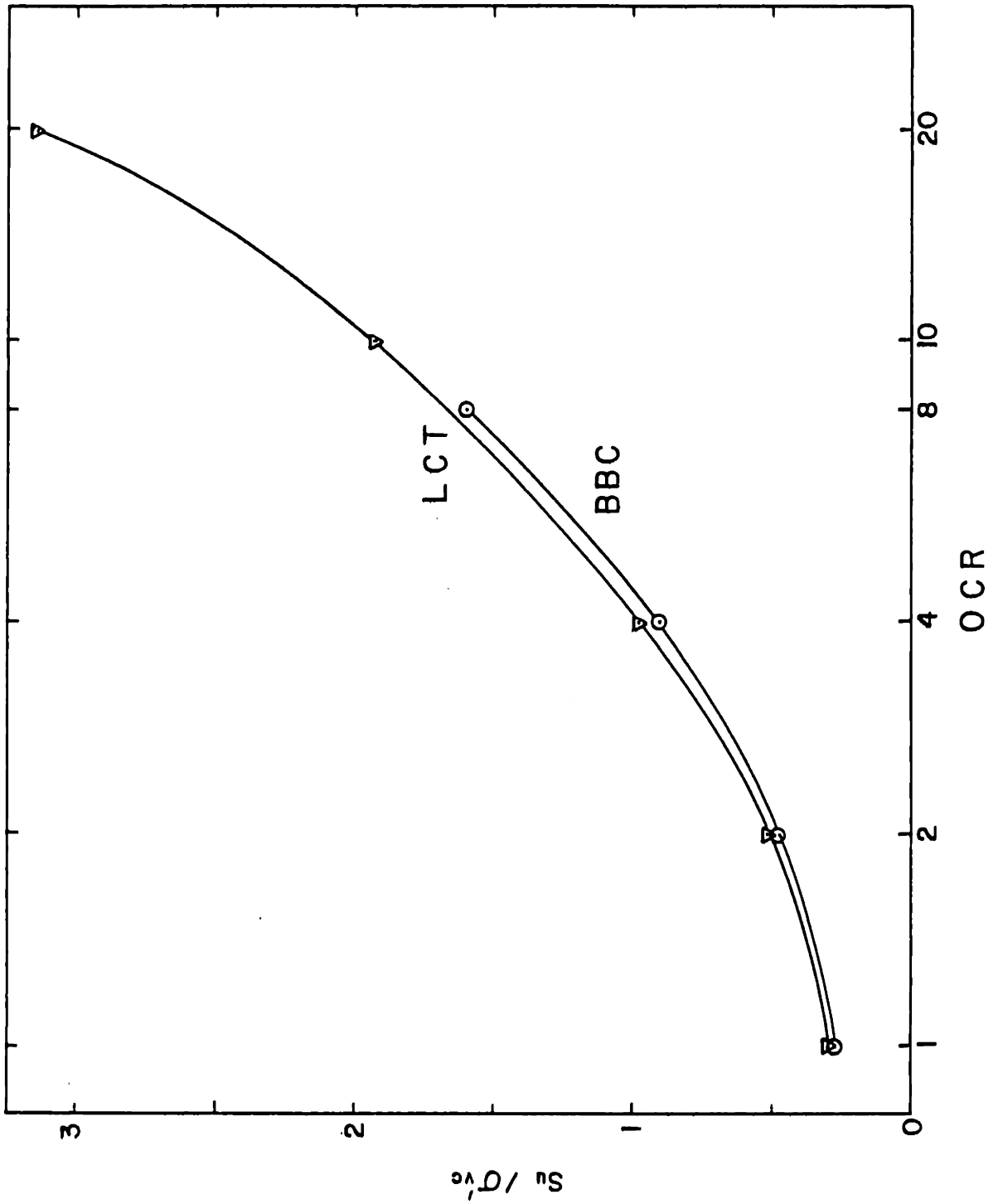


Figure 6.7 Normalized undrained strength for CIUC tests on BBC and LCT

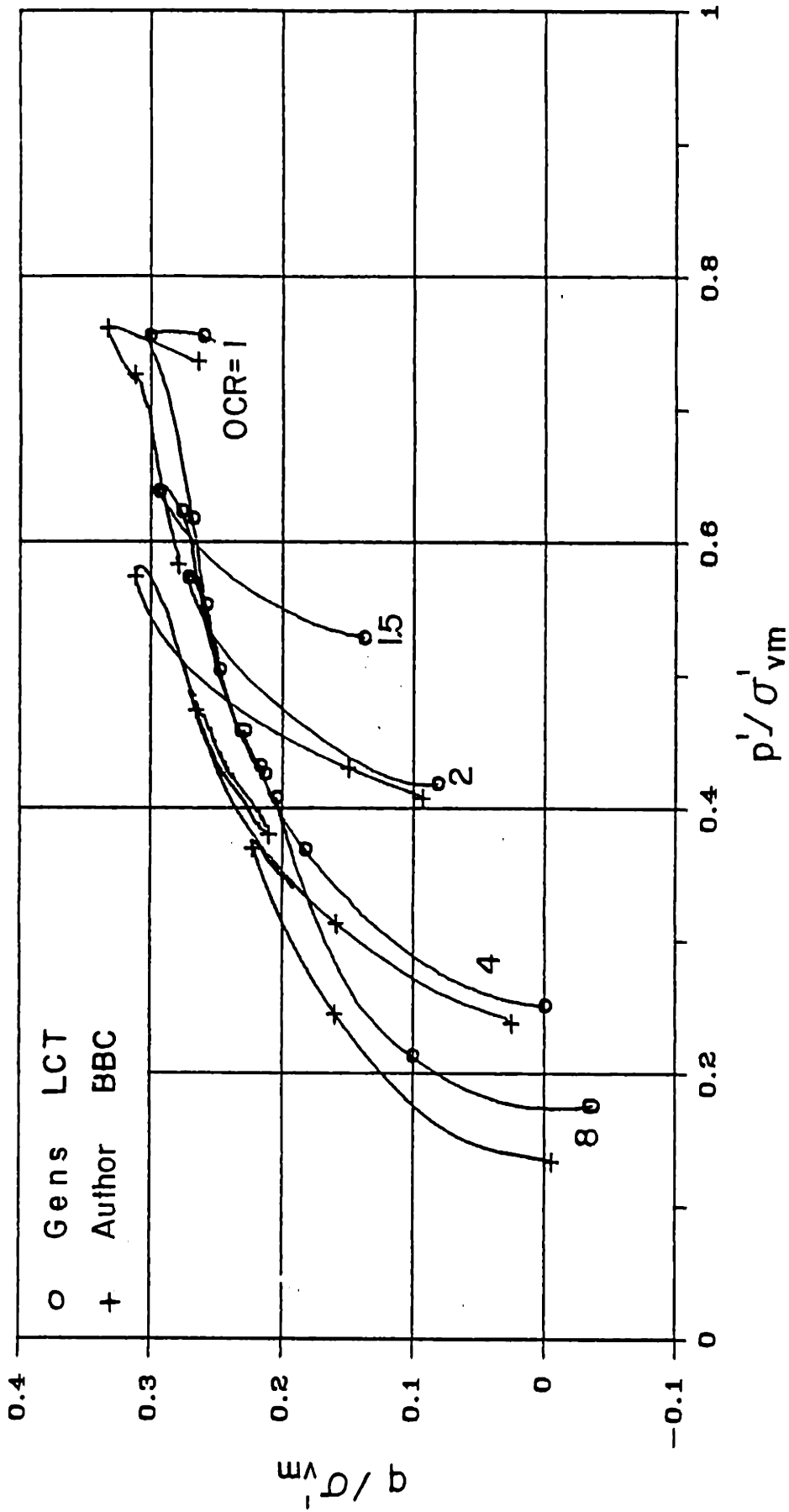


Figure 6.8 Stress paths for CK₀UC tests on BBC and LCT

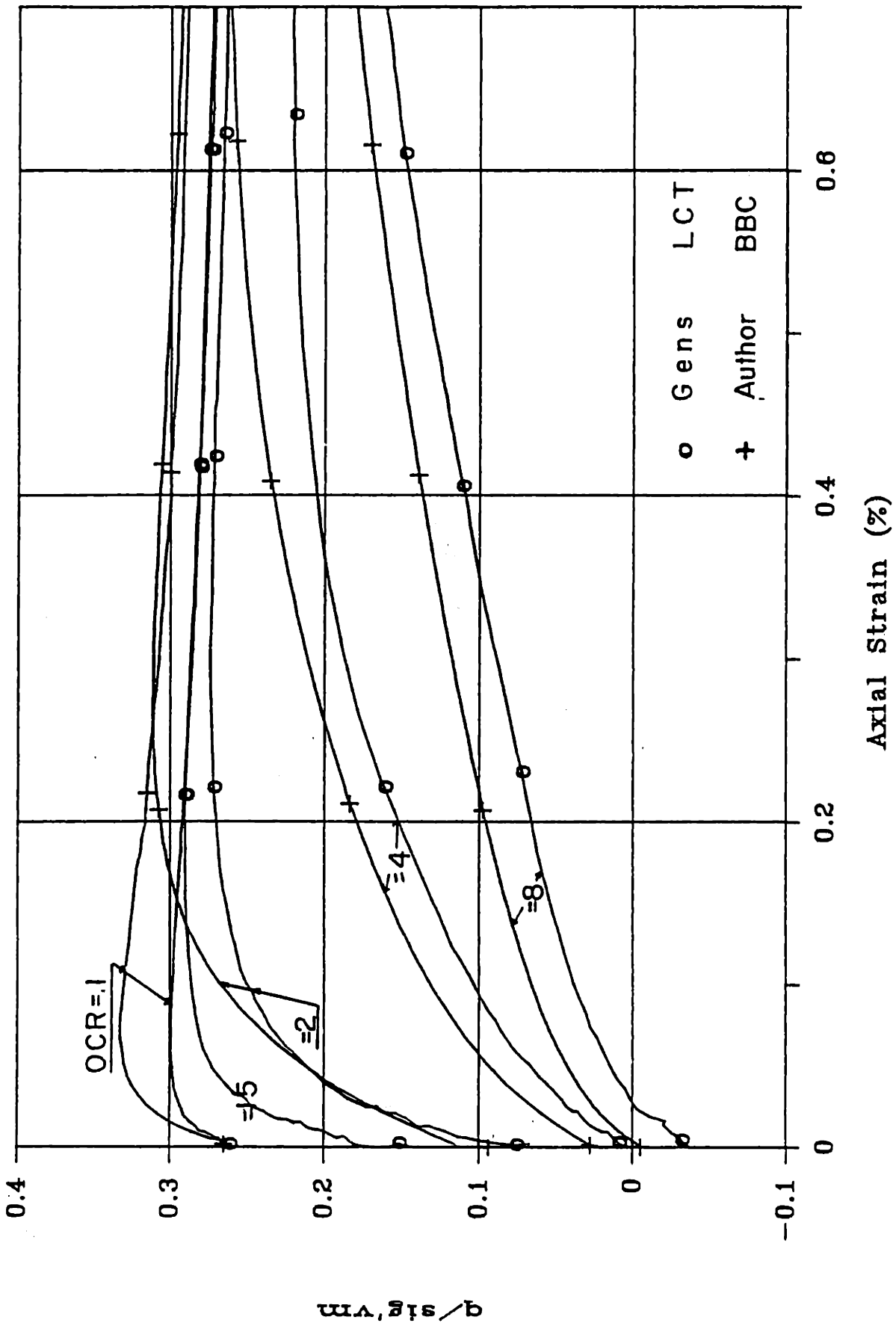


Figure 6.9 Stress-strain curves for CK_{0JG} tests on BBC and LCT

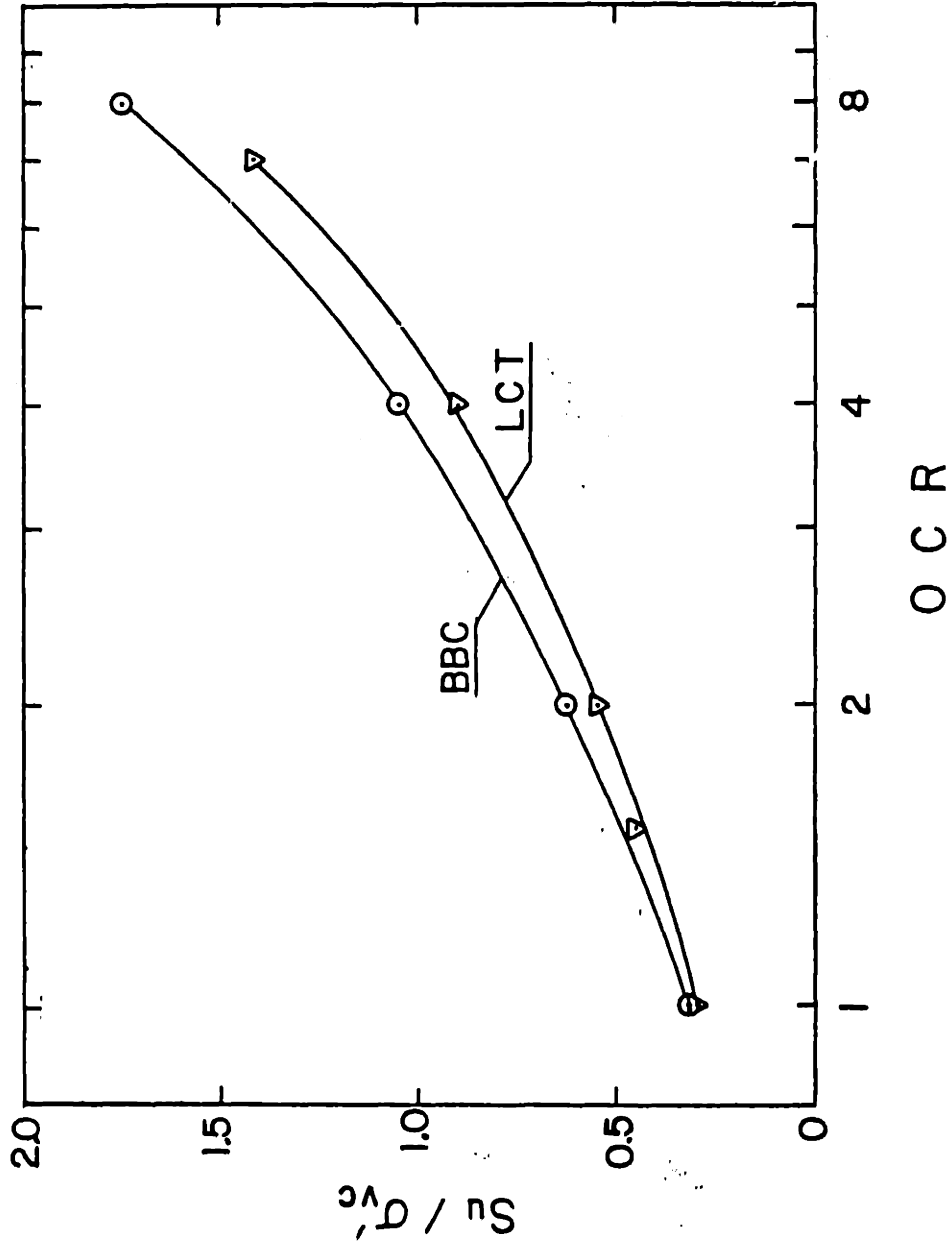


Figure 6.10 Normalized undrained strength for CK_{OUC} tests on BBC and LCT

CHAPTER 7

SPECIAL TESTS

Two unconventional tests were run on Resedimented Boston Blue Clay in the standard MIT triaxial cells. Both addressed very specific questions about the undrained behavior of BBC, specifically:

1) What are the behavioral characteristics of the soil after it has been sheared in an undrained mode beyond its peak resistance? This question was addressed by test CK_0UC1 , run on a normally consolidated sample. In this test, the first stage of undrained shearing beyond the peak was discussed in previous chapters. The second stage is discussed below.

2) What is the behavior of overconsolidated BBC during undrained cyclic triaxial shearing? Test $CK_0U-Cyc-4$ was cyclically sheared at a constant stress level. The undrained cyclic behavior of BBC in Direct-Simple-Shear is treated in detail by Malek (1986).

7.1 Test CK_0UC1

This test was performed to investigate drained and undrained behavior at a low stress ratio, following undrained triaxial compression shearing of the soil beyond its peak shear strength. As shown in Fig. 7.1, the test involved the following stages:

Stage 1: Anisotropic consolidation with $K_0=0.47$ to a normally consolidated vertical effective stress of 4 kg/cm^2 (Path AB).

Stage 2: Undrained shear to an axial strain of 1.2% (Path BC). Results of stages 1 and 2 of the test were discussed earlier.

Stage 3: Anisotropic consolidation (or drained shear) at a constant low

value of the stress ratio, $K=0.34$, obtained at the end of stage 2. The usual procedure was followed during consolidation except that the Load Increment Ratio (LIR) was lowered to a value of 0.03 ± 0.01 . This reduction was necessary because of the unstable structure of the sample at this low stress ratio and its proximity to the failure envelope. The stress path was therefore followed very closely along $K=0.34$, to an effective vertical stress of 6 kg/cm^2 *. This stress level was considered sufficiently high to eliminate most of the effects of undrained shearing** during stage 2 and achieve a normally consolidated sample.

Stage 4: Undrained shear at the standard rate of 0.5% strain per hour until the limit of travel of the piston (Path DE).

7.1.1 Volumetric Behavior

One of the expected consequences of a variation in the stress ratio is the shifting of the compression curve. This shift was discussed in section 4.2, when comparing isotropic ($K=1$) to anisotropic ($K_0=0.47$) consolidation. It was found that a decrease in K was associated with a shift of compression curves to the left, if plotted in terms of mean stresses, σ'_{oct} . The inverse trend was true if vertical stresses were plotted instead. The positive pore pressures generated during shear resulted in a decrease of the effective stresses. The compression curve for the second consolidation ($K=0.34$) should therefore bend toward its theoretical position (to the right for vertical stresses, to the left for octahedral stresses). The compression curves are shown in Fig. 7.2 in stages 1 and 3 as before and after undrained shearing, respectively, as a function of the

* A larger stress was risky because of the apparatus limitations.

**Equal to 1.5 times the maximum past pressure as recommended by Ladd and Foott (1974).

volumetric strains. The problems created by the friction of the piston, discussed in section 4.1.1, obscured the predicted trends, but the compression curves of the two phases seem to be parallel to each other. The range covered by the stage 3 consolidation is not wide enough to draw definite conclusions. But, because of the apparent similarity of the two curves, one may infer that the undrained shearing in stage 2 did not involve significant structural changes of the soil. Therefore, the differences in the undrained behavior during the undrained shearing stages 2 and 4 are mostly due to differences in the stress ratio during consolidation.

7.1.2 Undrained Behavior

The results of undrained shearing in stages 2 and 4 in test CK₀UC1 are plotted in Fig. 7.3 through 7.5 together with test results reported by Braathen (1966) on isotropically normally consolidated resedimented BBC. The stress paths in Fig. 7.3 are normalized by the consolidation stress, σ'_{vc} . The stress strain data are shown in Fig. 7.4, where the small level of axial strain reached during stages 2 and 4 can be seen. Obliquity data (σ'_1/σ'_3) are also plotted as a function of strain in Fig. 7.5. A summary of the data at failure is provided in Table 7.1. Maximum obliquity or ultimate data are not given, since neither was reached during the tests.

The horizontal path, DD', noticed in Figs. 7.4 and 7.5 corresponds to undrained creep of the soil at constant deviator stress during the 10 hours following the end of stage 3 consolidation.

The increased brittleness associated with decreasing values of the consolidation stress ratio, K can be seen in the stress-strain curves of Fig. 7.4. The same trend is observed in results from Gens (1982), and

Donaghe and Townsend (1978). The normalized undrained shear strength, s_u/σ'_{vc} , is also dependent on K ; an increase of this ratio with a decreasing K is seen in Fig. 7.4. Donaghe and Townsend (1978), Gens (1982) and Khera and Krizek (1967) found the same dependence of peak shear strength on the consolidation stress ratio, K .

This increased brittleness and strength directly affect the stress-strain characteristics (Fig. 7.4). As an illustration, Fig. 7.6 presents the axial strains found at peak, ϵ_{ap} , where a marked reduction is noted as K decreases. Gens (1982), Donaghe and Townsend (1978) and Broms and Ratnam (1963) have reported similar variations. On the other hand, comparison soil of stiffness after consolidation at low stress ratios is difficult because of the small strain levels involved and hence the limited reliability of the data. A stiffer response as K decreases can be seen in the stress-strain curves of Fig. 7.4. Gens (1982) also found a sharp increase in stiffness as K decreases.

When comparing the shapes of the effective stress paths observed in stages 2 and 4 (Figs. 7.1 and 7.3), it can be seen that a loop is formed in stage 4. This behavior may be attributed to the decrease in the stress ratio, K , since the strain rate was not changed (0.5% per hour). On the other hand, Gens (1982) performed a series of tests on anisotropically consolidated samples sheared at two different rates and observed similar loops at the higher shearing rate. He concluded that errors in pore pressure measurements associated with the higher rates of shearing may be the cause of the obscured loops in effective stress paths.

7.2 Cyclic Loading: Test CK₀U-Cyc-4

7.2.1 Procedure

The sample used for this test comes from the same batch as the other

samples. Trimming and set-up procedures are explained in Chapter 3, and six spiral filter strips were coiled around the specimen. Saturation and consolidation phases followed the same steps as the standard static tests. A vertical effective stress of 4 kg/cm^2 was reached during anisotropic consolidation ($K_0=0.47$) and then the sample was rebounded to an OCR of 4 (i.e., to $\sigma'_{vc}=1 \text{ kg/cm}^2$ and $K=0.8$).

Undrained cyclic shearing was then applied symmetrically about $q_{\text{static}}=0.1 \text{ kg/cm}^2$ as illustrated in Fig. 7.7. The cyclic amplitude was chosen as a percentage of the static undrained strength found from test CK₀UC4 and a cyclic period $t_{\text{cyc}}=48 \text{ min}$ was imposed. Positive as well as negative forces therefore had to be applied to the piston. This was done by means of a double acting bellofram air jack.

A purely mechanical system was assembled. A small pivot wheel was attached to the end of a slotted bar, the position of which could be adjusted and fixed to the shaft of a loading triaxial machine (see Plate 7.1). The triaxial loading frame was chosen to provide a large range of low speeds that was needed for the experiment. The distance between the pivot wheel and the axis of the driving shaft set the amplitude of the sinusoidal function.

The wheel was connected to a pneumatic regulator through a bicycle chain that fit in the teeth of a gear attached to the air pressure control knob on the regulator (see Plate 7.2). To keep the chain under tension at all times, a counter-weight of 2 kg was hung on the free end of the chain. This regulator controlled the pressure of air sent to the upper, or compression side, of the bellofram air jack (see Plate 7.3).

To allow the sample to be placed under tension, a constant pressure air supply was connected to the lower bellows chamber. By adjusting the

air pressure to the lower bellows side, the static pressure throughout the loading cycle could be maintained at the desired level (see Fig. 7.8). Increasing the air pressure caused the sample to be under tension during a portion of the loading cycle.

The system was initially calibrated using a load cell installed in place of the sample. First, stress amplitude was adjusted to the desired value by varying the distance between the pivot wheel and the driving shaft axis. Then, static pressure was adjusted by varying the air pressure to the lower bellows chamber.

With this type of driving system, it was impossible to synchronize the readings with particular points in the stress path. Moreover, the interval of time separating each reading being constant, the recorded data points were poorly distributed. An accumulation of data was reported around peaks, with only a few points in the middle of a cycle. To compensate for the lack of systematic control on the readings, a large number of measurements were taken, typically, 40 to 50 readings per cycle.

7.2.2 Presentation of results

Two values of the cyclic stresses, q_{cyclic} , were used throughout the test to achieve a constant value of the cyclic stress ratio (CSR) in each phase. The CSR is defined by $(q_{\text{static}} + q_{\text{cyclic}})/s_u$, where $q_{\text{static}}=0.1$ kg/cm² and $s_u=1.05$ kg/cm², as obtained from test CK₀UC4. In phase A, the CSR was fixed at 0.4, and the test was stopped after about 120 cycles. A period of 10 days followed in which the stresses were kept constant, equal to the initial effective stress state measured at the beginning of phase A. The CSR was then increased to 0.6, in phase B which lasted for 48 cycles. Cyclic conditions are summarized below:

Phase	CSR	q_{max}	q_{cyc}	N_{cyc}
A	0.4	0.415	0.315	120
B	0.6	0.630	0.530	48

PHASE A, CSR=0.4:

Figs. 7.8 through 7.10 present the stress path, the stress-strain and the pore pressure-strain curves, respectively, for the cycles $N=1, 10, 20, 30, 40$ and 80 . The stress-strain, and particularly the pore pressure change, curves show a very consistent trend. Figs. 7.9 and 7.10 indicate some dilatancy as expressed by an observed swelling (Fig. 7.9) and an average negative pore pressure (Fig. 7.10). After an initial slight migration of the stress path to the right, a stable closed hysteresis loop formed after $N=40$ involving no failure of the soil.

This behavior was also observed by Sangrey et al. (1969). Below a certain level of cyclic stress, migration of the effective stress path eventually ceases, i.e., no additional accumulation of pore pressures takes place, and the behavior in each cycle becomes recoverable. They used the terminology adopted by Larew and Leonards (1962) and referred to this stress level as the "critical level of repeated stress."

In light of these observations, and in order to avoid long-term tests, the test was stopped, monitored for a few days, and sheared again at a higher CSR.

INTERMEDIATE PHASE:

As soon as the cyclic shear of phase A was stopped, the stresses were adjusted to the effective stresses existing at the end of consolidation before cyclic loading, i.e., $\sigma'_{vc}=1 \text{ kg/cm}^2$ and $K=0.8$.

During this period, which lasted 10 days, more swelling was noticed as the axial strain varied from -0.21 to -0.26%. Vertical effective stresses decreased by 0.3 kg/cm² and pore pressure increased by 0.05 kg/cm². These variations are related to changes in air pressure and stick-slip phenomenon occurring in the piston. The final state of stress at the end of this intermediate phase was:

$$p' = 0.778 \text{ kg/cm}^2$$

$$q = -0.09 \text{ kg/cm}^2$$

$$u = 1.970 \text{ kg/cm}^2$$

PHASE B, CSR=0.6.

The effective stress path is presented for selected cycles (N=1, 8, 20, 25, 30 and 35) in Fig. 7.11. The stress-strain curves are shown in Fig. 7.12. As noted in phase A, an initial migration of the effective stress path to the right is observed, which reverses after the 8th cycle. As migration to the left proceeds the shape of the effective stress path during each cycle changes. The variation in pore pressures is shown in Fig. 7.13 and indicates a significant increase (per cycle) as the failure envelope is approached.

Two distinct phases in the stress-strain behavior can be observed in Fig. 7.12. In the initial stage, the soil is stiff and exhibits small hysteresis loops. This means that, at early cyclic stages of this overconsolidated soil, the sample behaves almost elastically and develops low strains. But as cycles are added, the small permanent pore pressures generated in the individual cycles accumulate, the effective stresses decrease and approach the failure envelope. At this stage, strains and pore pressures become larger and a characteristic "S-shape" develops in the

stress-strain curves. This shape may well be exhibited by the different strain rates observed in a cycle. This is illustrated in Fig. 7.11 and 7.12 where strain rates are shown at discrete locations of cycle $N=35$.

Figure 7.14 shows the development of maximum and minimum axial strains, ϵ_a , (in each cycle), vs the number of cycles, N . For $N > 25$ cycles, $|\epsilon_a|_{\max}$ increases slightly, but after $N=25$, major increases in $|\epsilon_a|_{\max}$ take place. The same observations are valid for the pore pressures plotted in Fig. 7.15. The average pore pressure measured in a cycle reaches a minimum value at cycle $N=8$, then increases steadily with N .

The effective stress path of cycle $N=35$ is plotted in Fig. 7.11, where strain rate effects have a predominant role. A high friction angle (54°) and negative effective stresses are observed as a result of the larger strains developed in the cycle. This is particularly obvious in Fig. 7.12 where the data corresponding to constant time interval are marked. The strain rate reaches a maximum of 92% axial strain per hour and averages around 0.1% per hour at the peaks. The high strain rates observed induce non-uniform distribution of pore pressures in the sample resulting in wrong estimates of the effective stresses.

Results of q , ϵ_a and change in pore pressures, du , during the initial part of the test are plotted in terms of the number of cycles ($N=1$ to 10) in Fig. 7.16, 7.17, and 7.18, respectively. The number of data taken per cycle, and their concentration around the peaks give a good illustration of the discussion in 7.2.1. Figs. 7.19 through 7.21 show the same type of curves at high cycle numbers N . The first plot of each series corresponds to the applied sinusoidal load function, the second and third plots represent the axial strain and pore pressure response, respectively. The following comments can be made:

1) The applied load has a constant amplitude until about 25 cycles when significant strains and pore pressures start to develop, thus preventing good control of the imposed cyclic stress.

2) Cyclic strain amplitudes are initially small, but increase steadily and permanent strains develop.

3) After a certain number of cycles, the rate of increase in cyclic strain amplitude or the rate of permanent strain development accelerates, and the rate of build-up of pore pressures increases.

4) At the larger number of cycles, strain development becomes asymmetrical, with large strains occurring in compression.

5) The major softening observed from the strain response curves indicates that cyclic failure was reached.

TABLE 7.1

Parameter	CIU-P1 Braathen	CK ₀ UC1A Stage 2	CK ₀ UC1B Stage 4
K	1	0.47	0.34
ϵ_f (%)	9.54	0.066	0.053
A_f	1.347	0.321	0.040
ϕ'_f	32.7	25.9	32.6
S_u/σ'_{vc}	0.283	0.334	0.365
E_{50}/σ'_{vc}	139	215	?
E_{50}/s_u	493	645	?
$\Delta u/\sigma'_{vc}$	0.76	0.046	0.002

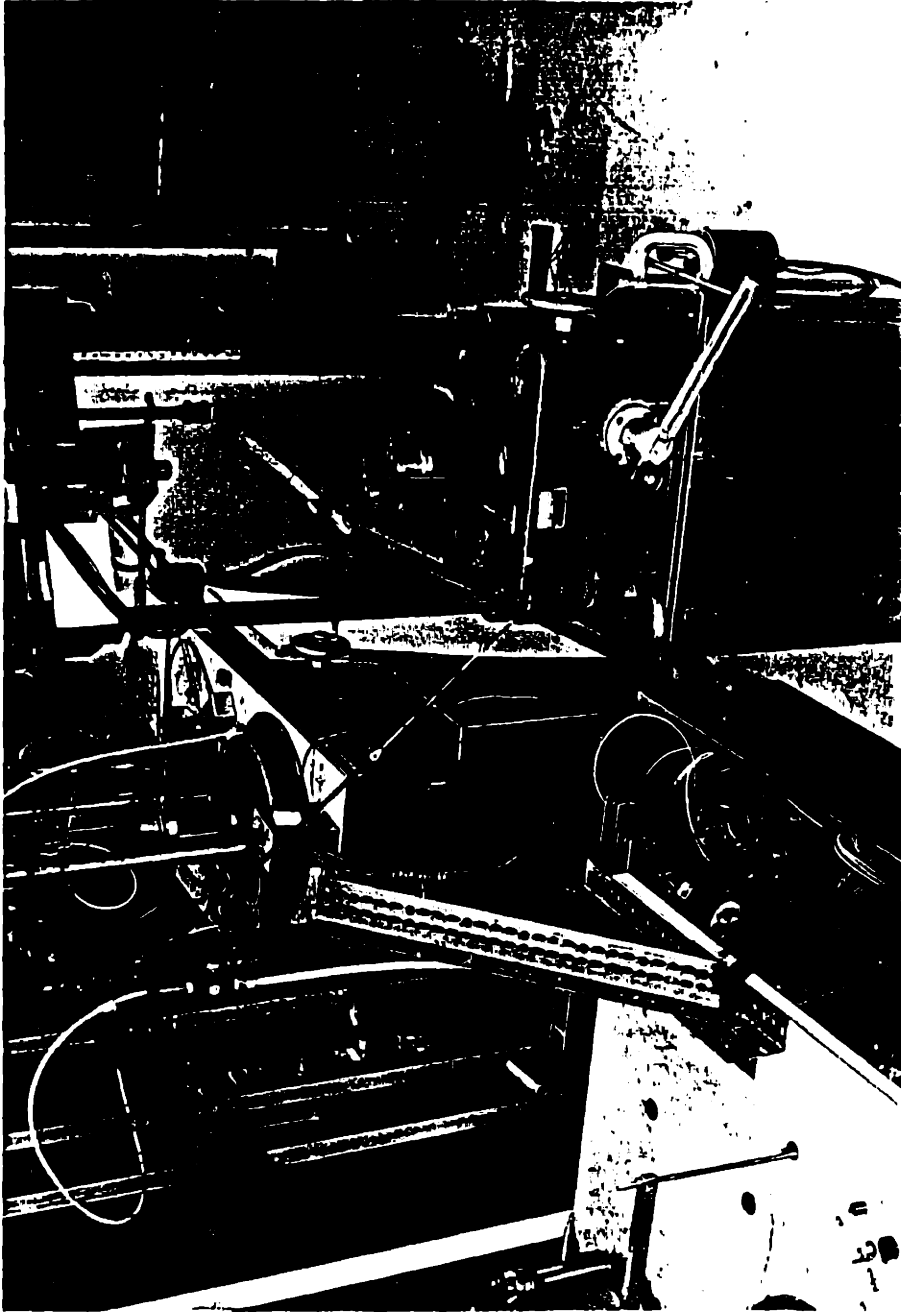


Plate 7.1

Driving system with the pivot wheel, adjusting arm
and mechanical counter

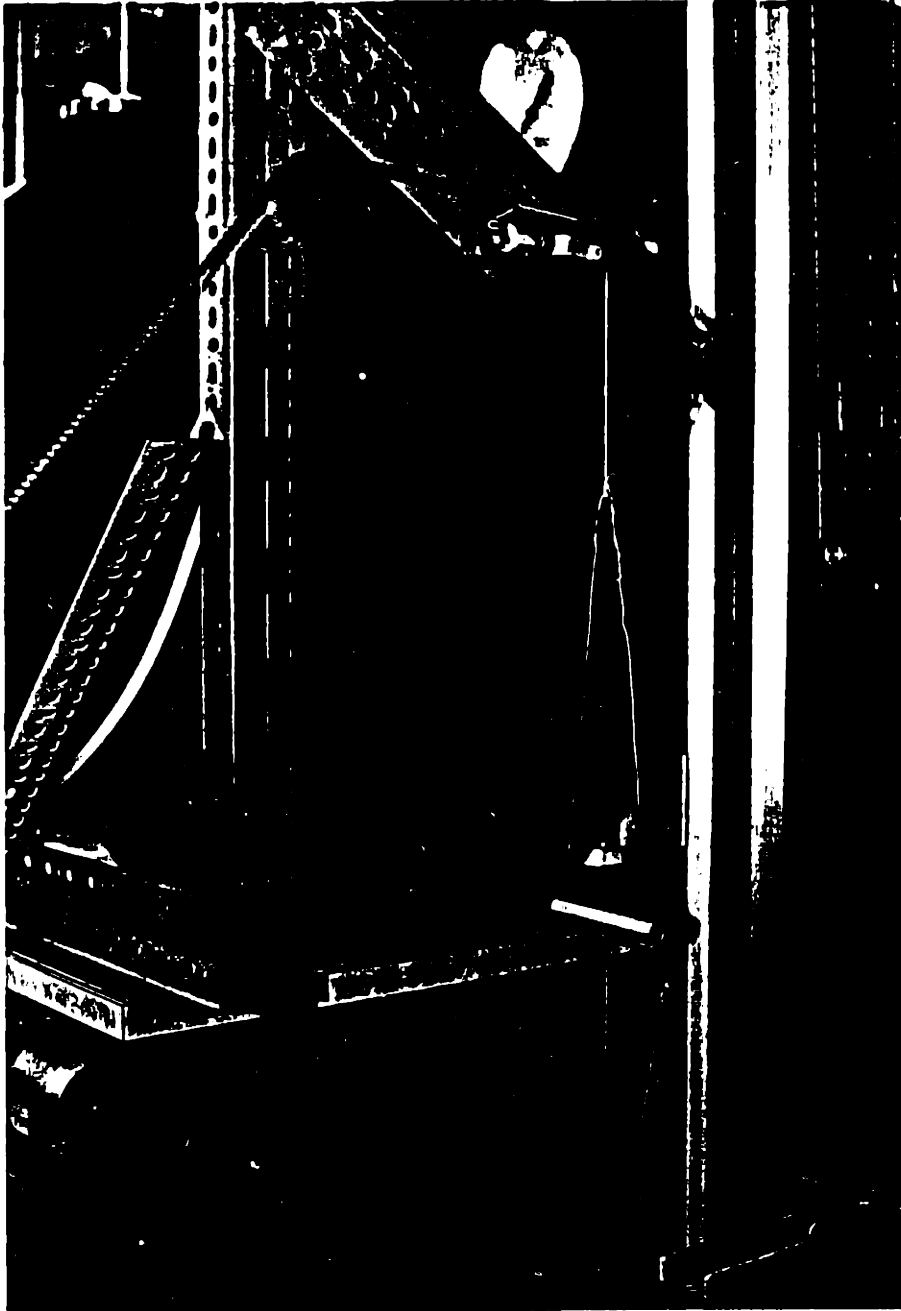


Plate 7.2

Air regulator wheel



Plate 7.3 Belloframe air jack with upper chamber connection

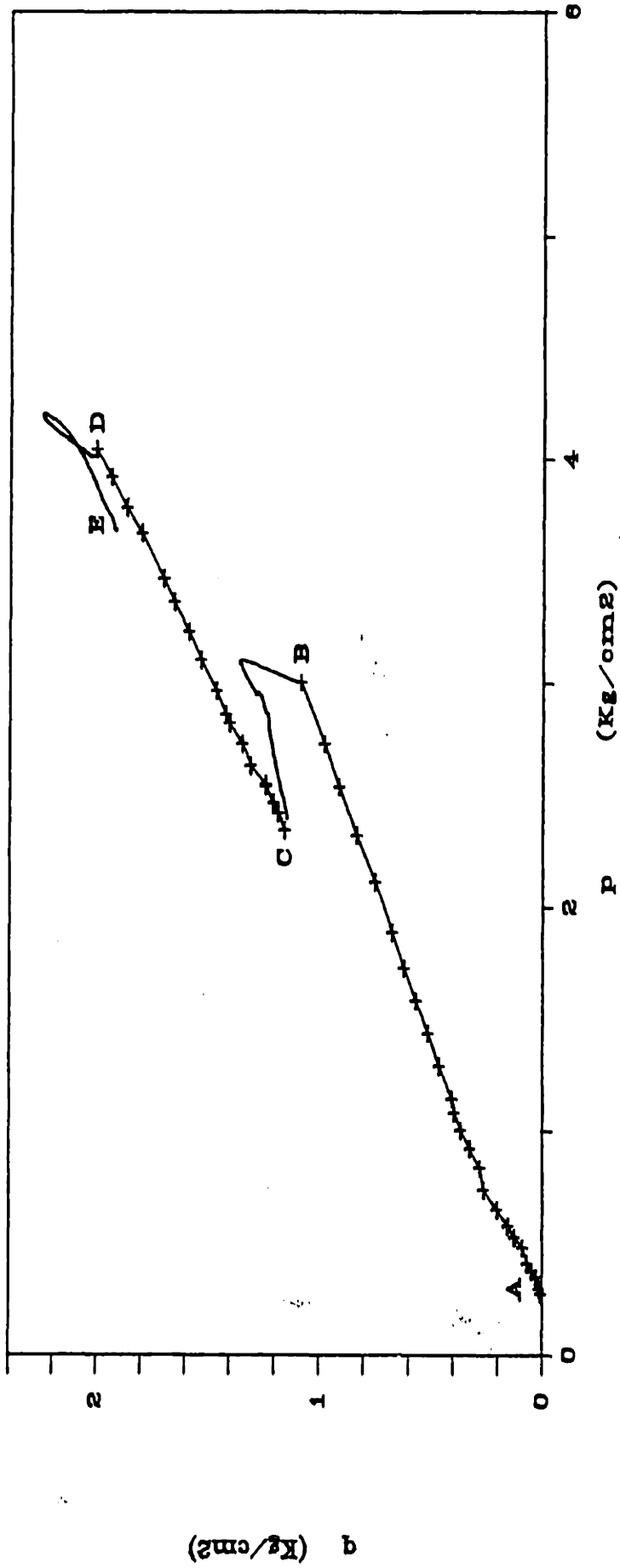


Figure 7.1 Stress path for test CK₀UC1

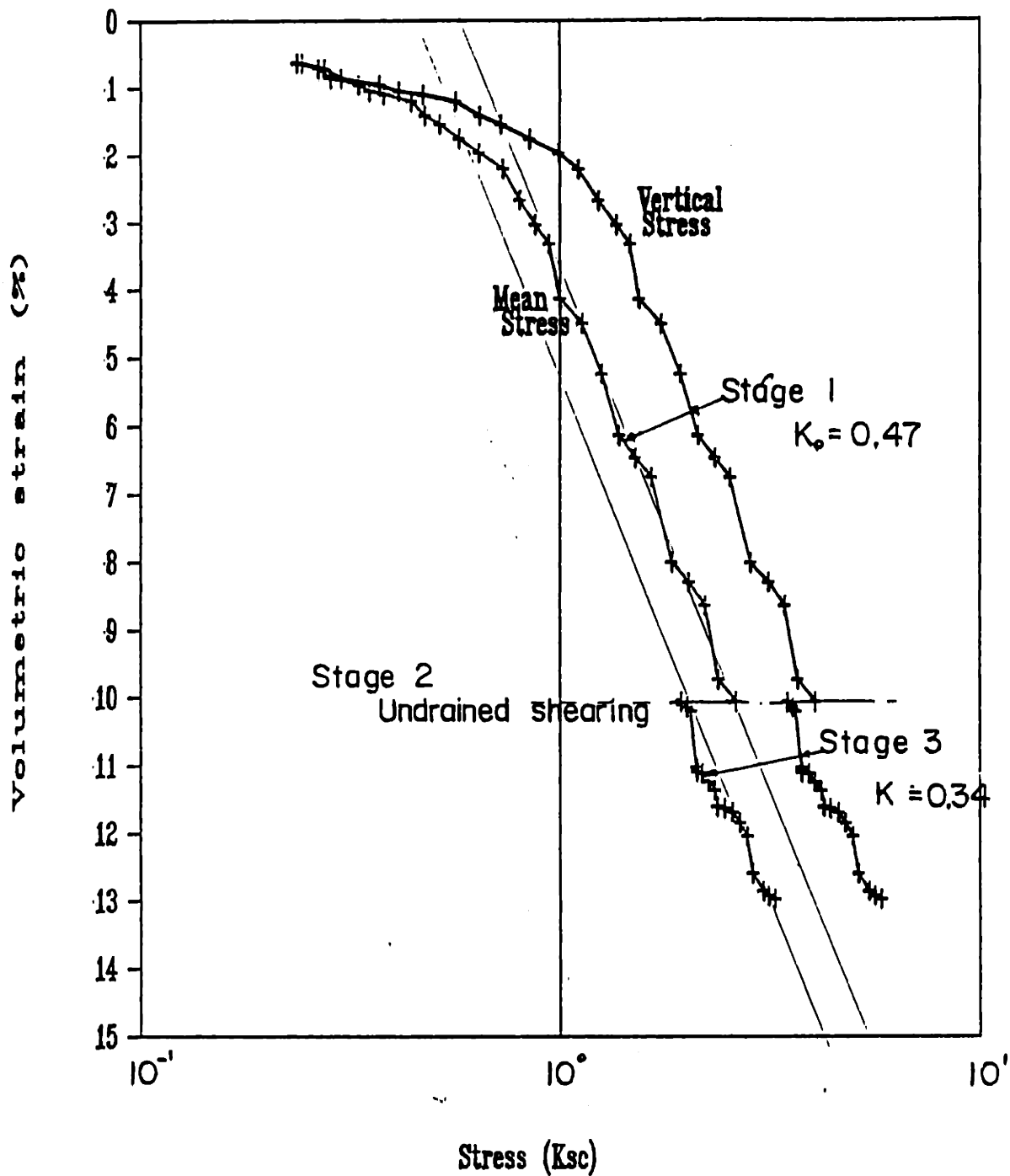


Figure 7.2 Compression curves of test CK₀UC1

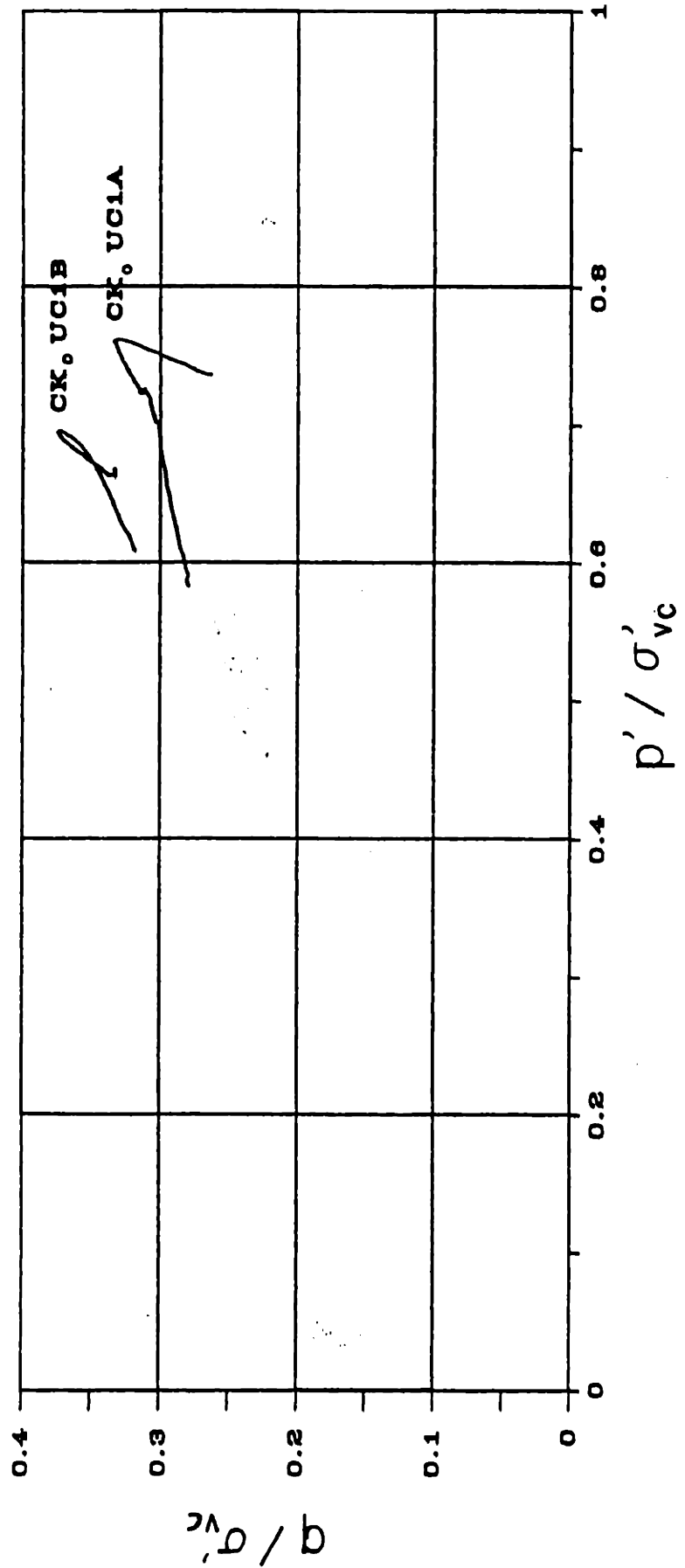


Figure 7.3 Normalized stress path for test CK₀UC1

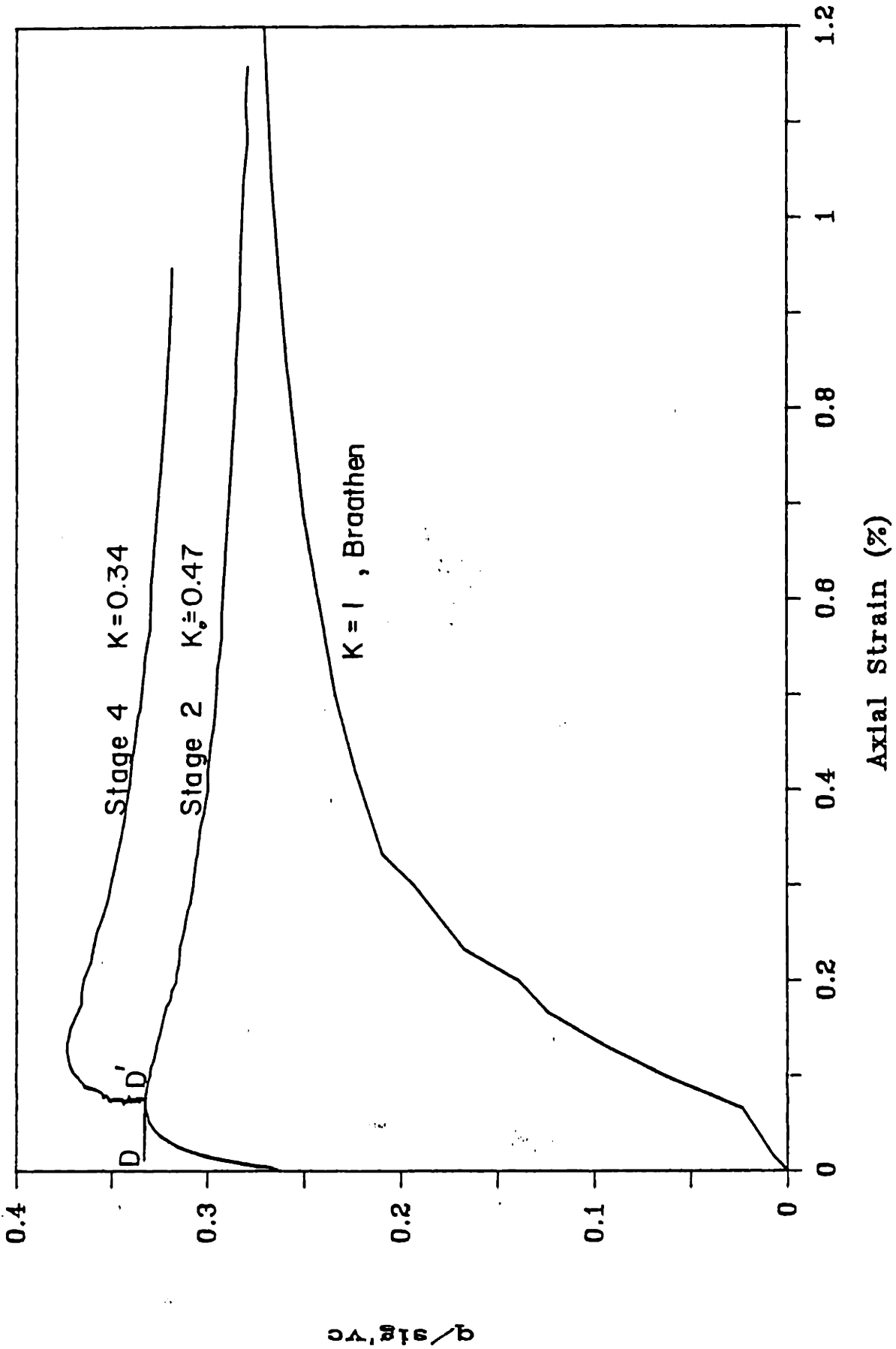


Figure 7.4 Stress-strain curves of NC samples at different values of K

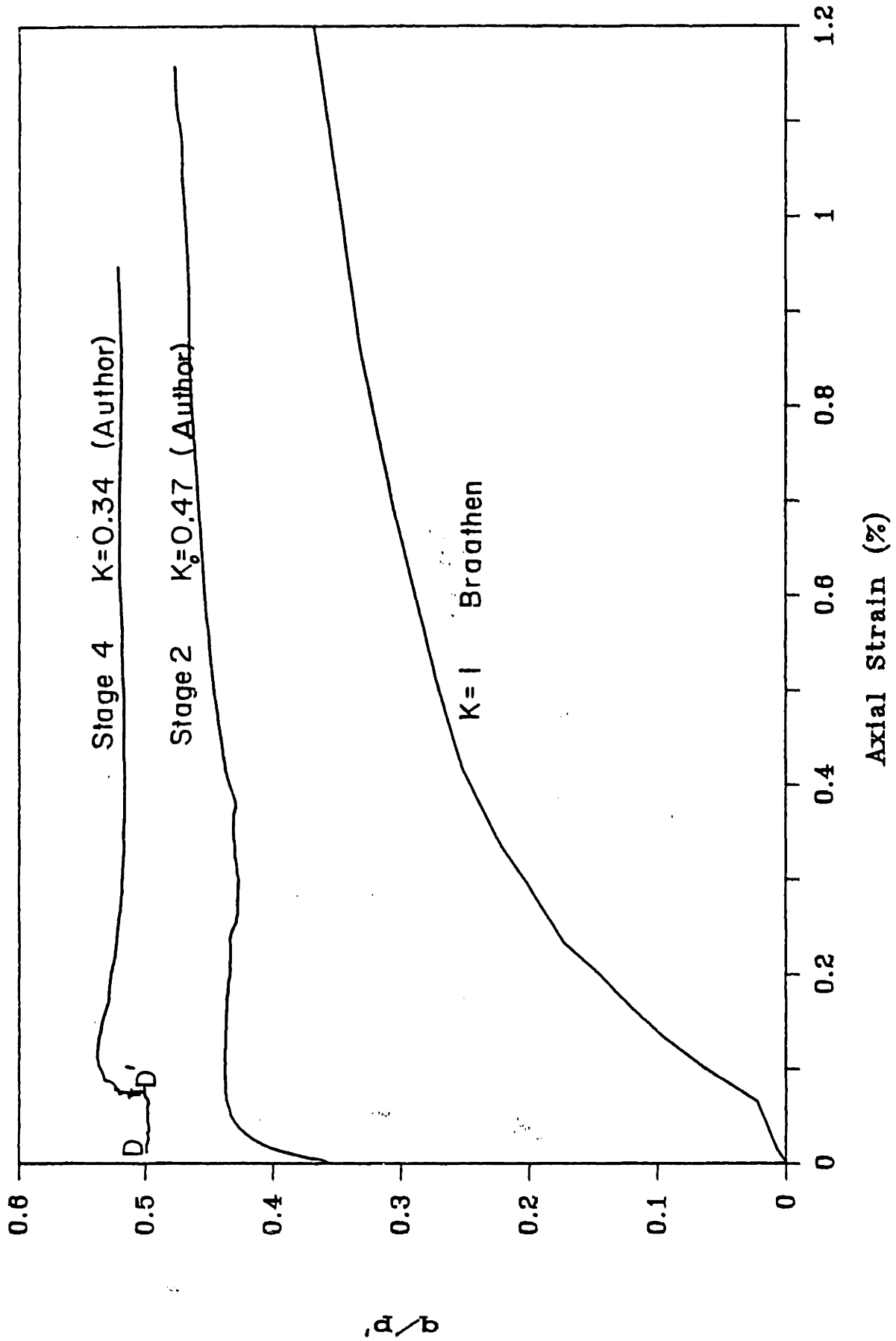


Figure 7.5 Obliquity-strain curves of NC samples at different values of K

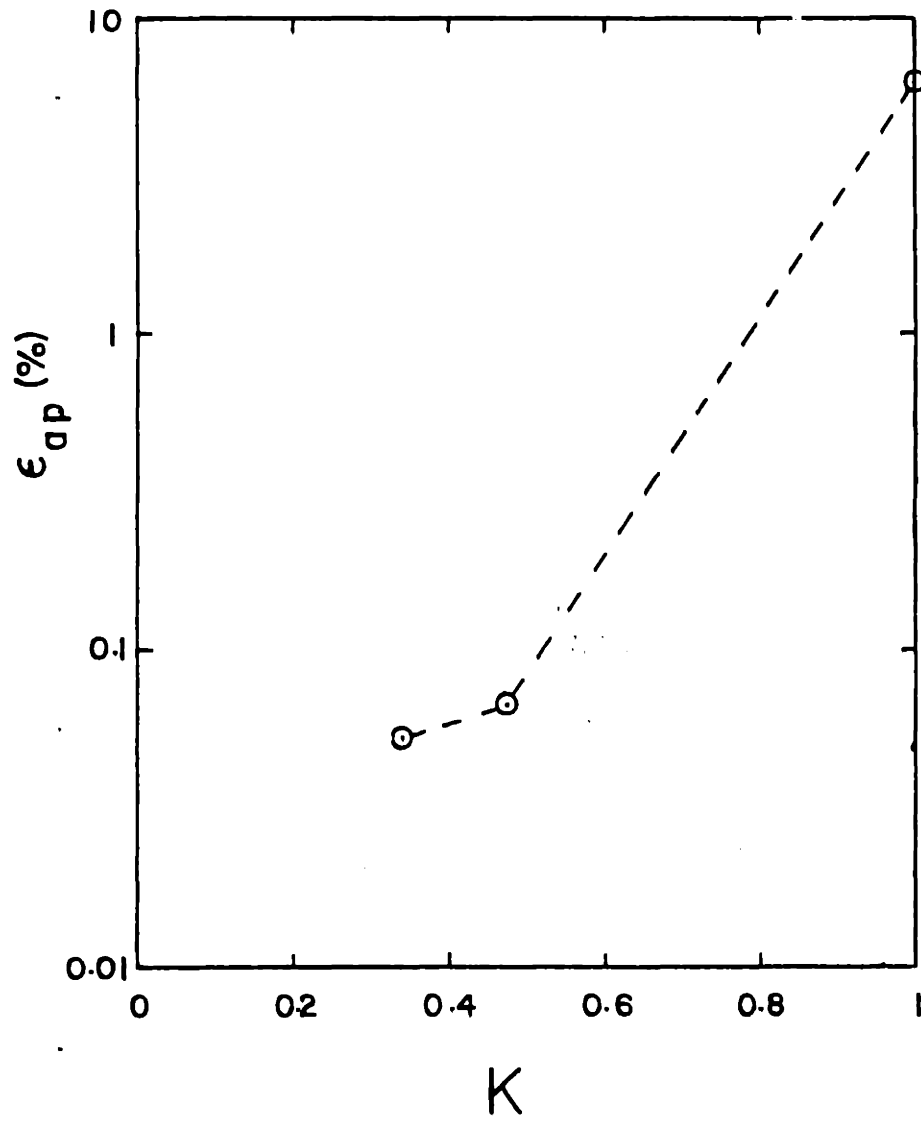


Figure 7.6 Axial strains at peak vs stress ratio K for NC samples on BBC

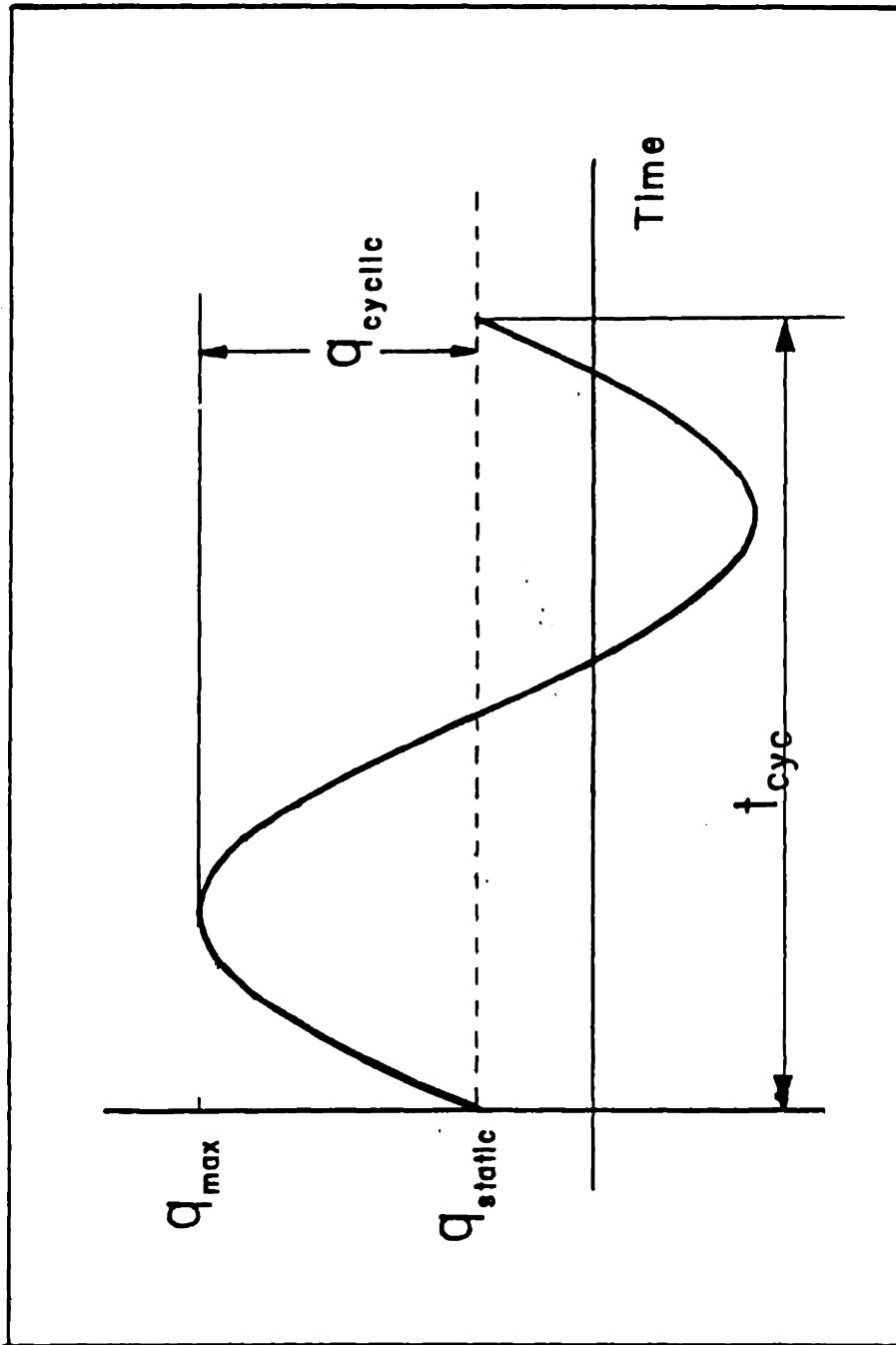


Figure 7.7 Definition of stresses during cyclic loading

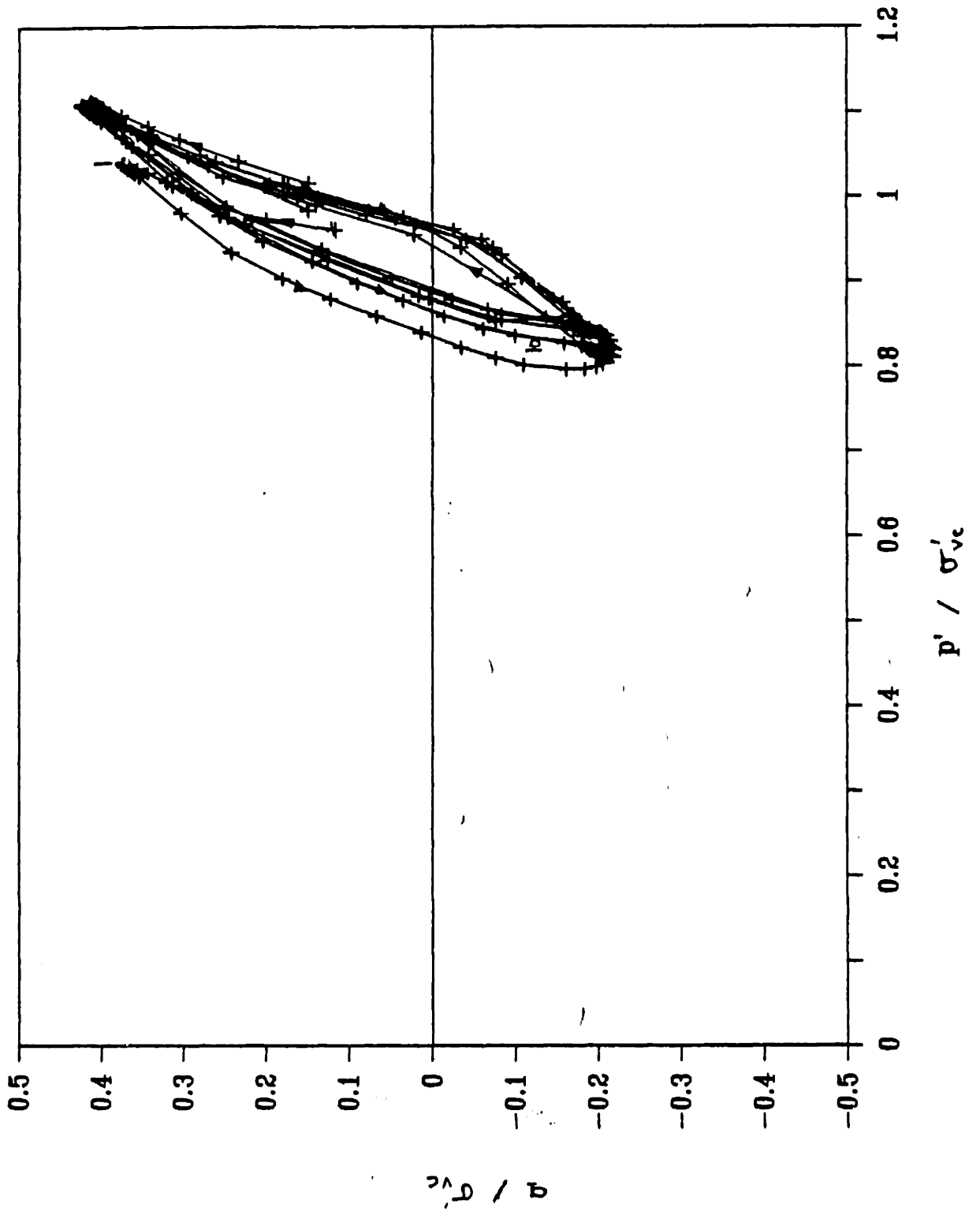


Figure 7.8 Stress paths for cyclic loading (CSR=40%)

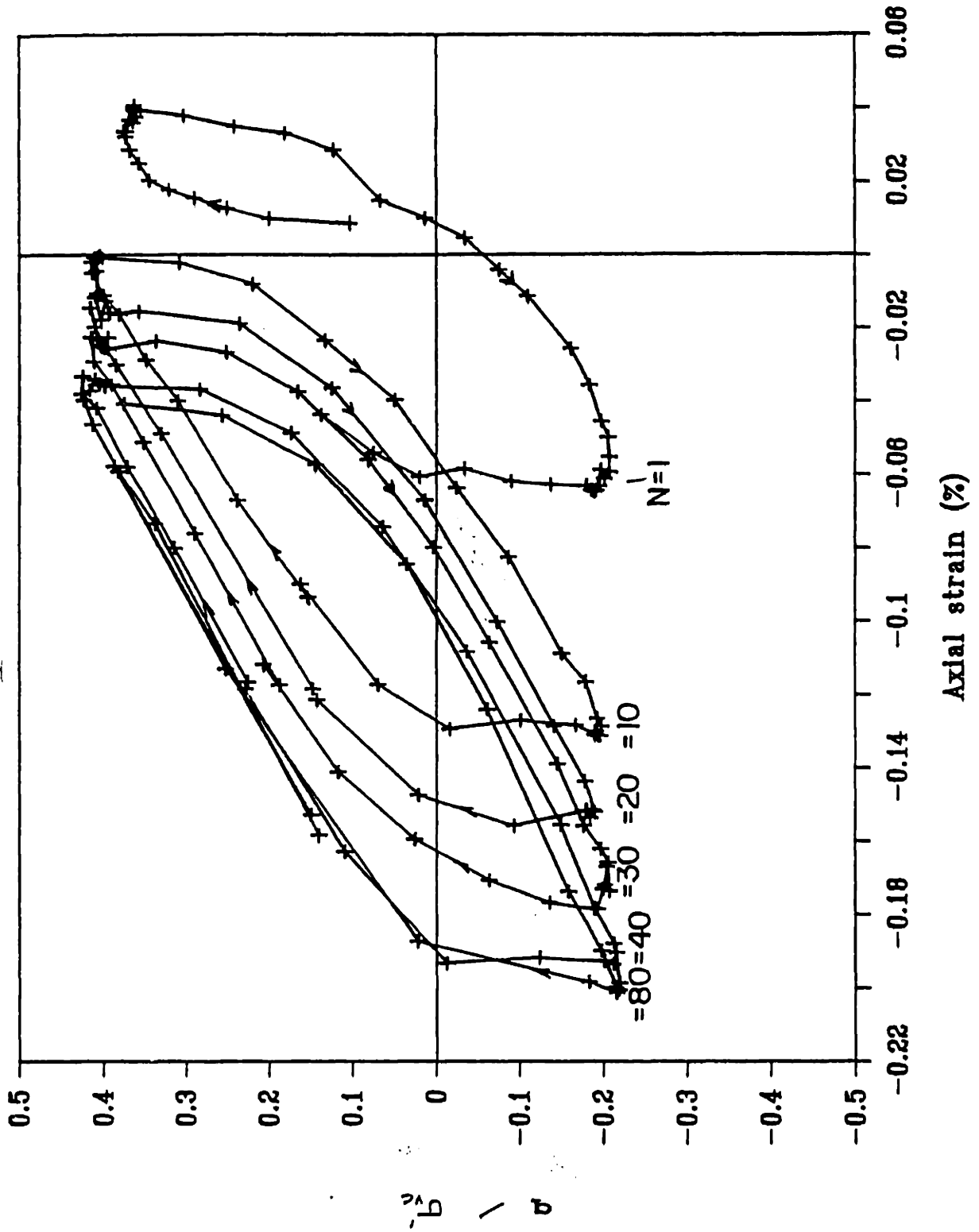


Figure 7.9 Stress-strain curves for cyclic loading (CSR=40%)

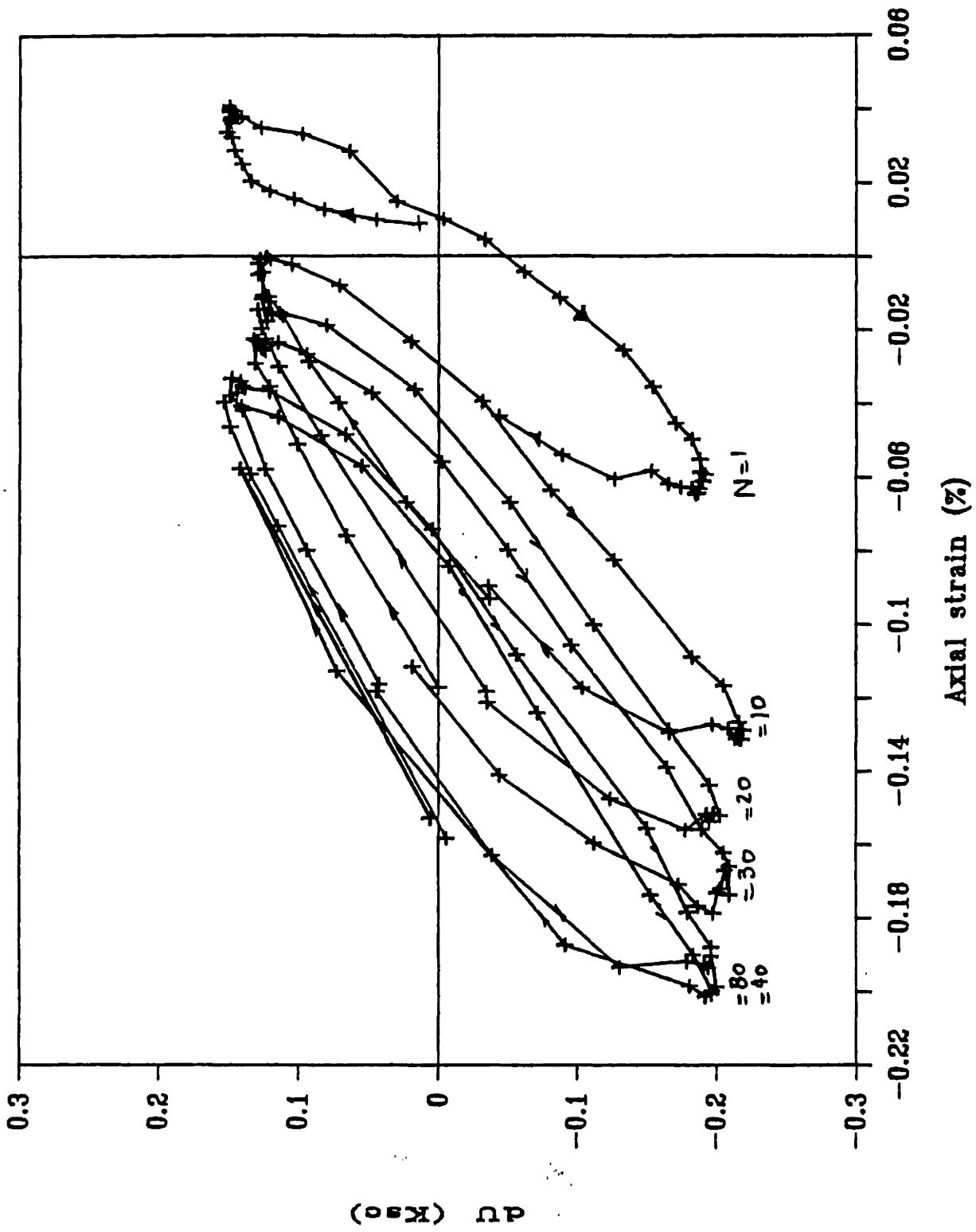


Figure 7.10 Excess pore pressure vs strain for cyclic loading
(CSR=40%)

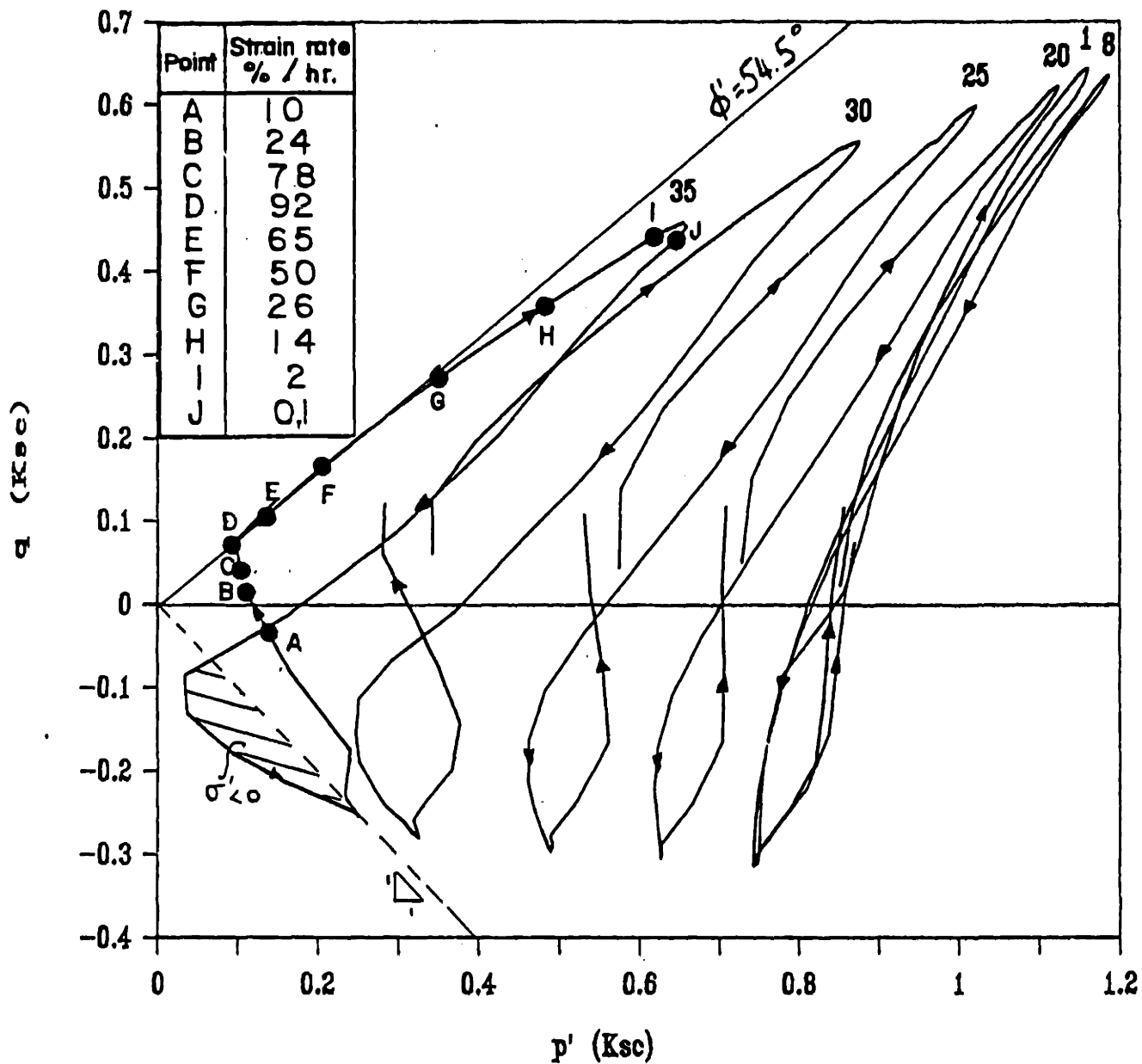


Figure 7.11 Stress paths for cyclic loading (CSR=60%)

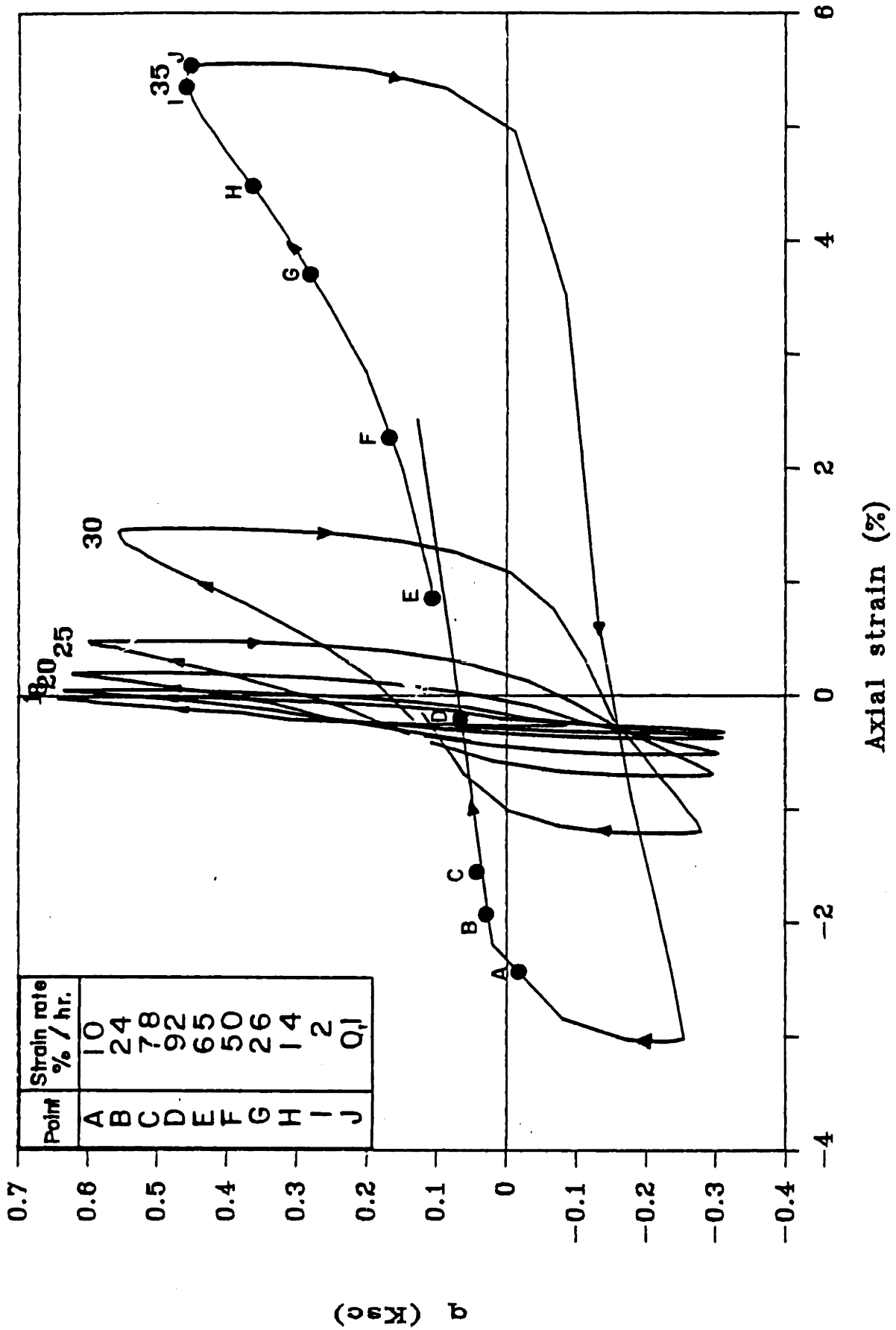


Figure 7.12 Stress-strain curves for cyclic loading (CSR=60%)

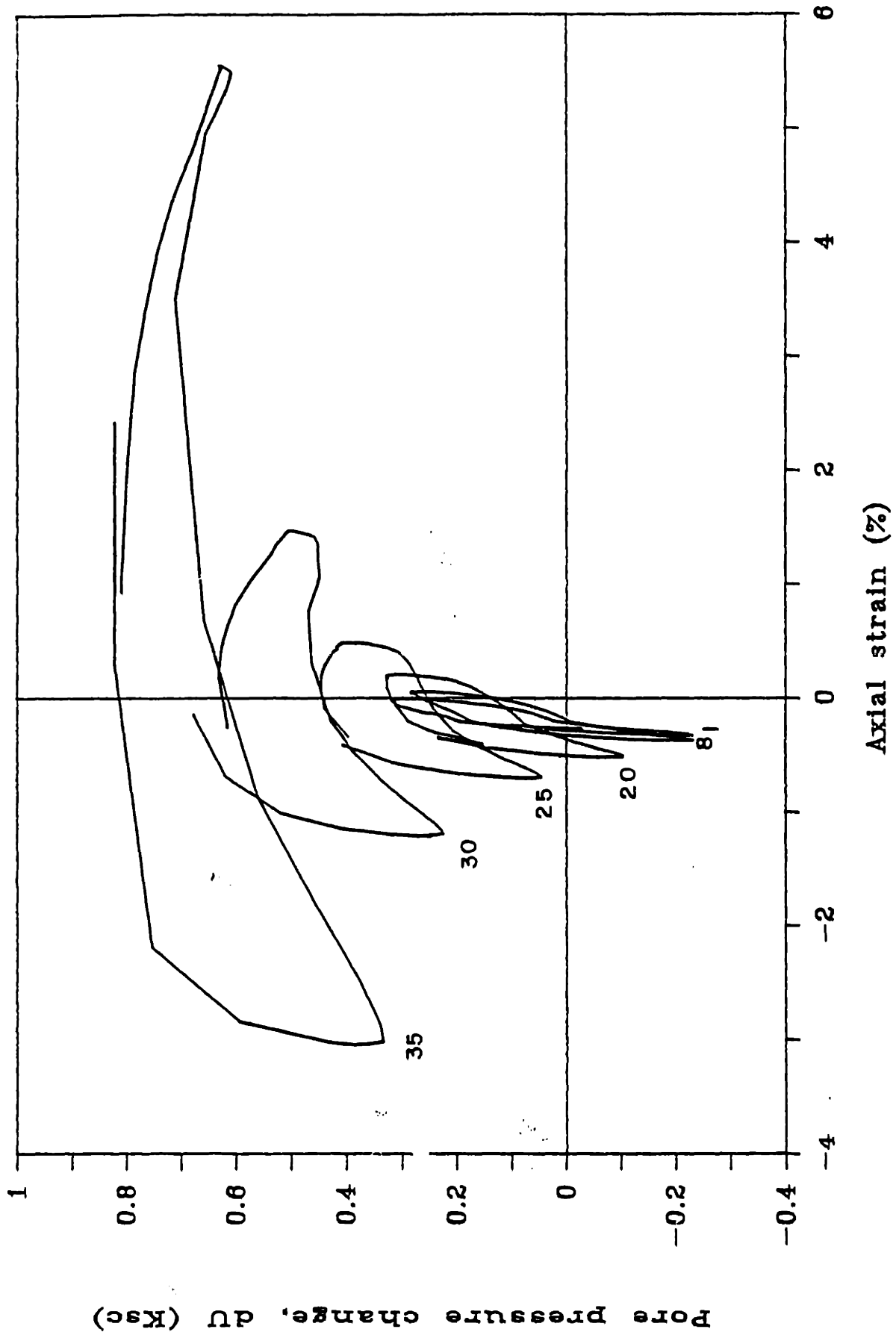


Figure 7.13 Excess pore pressure vs strain for cyclic loading (CSR=60%)

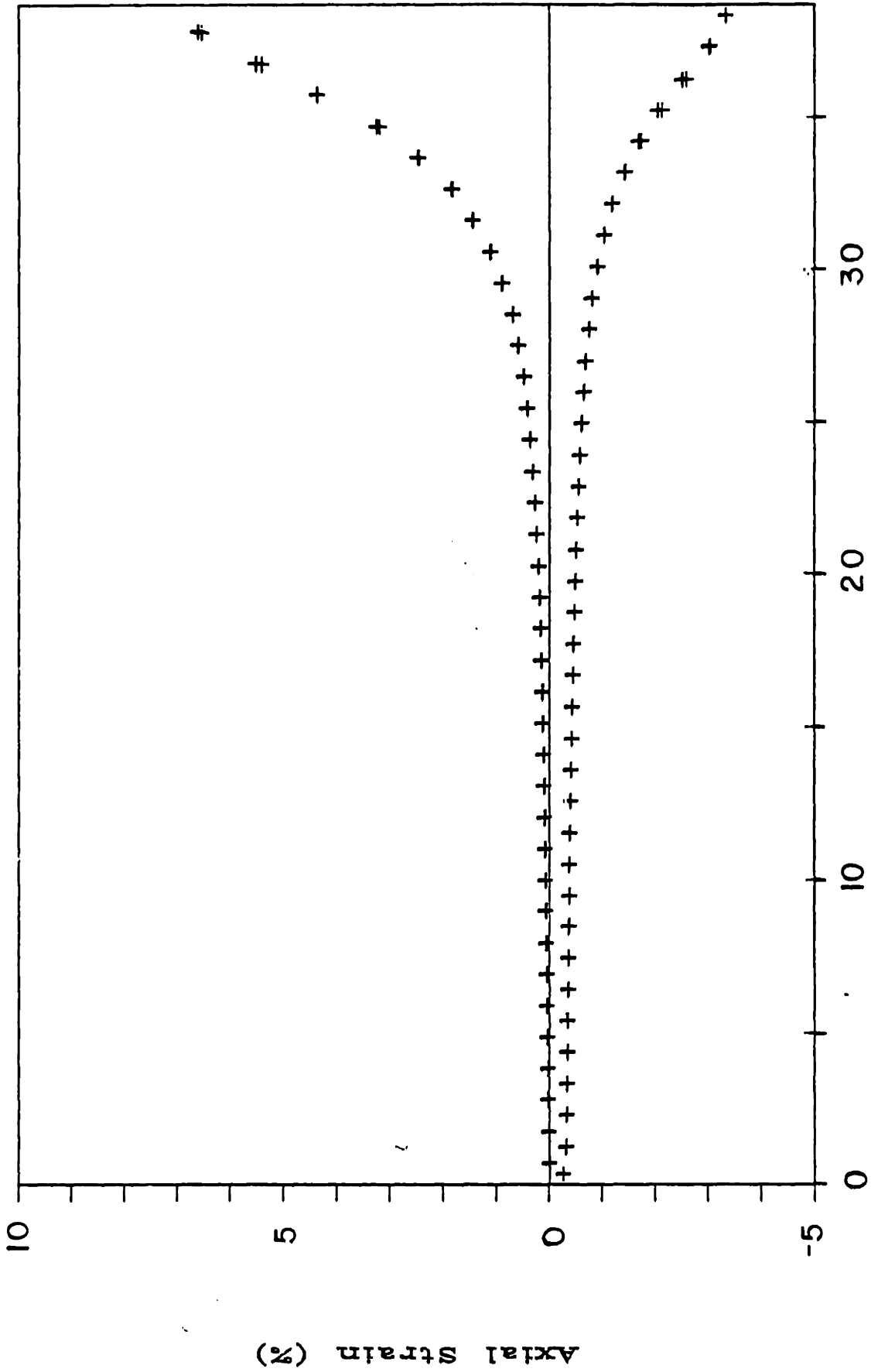
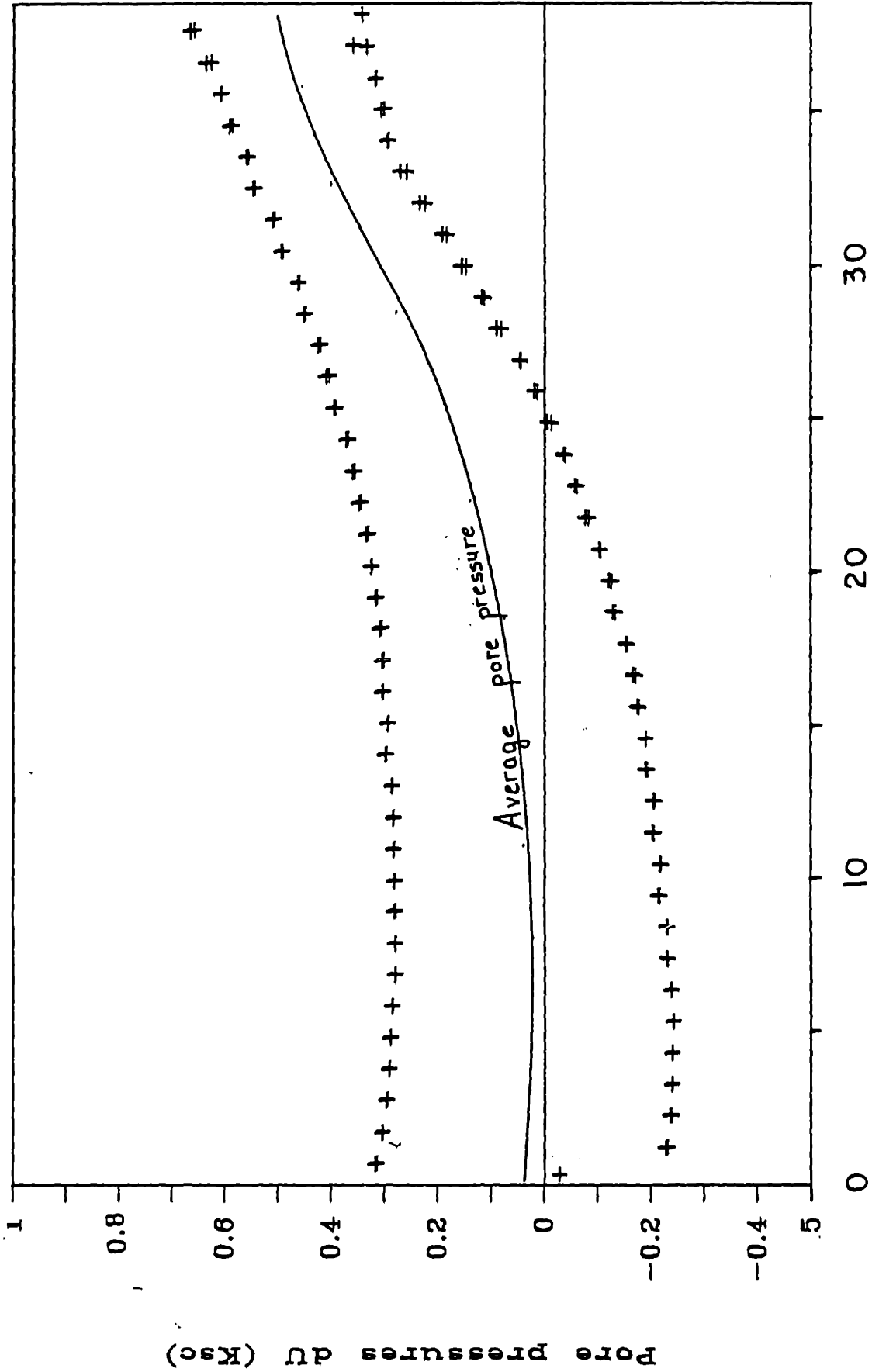


Figure 7.14 Minimum and maximum axial strain during cyclic loading (CSR=60%)



Number of cycles, N

Figure 7.15 Minimum and maximum pore pressure during cyclic loading (CSR=60%)

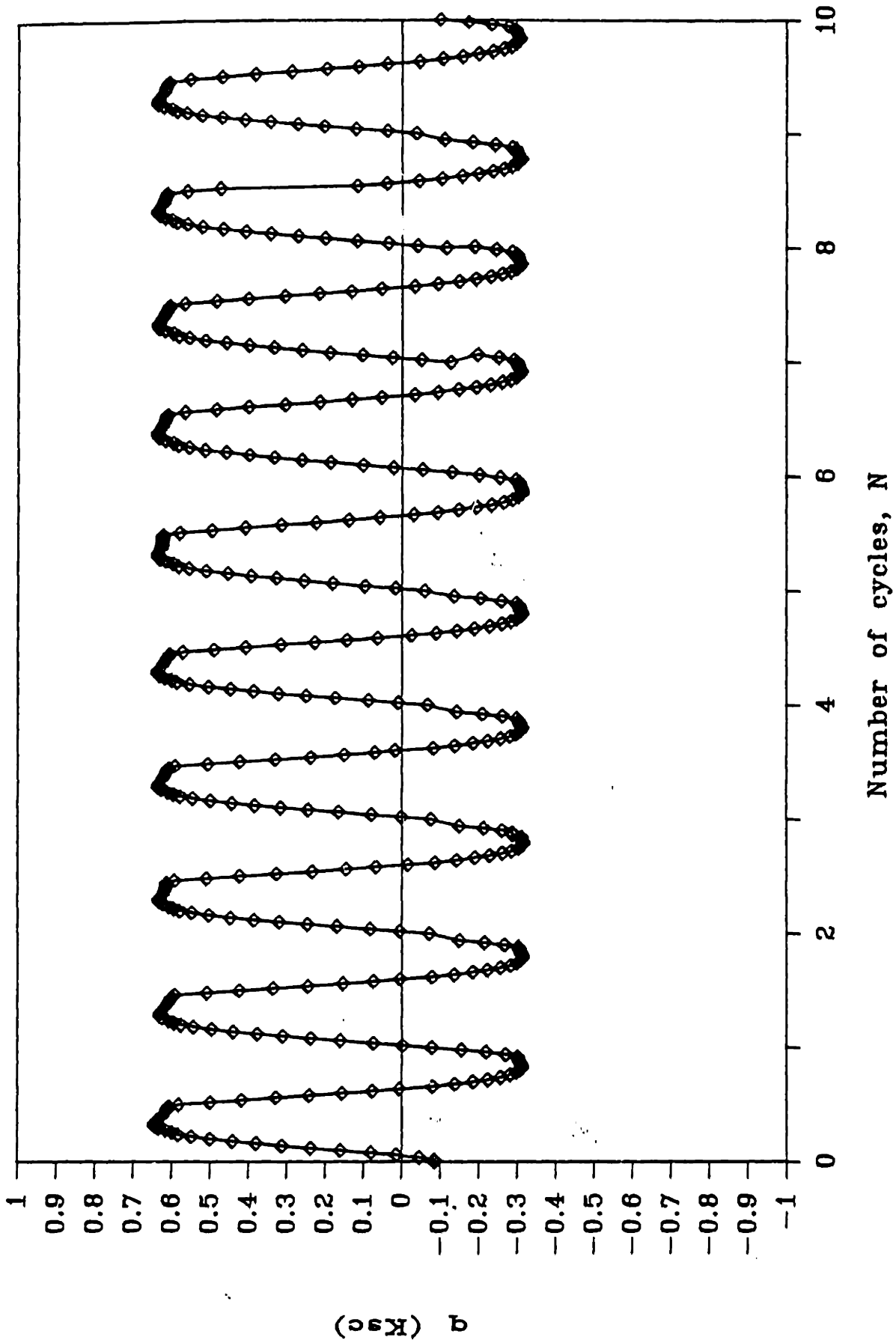


Figure 7.16 Applied shear stress for low number of cycles (CSR=60%)

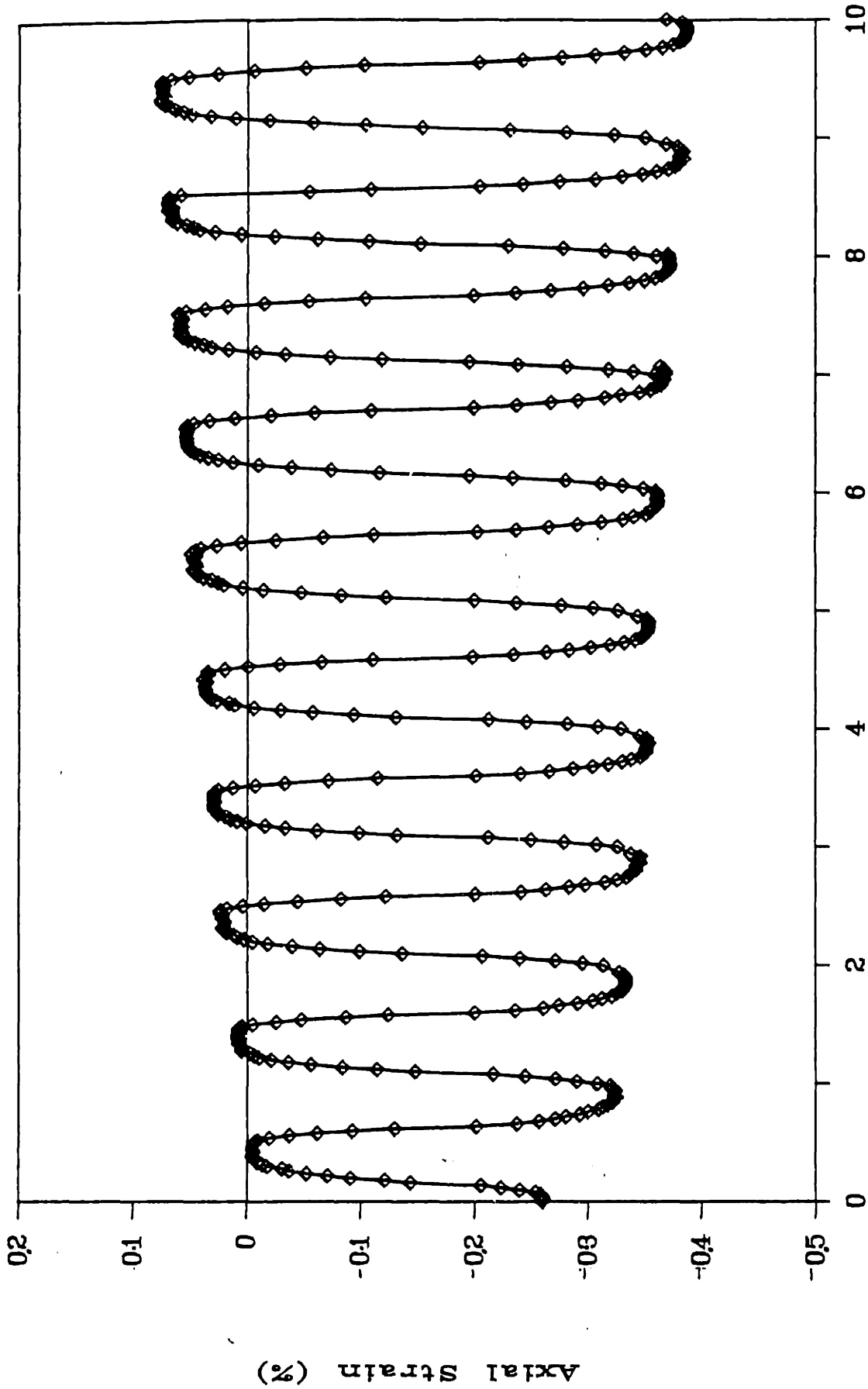


Figure 7.17 Axial strain response for low number of cycles (CSR=60%)

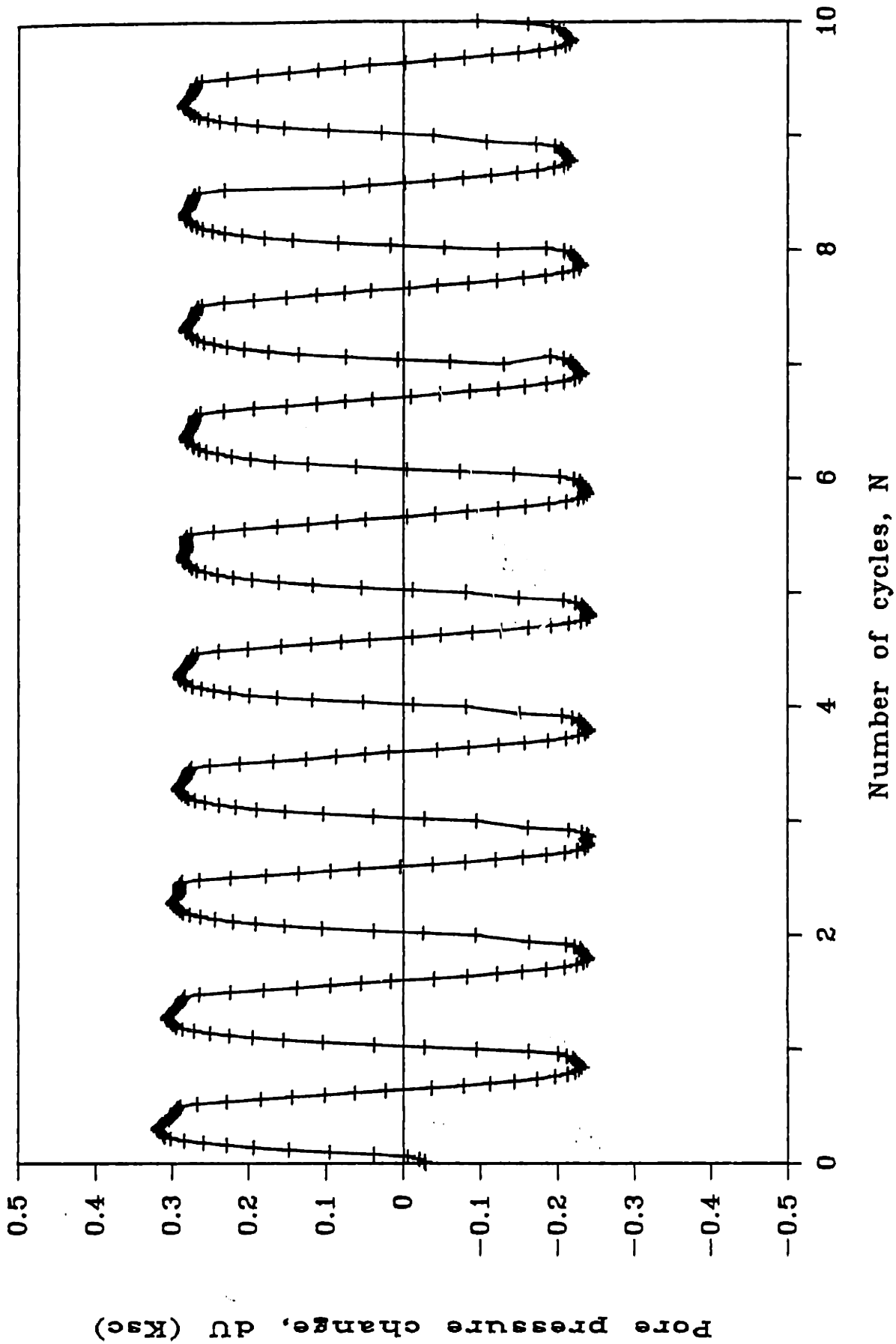
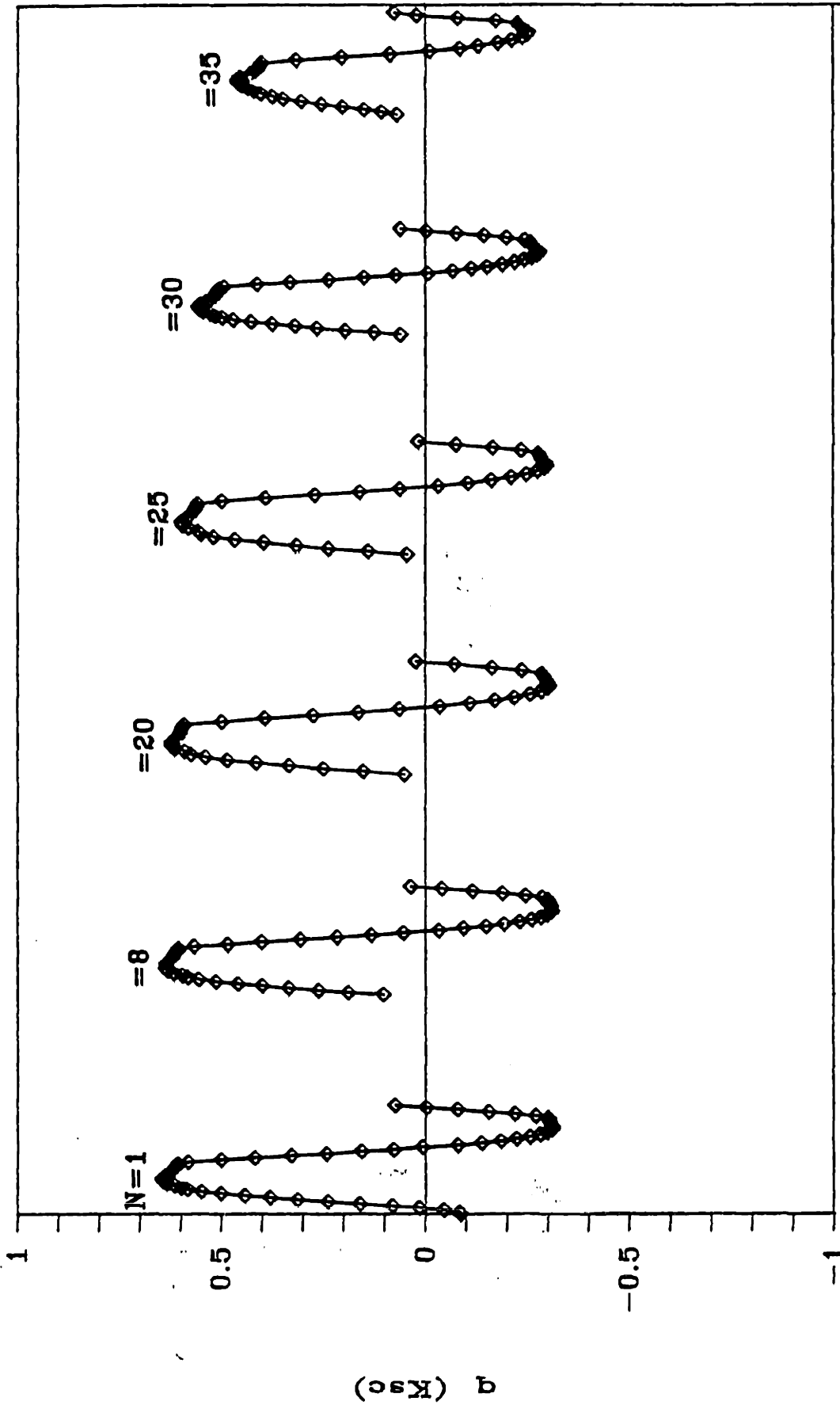


Figure 7.18 Pore pressure response for low number of cycles (CSR=60%)



N
Figure 7.19 Applied shear stress for N=1,8,20,25,30 and 35
(CSR=60%)

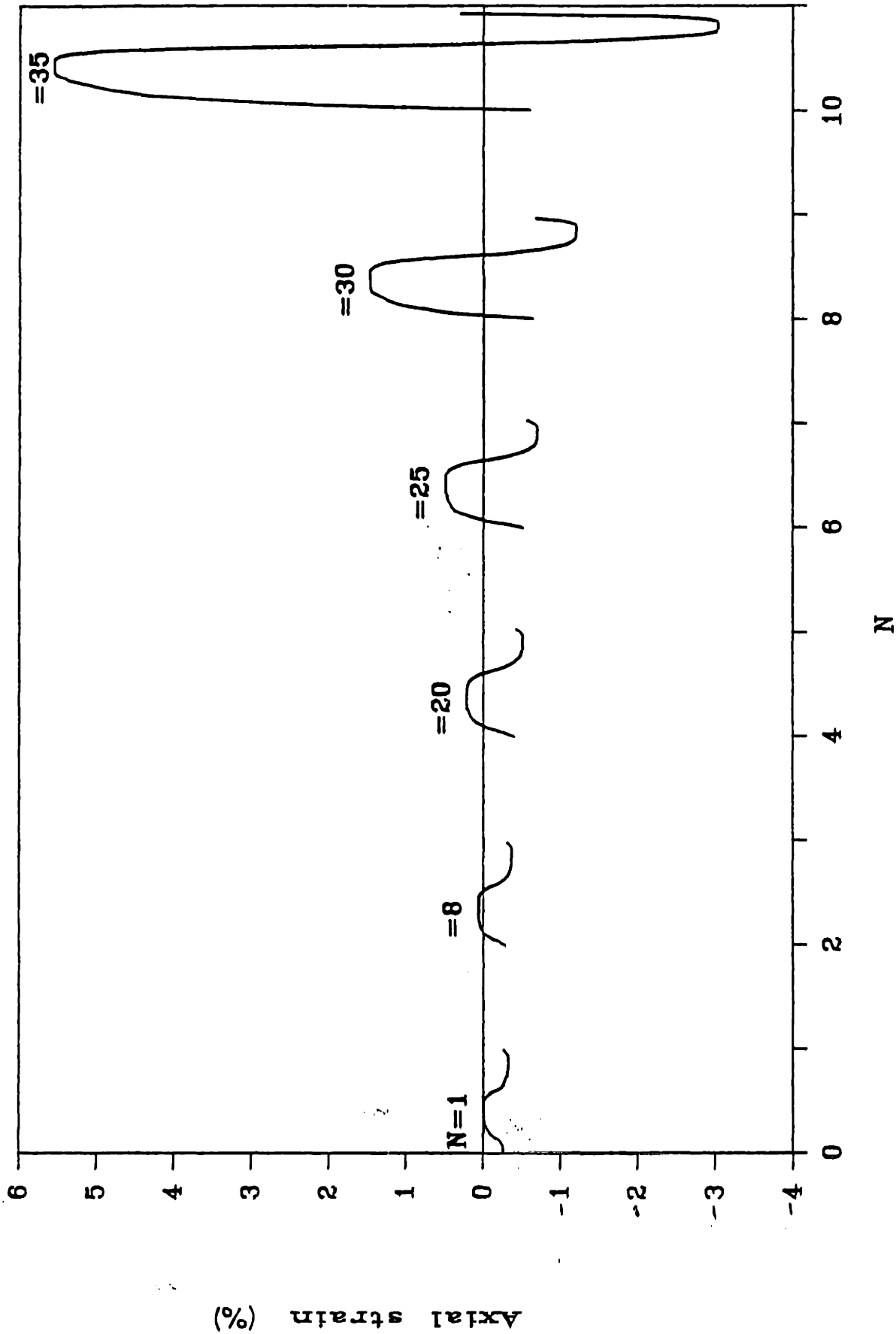
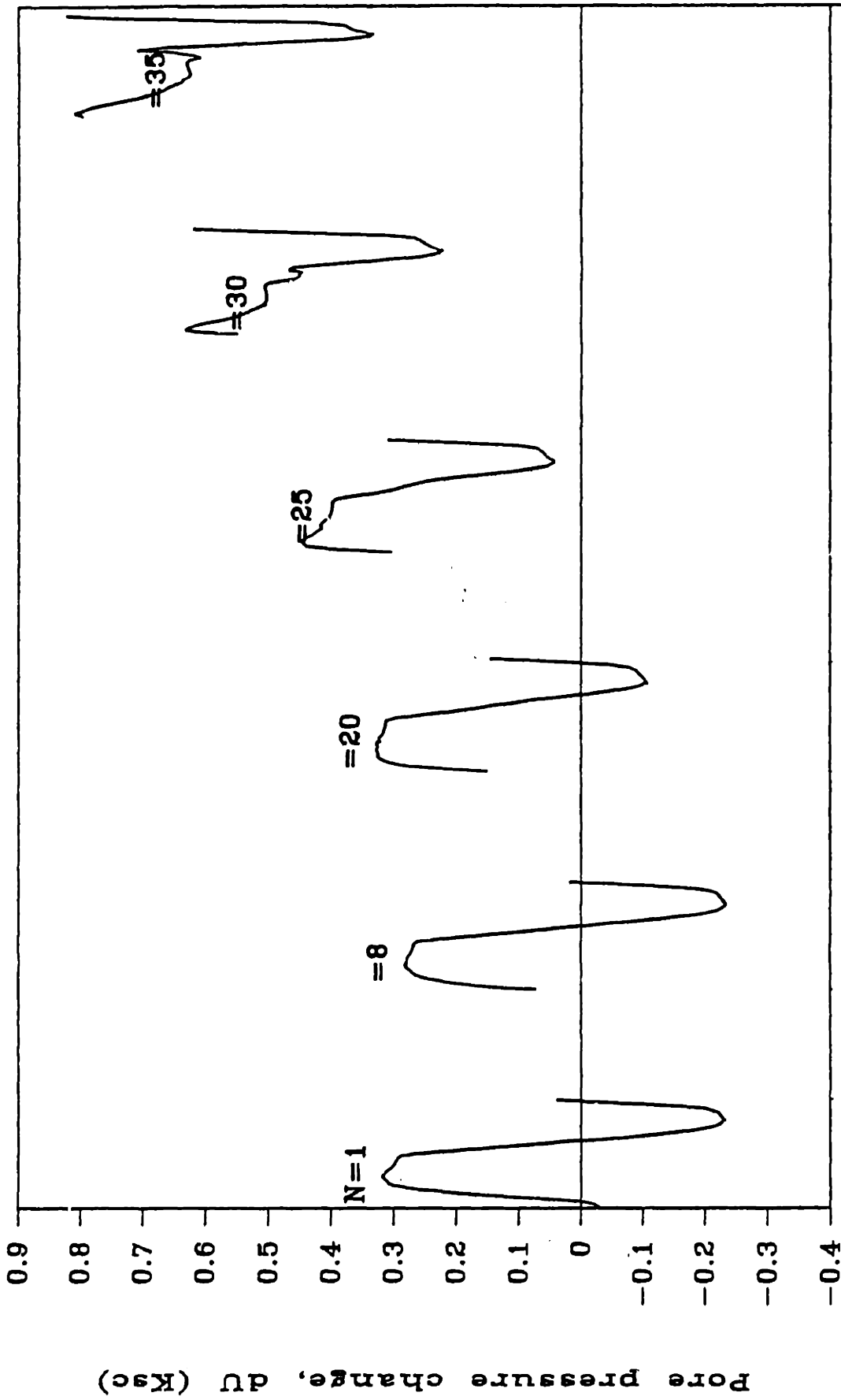


Figure 7.20 Axial strain response for N=1,8,20,25,30 and 35 (CSR=60%)



N

Figure 7.21 Pore pressure response for $N=1, 8, 20, 25, 30$ and 35 (CSR=60%)

CHAPTER 8

CONCLUSIONS AND RECOMMENDATIONS

8.1 Conclusions

This research utilizes the triaxial apparatus and the standard incremental oedometer device to investigate the volumetric and undrained behavior of resedimented Boston Blue Clay (BBC), a low plasticity (PI=21%, LL=42%) silty clay. Results of tests on isotropically and anisotropically (K_0) consolidated samples are presented and compared to existing data on resedimented BBC and to the behavior of another reconstituted low plasticity clay (PI=12%, LL=25%), Lower Cromer Till.

Previous investigations on resedimented BBC since 1961 are summarized and results are compiled in Chapter 2. The data reported in these studies involves significant scatter because of differing factors such as sedimentation methods, testing procedures and storage time resulting in different index properties, water content and engineering properties. The relative influence of each factor is assessed and separated in Chapters 4 and 5, where the volumetric and undrained behavior of the clay is discussed. The findings of those chapters are summarized below.

Soil compressibility in the normally consolidated state, as expressed by the slope of the virgin compression line (VCL) in a plot of axial strain, ϵ_a , vs. $\log \sigma'$, is independent of the consolidation stress ratio (K). However, for a given value of the vertical stress, σ'_v , the isotropically consolidated samples are more compressible (Fig. 4.3) than the anisotropically (K_0) consolidated samples. On the other hand, no definitive conclusions could be reached with regard to the position of the VCL in a void ratio, e , vs. $\log \sigma'$ plot due to the large scatter of the

triaxial and oedometer data resulting from thixotropic, and hence storage time, effects on resedimented BBC behavior. O'Neill (1985) found that thixotropy (storage time after resedimentation) increases the preconsolidation pressure of the clay, σ'_p . Measured behavior during anisotropic consolidation described herein suggests that thixotropy also tends to increase the lateral effective stress ratio (K_0) during K_0 -consolidation (with no lateral straining).

Soil compressibility measured during K_0 -consolidation in the triaxial equipment is similar to data obtained in oedometer tests and indicates that the overconsolidated behavior of BBC is very non-linear. During rebound, soil stiffness, as expressed by the swelling ratio*, SR, increases significantly with the overconsolidation ratio ($OCR=\xi$) and is higher than the recompression ratio*, RR, of the clay at a given value of ξ .

During undrained shearing of anisotropically consolidated samples, significant brittleness is observed in compression tests due to the development of failure planes and clear instabilities take place in extension tests due to necking of the sample. This gives rise to significant scatter in the measured data at high strain levels and reduces their reliability.

Comparing compression to extension behavior of K_0 -NC samples of resedimented BBC during undrained shearing, results show that:

a) the undrained strength s_u (at peak shearing resistance) in compression is twice as high as extension. This is principally due to the significantly lower excess pore pressures;

* slope of the ϵ_a vs. $\log \sigma'$ plot.

- b) the friction angle at peak, ϕ'_p , in compression is smaller by 5° ;
- c) the undrained stiffness of the soil as expressed by the secant Young's modulus, E_{50} , at 50% of the incremental shear stress required to reach peak resistance (i.e., $\Delta q/\Delta q_{\max}=50\%$) is 10 times larger.

Comparing the effective stress envelopes at peak undrained strength for isotropically consolidated samples (CIUC) vs. K_0 -consolidated samples (CK_0UC), results for various OCR indicates no dependence on the consolidated stress ratio. However, CK_0UC samples exhibit a higher undrained shear strength (by 12%), smaller axial strain at peak and a significantly larger stiffness, E_{50} , than the CIUC samples. This behavior applies to all OCR's considered (OCR=1,2,4 and 8).

The behavior of resedimented BBC is compared to reconstituted Lower Cromer Till (LCT) in Chapter 6. The two clays exhibit the same general trends with differences that are compatible with the lower plasticity of LCT. Comparing the volumetric and undrained behavior of BBC to LCT, results show that:

- a) BBC is two times more compressible than LCT, for both the normal and overconsolidated range.
- b) The position of the virgin compression line (VCL) depends on the consolidation stress ratio (k). For a same octahedral stress, σ'_{oct} , larger water content changes are observed for lower values of K . This behavior is valid for both BBC and LCT.
- c) During undrained triaxial compression shearing, larger negative shear-induced pore pressures develop in the case of normally consolidated samples of LCT. The situation is reversed for the overconsolidated samples.
- d) Anisotropically consolidated (K_0) samples of BBC sheared undrained

in compression show a more pronounced undrained brittleness than samples of LCT. This is related to the lower plasticity of LCT and to the lower consolidation stress ratio, K_0 , used for LCT.

Two "special" tests are described in Chapter 7. The first test (CK₀UC1) investigates the drained and undrained behavior at a very low stress ratio ($K=0.34$) of a sample presheared beyond its peak undrained strength (i.e., after reaching the strain softening stage). Results indicate that, by decreasing the stress ratio ($K=0.34$) during consolidation, the soil exhibits the following behavior:

a) during consolidation, the soil has the same compression ratio, CR, as the intact soil (consolidated at $K=0.47$) but has a reduced void ratio (or water content) for the same octahedral stress, σ'_{oct} , i.e., differences in a reduction in K causes a shift of the virgin compression line on a w vs $\log \sigma'$ plot to the left, Fig. 7.2;

b) during undrained compression shearing, a decrease in K increases soil brittleness (strain softening susceptibility) of the sample, increases the stiffness at small strains, and decreases the axial strain required to reach peak resistance.

The second test (CK₀U-Cyc-4) is cyclically sheared at constant stress levels. two values of the cyclic stress ratio, CSR ($= q_{static} + q_{cyclic} / s_u$ (see Fig. 7.7 for definition of stresses) are used. A CSR of 0.4 is first applied for which stable conditions are reached at cycle $N=40$. The CSR is then increased to 0.6, where failure is observed at cycle $N=25$. Results from undrained cyclic shearing, at CSR=0.6, show that:

1) Failure occurs gradually as permanent strains develop, increasing the cyclic strain amplitude. The rate of strain development is increased after $N=25$ cycles.

2) The average pore pressures measured in a cycle reach a minimum value at cycle $N=8$, then increase steadily.

3) At large cycles, characteristic "S-shape" develop in the stress-strain curves. This is attributed to the different strain rates observed in a cycle. A maximum of 92% axial strain per hour is measured in the middle of a cycle where only an average of 0.1% axial strain per hour is observed around the peaks.

8.2 Recommendations

Further research on resedimented BBC is recommended in the following areas:

1) Thixotropy:

A comprehensive study of thixotropic effects on resedimented BBC is of critical importance because of their strong and undesirable influence on behavior. Since the storage time for all samples cannot realistically be kept constant, this study should attempt to: 1) Quantify the effects of thixotropy on various important aspects of behavior and derive consistent and reliable correction factors for the time of storage of various samples; and, 2) develop a basic understanding of thixotropy in order to minimize its effects in proved methods of sedimentation.

2) Virgin Compression Line (VCL):

The position of the VCL in e - $\log \sigma'$ space needs to be defined for different values of K . This could be accomplished in the triaxial cells by consolidating samples along different radial stress paths.

3) Extension:

No reliable data regarding BBC behavior during undrained triaxial extension shearing are available. A complete series of isotropically and anisotropically (K_0) consolidated extension tests should be performed.

4) Strain Rate:

A comprehensive study of the effects of strain rate during undrained shearing of BBC is required.

5) Water Content:

The importance of careful and accurate water content measurements should be kept in mind.

REFERENCES

Note: ASCE = American Society of Civil Engineers
 ASTM = American Society of Testing and Materials
 ICSMFE = International Conference on Soil Mechanics
 and Foundation Engineering
 JGED = Journal of the Geotechnical Engineering
 Division
 JSMFD = Journal of the Soil Mechanics and Foundations
 Division
 MIT = Massachusetts Institute of Technology
 STP = Special Technical Publication
 GTJ = Geotechnical Testing Journal

AKAI, K. AND T. ADACHI (1965)

"Study of the One-Dimensional Consolidation and the Shear Strength Characteristics of Fully Saturated Clay; in Terms of Effective Stress," 6th ICSMFE, Montreal, Vol. 1, Paper 2/2, pp. 146-150.

AMERASINGHE, S.E. AND R.H.G. PARRY (1975)

"Anisotropy in Heavily Overconsolidated Kaolin," JGED, ASCE, Vol. 101, pp. 1277-1293.

ANDERSEN, K.H., J.H. POOL, S.F. BROWN AND W.F. ROSENBRAND (1980)

"Cyclic and Static Laboratory Tests on Drammen Clay," JGED, ASCE, Vol. 106, GT5, pp. 499-529.

ANDRAWS, K.Z. AND M.A. EL-SOBY (1973)

"Factors Affecting Coefficient of Earth Pressure K_0 ," JSMFD, ASCE, Vol. 99, No. 5177, pp. 527-539.

ATKINSON, J.H., J.S. EVANS AND E.W. HO (1965)

"Non-Uniformity of Triaxial Samples due to Consolidation with Radial Drainage," Geotechnique 35, No. 3, pp. 353-355.

AYAN, K.D.J. (1985)

"Undrained Triaxial Strength-Deformation Behavior of Harrison Bay Arctic Silts," M.Sc. Thesis, Dept. of Civil Eng., MIT, Cambridge, MA, 352 p.

AZZOUZ, A.S. AND M.M. BALIGH (1984)

"Behavior of Friction Piles in Plastic Empire Clays," Res. Rpt. R84-14, Order No. 771, Dept. of Civil Eng., MIT, Cambridge, MA, 902 p.

BAILEY, W.A. (1961)

"Effects of Salt on the Shear Strength of Boston Blue Clay," S.B. Thesis, Dept. of Civil Eng., MIT, Cambridge, MA

BENSARI, J.E. (1984)

"Stress-Strain Characteristics from Undrained and Drained Triaxial Tests on Resedimented Boston Blue Clay," M.Sc. Thesis, Dept. of Civil Eng. MIT, Cambridge, MA, 193 p.

- BISHOP, A.W. (1958)
"Test Requirements for Measuring the Coefficient of Earth Pressure at Rest," Conf. Earth Pressure Problems, Brussels, pp. 2-14.
- BISHOP, A.W. AND D.J. HENKEL (1962)
"The Measurement of Soil Properties in the Triaxial Test," 2nd ed., Edward Arnold Pub. Ltd., London, 227 p.
- BOVEE, R. AND C.C. LADD (1970)
"M.I.T. Plane Strain Device," Res. in Earth Physics, Phase Rpt. 12, Dept. of Civil Eng., MIT, Cambridge, MA
- BRAATHEN, N.F. (1966)
"Investigation of Effects of Disturbance on Undrained Shear Strength of Boston Blue Clay," S.M. Thesis, Dept. of Civil Eng., MIT, Cambridge, MA
- BROMS, B. AND M.V. RATNAM (1963)
"Shear Strength of Anisotropically Consolidated Clay," JSMFD, Proc. ASCE, Vol. 89, SM6, pp. 1-26.
- BROOKER, E.W. and H.O. IRELAND (1965)
"Earth Pressure of Rest Related to Stress History," Canadian Geot. Journal, Vol. 2, No. 1, pp. 1-15.
- BURLAND, J.B. and SYMES, M.J.P.R. (1980)
"A Simple Axial Displac Gauge for Use in the Triaxial Apparatus," Geotechnique, 32, No. 1, pp. 62-65.
- DICKEY, J.W. (1967)
"A Plane Strain Shearing Device for Testing Clays," M.Sc. Thesis Dept. of Civil Eng., MIT, Cambridge, MA
- DICKEY, J.W., LADD, C.C. and RIXNER, J.J. (1968)
"A Plane Strain Shear Device for Testing Clays," Res. Rpt. R68-3, Soil Publication 237, MIT, Cambridge, MA, 162 p.
- DONAGHE, R.T. AND TOWNSEND (1978)
"Effects of Anisotropic versus Isotropic Consolidation in Consolidated Undrained Triaxial Compression Tests of Cohesive Soils," Geot. Testing Journal, GTJ, Vol. 1, No. 4, pp. 173-189.
- GENS, A. (1982)
"Stress-Strain and Strength Characteristics of a Low Plasticity Clay," Ph.D. Thesis, Imperial College, London, 856 p.
- GERMAINE, J.T. (1982)
"Development of the Directional Shear Cell for Measuring Cross Anisotropic Clay Properties," Ph.D. Thesis, Dept. of Civil Eng., MIT, Cambridge, MA, 530 p.
- GERMAINE, J.T. (1985)
"Laboratory Measurement of Clay Behavior," MIT Special Summer Course 1.60S, Dept. of Civil Eng., MIT, Cambridge, MA, 131 p.

- HEAD, K.H. (1982)
Manual of Soil Laboratory Testing, Vol. 2, John Wiley & Sons, New York,
748 p.
- HENKEL, D.J. AND V.A. SOWA (1963)
"The Influence of Stress History on Stress Paths in the Undrained Triaxial
Tests on Clays," Laboratory Shear Testing of Soils, STP 361, ASTM, pp.
280-291.
- HIGHT, D.W. (1983)
"Laboratory Investigations of Sea-Bed Clays," Ph.D. Thesis, Imperial
College, London, 780 p.
- HIGHT, D.W., A. GENS AND R.J. JARDINE (1985)
"Evaluation of Geotechnical Parameters from Triaxial Tests on Offshore
Clay," Proc. Symp. Underwater Tech. Conf. on Offshore Tech., London, 31 p.
- JACKSON, W.T. (1963)
"Stress Paths and Strains in a Saturated Clay," M. Sc. Thesis, Dept. of
Civil Eng., MIT, Cambridge, MA, 101 p.
- JAKY, J. (1948)
"Pressure in Silos," Proc 2nd ICSMFE, London, Vol. 1, pp. 103-107.
- JARDINE, R.S., SYMES, M.J.P.R. and J.B. BURLAND (1984)
"The Measurement of Soil Stiffness in the Triaxial Apparatus,"
Geotechnique, 34, No. 3, pp. 323-340.
- KAVVADAS, M. (1982)
"Non-linear Consolidation around Driven Piles in Clays," Ph.D. Thesis,
Dept. of Civil Eng., MIT, Cambridge, MA
- KENNEY, T.C. (1964)
"Sea-Level Movements and the Geologic Histories of the Post-Glacial Marine
Soils at Boston, Nicolet, Ottawa and Oslo," Geotechnique, 14, No. 3, pp.
203-230.
- KHERA, R.P. AND R.J. KRIZEK (1967)
"Strength Behavior of Anisotropically Consolidated Remoulded Clay,"
Highway Research Record, 190, pp. 8-18.
- KINNER, E.B. AND C.C. LADD (1970)
"Load-Deformation Behavior of Saturated Clays during Undrained Shear,"
Res. in Earth Physics, Phase Rpt. No. 13, Res. Rpt. R70-27, MIT,
Cambridge, MA, 302 p.
- KOUTSOFTAS, D.C. AND C.C. LADD (1985)
"Design Strengths for an Offshore Clay," JGE, Vol. 111, No. 3, March, pp.
337-355.
- KOUTSOFTAS, D.C., (1981)
"Undrained Shear Behavior of a Marine Clay," ASTM STP 740, Yong and
Townsend ed., pp. 254-276.

- LADD, C.C. (1965)
 "Stress-Strain Behavior of Anisotropically Consolidated Clays during Undrained Shear," 6th ICSMFE, Montreal, Vol. 1, Paper 2/31, pp. 282-286.
- LADD, C.C. (1985)
 "Overview of Clay Behavior," MIT Special Summer Course 1.60S, Dept. of Civil Eng., MIT, Cambridge, MA, 99 p.
- LADD, C.C. AND L. EDGERS (1972)
 "Consolidated-Undrained Direct-Simple-Shear Tests on Saturated Clays," Res. Rpt. R72-82, No. 284, Dept. of Civil Eng, MIT, Cambridge, MA, 354 p.
- LADD, C.C., BOVEE, L. EDGERS AND RIXNER (1971)
 "Consolidated-Undrained Plane Strain Shear Tests on Boston Blue Clay," Res. in Earth Physics, Phase rpt. No. 15, Dept. of Civil Eng, MIT, Cambridge, MA, 243 p.
- LADD, C.C. and R. FOOTT (1974)
 "New Design Procedure for Stability of Soft Clays," Proc. ASCE, JGED, Vol. 100, GT7, pp. 763-786.
- LADD, C.C., R. FOOTT, K. ISHIHARA, F. SCHLOSSER and H.G. POULOS (1977)
 "Stress Deformation and Strength Characteristics," 9th ICSMFE, Tokyo, pp. 421-494.
- LADD, C.C. AND U. LUSCHER (1965)
 "Engineering Properties of Soils Underlying the MIT Campus," Res. Rpt. R65-58, Dept. of Civil Eng, MIT, Cambridge, MA.
- LADD, C.C. and VARALLYAY, J. (1965)
 "The Influence of Stress System on the Behavior of Saturated Clays during Undrained Shear," Res. Rpt. R65-11, MIT, Cambridge, MA, Soil Publication No. 177, 263 p.
- LADE, P.V., and TSAI, J. (1985)
 "Effects of Localization in Triaxial Tests on Clay," 11th ICSMFE, San Francisco, Vol. 2, pp. 549-552, 1/A/33.
- LAMBE, T.W. (1951)
 Soil Testing for Engineers, John Wiley & Sons, New York.
- LAREW, H.G. AND G.A. LEONARDS (1962)
 "A Strength Criterion for Repeated Loads," Proc. HRB 41.
- LEE, K.L. AND R.A. MORRISON (1970)
 "Strength of Anisotropically Consolidated Compacted Clay," JSMFD, ASCE, Vol. 96, SM6, pp. 2025-2043.
- LUTZ, D.G. (1985)
 Personal Communication.
- MALEK, A. (1986)
 Ph.D. Thesis in Preparation, Dept. of Civil Eng., MIT, Cambridge, MA

- MAYNE, P.W. AND F.H. KULHAWY (1982)
 "Ko-OCR Relationship in Soil," JGED, ASCE, Vol. 108, GT6, pp. 851-872.
- MIT (1986)
 "Behavior of Piles Supporting Tension Leg Platforms," Progress Rpt. 2, Sea Grant Program, unpublished.
- MITACHI, T. AND S. KITAGO (1976)
 "Change in Undrained Shear Strength Characteristics of Saturated Remolded Clay due to Swelling," Soils and Foundations, Vol. 16, No. 1, pp. 45-58.
- MITCHELL, J.K. (1956)
 "The Importance of Structure to the Engineering Behavior of Clay," Ph.D. Thesis, Dept. of Civil Eng., MIT, Cambridge, MA
- MITCHELL, J.K. (1976)
 Fundamentals of Soil Behavior, John Wiley & Sons, New York, 422 p.
- OLSON, R.E. and L.M. CAMPBELL (1967)
 "Bushing Friction in Triaxial Shear Testing," Materials Research and Standards, Vol. 7, No. 2, Feb., pp. 45-52.
- O'NEILL, D.A. (1985)
 "Undrained Strength Anisotropy of an Overconsolidated Thixotropic Clay," M.Sc. Thesis, Dept. of Civil Eng., MIT, Cambridge, MA.
- PARRY, R.H.G., and V. NADARAJAH (1973)
 "Observations on Laboratory Prepared, Lightly Overconsolidated Specimens of Kaolin," Geotechnique 24, No. 3, pp. 345-358.
- PARRY, R.H.G., (1960)
 "Triaxial Compression and Extension Tests on Remoulded Saturated Clay," Geotechnique 10, pp. 166-180.
- PRESTON, W.B. (1965)
 "The Effects of Sample Disturbance on the Undrained Strength Behavior of Boston Blue Clay," M.S. Thesis, Dept. of Civil Eng., MIT, Cambridge, MA, 193 p.
- RICHARDSON, A.M. JR. AND R.V. WHITMAN (1963)
 "Effect of Strain Rate upon Undrained Shear Resistance of Saturated Remolded Fat Clay," Geotechnique, 13, No. 4, pp. 310-346.
- ROSCOE, K.H. AND J.B. BURLAND (1968)
 "On the Generalized Stress-Strain Behaviour of 'Wet' Clay," Engineering Plasticity, J. Heyman ed., Cambridge U. Press, pp. 535-609.
- ROWE, P.W. and L. BARDEN (1964)
 "Importance of Free Ends in Triaxial Testing," Proc. JSMFE, ASCE, Vol. 90, SMI, Jan., pp. 1-27.
- SANGREY, D.A., D.J. HENKEL AND M.I. ESRIG (1969)
 "The Effective Stress Response of a Saturated Clay Soil to Repeated

Loading," Canadian Geot. Journal, 6, pp. 241-252.

SCHMIDT, B. (1966)

Discussion of "Earth Pressure of Rest Related to Stress History," Canadian Geot. Journal, Vol. 3, No. 4, pp. 239-242.

WISSA, A. (1961)

"A Study of the Effects of Environmental Changes on the Stress-Strain Properties of Kaolinite," M. S. Thesis, Dept. of Civil Eng., MIT, Cambridge, MA

WHITTLE, A. J. (1987)

Ph.D. Thesis in Preparation, MIT, Cambridge, MA

Appendix A

Resedimented BBC Batch Data

A-1 Procedures

The equipment used, as well as the procedure followed are treated in great depth by Germaine (1982). The mixing, sedimentation, and consolidation equipment corresponds exactly to the one described by Germaine (1982). The procedures followed are also identical.

The Boston Blue Clay powder used in this research was recycled from the clay used to make the previous 12 batches. This clay was air dried, ground, passed through #40 sieve, and saved in large bins. Salt concentration of the powdered phase was found to be 9.9 g salt per kg of soil.

The actual quantities of material mixed to make the required final volume achieve 100% water content, 16 g/l salt concentration, and 0.01% (volume) phenol content, was:

14.499 kg	water,
14.765 kg	powdered clay with 9.9 g salt /kg of clay,
88.45 g	salt, and
1.45 ml	phenol,

giving a final salt concentration of 16.18 g/l.

A-2 Tabulated Results from the Consolidation of the Batch

TABLE A-1 SUMMARY OF CONSOLIDATION DATA FOR RESEDIMENTED BBC
Batch No. 113

INC	σ_{vc} (kg/cm ²)	Final Ht (cm)		Water Content (%)		Void Ratio (e)		Elapsed Time (min)		Cv x 10 ³ (cm ² /sec)	Cc	Av (cm ² /kg)	K _v x10 ⁷ (cm/sec)
		Primary	Increment	Primary	Increment	Primary	Increment	Primary	Increment				
0	0	-											
1	0.0078	-	23.430	-		-		-					
2	0.0156	-	20.900	-	79.62	-	2.214	-	2500	1.19	0.767	14.78	5.68
3	0.0313	19.393	19.359	71.29	71.10	1.982	1.977	1600	3820	1.02	0.718	6.86	2.44
4	0.0625	18.005	17.976	63.61	63.45	1.768	1.764	1150	1560	2.07	0.618	2.98	2.30
5	0.125	16.794	16.778	56.91	56.82	1.582	1.580	620	7155	2.17	0.525	1.26	1.10
6	0.25	15.767	15.756	51.23	51.17	1.424	1.423	400	2775	2.78	0.434	0.55	0.64
7	0.46	15.017	15.003	47.08	47.01	1.309	1.307	225	1965	4.99	0.394	0.25	0.55
8	1	14.156	14.156	42.32	42.32	1.175	1.176	170	3030	82.31	0.007	0.004	0.151
9	0.50	14.168	14.170	42.38	42.40	1.178	1.179	12	960	18.36	0.023	0.028	0.236
10	0.25	14.195	14.210	42.62	42.62	1.185	1.185	170	5795				

Appendix B

Miscellaneous details in the triaxial tests

B-1 B-Parameter

The B-Parameter ($\Delta u/\Delta \sigma_c$) is measured at each step during saturation. A good assessment of this parameter is essential to insure 100% saturation.

The following steps were followed:

- a -Isolate the system by closing all the valves (drainage and cell).
- b -Increase the pressure in the back pressure and cell lines to the desired values, without connecting them to the system.
- c -Lock the piston in place, and add the necessary weights to achieve isotropic conditions.
- d -Record the value of the pore pressure, u_0 .
- e -Open the cell pressure valve, release the piston and start timing.
- f -Record the value of the pore pressure for 1, 5, 10, 15, 30, 60, and 120 seconds.
- g -Open the drainage lines.
- h -The value of B to use is taken at a consistent time interval (e.g. at 30 seconds). The sample is considered saturated if B is at least equal to 0.97 before 30 seconds.

B-2 Membrane correction

A stress correction to the vertical stress is used to account for membrane resistance. The correction is based on Bishop and Henkel's (1962) procedure, and the following assumptions:

- a -Rubber is perfectly elastic with a poisson's ratio of one half. No hoop tension is therefore induced in the membrane, and no correction is applied to the lateral pressure. This is only true for undrained shear.

b -Membrane when held against the sample by the cell pressure is capable of taking compression.

c -Sample does not develop a single shear plane.

d -Compression modulus is identical to that measured in extension.

Based on the above mentioned assumptions, and using Bishop and Henkel's (1962) formula, the correction factor adopted for the membrane (two prophylactic thin membranes) is:

$$C_m = 1.942 \epsilon_a \quad (\text{Kg})$$

where ϵ_a is the cumulative axial strain.

B-3 Filter Drain Correction

A stress correction to the vertical stress is used to account for vertical filter drain resistance. This correction is based on Bishop and Henkel's (1962) findings of comparative tests with and without drains. It was found that the resistance increases linearly with axial strain, ϵ_a , and reaches a stable condition at $\epsilon_a=2\%$.

The correction adopted for compression tests where 8 strips, 1/4 in. wide, are used amounts to:

$$\begin{aligned} C_f &= 0.406 \epsilon_a(\%) \quad (\text{Kg}), & \epsilon_a < 2\% \\ C_f &= 0.813 \quad (\text{Kg}), & \epsilon_a > 2\% \end{aligned}$$

Filter strips are helicoidaly coiled around the sample during extension tests. No correction is applied in this case.

B-4 Area Correction

This represents the largest source of errors in any test without direct measurements. Cylindrical and Parabolic corrections are the most commonly used.

During consolidation, the cylindrical correction is used. During undrained shearing, parabolic correction is used for compression tests,

whereas the cylindrical one is applied for the extension data.

1 - Cylindrical

The corrected area, A_c , is computed with the assumption that the sample deforms cylindrically (see Fig. B1). A simple geometrical equation is derived:

$$A_c = A_0 \frac{1 - \frac{\Delta V}{V_0}}{1 - \frac{\Delta H}{H_0}}$$

2 - Parabolical

For these tests run in compression with rough ends, the parabolic area correction is used to calculate the stresses at the maximum area.

The derivation of the formula used is based on the following assumptions (see Fig. B2):

1) The rough end condition implies no lateral movement of the soil at both ends.

2) The sample is uniform and deforms therefore symmetrically. The resulting shape is a paraboloid, whose axis of revolution is the vertical one and whose plane of symmetry is a plane perpendicular to the vertical axis inscribing the largest diameter circle.

3) For undrained tests, the condition of no volume change prevails, and the displacement of the soil is symmetrical.

In order to proceed in the calculations the equation of the parabola is derived, is the intersection of any vertical plane with the deformed sample. Due to the symmetry of the problem, one can study only half of the parabola (Fig. B3). The boundary conditions are:

$$h=0 \quad r=r_{\max}$$

$$h=0 \quad \frac{dr}{dh} = 0 \quad (\text{see orientation of axis in Fig. B3})$$

$$h=h_d \quad r=r_o$$

The general form of a parabola being

$$r = ah^2 + bh + c$$

and solving for the boundary conditions:

$$r = (r_o - r_{\max}) \left(\frac{h}{h_d}\right)^c + r_{\max} \quad (\text{B.1})$$

The third assumption tells us that the deformed shape has the same volume as the initial one. Hence,

$$\begin{aligned} \text{Volume of shaded area in Fig. B3} &= \int_0^{h_d} \pi r^2 dh \\ &= \pi \int_0^{h_d} \left[(r_o - r_{\max}) \left(\frac{h}{h_d}\right)^2 + r_{\max} \right]^2 dh \end{aligned}$$

The integration of this polynome is very straightforward, and leads to:

$$8 \frac{h_d}{h_o} \left(\frac{r_{\max}}{r_o}\right)^2 + 4 \frac{h_d}{h_o} \left(\frac{r_{\max}}{r_o}\right) + 3 \frac{h_d}{h_o} - 15 = 0 \quad (\text{B.2})$$

The roots of Eq. B.2 are of the form

$$\frac{r_{\max}}{r_o} = -\frac{1}{4} \pm \frac{\sqrt{-20(h_d/h_o)^2 + 120h_d}}{8h_d/h_o} \quad (\text{B.3})$$

Substituting the strain $\epsilon_a = \frac{h_o - h_d}{h_o} = 1 - \frac{h_d}{h_o}$ in B.3, we finally get:

$$\frac{r_{\max}}{r_o} = -\frac{1}{4} + \frac{\sqrt{400 - 320\epsilon_a - 80\epsilon_a^2}}{16(1 - \epsilon_a)}$$

$$\text{and } \frac{A_{\max}}{A_o} = \frac{\pi r_{\max}^2}{\pi r_o^2} = \left[-\frac{1}{4} + \frac{\sqrt{400 - 320\epsilon_a - 80\epsilon_a^2}}{16(1 - \epsilon_a)} \right]^2$$

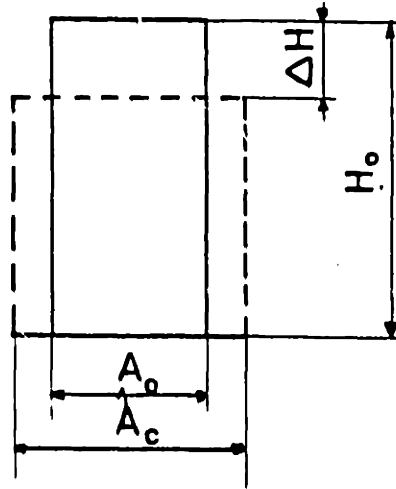


Figure B.1 Cylindrical Deformation of Sample.

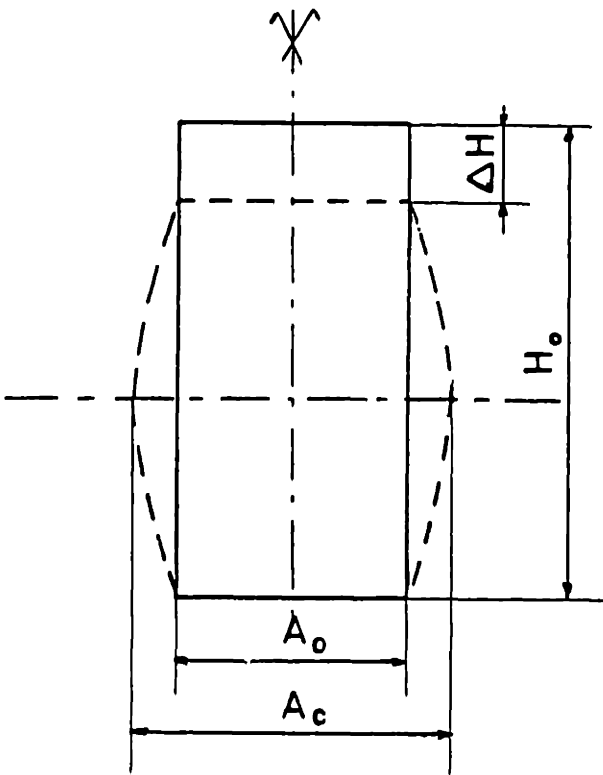


Figure B.2 Parabolical Deformation of Sample.

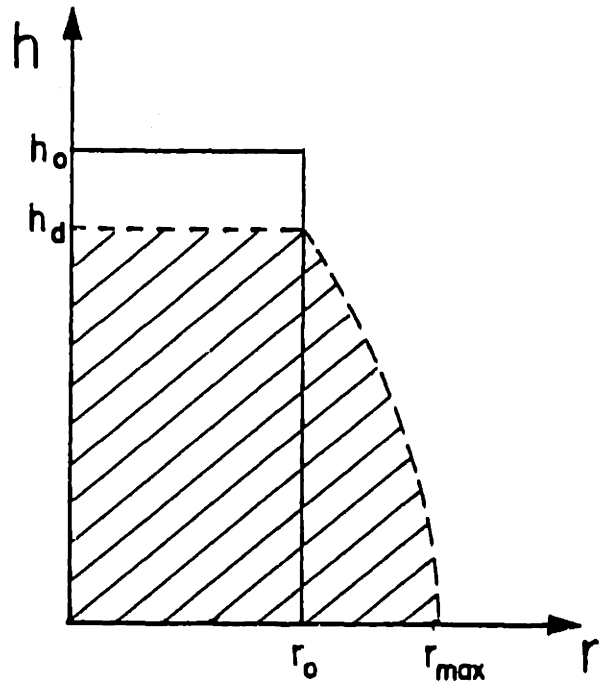


Figure B.3 Orientation of Axis for Parabolical Correction.

APPENDIX C

TRIAXIAL TEST DATA

CONSOLIDATED - UNDRAINED TRIAXIAL TEST

PROJECT BATCH 113
 SOIL TYPE BOSTON BLUE CLAY
 LOCATION Resedimented
 BORING NO. - SAMPLE NO. -
 DEPTH -

TEST NO. CK0UC1
 TYPE OF TEST CKUC
 APPARATUS NO. WFE-4
 TESTED BY PF
 DATE October 1985

WATER CONTENT

INITIAL, BASED ON TRIMMINGS 41.5 %
 INITIAL, BASED ON SAMPLE 43.8 %
 FINAL, BASED ON SAMPLE 32.8 %

ATTERBERG LIMITS

W_p _____ %
 W_L _____ %
 I_p _____ % I_L _____

PHASE RELATIONSHIPS

ρ_{WET} 1.772 g/cc ρ_{DRY} 1.233 g/cc
 e_i _____ e_f _____
 S_i _____ % $S_{precons}$ _____ %
 G_s 2.788

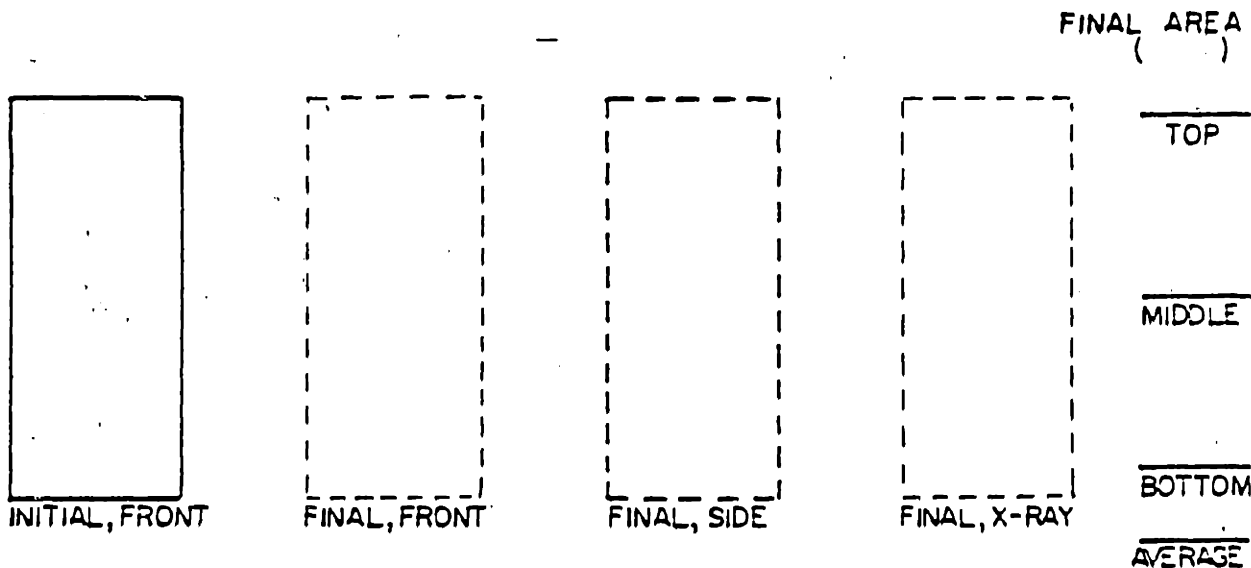
MISCELLANEOUS

B _____ %
 SATURATION ΔV -0.53 cm^3
 CONSOLIDATION ΔV _____
 MEMBRANES 0 THICK 2 THIN
 CORRECTION FACTOR 1.942, E
 FILTER STRIPS 8 X 1/4"
 CONFIGURATION Vertical
 CORRECTION FACTOR 0.4064 x E%
 AREA CORRECTION Right cylinder

GRAIN SIZE

% -#200 _____
 % -2 μ _____
 C_u _____ C_c _____

SAMPLE APPEARANCE



COMMENTS _____

CONSOLIDATED - UNDRAINED TRIAXIAL TEST

PROJECT BATCH 113 TYPE OF TEST CK₀UC TEST NO. CK₀UC1A

STRESS HISTORY

IN SITU CONDITIONS

σ'_{vo} 0.25 kg/cm²
 σ'_p 1.00 kg/cm²
 OCR 4

TORVANE STRENGTH _____
 TORVANE W_c _____ %

TEST CONDITIONS

σ'_{vc} 0.24 kg/cm²
 σ'_p 4.08 kg/cm²
 OCR 1.00
 K_c 0.47 U_b 2 kg/cm²
 STRAIN RATE 0.5 %/HOUR
 FINAL E_a _____ %

STRENGTH DATA

AT MAXIMUM q

E_a 0.066 %
 q/σ'_{vc} 0.324
 p/σ'_{vc} 0.740
 $\Delta u - \Delta \sigma_h / \sigma'_{vc}$ 0.046
 ϕ' 25.9
 A_f 0.642
 TIME TO q_{max} 8 minutes

AT MAXIMUM OBLIQUITY

E_a 0.108 %
 q/σ'_{vc} 0.320
 p/σ'_{vc} 0.731
 $\Delta u - \Delta \sigma_h / \sigma'_{vc}$ 0.052
 ϕ' 26.0
 $E_u(50\%) / q_f$ _____

TIME RECORD

SET UP 10/17/85
 START OF CONSOLIDATION 10/22/85
 START OF SHEAR 11/02/85
 END OF SHEAR 11/02/85
 REMOVAL _____
 TOTAL TIME IN APPARATUS _____
 CONSOLIDATION-SHEAR Δt 30 minutes

HYPERBOLIC STRESS-STRAIN PARAMETERS

G_i / σ'_{vc} _____
 R_f _____
 r^2 _____

RADIOGRAPHY

kV _____ mA _____
 EXPOSURE TIME _____

REMARKS

1st shear up to 1.16% axial strain.

CONSOLIDATED - UNDRAINED TRIAXIAL TEST

PROJECT BATCH 113 TYPE OF TEST CK₀UC TEST NO. CK₀UC1A

SAMPLE DIMENSIONS

	L (cm)	A (cm ²)	V (cm ³)	ϵ_0 (D) (%)	ϵ_{vol} (D) (%)	W
INITIAL	8.034	9.998*	80.33	-	-	
PRECONSOLIDATION	8.016	9.957	79.81	0.23	0.63	
PRESHEAR	7.264	9.946	72.25	9.59	10.06	
POST SHEAR	7.179	10.064	72.25	10.65	10.06	
FINAL						
FINAL MEASURED						

(a) Measured
(b) Based on initial dimensions
* Assumed value

CONSOLIDATION DATA

STRESSES IN kg/cm²

STEP	1	2	3	4	5	6	7	8	9	10
σ'_{vc}	0.24	0.28	0.30	0.37	0.42	0.48	0.57	0.65	0.73	0.85
σ'_{hc}	0.25	0.26	0.28	0.31	0.32	0.34	0.38	0.40	0.42	0.44
t_c (HRS)										
ϵ_0 (%)	0.23	0.23	0.38	0.46	0.54	0.60	0.63	0.84	0.95	1.18
ϵ_{vol} (%)	0.63	0.72	0.86	0.96	1.05	1.11	1.21	1.42	1.54	1.76
K_c	1.04	0.95	0.91	0.84	0.78	0.71	0.68	0.61	0.57	0.52

STEP	11	12	13	14	15	16	17	18	19	20
σ'_{vc}	1.00	1.11	1.24	1.37	1.48	1.55	1.75	1.95	2.15	2.35
σ'_{hc}	0.47	0.55	0.59	0.63	0.68	0.73	0.82	0.92	1.01	1.10
t_c (HRS)										
ϵ_0 (%)	1.41	1.58	2.05	2.42	2.71	3.59	3.87	4.60	5.56	5.82
ϵ_{vol} (%)	1.97	2.20	2.66	3.03	3.31	4.13	4.49	5.23	6.14	6.46
K_c	0.47	0.49	0.47	0.46	0.46	0.47	0.47	0.47	0.47	0.47

STEP	21	22	23	24	25	26	27	28	29	30
σ'_{vc}	2.56	2.86	3.15	3.45	3.70	4.08				
σ'_{hc}	1.21	1.36	1.48	1.62	1.74	1.91				
t_c (HRS)										
ϵ_0 (%)	6.06	7.38	7.63	8.18	9.3	9.59				
ϵ_{vol} (%)	6.75	8.01	8.29	8.63	9.74	10.06				
K_c	0.47	0.47	0.47	0.47	0.47	0.47				

GEOTECHNICAL LABORATORY
DEPT. OF CIVIL ENGR.
M.I.T.

CONSOLIDATED - UNDRAINED TRIAXIAL TEST

PROJECT Batch 113 TYPE OF TEST _____ TEST NO. CK0UC1B

STRESS HISTORY

IN SITU CONDITIONS

σ'_{vo} _____
 σ'_p _____
 OCR _____

TORVANE STRENGTH _____
 TORVANE W_c _____ %

TEST CONDITIONS

σ'_{vc} 6.04 ksc
 σ'_p 6.04 ksc
 OCR 1
 K_c 0.336 U_D 2
 STRAIN RATE 0.5 %/HOUR
 FINAL ϵ_a _____ %

STRENGTH DATA

AT MAXIMUM q

ϵ_a 0.053 %
 q/σ'_{vc} 0.365
 p/σ'_{vc} 0.677
 $\Delta u - \Delta \sigma_h / \sigma'_{vc}$ 0.002
 ϕ' 32.6
 A_f 0.04
 TIME TO q_{max} 6 min

AT MAXIMUM OBLIQUITY \equiv End of test

ϵ_a 0.874 %
 q/σ'_{vc} 0.311
 p/σ'_{vc} 0.594
 $\Delta u - \Delta \sigma_h / \sigma'_{vc}$ 0.03
 ϕ' 31.5

$E_u(50\%) / q_f$ 460

TIME RECORD

SET UP _____
 START OF CONSOLIDATION 11/02/85
 START OF SHEAR 11/06/85
 END OF SHEAR 11/06/85
 REMOVAL 11/06/85
 TOTAL TIME IN APPARATUS 21 days
 CONSOLIDATION-SHEAR Δt _____

HYPERBOLIC STRESS-STRAIN PARAMETERS

G_i / σ'_{vc} _____
 R_f _____
 r^2 _____

RADIOGRAPHY

kV _____ mA _____
 EXPOSURE TIME _____

REMARKS

CONSOLIDATED - UNDRAINED TRIAXIAL TEST

PROJECT Batch 113 TYPE OF TEST _____ TEST NO. CK0UC1B

SAMPLE DIMENSIONS

	L (cm)	A (cm)	V. (cm)	ϵ_a ^(b) (%)	ϵ_{vol} ^(b) (%)	W ()
INITIAL	(a)	(a)				
PRECONSOLIDATION	7.179	10.064	72.25	10.65	10.06	
PRESHEAR	6.521	10.698	69.76	18.84	13.16	
POST SHEAR						
FINAL	6.185			19.79		
FINAL MEASURED	6.230 (a)	(a)				

(a) Measured
 (b) Based on initial
 dimensions

CONSOLIDATION DATA

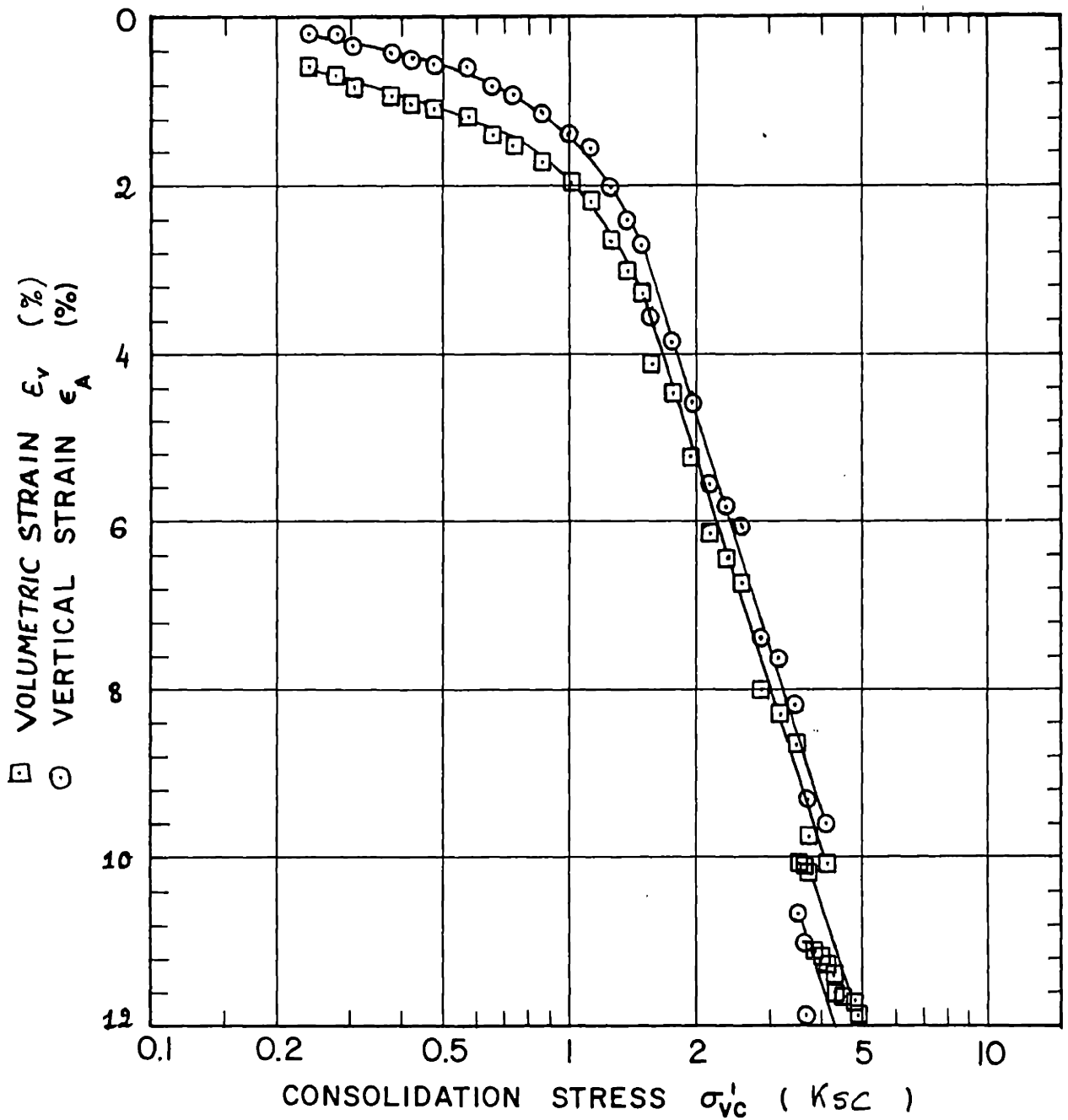
STRESSES IN ksc

STEP	1	2	3	4	5	6	7	8	9	10
σ'_{vc}	3.497	3.605	3.672	3.70	3.788	3.939	4.073	4.222	4.279	4.428
σ'_{hc}	1.184	1.228	1.253	1.295	1.302	1.320	1.378	1.413	1.435	1.499
t_c (HRS)										
ϵ_a (%)	10.645	11.012	11.85	14.44	14.54	14.57	14.87	15.17	15.65	15.67
ϵ_{vol} (%)	10.06	10.15	10.21	11.03	11.09	11.12	11.24	11.37	11.60	11.63
K_c	0.34	0.34	0.34	0.34	0.34	0.34	0.34	0.34	0.34	0.34

STEP	11	12	13	14	15	16	17	18	19	20
σ'_{vc}	4.634	4.813	5.011	5.164	5.465	5.648	5.851	6.044		
σ'_{hc}	1.568	1.637	1.699	1.753	1.861	1.904	1.970	2.029		
t_c (HRS)										
ϵ_a (%)	15.76	15.98	16.41	17.94	18.33	18.47	18.56	18.84		
ϵ_{vol} (%)	11.69	11.85	12.04	12.59	12.89	12.92	12.97	13.16		
K_c	0.34	0.34	0.34	0.34	0.34	0.34	0.34	0.34		

STEP	21	22	23	24	25	26	27	28	29	30
σ'_{vc}										
σ'_{hc}										
t_c (HRS)										
ϵ_a (%)										
ϵ_{vol} (%)										
K_c										

GEOTECHNICAL LABORATORY
 DEPT. OF CIVIL ENGR.
 M.I.T.



Sample No.	w_N (%)	Estimated		
Depth	w_L (%)	σ'_{vo}	σ'_p	
Soil Type	w_p (%)	CR 0.155	RR	
	I_p (%)	G_s	e_0	S (%)
○ At t_p or	hr	Remarks		
● At ()	hr			

GEOTECHNICAL LABORATORY
DEPT. OF CIVIL ENGR.
M.I.T.

COMPRESSION CURVE
TEST NO. CK₀UC1

FIGURE

Test CKJUC1A
Batch 113

Sig'vm = 3.681 Kg/cm2
Sig'vc = 3.681 Kg/cm2

Su = 1.320 Kg/cm2

v. strain %	q ----- sig'vc	p' ----- sig'vc	dU-dSIGh ----- sig'vc	sig'v ----- sig'h	Eu ----- Su	dQ ----- dQf	A
0.0018	0.2636	0.7363	0.0013	2.1155	656.60	0.0007	****
0.0019	0.2647	0.7366	0.0022	2.1223	969.70	0.0173	0.9351
0.0051	0.2732	0.7394	0.0078	2.1722	1356.6	0.1396	0.4077
0.0121	0.2925	0.7478	0.0186	2.2851	1535.9	0.4195	0.3227
0.0209	0.3088	0.7547	0.0280	2.3848	1357.1	0.6545	0.3108
0.0312	0.3201	0.7595	0.0346	2.4574	1128.4	0.8193	0.3057
0.0438	0.3281	0.7619	0.0402	2.5128	912.61	0.9348	0.3115
0.0586	0.3314	0.7615	0.0438	2.5411	715.85	0.9826	0.3232
0.0663	0.3327	0.7612	0.0456	2.5529	644.77	1.0009	0.3299
0.0839	0.3318	0.7579	0.0478	2.5573	502.91	0.9879	0.3503
0.1003	0.3298	0.7534	0.0501	2.5576	409.08	0.9596	0.3783
0.1083	0.3294	0.7518	0.0513	2.5599	376.42	0.9534	0.3902
0.1252	0.3269	0.7469	0.0540	2.5567	313.67	0.9173	0.4264
0.1436	0.3247	0.7426	0.0563	2.5544	264.30	0.8857	0.4608
0.1627	0.3225	0.7380	0.0588	2.5524	224.98	0.8532	0.4997
0.1804	0.3191	0.7326	0.0610	2.5440	191.80	0.8049	0.5492
0.1984	0.3161	0.7281	0.0625	2.5344	165.15	0.7605	0.5954
0.2175	0.3148	0.7256	0.0640	2.5333	147.24	0.7428	0.6241
0.2357	0.3141	0.7230	0.0659	2.5362	133.91	0.7317	0.6520
0.2540	0.3117	0.7259	0.0607	2.5055	118.68	0.6976	0.6303
0.2721	0.3101	0.7239	0.0613	2.4990	107.22	0.6742	0.6586
0.2901	0.3081	0.7204	0.0628	2.4948	96.41	0.6452	0.7055
0.3074	0.3068	0.7159	0.0661	2.5002	82.468	0.6264	0.7640
0.3244	0.3058	0.7106	0.0703	2.5110	81.996	0.6120	0.8317
0.3414	0.3045	0.7061	0.0734	2.5164	75.552	0.5925	0.8970
0.3585	0.3035	0.7040	0.0745	2.5155	70.256	0.5779	0.9345
0.3981	0.2996	0.6895	0.0850	2.5369	57.426	0.5219	1.1803
0.4310	0.2988	0.6801	0.0936	2.5676	51.951	0.5107	1.3278
0.4795	0.2957	0.6651	0.1053	2.6015	42.837	0.4660	1.6361
0.5276	0.2945	0.6554	0.1136	2.6321	37.502	0.4478	1.8376
0.5760	0.2925	0.6455	0.1214	2.6575	32.292	0.4193	2.0973
0.9078	0.2832	0.6066	0.1514	2.7514	14.307	0.2839	3.8626
1.0376	0.2811	0.5960	0.1602	2.7862	11.331	0.2545	4.5571
1.1583	0.2787	0.5834	0.1700	2.8301	8.9199	0.2200	5.5928

Test CKoUC1B
Batch 113

Sig'vm = 6.035 Kg/cm2
Sig'vc = 6.035 Kg/cm2

Su = 2.2575 Kg/cm2

v. strain %	q ----- sig'vc	p' ----- sig'vc	dU-dSIGh ----- sig'vc	sig'v ----- sig'h	Eu ----- Su	dQ ----- dQf	A
0.0121	0.3329	0.6670	0.0015	2.9935	7.3438	0.0001	2486.9
0.0445	0.3328	0.6671	0.0013	2.9910	0.4734	-0.003	-5.199
0.0648	0.3325	0.6675	0.0015	2.9855	-1.931	-0.009	-1.959
0.0689	0.3325	0.6660	0.0029	2.9944	-1.721	-0.009	-3.832
0.0706	0.3326	0.6639	0.0050	3.0075	-1.472	-0.008	-7.029
0.0718	0.3421	0.6674	0.0111	3.1040	69.799	0.2240	0.6048
0.0984	0.3678	0.6870	0.0178	3.3043	190.11	0.8477	0.2565
0.1036	0.3705	0.6894	0.0180	3.3242	194.67	0.9145	0.2405
0.1111	0.3724	0.6916	0.0176	3.3336	190.58	0.9604	0.2241
0.1169	0.3729	0.6927	0.0170	3.3328	183.62	0.9735	0.2128
0.1262	0.3736	0.6944	0.0159	3.3293	172.93	0.9897	0.1955
0.1337	0.3734	0.6951	0.0149	3.3219	162.52	0.9854	0.1841
0.1372	0.3730	0.6957	0.0136	3.3115	156.60	0.9741	0.1709
0.1494	0.3718	0.6955	0.0125	3.2969	139.62	0.9455	0.1618
0.1743	0.3659	0.6914	0.0108	3.2486	101.76	0.8032	0.1639
0.1806	0.3660	0.6915	0.0108	3.2494	98.432	0.8052	0.1632
0.1847	0.3660	0.6919	0.0103	3.2461	96.118	0.8040	0.1562
0.1980	0.3650	0.6913	0.0099	3.2371	86.960	0.7798	0.1548
0.2021	0.3645	0.6911	0.0096	3.2320	83.983	0.7683	0.1527
0.2189	0.3611	0.6884	0.0088	3.2067	69.276	0.6861	0.1578
0.2501	0.3580	0.6852	0.0089	3.1886	54.003	0.6109	0.1782
0.2663	0.3546	0.6814	0.0093	3.1704	43.848	0.5276	0.2155
0.2866	0.3517	0.6776	0.0101	3.1580	35.302	0.4565	0.2703
0.3046	0.3498	0.6745	0.0113	3.1555	29.989	0.4117	0.3364
0.3295	0.3472	0.6706	0.0126	3.1467	23.381	0.3466	0.4438
0.3462	0.3454	0.6673	0.0140	3.1461	19.542	0.3039	0.5633
0.3665	0.3433	0.6638	0.0154	3.1425	15.383	0.2526	0.7429
0.3914	0.3415	0.6606	0.0168	3.1403	11.922	0.2083	0.9835
0.4059	0.3403	0.6579	0.0184	3.1435	9.9541	0.1799	1.2454
0.4313	0.3390	0.6549	0.0199	3.1462	7.7307	0.1478	1.6383
0.4504	0.3374	0.6519	0.0213	3.1456	5.5045	0.1087	2.3875
0.4765	0.3360	0.6491	0.0227	3.1473	3.6710	0.0757	3.6636
0.4846	0.3347	0.6462	0.0241	3.1486	2.1212	0.0428	6.8808
0.5083	0.3337	0.6438	0.0255	3.1521	0.9755	0.0186	16.764
0.5245	0.3329	0.6416	0.0269	3.1567	0.1199	-0.001	-233.9
0.5361	0.3326	0.6409	0.0273	3.1583	-0.152	-0.007	-42.42
0.5685	0.3297	0.6346	0.0307	3.1631	-2.864	-0.078	-4.778
0.6171	0.3288	0.6313	0.0331	3.1749	-3.381	-0.099	-4.061
0.6698	0.3269	0.6273	0.0352	3.1760	-4.713	-0.147	-2.901
0.7069	0.3253	0.6242	0.0368	3.1769	-5.637	-0.185	-2.419
0.7556	0.3234	0.6215	0.0379	3.1704	-6.609	-0.231	-1.997
0.8002	0.3218	0.6188	0.0392	3.1672	-7.335	-0.271	-1.761
0.8471	0.3204	0.6162	0.0403	3.1664	-7.801	-0.304	-1.610
0.8964	0.3192	0.6123	0.0430	3.1778	-8.106	-0.334	-1.564
0.9473	0.3182	0.6092	0.0451	3.1871	-8.232	-0.358	-1.528

CONSOLIDATED - UNDRAINED TRIAXIAL TEST

PROJECT Batch 113
 SOIL TYPE Boston Blue Clay
 LOCATION Resedimented
 BORING NO. - SAMPLE NO. -
 DEPTH -

TEST NO. CK₀UC2
 TYPE OF TEST CK₀UC
 APPARATUS NO. WFE-6
 TESTED BY PF
 DATE Nov 1985

WATER CONTENT

INITIAL, BASED ON TRIMMINGS 42.2 %
 INITIAL, BASED ON SAMPLE 44.5 %
 FINAL, BASED ON SAMPLE 34.9 %

ATTERBERG LIMITS

W_p _____ %
 W_L _____ %
 I_p _____ % I_L _____

PHASE RELATIONSHIPS

WET 1.846 g/cc DRY 1.28 g/cc
 e_i 1.123 e_f 0.973
 S_i 104 % S_{precons} _____ %
 G_s 2.788

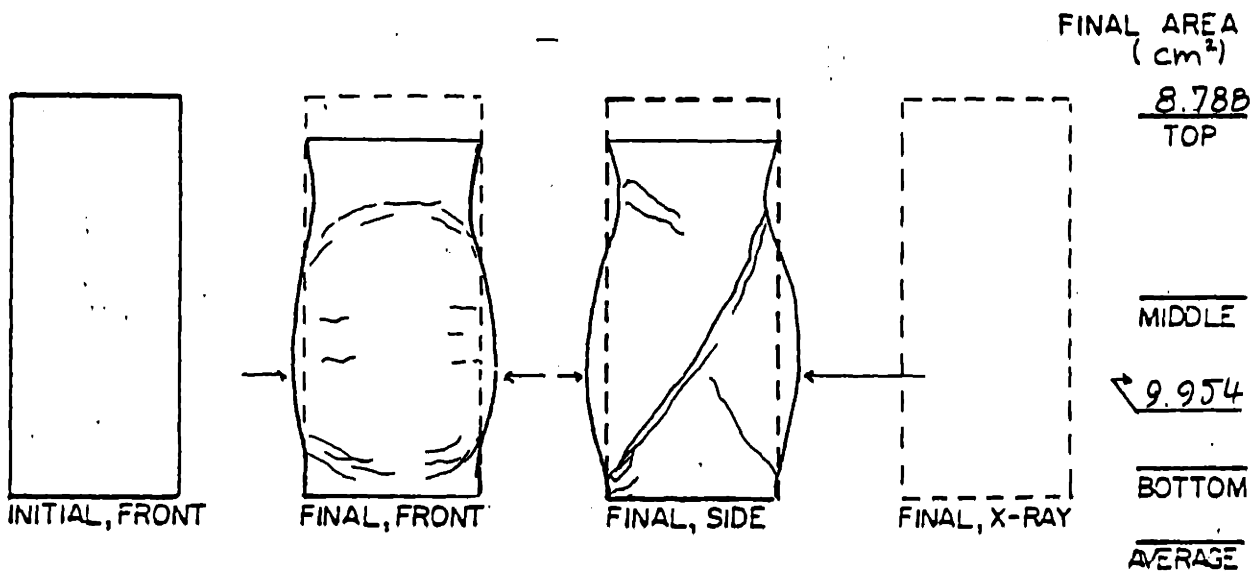
MISCELLANEOUS

B 110 %
 SATURATION ΔV -0.15
 CONSOLIDATION ΔV 7.51
 MEMBRANES 0 THICK 2 THIN
 CORRECTION FACTOR 1.942 × E
 FILTER STRIPS 8 × 1/4"
 CONFIGURATION Vertical
 CORRECTION FACTOR 0.4064 × E%
 AREA CORRECTION Parabolic

GRAIN SIZE

% -#200 _____
 % -#20 _____
 C_u _____ C_c _____

SAMPLE APPEARANCE



COMMENTS Dry weight is not reliable

CONSOLIDATED - UNDRAINED TRIAXIAL TEST

PROJECT Batch 113 TYPE OF TEST CK₀UC TEST NO. CK₀UC2

STRESS HISTORY

IN SITU CONDITIONS

σ'_{v0} 0.25 kg/cm²
 σ'_p 1.00 kg/cm²
 OCR 4

TORVANE STRENGTH _____
 TORVANE w_c _____ %

TEST CONDITIONS

σ'_{vc} 0.25 kg/cm²
 σ'_p 4.09 kg/cm²
 OCR 2.04

K_c 0.63 U_b 1.81 kg/cm²
 STRAIN RATE 0.5 %/HOUR
 FINAL ϵ_a _____ %

STRENGTH DATA

AT MAXIMUM q

ϵ_a 0.3 %
 q/σ'_{vc} 0.626
 p/σ'_{vc} 1.159
 $\Delta u - \Delta \sigma_h / \sigma'_{vc}$ 0.024
 ϕ' 32.5
 A_f 0.216
 TIME TO q_{max} 35 minutes

TIME RECORD

SET UP 10/29/85
 START OF CONSOLIDATION 11/03/85
 START OF SHEAR 11/16/85
 END OF SHEAR 11/18/85
 REMOVAL 11/18/85
 TOTAL TIME IN APPARATUS 21 days
 CONSOLIDATION-SHEAR Δt 30 min

REMARKS

AT MAXIMUM OBLIQUITY

ϵ_a 0.16 %
 q/σ'_{vc} 0.597
 p/σ'_{vc} 1.081
 $\Delta u - \Delta \sigma_h / \sigma'_{vc}$ 0.146
 ϕ' 33.5

$E_u(50\%) / q_f$ _____

HYPERBOLIC STRESS-STRAIN PARAMETERS

G_i / σ'_{vc} _____
 R_f _____
 r^2 _____

RADIOGRAPHY

kV - mA -
 EXPOSURE TIME -

CONSOLIDATED - UNDRAINED TRIAXIAL TEST

PROJECT Batch 113 TYPE OF TEST CK₀UC TEST NO. CK₀UC2

SAMPLE DIMENSIONS

	L (cm)	A (cm ²)	V (cm ³)	ϵ_0 ^(D) (%)	ϵ_{vol} ^(D) (%)	W
INITIAL	8.025	9.714	77.95	0	0	
PRECONSOLIDATION	8.021	9.709	77.88	0.05	0.10	
PRESHEAR	7.346	9.589	70.45	8.45	9.63	
POST SHEAR						
FINAL	7.032			12.37		
FINAL MEASURED						

(a) Measured on initial dimensions
(b) Based on initial dimensions

CONSOLIDATION DATA

STRESSES IN kg / cm²

STEP	1	2	3	4	5	6	7	8	9	10
σ'_{vc}	0.25	0.28	0.31	0.35	0.38	0.41	0.47	0.55	0.65	0.75
σ'_{hc}	0.25	0.26	0.28	0.29	0.30	0.30	0.31	0.34	0.37	0.40
t_c (HRS)	12.5	8	7	6	8	7.5	9	8	6	7.5
ϵ_0 (%)	0.05	0.13	0.17	0.23	0.28	0.35	0.44	0.59	0.70	0.83
ϵ_{vol} (%)	0.10	0.19	0.23	0.32	0.39	0.45	0.54	0.69	0.82	0.98
K_c	1.03	0.95	0.89	0.83	0.78	0.74	0.67	0.61	0.56	0.53

STEP	11	12	13	14	15	16	17	18	19	20
σ'_{vc}	0.85	0.95	1.05	1.16	1.25	1.40	1.60	1.80	2.00	2.25
σ'_{hc}	0.42	0.45	0.49	0.54	0.59	0.66	0.75	0.84	0.94	1.06
t_c (HRS)	10.5	5.5	19	6.5	7	10	5	9	9.5	24
ϵ_0 (%)	0.97	1.08	1.28	1.38	1.56	2.02	2.95	3.81	4.15	5.18
ϵ_{vol} (%)	1.12	1.23	1.50	1.64	1.85	2.36	3.36	4.41	4.80	6.03
K_c	0.49	0.47	0.47	0.47	0.47	0.47	0.47	0.47	0.47	0.47

STEP	21	22	23	24	25	26	27	28	29	30
σ'_{vc}	2.50	2.75	3.00	3.25	3.50	3.75	4.09	3.82	3.50	3.25
σ'_{hc}	1.18	1.29	1.41	1.53	1.65	1.76	1.92	1.95	1.75	1.68
t_c (HRS)	6	7.5	10.5	6.5	8.5	8.5	2.5	3	9.5	10
ϵ_0 (%)	5.29	6.22	6.69	6.91	7.75	7.99	8.64	8.63	8.61	8.60
ϵ_{vol} (%)	6.18	7.21	7.75	7.99	8.84	9.13	9.88	9.87	9.83	9.80
K_c	0.47	0.47	0.47	0.47	0.47	0.47	0.47	0.51	0.50	0.52

GEOTECHNICAL LABORATORY
DEPT. OF CIVIL ENGR.
M.I.T.

CONSOLIDATED - UNDRAINED TRIAXIAL TEST

PROJECT BATCH 113 TYPE OF TEST CEUC/E TEST NO. CK6UC2

STEP	31	32	33	34	35	36	37	38	39	40
σ'_{vc}	3.00	2.50	2.00							
σ'_{hc}	1.60	1.44	1.26							
t_c (HRS)	10	13	25							
E_D (%)	8.68	8.52	8.45							
E_{vol} (%)	9.78	9.70	9.63							
K_c	0.53	0.58	0.63							

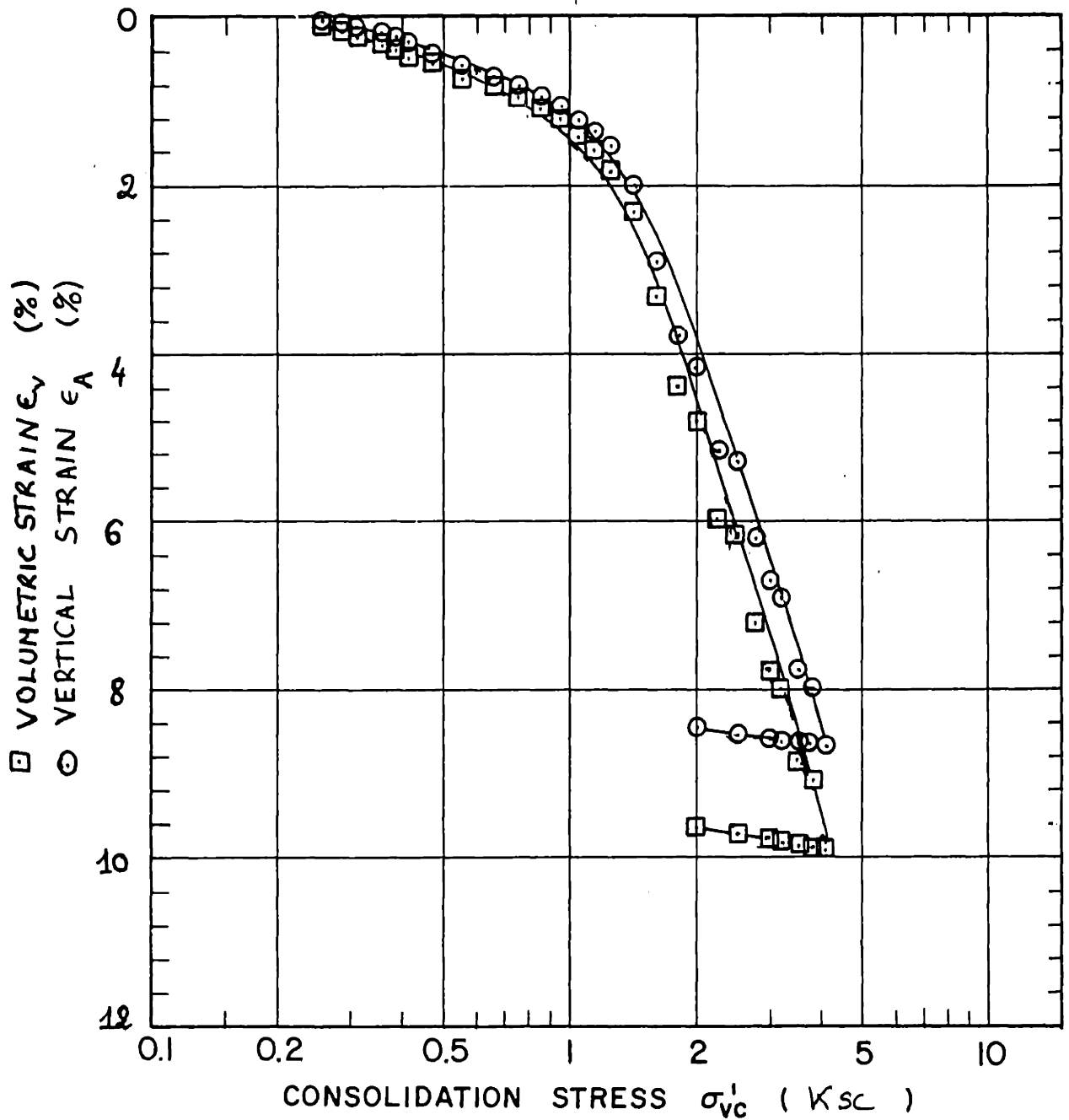
STEP	41	42	43	44	45	46	47	48	49	50
σ'_{vc}										
σ'_{hc}										
t_c (HRS)										
E_D (%)										
E_{vol} (%)										
K_c										

STEP	51	52	53	54	55	56	57	58	59	60
σ'_{vc}										
σ'_{hc}										
t_c (HRS)										
E_D (%)										
E_{vol} (%)										
K_c										

REMARKS

• AXIAL AND VOLUMETRIC STRAINS ARE REFERENCED TO THE PRECONSOLIDATION DIMENSIONS.

GEOTECHNICAL LABORATORY
DEPT. OF CIVIL ENGR.
M.I.T.



Sample No.	w_N (%)	Estimated	
Depth	w_L (%)	σ'_{v0}	σ'_p
Soil Type BBC	w_P (%)	CR 0.170	RR 0.0077
	I_P (%)	G_s 2.78	e_0 1.183 S (%) 104

○ At t_p or hr Remarks
 ● At () hr

GEOTECHNICAL LABORATORY
 DEPT. OF CIVIL ENGR.
 M.I.T.

COMPRESSION CURVE
 TEST NO. CK₀UC2

FIGURE

Test CKoUC2
Batch 113

Sig'vm = 4.088 Kg/cm²
Sig'vc = 1.9985 Kg/cm²

Su = 1.246 Kg/cm²

v. strain	q	p'	dU-dSIGh	sig'v	Eu	dQ	A
%	sig'vc	sig'vc	sig'vc	sig'h	Su	dQf	
0.0003	0.1850	0.8149	0	1.5877	373.53	0.0002	0
0.0001	0.1869	0.8160	0.0013	1.5942	6807.3	0.0044	0.1676
0.0025	0.2329	0.8355	0.0542	1.7733	6143.3	0.1094	0.2814
0.0073	0.2572	0.8443	0.0851	1.8762	3185.4	0.1647	0.2937
0.0104	0.2712	0.8495	0.1027	1.9383	2656.6	0.1967	0.2966
0.0160	0.2985	0.8603	0.1356	2.0628	2272.7	0.2590	0.2976
0.0191	0.3121	0.8662	0.1510	2.1265	2132.3	0.2899	0.2963
0.0279	0.3502	0.8831	0.1934	2.3143	1899.8	0.3767	0.2922
0.0312	0.3622	0.8889	0.2061	2.3757	1825.5	0.4042	0.2903
0.0447	0.4086	0.9132	0.2500	2.6194	1606.8	0.5099	0.2792
0.0549	0.4385	0.9307	0.2747	2.7815	1480.3	0.5781	0.2706
0.0782	0.4942	0.9696	0.3084	3.0796	1268.9	0.7054	0.2488
0.1021	0.5372	1.0064	0.3207	3.2900	1107.5	0.8033	0.2273
0.1182	0.5590	1.0295	0.3181	3.3765	1015.7	0.8531	0.2123
0.1385	0.5807	1.0558	0.3089	3.4448	917.35	0.9026	0.1948
0.1645	0.5992	1.0840	0.2894	3.4725	808.45	0.9448	0.1742
0.1862	0.6093	1.1033	0.2711	3.4671	731.62	0.9678	0.1594
0.2159	0.6176	1.1243	0.2455	3.4374	643.15	0.9866	0.1415
0.2650	0.6233	1.1484	0.2088	3.3741	530.78	0.9996	0.1187
0.2781	0.6221	1.1517	0.1998	3.3495	504.49	0.9970	0.1140
0.3137	0.6220	1.1601	0.1829	3.3118	447.15	0.9966	0.1043
0.4556	0.6069	1.1568	0.1592	3.2074	297.29	0.9623	0.0940
0.7346	0.5841	1.1107	0.2061	3.2188	174.43	0.9103	0.1288
1.0001	0.5690	1.0740	0.2500	3.2533	123.25	0.8757	0.1631
1.4232	0.5543	1.0256	0.3168	3.3522	83.302	0.8422	0.2143
1.8280	0.5437	0.9931	0.3600	3.4195	62.999	0.8180	0.2503
2.5103	0.5360	0.9615	0.4076	3.5189	44.892	0.8005	0.2896
3.5073	0.5247	0.9262	0.4549	3.6135	31.101	0.7748	0.3336
4.0144	0.5181	0.9102	0.4739	3.6430	26.646	0.7598	0.3544
4.5760	0.5138	0.8981	0.4888	3.6737	23.070	0.7499	0.3700
7.1003	0.4936	0.8564	0.5290	3.7221	13.960	0.7040	0.4243
9.0101	0.4836	0.8435	0.5324	3.6881	10.644	0.6812	0.4394
11.137	0.4639	0.8181	0.5410	3.6206	8.0439	0.6363	0.4755
13.077	0.4333	0.8008	0.5554	3.6094	6.5894	0.6119	0.5088
14.796	0.4200	0.7602	0.5702	3.4696	5.1028	0.5361	0.5968

CONSOLIDATED -- UNDRAINED TRIAXIAL TEST

PROJECT Batch 113
 SOIL TYPE BOSTON BLUE CLAY
 LOCATION RESEMENTED
 BORING NO. - SAMPLE NO. -
 DEPTH -

TEST NO. CK00cd
 TYPE OF TEST CK00C
 APPARATUS NO. WFF-4
 TESTED BY PF
 DATE Nov-Dec 1985

WATER CONTENT

INITIAL, BASED ON TRIMMINGS 41.5 %
 INITIAL, BASED ON SAMPLE 42.4 %
 FINAL, BASED ON SAMPLE 35.3 %

ATTERBERG LIMITS

W_p _____ %
 W_L _____ %
 I_p _____ % I_L _____

PHASE RELATIONSHIPS

ρ_{WET} 1.810 g/cc ρ_{DRY} 1.27 g/cm³
 e_i 1.193 e_f 0.988
 S_i 99 % $S_{precons}$ _____ %
 G_s 2.788

MISCELLANEOUS

B 98 %
 SATURATION ΔV -0.18
 CONSOLIDATION ΔV 7.03
 MEMBRANES 0 THICK 2 THIN
 CORRECTION FACTOR 1.942 * E
 FILTER STRIPS 8 X 1/4"
 CONFIGURATION VERTICAL
 CORRECTION FACTOR 0.4264 * E%
 AREA CORRECTION PARABOLIC

GRAIN SIZE

% -#200 _____
 % -2 μ _____
 C_u _____ C_c _____

SAMPLE APPEARANCE

				FINAL AREA (cm ²)
INITIAL, FRONT	FINAL, FRONT	FINAL, SIDE	FINAL, X-RAY	<u>7.766</u> TOP
				<u>10.304</u> MIDDLE
				<u>8.471</u> BOTTOM
				<u> </u> AVERAGE

COMMENTS Diameter not measured during set-up
so assumed diameter based on test TB.

CONSOLIDATED - UNDRAINED TRIAXIAL TEST

PROJECT BATCH 113 TYPE OF TEST CK₀UC TEST NO. CK₀UC4

STRESS HISTORY

IN SITU CONDITIONS

σ'_{vo} 0.25 kg/cm²
 σ'_p 1.00 kg/cm²
OCR 4

TEST CONDITIONS

σ'_{vc} 0.25 kg/cm²
 σ'_p 4.10 kg/cm²
OCR 4.06
 K_c 0.819 U_b 2 kg/cm²
STRAIN RATE 0.5 %/HOUR
FINAL ϵ_a 5.4 %

TORVANE STRENGTH _____
TORVANE W_c _____ %

STRENGTH DATA

AT MAXIMUM q

ϵ_a 1.064 %
 q/σ'_{vc} 1.017
 p/σ'_{vc} 1.822
 $\Delta u - \Delta \sigma_h / \sigma'_{vc}$ 0.016
 ϕ' 33.9
 A_f 0.018
TIME TO q_{max} 2 hours

AT MAXIMUM OBLIQUITY

ϵ_a 0.417 %
 q/σ'_{vc} 0.908
 p/σ'_{vc} 1.542
 $\Delta u - \Delta \sigma_h / \sigma'_{vc}$ 0.186
 ϕ' 36.0

$E_u(50\%)/q_f$ _____

TIME RECORD

SET UP 11/13/85
START OF CONSOLIDATION 11/17/85
START OF SHEAR 12/06/85
END OF SHEAR 12/09/85
REMOVAL 12/09/85
TOTAL TIME IN APPARATUS 27 days
CONSOLIDATION-SHEAR Δt 310 minutes

HYPERBOLIC STRESS-STRAIN PARAMETERS

G_i/σ'_{vc} _____
 R_f _____
 r^2 _____

RADIOGRAPHY

kV _____ mA _____
EXPOSURE TIME _____

REMARKS

CONSOLIDATED - UNDRAINED TRIAXIAL TEST

PROJECT BATCH 113 TYPE OF TEST CK₀UC TEST NO. _____ CKUC4

SAMPLE DIMENSIONS

	L (cm)	A (cm ²)	V (cm ³)	ϵ_0 ^(D) (%)	ϵ_{vol} ^(D) (%)	W (gms)
INITIAL	8.012	9.712	77.79	0	0	140.8
PRECONSOLIDATION	7.986	9.712	77.56	0.3	0.3	
PRESHEAR	7.331	9.621	70.53	8.15	9.06	
POST SHEAR						
FINAL	7.577			5.41		
FINAL MEASURED						98.88

(a) Measured
(b) Based on initial dimensions

CONSOLIDATION DATA

STRESSES IN kg/cm²

STEP	1	2	3	4	5	6	7	8	9	10
σ'_{vc}	0.30	0.33	0.37	0.41	0.48	0.55	0.65	0.75	0.85	1.01
σ'_{hc}	0.27	0.28	0.29	0.31	0.31	0.34	0.36	0.39	0.42	0.48
t_c (HRS)										
ϵ_0 (%)	0.04	0.08	0.15	0.21	0.33	0.44	0.60	0.73	0.87	1.10
ϵ_{vol} (%)	0.03	0.08	0.15	0.24	0.32	0.43	0.57	0.68	0.84	1.10
K_c	0.89	0.85	0.79	0.74	0.66	0.61	0.55	0.51	0.49	0.48

STEP	11	12	13	14	15	16	17	18	19	20
σ'_{vc}	1.09	1.21	1.30	1.40	1.51	1.61	1.76	1.91	2.05	2.20
σ'_{hc}	0.54	0.57	0.61	0.65	0.72	0.77	0.83	0.90	0.97	1.03
t_c (HRS)										
ϵ_0 (%)	1.17	1.33	1.48	1.67	1.95	2.42	2.79	3.55	4.08	4.19
ϵ_{vol} (%)	1.24	1.41	1.60	1.84	2.22	2.79	3.20	4.04	4.47	4.80
K_c	0.50	0.47	0.47	0.47	0.47	0.47	0.47	0.47	0.47	0.47

STEP	21	22	23	24	25	26	27	28	29	30
σ'_{vc}	2.35	2.55	2.75	3.00	3.34	3.50	3.75	4.10	3.74	3.50
σ'_{hc}	1.10	1.20	1.29	1.41	1.65	1.64	1.76	1.93	1.88	1.87
t_c (HRS)										
ϵ_0 (%)	4.29	5.55	5.85	6.23	7.29	7.42	7.64	8.69	8.67	8.66
ϵ_{vol} (%)	4.94	6.27	6.65	6.80	8.37	8.48	8.74	9.71	9.70	9.67
K_c	0.47	0.47	0.47	0.47	0.50	0.47	0.47	0.47	0.50	0.53

GEOTECHNICAL LABORATORY
DEPT. OF CIVIL ENGR.
M.I.T.

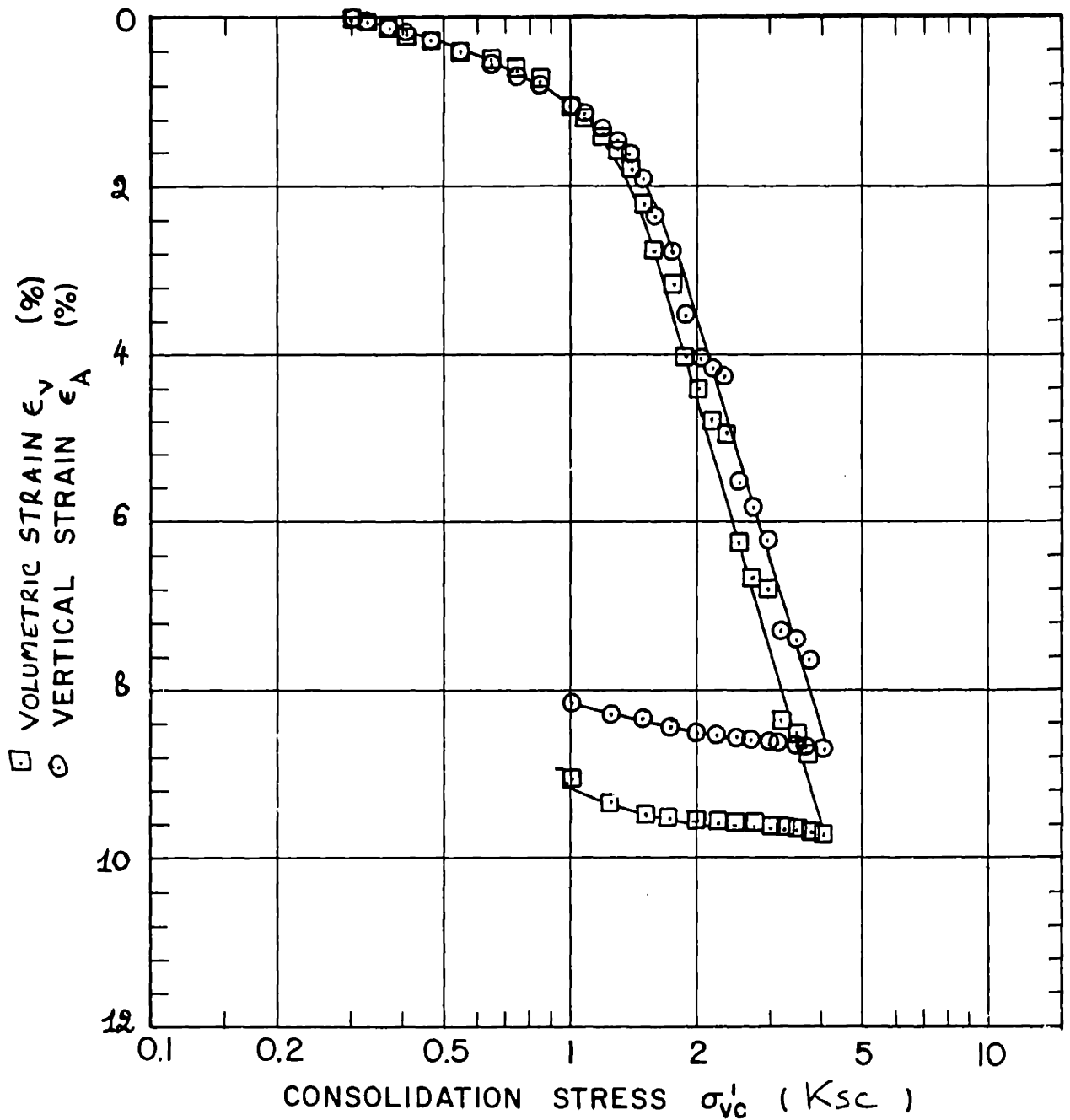
STEP	31	32	33	34	35	36	37	38	39	40
σ'_{vc}	3.25	3.01	2.75	2.50	2.25	2.0	1.75	1.50	1.25	1.01
σ'_{hc}	1.84	1.81	1.78	1.73	1.71	1.67	1.63	1.35	1.09	0.83
t_c (HRS)										
E_o (%)	8.64	8.62	8.59	8.57	8.53	8.49	8.43	8.36	8.31	8.15
E_{vol} (%)	9.66	9.64	9.63	9.61	9.59	9.57	9.53	9.43	9.32	9.06
K_c	0.57	0.60	0.65	0.69	0.76	0.84	0.93	0.90	0.87	0.82

STEP	41	42	43	44	45	46	47	48	49	50
σ'_{vc}										
σ'_{hc}										
t_c (HRS)										
E_o (%)										
E_{vol} (%)										
K_c										

STEP	51	52	53	54	55	56	57	58	59	60
σ'_{vc}										
σ'_{hc}										
t_c (HRS)										
E_o (%)										
E_{vol} (%)										
K_c										

REMARKS

AXIAL AND VOLUMETRIC STRAINS ARE REFERENCED TO THE PRECONSOLIDATION DIMENSIONS.



Sample No.

w_N (%)

Estimated

Depth

w_L (%)

σ'_{v0} σ'_p

Soil Type BBC

w_p (%)

CR 0.172 RR 0.010

I_p (%)

G_s 2.78 e_0 1.193 S (%) 99

○ At t_p or hr

Remarks

● At () hr

GEOTECHNICAL LABORATORY
DEPT. OF CIVIL ENGR.
M.I.T.

COMPRESSION CURVE

TEST NO. Ck₀Uc4

FIGURE

Test CKoUC4
Batch 113

Sig'vm = 4.097 Kg/cm²
Sig'vc = 1.0496 Kg/cm²

Su = 1.059 Kg/cm²

v. strain %	q ----- sig'vc	p' ----- sig'vc	dU-dSIGh ----- sig'vc	sig'v ----- sig'h	Eu ----- Su	dQ ----- dQf	A
0.0003	0.0936	0.9063	0.0013	1.2304	2357.2	0.0000	****
0.0048	0.1275	0.9277	0.0139	1.3187	1585.9	0.0370	0.2050
0.0131	0.1804	0.9448	0.0497	1.4722	1380.5	0.0949	0.2861
0.0186	0.2122	0.9562	0.0702	1.5706	1310.4	0.1296	0.2958
0.0246	0.2448	0.9691	0.0898	1.6759	1252.1	0.1651	0.2970
0.0324	0.2841	0.9854	0.1129	1.8102	1190.3	0.2081	0.2965
0.0461	0.3419	1.0123	0.1440	2.0203	1085.3	0.2713	0.2899
0.0602	0.3900	1.0411	0.1633	2.1981	990.96	0.3238	0.2754
0.0743	0.4324	1.0687	0.1780	2.3591	916.13	0.3701	0.2627
0.0874	0.4682	1.0925	0.1901	2.5003	859.75	0.4093	0.2537
0.1013	0.5030	1.1161	0.2014	2.6410	809.83	0.4473	0.2459
0.1156	0.5353	1.1392	0.2103	2.7728	764.62	0.4825	0.2381
0.1305	0.5649	1.1616	0.2177	2.8936	722.78	0.5149	0.2309
0.1448	0.5916	1.1820	0.2240	3.0041	687.56	0.5441	0.2249
0.1587	0.6161	1.2018	0.2286	3.1042	658.31	0.5709	0.2187
0.1807	0.6532	1.2332	0.2344	3.2529	618.63	0.6114	0.2094
0.2034	0.6873	1.2656	0.2360	3.3771	582.92	0.6486	0.1988
0.2266	0.7182	1.2961	0.2362	3.4854	550.25	0.6823	0.1891
0.2493	0.7473	1.3274	0.2341	3.5764	523.37	0.7141	0.1791
0.2814	0.7844	1.3696	0.2290	3.6812	489.73	0.7547	0.1657
0.3287	0.8314	1.4290	0.2165	3.7828	447.60	0.8060	0.1467
0.3775	0.8723	1.4863	0.2000	3.8412	411.20	0.8507	0.1284
0.4506	0.9202	1.5662	0.1681	3.8492	365.58	0.9030	0.1017
0.5535	0.9637	1.6633	0.1147	3.7552	313.21	0.9506	0.0659
0.8012	1.0043	1.7711	0.0477	3.6197	226.45	0.9950	0.0262
1.0489	1.0092	1.8047	0.0185	3.5372	173.88	1	0.0101
1.0762	1.0089	1.8085	0.0145	3.5235	169.41	1	0.0079
1.1425	1.0090	1.8188	0.0045	3.4918	159.60	1	0.0024
1.8064	0.9849	1.7843	0.0151	3.4640	98.303	0.9737	0.0084
2.0066	0.9788	1.7606	0.0324	3.5040	87.894	0.9671	0.0183
2.6662	0.9623	1.7220	0.0545	3.5334	64.923	0.9491	0.0314
3.5206	0.9481	1.6882	0.0742	3.5623	48.367	0.9335	0.0434
5.0110	0.9292	1.6445	0.0988	3.5980	33.233	0.9128	0.0591
6.0277	0.9146	1.6287	0.1006	3.5618	27.150	0.8970	0.0612
7.0171	0.9024	1.6139	0.1030	3.5366	22.976	0.8836	0.0637
8.0254	0.8874	1.5899	0.1119	3.5263	19.719	0.8672	0.0705
9.0345	0.8766	1.5743	0.1168	3.5130	17.280	0.8554	0.0745
10.026	0.8605	1.5544	0.1209	3.4804	15.251	0.8378	0.0788
12.004	0.8183	1.4885	0.1446	3.4417	12.041	0.7917	0.0997
12.932	0.8072	1.4711	0.1512	3.4319	11.000	0.7796	0.1059

CONSOLIDATED - UNDRAINED TRIAXIAL TEST

PROJECT BATCH 113
 SOIL TYPE BOSTON BLUE CLAY
 LOCATION RESEDIMENTED
 BORING NO. - SAMPLE NO. -
 DEPTH -

TEST NO. CK0UC8
 TYPE OF TEST CK0UC
 APPARATUS NO. WFF-6
 TESTED BY PF
 DATE Nov-Dec 1985

WATER CONTENT

INITIAL, BASED ON TRIMMINGS 42 %
 INITIAL, BASED ON SAMPLE 43.7 %
 FINAL, BASED ON SAMPLE 35.6 %

ATTERBERG LIMITS

W_p _____ %
 W_L _____ %
 I_p _____ % I_L _____

PHASE RELATIONSHIPS

ρ_{WET} 1.816 g/cc ρ_{DRY} 1.263 g/cc
 e_i 1.207 e_f 1.013
 S_i 100.9 % Sprecons _____ %
 G_s 2.788

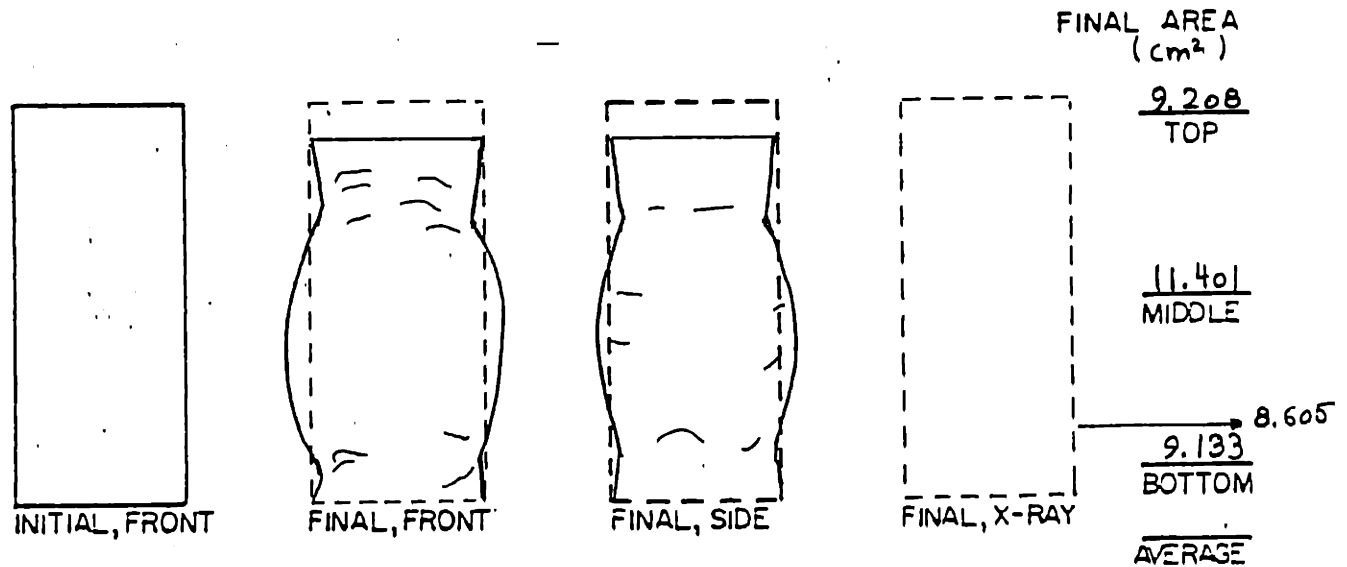
MISCELLANEOUS

B _____ %
 SATURATION ΔV -0.26 cm³
 CONSOLIDATION ΔV 6.77 cm³
 MEMBRANES 0 THICK 2 THIN
 CORRECTION FACTOR 1.942 x E
 FILTER STRIPS 8 X 1/4"
 CONFIGURATION VERTICAL
 CORRECTION FACTOR 0.4064 x E%
 AREA CORRECTION PARABOLIC

GRAIN SIZE

% -#200 _____
 % -2 μ _____
 C_u _____ C_c _____

SAMPLE APPEARANCE



COMMENTS Final dry weight was measured one month later.

CONSOLIDATED - UNDRAINED TRIAXIAL TEST

PROJECT BATCH 113 TYPE OF TEST CK₀UC TEST NO. CK₀UC8

STRESS HISTORY

IN SITU CONDITIONS

σ'_{v0} 0.25 kg/cm²
 σ'_p 1.00 kg/cm²
 OCR 4

TORVANE STRENGTH _____
 TORVANE W_c _____ %

TEST CONDITIONS

σ'_{vc} 0.25 kg/cm²
 σ'_p 4.10 kg/cm²
 OCR 8.04
 K_c 1.10 U_b 2.00 kg/cm²
 STRAIN RATE 0.5 %/HOUR
 FINAL E_0 5.6 %

STRENGTH DATA

AT MAXIMUM q

E_0 2.97 %
 q/σ'_{vc} 1.749
 p/σ'_{vc} 2.939
 $\Delta u - \Delta \sigma_h / \sigma'_{vc}$ -0.098
 ϕ' 36.5
 A_f -0.053
 TIME TO q_{max} 6 hours

AT MAXIMUM OBLIQUITY

E_0 0.597 %
 q/σ'_{vc} 1.312
 p/σ'_{vc} 2.008
 $\Delta u - \Delta \sigma_h / \sigma'_{vc}$ 0.401
 ϕ' 40.8

$E_{u(50\%)} / q_f$ _____

TIME RECORD

SET UP 11/21/85
 START OF CONSOLIDATION 11/25/85
 START OF SHEAR 12/16/85
 END OF SHEAR 12/19/85
 REMOVAL 12/19/85
 TOTAL TIME IN APPARATUS 29 days
 CONSOLIDATION-SHEAR Δt 30 minutes

HYPERBOLIC STRESS-STRAIN PARAMETERS

G_i / σ'_{vc} _____
 R_f _____
 r_2 _____

RADIOGRAPHY

kV _____ mA _____
 EXPOSURE TIME _____

REMARKS

CONSOLIDATED - UNDRAINED TRIAXIAL TEST

PROJECT BATCH 113 TYPE OF TEST CKUC TEST NO. CKUC8

SAMPLE DIMENSIONS

	L (cm)	A (cm ²)	V (cm ³)	ϵ_o (D) (%)	ϵ_{vol} (D) (%)	W
INITIAL	8.008	9.834	78.75	0	0	
PRECONSOLIDATION	7.993	9.834	78.61	0.19	0.18	
PRESHEAR	7.307	9.832	71.84	8.55	8.61	
POST SHEAR						
FINAL	7.558			5.62		
FINAL MEASURED						

(a) Measured
(b) Based on initial
dimensions

CONSOLIDATION DATA

STRESSES IN kg/cm²

STEP	1	2	3	4	5	6	7	8	9	10
σ'_{vc}	0.28	0.31	0.33	0.39	0.44	0.49	0.55	0.63	0.70	0.80
σ'_{hc}	0.26	0.27	0.28	0.29	0.31	0.32	0.35	0.35	0.37	0.40
t_c (HRS)										
ϵ_o (%)	0.02	0.04	0.07	0.14	0.22	0.29	0.39	0.50	0.61	0.75
ϵ_{vol} (%)	0.03	0.06	0.09	0.15	0.25	0.33	0.43	0.53	0.65	0.80
K_c	0.94	0.89	0.84	0.75	0.70	0.65	0.63	0.55	0.53	0.50

STEP	11	12	13	14	15	16	17	18	19	20
σ'_{vc}	0.92	1.05	1.15	1.25	1.35	1.44	1.50	1.60	1.74	1.90
σ'_{hc}	0.44	0.50	0.54	0.59	0.64	0.72	0.70	0.75	0.82	0.89
t_c (HRS)										
ϵ_o (%)	0.87	1.08	1.17	1.36	1.61	1.67	1.87	2.37	3.10	3.39
ϵ_{vol} (%)	0.92	1.18	1.35	1.45	1.85	1.96	2.16	2.71	3.51	3.86
K_c	0.48	0.47	0.47	0.47	0.47	0.50	0.47	0.47	0.47	0.47

STEP	21	22	23	24	25	26	27	28	29	30
σ'_{vc}	2.09	2.25	2.50	2.76	3.00	3.25	3.50	3.75	4.10	3.75
σ'_{hc}	0.99	1.06	1.18	1.30	1.41	1.53	1.65	1.76	1.93	1.83
t_c (HRS)										
ϵ_o (%)	5.62	5.73	6.39	6.79	7.17	7.91	8.29	8.67	9.46	9.45
ϵ_{vol} (%)	5.47	5.55	6.36	6.84	7.25	7.96	8.40	8.79	9.67	9.64
K_c	0.47	0.47	0.47	0.47	0.47	0.47	0.47	0.47	0.47	0.49

GEOTECHNICAL LABORATORY
DEPT. OF CIVIL ENGR.

M.I.T.

CONSOLIDATED - UNDRAINED TRIAXIAL TEST

PROJECT BATCH 113 TYPE OF TEST CKUC TEST NO. CK6UC8

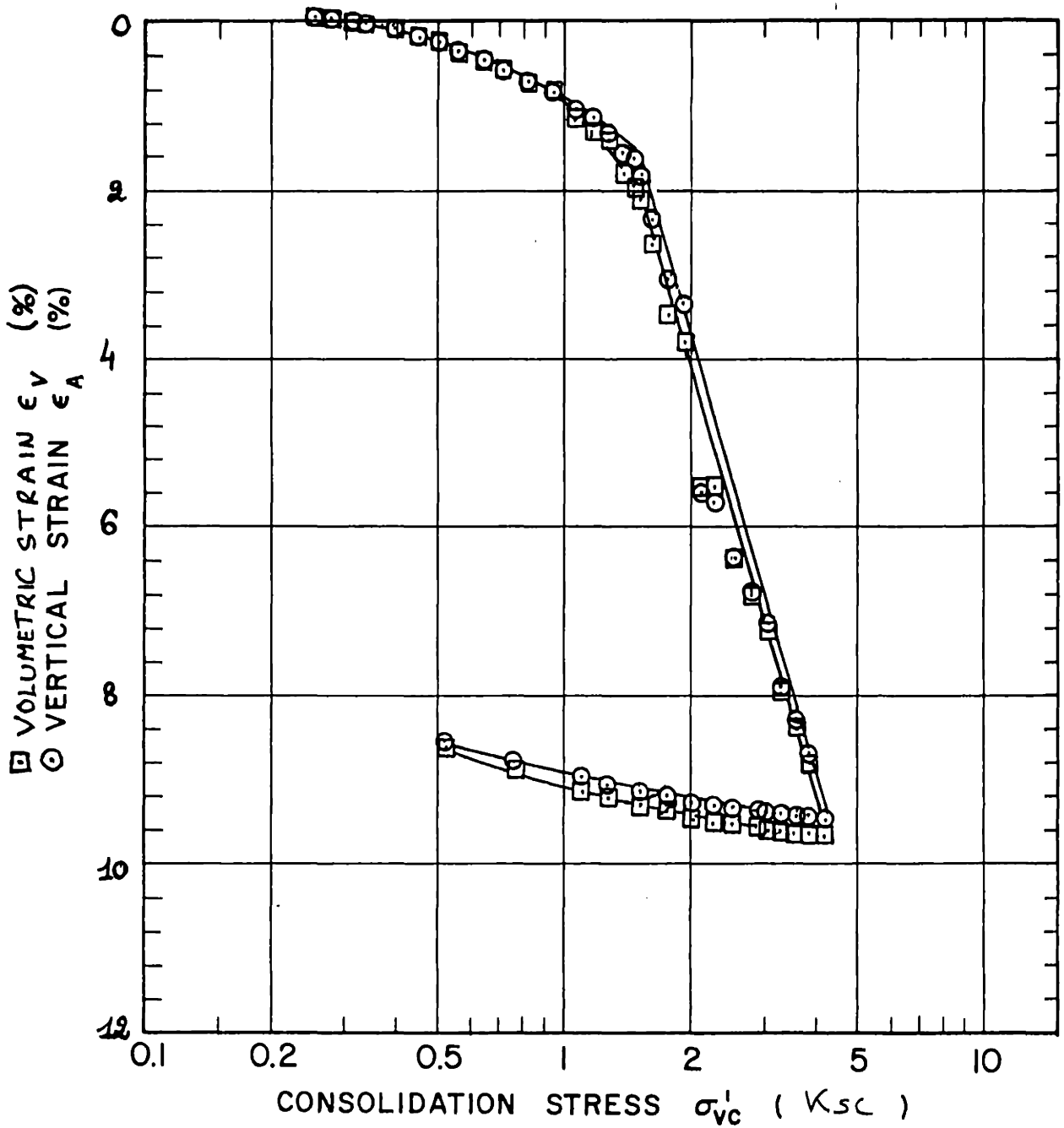
STEP	31	32	33	34	35	36	37	38	39	40
σ'_{vc}	3.49	3.24	3.00	2.75	2.50	2.25	2.00	1.75	1.50	1.25
σ'_{hc}	1.74	1.68	1.60	1.52	1.44	1.35	1.27	1.16	1.06	0.96
t_c (HRS)										
ϵ_o (%)	9.43	9.41	9.39	9.36	9.33	9.30	9.26	9.20	9.15	9.06
ϵ_{vol} (%)	9.63	9.62	9.59	9.55	9.53	9.50	9.45	9.36	9.30	9.21
K_c	0.50	0.52	0.53	0.55	0.58	0.60	0.63	0.67	0.71	0.77

STEP	41	42	43	44	45	46	47	48	49	50
σ'_{vc}	1.09	0.75	0.51							
σ'_{hc}	0.97	0.71	0.56							
t_c (HRS)										
ϵ_o (%)	8.97	8.78	8.55							
ϵ_{vol} (%)	9.12	8.87	8.61							
K_c	0.89	0.94	1.10							

STEP	51	52	53	54	55	56	57	58	59	60
σ'_{vc}										
σ'_{hc}										
t_c (HRS)										
ϵ_o (%)										
ϵ_{vol} (%)										
K_c										

REMARKS

STRAINS ARE REFERENCED TO THE PRECONSOLIDATION DIMENSIONS



Sample No.	w_N (%)	Estimated		
Depth	w_L (%)	σ'_{vo}	σ'_p	
Soil Type	w_p (%)	CR 0.171	RR 0.01	
	I_p (%)	G_s	e_0	S (%)
○ At t_p or	hr	Remarks		
● At ()	hr			

GEOTECHNICAL LABORATORY
DEPT. OF CIVIL ENGR.
M.I.T.

COMPRESSION CURVE
TEST NO. CK6UC8

FIGURE

Test CKoUCB
Batch 113

Sig'vm = 4.103 Kg/cm2
Sig'vc = .5123 Kg/cm2

Su = .892 Kg/cm2

v. strain %	q ----- sig'vc	p' ----- sig'vc	dU-dSIGh ----- sig'vc	sig'v ----- sig'h	Eu ----- Su	dQ ----- dQf	A
0.0002	-0.045	1.0459	0.0001	0.9158	1153.6	-0.000	-0.100
0.0016	-0.030	1.0518	0.0103	0.9439	1290.3	0.0082	0.3531
0.0024	-0.021	1.0535	0.0177	0.9602	1292.5	0.0132	0.3759
0.0032	-0.013	1.0551	0.0240	0.9746	1236.0	0.0175	0.3819
0.0040	-0.003	1.0577	0.0316	0.9933	1280.6	0.0232	0.3811
0.0051	0.0076	1.0597	0.0406	1.0144	1266.7	0.0294	0.3858
0.0061	0.0236	1.0626	0.0534	1.0454	1348.4	0.0384	0.3897
0.0065	0.0290	1.0638	0.0579	1.0562	1358.1	0.0414	0.3912
0.0085	0.0512	1.0684	0.0759	1.1007	1338.6	0.0538	0.3944
0.0103	0.0695	1.0717	0.0905	1.1388	1317.3	0.0641	0.3952
0.0118	0.0846	1.0744	0.1030	1.1709	1293.4	0.0725	0.3975
0.0144	0.1084	1.0783	0.1225	1.2235	1247.1	0.0859	0.3994
0.0192	0.1490	1.0857	0.1557	1.3181	1178.6	0.1086	0.4013
0.0310	0.2308	1.0992	0.2238	1.5315	1034.0	0.1544	0.4058
0.0476	0.3207	1.1194	0.2937	1.8030	889.86	0.2047	0.4016
0.0673	0.4050	1.1456	0.3515	2.0938	773.66	0.2519	0.3905
0.0941	0.4985	1.1842	0.4064	2.4540	667.58	0.3043	0.3738
0.1619	0.6703	1.2857	0.4764	3.1782	509.93	0.4004	0.3330
0.2028	0.7518	1.3498	0.4938	3.5140	453.42	0.4460	0.3098
0.2584	0.8501	1.4426	0.4993	3.8701	399.59	0.5011	0.2788
0.3766	1.0342	1.6385	0.4874	4.4228	330.28	0.6042	0.2258
0.5141	1.2146	1.8669	0.4388	4.7238	282.21	0.7052	0.1741
0.6813	1.3853	2.1245	0.3519	4.7480	241.74	0.8007	0.1230
0.9150	1.5418	2.4114	0.2203	4.5461	199.65	0.8884	0.0694
1.2011	1.6478	2.6476	0.0888	4.2963	162.24	0.9477	0.0262
1.5159	1.7004	2.7886	0.0003	4.1252	132.53	0.9772	0.0001
1.8156	1.7230	2.8567	-0.046	4.0396	112.08	0.9898	-0.013
3.0648	1.7396	2.9260	-0.099	3.9325	67.023	0.9991	-0.027
3.8137	1.7303	2.9243	-0.108	3.8983	53.581	0.9939	-0.030
4.6561	1.7235	2.9217	-0.112	3.8771	43.722	0.9901	-0.031
5.9310	1.6980	2.8981	-0.107	3.8298	33.829	0.9758	-0.030
7.0876	1.6666	2.8546	-0.094	3.8059	27.800	0.9583	-0.027
8.0422	1.6402	2.8114	-0.076	3.801	24.122	0.9435	-0.022
9.0893	1.6280	2.7974	-0.075	3.7843	21.189	0.9366	-0.022
10.045	1.6123	2.7776	-0.072	3.7671	18.993	0.9278	-0.021
11.113	1.5889	2.7513	-0.067	3.7338	16.926	0.9147	-0.020
12.118	1.5679	2.7274	-0.062	3.7045	15.323	0.9030	-0.019
13.115	1.5427	2.7088	-0.066	3.6459	13.937	0.8889	-0.020
14.140	1.5218	2.6869	-0.065	3.6123	12.757	0.8772	-0.020
14.886	1.4971	2.6543	-0.061	3.5877	11.927	0.8633	-0.019

CONSOLIDATED - UNDRAINED TRIAXIAL TEST

PROJECT BATCH 113
 SOIL TYPE BOSTON BLUE CLAY
 LOCATION RESIDENTIAL
 BORING NO. - SAMPLE NO. -
 DEPTH -

TEST NO. CK0UF2
 TYPE OF TEST CKUF
 APPARATUS NO. WFE-7
 TESTED BY PF
 DATE December 1985

WATER CONTENT

INITIAL, BASED ON TRIMMINGS _____ %
 INITIAL, BASED ON SAMPLE 43.7 %
 FINAL, BASED ON SAMPLE 36.5 %

ATTERBERG LIMITS

W_p _____ %
 W_L _____ %
 I_p _____ % I_L _____ %

PHASE RELATIONSHIPS

γ_{WET} 1.834 g/cc γ_{DRY} 1.276 g/cc
 e_i 1.185 e_f 0.969
 S_i 102 % $S_{precons}$ _____ %
 G_s 2.788

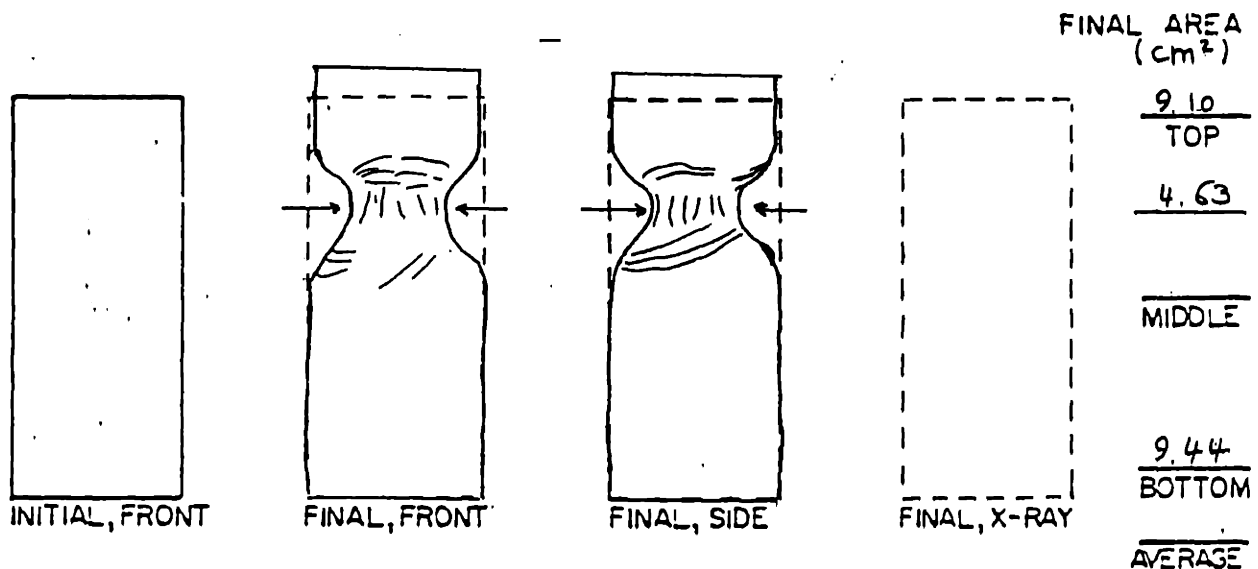
MISCELLANEOUS

B _____ %
 SATURATION ΔV -0.23 cm^3
 CONSOLIDATION ΔV 7.57 cm^3
 MEMBRANES 0 THICK 2 THIN
 CORRECTION FACTOR 1.942 \pm E
 FILTER STRIPS 7 X 1/4"
 CONFIGURATION SPIRAL
 CORRECTION FACTOR NO
 AREA CORRECTION RIGHT CYLINDER

GRAIN SIZE

% -#200 _____
 % -2 μ _____
 C_u _____ C_c _____

SAMPLE APPEARANCE



COMMENTS _____

CONSOLIDATED - UNDRAINED TRIAXIAL TEST

PROJECT BATCH 113 TYPE OF TEST CK₀UE TEST NO. CK₀UE2

STRESS HISTORY

IN SITU CONDITIONS

σ'_{vo} 0.25 kg/cm²
 σ'_p 1.00 kg/cm²
 OCR 4

TORVANE STRENGTH _____
 TORVANE W_c _____ %

TEST CONDITIONS

σ'_{vc} 0.15 kg/cm²
 σ'_p 4.01 kg/cm²
 OCR 2.00
 K_c 0.625 u_b 2.0 kg/cm²
 STRAIN RATE 0.5 %/HOUR
 FINAL ϵ_o -9.8 %

STRENGTH DATA

AT MAXIMUM q

ϵ_o -10.80 %
 q/σ'_{vc} -0.318
 p/σ'_{vc} 0.340
 $\Delta u - \Delta\sigma_h / \sigma'_{vc}$ -0.036
 ϕ' -69.3°
 A_f 0.926
 TIME TO q_{max} 21.5 hours

TIME RECORD

SET UP 12/2/85
 START OF CONSOLIDATION 12/6/85
 START OF SHEAR 12/19/85
 END OF SHEAR 12/20/85
 REMOVAL 12/20/85
 TOTAL TIME IN APPARATUS 19 days
 CONSOLIDATION-SHEAR Δt 30 minutes

REMARKS

AT MAXIMUM OBLIQUITY

ϵ_o -10.1 %
 q/σ'_{vc} -0.314
 p/σ'_{vc} 0.330
 $\Delta u - \Delta\sigma_h / \sigma'_{vc}$ -0.023
 ϕ' -71.9°
 $E_u(50\%) / q_f$ _____

HYPERBOLIC STRESS-STRAIN PARAMETERS

G_i / σ'_{vc} _____
 R_f _____
 r^2 _____

RADIOGRAPHY

kV - mA -
 EXPOSURE TIME -

CONSOLIDATED - UNDRAINED TRIAXIAL TEST

PROJECT BATCH 113 TYPE OF TEST CK₀UE TEST NO. CK0UE2

SAMPLE DIMENSIONS

	L (cm)	A (cm ²)	V (cm ³)	ϵ_0 (D) (%)	ϵ_{vol} (D) (%)	W (gms)
INITIAL	7.978	9.707	77.44	0	0	142.0
PRECONSOLIDATION	7.968	9.707	77.34	0.13	0.13	
PRESHEAR	7.274	9.591	69.77	8.63	9.79	
POST SHEAR						
FINAL	8.759	-	-	9.79	-	
FINAL MEASURED	8.649	-	-	8.41	-	98.81

(a) Measured
(b) Based on initial
dimensions

CONSOLIDATION DATA

STRESSES IN hg/cm²

STEP	1	2	3	4	5	6	7	8	9	10
σ'_{vc}	0.21	0.25	0.28	0.31	0.35	0.39	0.44	0.52	0.60	0.70
σ'_{hc}	0.21	0.25	0.26	0.28	0.28	0.30	0.31	0.33	0.34	0.37
t_c (HRS)										
ϵ_0 (%)	0.07	0.12	0.17	0.22	0.27	0.33	0.42	0.53	0.65	0.79
ϵ_{vol} (%)	0.16	0.30	0.38	0.47	0.50	0.58	0.66	0.78	0.91	1.13
K_c	1.01	1.01	0.94	0.89	0.81	0.76	0.70	0.63	0.57	0.52

STEP	11	12	13	14	15	16	17	18	19	20
σ'_{vc}	0.83	1.00	1.18	1.30	1.45	1.60	1.80	2.00	2.25	2.50
σ'_{hc}	0.41	0.47	0.54	0.61	0.68	0.75	0.84	0.94	1.06	1.17
t_c (HRS)										
ϵ_0 (%)	0.95	1.17	1.47	1.76	2.83	3.13	4.10	4.43	5.60	5.88
ϵ_{vol} (%)	1.29	1.56	1.91	2.46	3.49	4.01	5.00	5.37	6.56	6.89
K_c	0.49	0.47	0.47	0.47	0.47	0.47	0.47	0.47	0.47	0.47

STEP	21	22	23	24	25	26	27	28	29	30
σ'_{vc}	2.75	3.00	3.26	3.50	3.74	4.01	3.78	3.47	3.25	3.00
σ'_{hc}	1.29	1.41	1.53	1.64	1.76	1.88	1.86	1.69	1.67	1.59
t_c (HRS)										
ϵ_0 (%)	6.38	7.20	7.52	7.71	8.38	8.82	8.80	8.80	8.78	8.76
ϵ_{vol} (%)	7.44	8.29	8.68	8.90	9.57	10.05	10.02	10.01	9.97	9.94
K_c	0.47	0.47	0.47	0.47	0.47	0.47	0.49	0.49	0.51	0.59

GEOTECHNICAL LABORATORY
DEPT. OF CIVIL ENGR.
M.I.T.

CONSOLIDATED - UNDRAINED TRIAXIAL TEST

PROJECT BATCH 113 TYPE OF TEST CK₀UE TEST NO. _____ CK0UE2

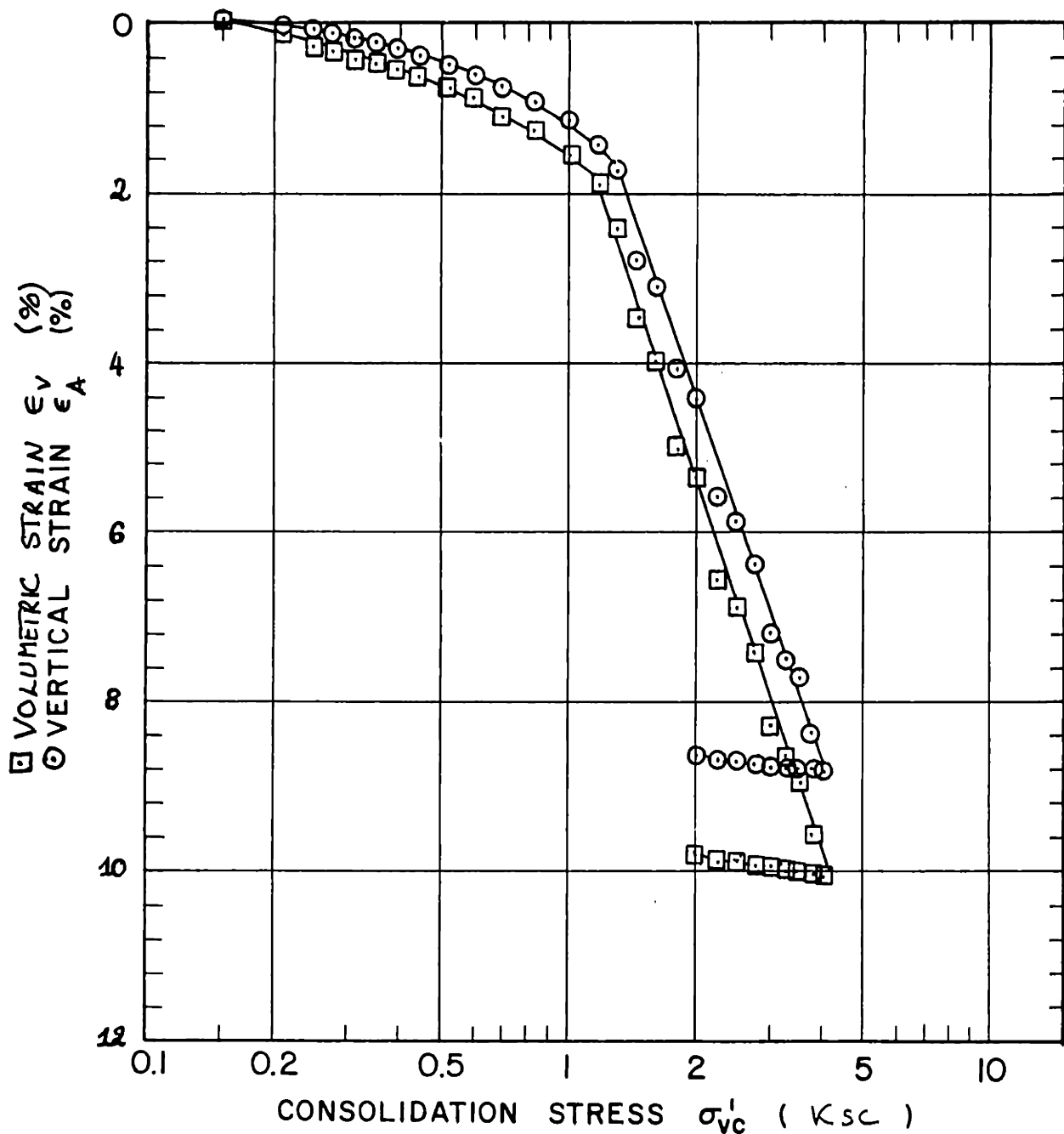
STEP	31	32	33	34	35	36	37	38	39	40
σ'_{vc}	2.76	2.50	2.25	2.00						
σ'_{hc}	1.51	1.42	1.33	1.25						
t_c (HRS)										
ϵ_D (%)	8.74	8.71	8.68	8.63						
ϵ_{vol} (%)	9.93	9.89	9.85	9.79						
K_c	0.58	0.57	0.59	0.63						

STEP	41	42	43	44	45	46	47	48	49	50
σ'_{vc}										
σ'_{hc}										
t_c (HRS)										
ϵ_D (%)										
ϵ_{vol} (%)										
K_c										

STEP	51	52	53	54	55	56	57	58	59	60
σ'_{vc}										
σ'_{hc}										
t_c (HRS)										
ϵ_D (%)										
ϵ_{vol} (%)										
K_c										

REMARKS

Axial & volumetric strains are referenced to the initial dimensions.



Sample No.	w_N (%)	Estimated		
Depth	w_L (%)	σ'_{v0}	σ'_p	
Soil Type	w_p (%)	CR 0.153	RR 0.007	
	I_p (%)	G_s	e_0	S (%)
○ At t_p or hr	Remarks			
● At () hr				

GEOTECHNICAL LABORATORY
 DEPT. OF CIVIL ENGR.
 M.I.T.

COMPRESSION CURVE
 TEST NO. CK₀UE 2

FIGURE

Test CKoUE2
Batch 113

Sig'vm = 4.005 Kg/cm2
Sig'vc = 1.9327 Kg/cm2

Su = -.623 Kg/cm2

v. strain %	q ----- sig'vc	p' ----- sig'vc	dU-dSIGh ----- sig'vc	sig'v ----- sig'h	Eu ----- Su	dQ ----- dQf	A
-0.001	0.1919	0.8080	0.0100	1.6232	891.76	-0.000	****
-0.004	0.1812	0.8047	0.0026	1.5812	1927.5	0.0207	-0.125
-0.008	0.1686	0.8009	-0.006	1.5334	1803.2	0.0452	0.1290
-0.010	0.1622	0.7988	-0.010	1.5096	1857.2	0.0576	0.1770
-0.015	0.1488	0.7950	-0.020	1.4606	1828.3	0.0837	0.2336
-0.020	0.1275	0.7895	-0.036	1.3854	1985.6	0.1250	0.2800
-0.026	0.1131	0.7863	-0.047	1.3362	1919.9	0.1530	0.2987
-0.035	0.0922	0.7819	-0.063	1.2673	1791.9	0.1938	0.3199
-0.043	0.0783	0.7796	-0.075	1.2235	1662.8	0.2207	0.3311
-0.053	0.0589	0.7767	-0.091	1.1641	1567.0	0.2586	0.3446
-0.061	0.0473	0.7753	-0.101	1.1300	1490.3	0.2811	0.3525
-0.074	0.0325	0.7739	-0.115	1.0877	1344.2	0.3099	0.3619
-0.085	0.0197	0.7725	-0.126	1.0524	1261.7	0.3347	0.3684
-0.100	0.0077	0.7712	-0.137	1.0203	1152.1	0.3580	0.3732
-0.128	-0.013	0.7681	-0.155	0.9650	1004.9	0.3997	0.3789
-0.153	-0.029	0.7643	-0.167	0.9256	904.50	0.4305	0.3785
-0.184	-0.046	0.7580	-0.178	0.8845	810.17	0.4634	0.3738
-0.204	-0.054	0.7532	-0.182	0.8640	755.41	0.4800	0.3692
-0.252	-0.073	0.7405	-0.187	0.8200	656.85	0.5155	0.3538
-0.304	-0.087	0.7265	-0.188	0.7851	574.56	0.5432	0.3371
-0.402	-0.108	0.6986	-0.181	0.7303	466.40	0.5848	0.3025
-0.503	-0.125	0.6722	-0.171	0.6859	393.30	0.6166	0.2711
-0.611	-0.139	0.6441	-0.158	0.6431	338.74	0.6452	0.2394
-0.700	-0.149	0.6226	-0.147	0.6119	304.49	0.6645	0.2158
-0.807	-0.161	0.5971	-0.133	0.5738	273.42	0.6875	0.1892
-0.911	-0.171	0.5749	-0.121	0.5410	248.58	0.7061	0.1669
-1.016	-0.179	0.5548	-0.109	0.5116	227.85	0.7217	0.1475
-1.516	-0.211	0.4747	-0.062	0.3827	166.06	0.7852	0.0777
-2.004	-0.228	0.4265	-0.031	0.3024	130.74	0.8173	0.0371
-2.502	-0.241	0.3903	-0.008	0.2346	108.11	0.8437	0.0098
-3.006	-0.244	0.3722	0.0077	0.2081	90.407	0.8476	-0.008
-4.034	-0.252	0.3466	0.0254	0.1564	68.732	0.8649	-0.028
-5.091	-0.271	0.3235	0.0306	0.0875	56.732	0.9010	-0.033
-7.040	-0.287	0.3200	0.0194	0.0542	42.397	0.9313	-0.020
-8.076	-0.287	0.3317	0.0079	0.0713	36.998	0.9323	-0.008
-9.02	-0.303	0.3298	-0.004	0.0418	34.216	0.9630	0.0047
-10.04	-0.316	0.3346	-0.021	0.0274	31.544	0.9891	0.0215
-10.80	-0.322	0.3443	-0.036	0.0332	29.649	0.9996	0.0350
-11.08	-0.317	0.3554	-0.041	0.0570	28.600	0.9897	0.0408
-12.48	-0.304	0.3802	-0.058	0.1106	24.771	0.9652	0.0587
-14.07	-0.308	0.3839	-0.067	0.1095	22.137	0.9723	0.0675
-15.04	-0.297	0.3986	-0.073	0.1446	20.282	0.9524	0.0746
-18.01	-0.282	0.4098	-0.069	0.1833	16.424	0.9232	0.0732
-20.00	-0.268	0.4135	-0.057	0.2130	14.342	0.8949	0.0627
-20.29	-0.261	0.4160	-0.054	0.2278	13.933	0.8819	0.0595

CONSOLIDATED - UNDRAINED TRIAXIAL TEST

PROJECT Batch 113
 SOIL TYPE Boston Blue Clay
 LOCATION Resedimented
 BORING NO. - SAMPLE NO. -
 DEPTH -

TEST NO. CK0UE4
 TYPE OF TEST CKUE
 APPARATUS NO. WFE-6
 TESTED BY PF
 DATE April 1986

WATER CONTENT

INITIAL, BASED ON TRIMMINGS 41.5 %
 INITIAL, BASED ON SAMPLE 43.2 %
 FINAL, BASED ON SAMPLE 35.7 %

ATTERBERG LIMITS

W_p _____ %
 W_L _____ %
 I_p _____ % I_L _____

PHASE RELATIONSHIPS

W_{wet} 1.815 g/cc DRY 1.27 g/cc
 e_i 1.199 e_f 0.956
 S_i 100.5 % Sprecons 104 %
 G_s 2.78

MISCELLANEOUS

B 102 %
 SATURATION ΔV -0.08 cm³
 CONSOLIDATION ΔV 7.64 cm³
 MEMBRANES 0 THICK 2 THIN
 CORRECTION FACTOR 1.942.e
 FILTER STRIPS 6 x 1/4"
 CONFIGURATION Spiral
 CORRECTION FACTOR _____
 AREA CORRECTION Right Cylinder

GRAIN SIZE

% -#200 _____
 % -#20 _____
 C_u _____ C_c _____

SAMPLE APPEARANCE

				FINAL AREA (cm ²)
				<u>9.511</u>
INITIAL, FRONT	FINAL, FRONT	FINAL, SIDE	FINAL, X-RAY	TOP
				<u>7.13</u>
				MIDDLE
				<u>9.25</u>
				BOTTOM
				<u>10.14</u>
				AVERAGE

COMMENTS _____

CONSOLIDATED - UNDRAINED TRIAXIAL TEST

PROJECT Batch 113 TYPE OF TEST CK₀UE TEST NO. CK0UE4

STRESS HISTORY

IN SITU CONDITIONS

σ'_{v0} 0.25 kg/cm²
 σ'_p 1.00 kg/cm²
 OCR 4.0

TORVANE STRENGTH _____
 TORVANE W_c _____ %

TEST CONDITIONS

σ'_{vc} 0.35 kg/cm²
 σ'_p 3.98 kg/cm²
 OCR 4.01

K_c 0.829 U_b 2 kg/cm²
 STRAIN RATE 0.5 %/HOUR
 FINAL ϵ_a -0.13 %

STRENGTH DATA

AT MAXIMUM q

ϵ_a -8.994 %
 q/σ'_{vc} -0.625
 p/σ'_{vc} 1.036
 $\Delta u - \Delta \sigma_h / \sigma'_{vc}$ -0.826
 ϕ' -37.1'
 A_f -0.167
 TIME TO q_{max} 18 hours

TIME RECORD

SET UP 3/23/86
 START OF CONSOLIDATION 3/25/86
 START OF SHEAR 4/10/86
 END OF SHEAR 4/11/86
 REMOVAL 4/11/86
 TOTAL TIME IN APPARATUS 20 days
 CONSOLIDATION-SHEAR Δt 30 minutes

REMARKS

AT MAXIMUM OBLIQUITY

ϵ_a -6.136 %
 q/σ'_{vc} -0.581
 p/σ'_{vc} 0.923
 $\Delta u - \Delta \sigma_h / \sigma'_{vc}$ -0.668
 ϕ' -39°

$E_{u(50\%)/q_f}$ _____

HYPERBOLIC STRESS-STRAIN PARAMETERS

G_i/σ'_{vc} _____
 R_f _____
 r^2 _____

RADIOGRAPHY

kV - mA -
 EXPOSURE TIME -

CONSOLIDATED - UNDRAINED TRIAXIAL TEST

PROJECT Batch 113 TYPE OF TEST CKUE TEST NO. CKUE4

SAMPLE DIMENSIONS

	L (cm)	A (cm ²)	V (cm ³)	$\epsilon_a^{(D)}$ (%)	$\epsilon_{vol}^{(D)}$ (%)	W (gms)
INITIAL	8.01	9.88	79.108	-	-	143.6
PRECONSOLIDATION	8.006	9.876	79.066	0.053	0.053	
PRESHEAR	7.123	10.033	71.468	11.068	9.658	
POST SHEAR	8.084	-	-	0.923		
FINAL	8.052	-	-	0.524		
FINAL MEASURED	8.00	-	-	-0.125		100.3

(a) Measured
(b) Based on initial
dimensions

CONSOLIDATION DATA

STRESSES IN kg/cm²

STEP	1	2	3	4	5	6	7	8	9	10
σ'_{vc}	0.39	0.45	0.51	0.58	0.67	0.78	0.88	1.00	1.15	1.30
σ'_{hc}	0.37	0.40	0.40	0.40	0.44	0.47	0.52	0.58	0.65	0.73
t_c (HRS)	24	7	8	10	9	14	7	8	8.5	8
ϵ_a (%)	0.09	0.16	0.27	0.45	0.73	1.20	1.73	2.40	3.31	3.48
ϵ_{vol} (%)	0.13	0.22	0.32	0.46	0.71	1.09	1.56	2.15	2.99	3.11
K_c	0.94	0.89	0.79	0.70	0.65	0.60	0.59	0.58	0.57	0.56

STEP	11	12	13	14	15	16	17	18	19	20
σ'_{vc}	1.40	1.50	1.60	1.69	1.80	1.90	2.00	2.19	2.40	2.60
σ'_{hc}	0.77	0.81	0.84	0.87	0.90	0.93	0.96	1.03	1.13	1.23
t_c (HRS)	8	10	8.5	7	12	9.5	7	7.25	10	14
ϵ_a (%)	4.63	4.89	5.00	5.34	6.05	6.17	6.31	8.04	8.31	8.52
ϵ_{vol} (%)	4.12	4.43	4.55	4.83	5.39	5.51	5.64	6.90	7.21	7.37
K_c	0.55	0.54	0.53	0.51	0.50	0.49	0.48	0.47	0.47	0.47

STEP	21	22	23	24	25	26	27	28	29	30
σ'_{vc}	2.80	3.00	3.20	3.40	3.58	3.78	3.98	3.78	3.58	3.29
σ'_{hc}	1.32	1.41	1.51	1.60	1.70	1.80	1.89	1.84	1.78	1.69
t_c (HRS)	10	8.5	7.5	9.5	7	7	40	8.5	12	11
ϵ_a (%)	9.05	9.73	10.05	10.38	10.66	10.96	11.51	11.51	11.50	11.48
ϵ_{vol} (%)	7.83	8.42	8.70	9.04	9.32	9.59	10.18	10.18	10.14	10.13
K_c	0.47	0.47	0.47	0.47	0.47 ^f	0.47 ^g	0.47 ^f	0.48 ^g	0.50	0.51

GEOTECHNICAL LABORATORY
DEPT. OF CIVIL ENGR.
M.I.T.

CONSOLIDATED - UNDRAINED TRIAXIAL TEST

PROJECT BATCH 113 TYPE OF TEST CKUE TEST NO. CK0UE4

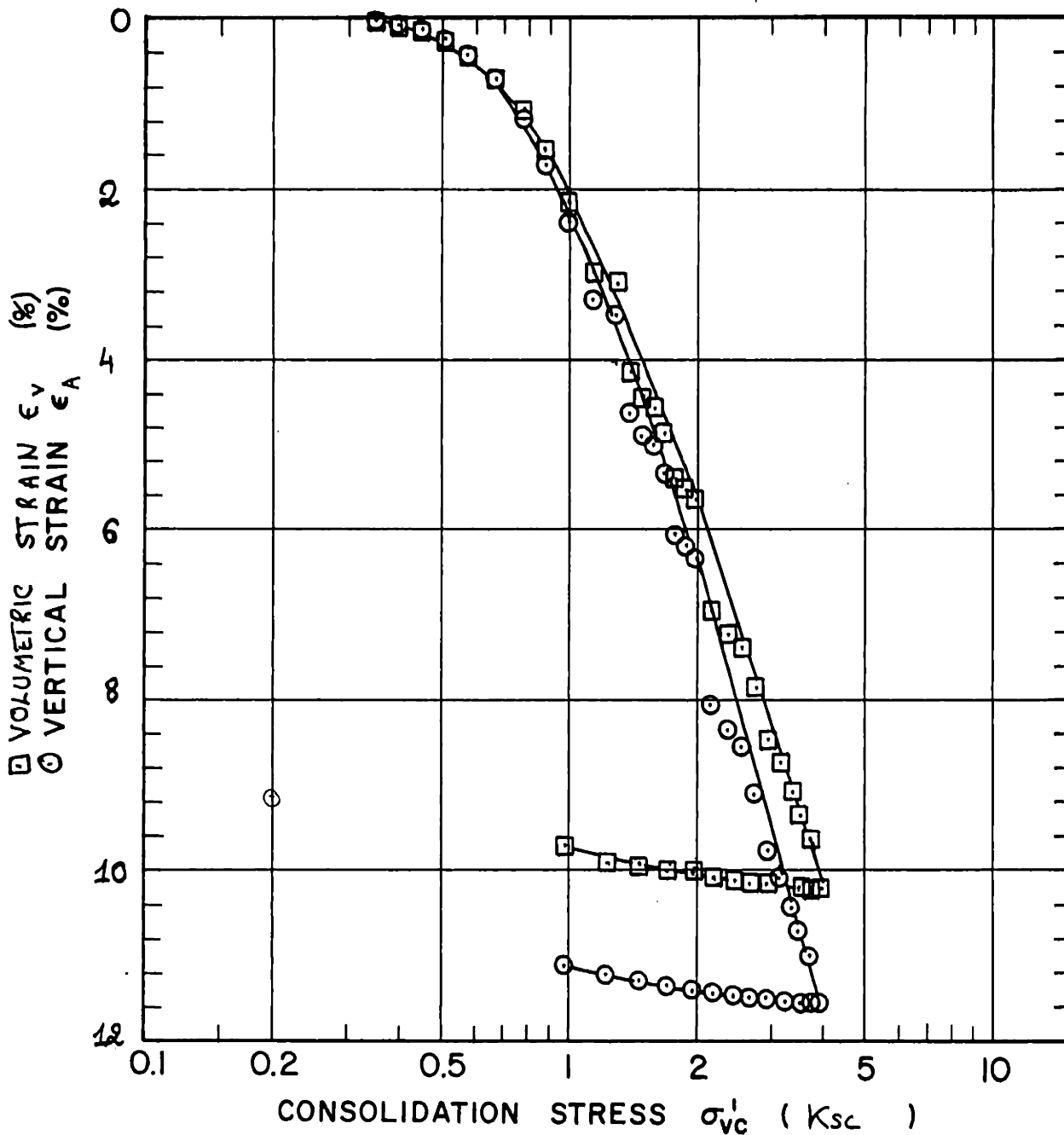
STEP	31	32	33	34	35	36	37	38	39	40
σ'_{vc}	2.98	2.73	2.49	2.24	1.99	1.74	1.49	1.25	1.00	
σ'_{hc}	1.59	1.50	1.43	1.34	1.25	1.15	1.05	0.95	0.83	
t_c (HRS)	10.75	7.5	7.5	10	8.5	7.5	9	7	24	
ϵ_o (%)	11.46	11.44	11.42	11.39	11.36	11.32	11.25	11.19	11.07	
ϵ_{vol} (%)	10.11	10.10	10.08	10.04	9.99	9.95	9.92	9.86	9.66	
K_c	0.53	0.55	0.57	0.60	0.63	0.66	0.70	0.76	0.83	

STEP	41	42	43	44	45	46	47	48	49	50
σ'_{vc}										
σ'_{hc}										
t_c (HRS)										
ϵ_o (%)										
ϵ_{vol} (%)										
K_c										

STEP	51	52	53	54	55	56	57	58	59	60
σ'_{vc}										
σ'_{hc}										
t_c (HRS)										
ϵ_o (%)										
ϵ_{vol} (%)										
K_c										

REMARKS

VOLUMETRIC AND AXIAL STRAINS ARE REFERENCED TO THE PRESHEAR DIMENSIONS.



Sample No.	w_N (%)	Estimated		
Depth	w_L (%)	σ'_{v0}	σ'_p	
Soil Type	w_P (%)	CR 0.152	RR 0.008	
	I_P (%)	G_s	e_0	S (%)

○ At t_p or hr Remarks

● At () hr

GEOTECHNICAL LABORATORY
DEPT. OF CIVIL ENGR.
M.I.T.

COMPRESSION CURVE
TEST NO. CK0UE4

FIGURE

CONSOLIDATED - UNDRAINED TRIAXIAL TEST

PROJECT Batch 113
 SOIL TYPE BOSTON BLUE CLAY
 LOCATION Resedimented
 BORING NO. — SAMPLE NO. —
 DEPTH —

TEST NO. CK0UE8
 TYPE OF TEST CK0UE
 APPARATUS NO. WFE-4
 TESTED BY PF
 DATE April 1986

WATER CONTENT

INITIAL, BASED ON TRIMMINGS 41.6 %
 INITIAL, BASED ON SAMPLE 43.2 %
 FINAL, BASED ON SAMPLE 35.5 %

ATTERBERG LIMITS

W_p _____ %
 W_L _____ %
 I_p _____ % I_L _____

PHASE RELATIONSHIPS

γ_{WET} 1.825 g/cc γ_{DRY} 1.27 g/cc
 e_i 1.188 e_f 0.948
 S_i 101 % $S_{precons}$ 104 %
 G_s 2.788

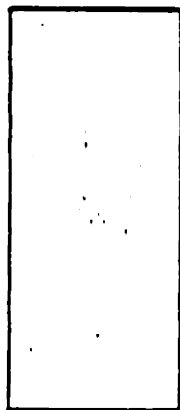
MISCELLANEOUS

B 92 %
 SATURATION ΔV 0.02
 CONSOLIDATION ΔV 7.28
 MEMBRANES 0 THICK 2 THIN
 CORRECTION FACTOR 1.942 - E
 FILTER STRIPS 6 X 1/4"
 CONFIGURATION Spiral
 CORRECTION FACTOR _____
 AREA CORRECTION Right Cylinder

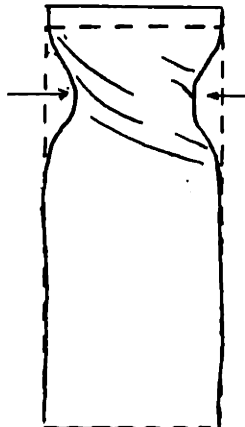
GRAIN SIZE

% -#200 _____
 % -#20 _____
 C_u _____ C_c _____

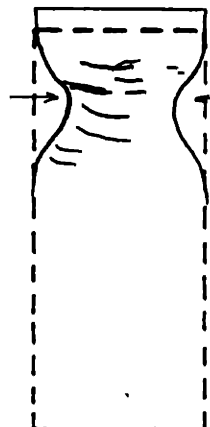
SAMPLE APPEARANCE



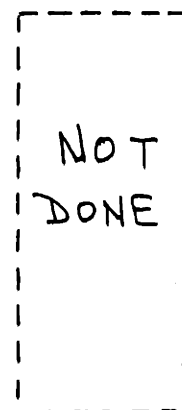
INITIAL, FRONT



FINAL, FRONT



FINAL, SIDE



FINAL, X-RAY

FINAL AREA
(cm^2)

9.06
TOP 5.67

9.08
MIDDLE

9.69
BOTTOM

AVERAGE

COMMENTS

GEOTECHNICAL LABORATORY
 DEPT. OF CIVIL ENGR.
 - M.I.T.

CONSOLIDATED - UNDRAINED TRIAXIAL TEST

PROJECT Batch 113 TYPE OF TEST CK₀UE TEST NO. CK₀UE8

STRESS HISTORY

IN SITU CONDITIONS

σ'_{vo} 0.25 kg/cm²
 σ'_p 1.00 kg/cm²
 OCR 4

TORVANE STRENGTH —
 TORVANE W_c — %

TEST CONDITIONS

σ'_{vc} 0.35 kg/cm²
 σ'_p 4.00 kg/cm²
 OCR 8.13
 K_c 1.07 U_b 2 kg/cm²
 STRAIN RATE 0.5 %/HOUR
 FINAL ϵ_o 10.991 %

STRENGTH DATA

AT MAXIMUM q

ϵ_o - 10.22 %
 q/σ'_{vc} - 1.384
 p/σ'_{vc} 3.329
 $\Delta u - \Delta \sigma_h / \sigma'_{vc}$ - 3.578
 ϕ' - 24.8
 A_f - 1.662
 TIME TO q_{max} 20.4 hrs

TIME RECORD

SET UP 3/23/86
 START OF CONSOLIDATION 3/25/86
 START OF SHEAR 4/12/86
 END OF SHEAR 4/13/86
 REMOVAL 4/14/86
 TOTAL TIME IN APPARATUS 25 days
 CONSOLIDATION-SHEAR Δt 30 minutes

REMARKS

AT MAXIMUM OBLIQUITY

ϵ_o - 4.73 %
 q/σ'_{vc} - 1.100
 p/σ'_{vc} 2.946
 $\Delta u - \Delta \sigma_h / \sigma'_{vc}$ - 2.241
 ϕ' - 29.2

$E_u(50\%)/q_f$ —

HYPERBOLIC STRESS-STRAIN PARAMETERS

G_i/σ'_{vc} —
 R_f —
 r_2 —

RADIOGRAPHY

kV — mA —
 EXPOSURE TIME —

CONSOLIDATED - UNDRAINED TRIAXIAL TEST

PROJECT Batch 113 TYPE OF TEST CK₀UE TEST NO. CK0UE8

SAMPLE DIMENSIONS

	L (cm)	A (cm ²)	V (cm ³)	ϵ_0 (D) (%)	ϵ_{vol} (D) (%)	W (gms)
INITIAL	8.002	9.763	78.12	0	0	142.54
PRECONSOLIDATION	7.993	9.763	78.04	0.11	0.11	
PRESHEAR	7.122	9.947	70.85	10.99	9.32	
POST SHEAR	8.225	-	-	-2.79		
FINAL	8.224	-	-	-2.77		
FINAL MEASURED	8.105	-	-	-1.29		99.55

(a) Measured
(b) Based on initial dimensions

CONSOLIDATION DATA

STRESSES IN kg/cm²

STEP	1	2	3	4	5	6	7	8	9	10
σ'_{vc}	0.40	0.44	0.51	0.58	0.67	0.78	0.88	1.00	1.15	1.30
σ'_{hc}	0.37	0.38	0.41	0.41	0.43	0.47	0.52	0.58	0.66	0.73
t_c (HRS)	24	7	8	10	9	12.5	7	8	8	8
ϵ_0 (%)	0.15	0.22	0.36	0.54	0.86	1.35	1.94	2.61	3.48	4.03
ϵ_{vol} (%)	0.14	0.21	0.37	0.53	0.81	1.20	1.72	2.29	3.09	3.61
K_c	0.94	0.87	0.80	0.70	0.65	0.60	0.59	0.58	0.57	0.56

STEP	11	12	13	14	15	16	17	18	19	20
σ'_{vc}	1.40	1.50	1.60	1.70	1.80	1.90	2.00	2.20	2.41	2.60
σ'_{hc}	0.77	0.81	0.84	0.87	0.90	0.93	0.96	1.04	1.13	1.22
t_c (HRS)	10	10.5	7	10	12	9.5	7	7.5	10.25	12.5
ϵ_0 (%)	4.38	4.66	5.20	5.59	5.81	5.97	6.99	7.74	8.23	8.52
ϵ_{vol} (%)	3.94	4.24	4.67	5.02	5.22	5.36	6.11	6.71	7.18	7.33
K_c	0.55	0.53	0.53	0.51	0.50	0.49	0.48	0.47	0.47	0.47

STEP	21	22	23	24	25	26	27	28	29	30
σ'_{vc}	2.81	3.00	3.20	3.40	3.60	3.80	4.00	3.80	3.60	3.30
σ'_{hc}	1.32	1.41	1.51	1.60	1.70	1.80	1.89	1.83	1.78	1.68
t_c (HRS)	10	7	7.5	9.5	7	7	40	8.5	12	11
ϵ_0 (%)	8.97	9.95	10.25	10.54	10.83	11.26	11.76	11.80	11.81	11.78
ϵ_{vol} (%)	7.73	8.51	8.81	9.09	9.36	9.74	10.29	10.30	10.28	10.25
K_c	0.47	0.47	0.47	0.47	0.47	0.47	0.47	0.48	0.49	0.51

GEOTECHNICAL LABORATORY
DEPT. OF CIVIL ENGR.
M.I.T.

CONSOLIDATED - UNDRAINED TRIAXIAL TEST

PROJECT BATCH 113 TYPE OF TEST CKUE TEST NO. CKUE8

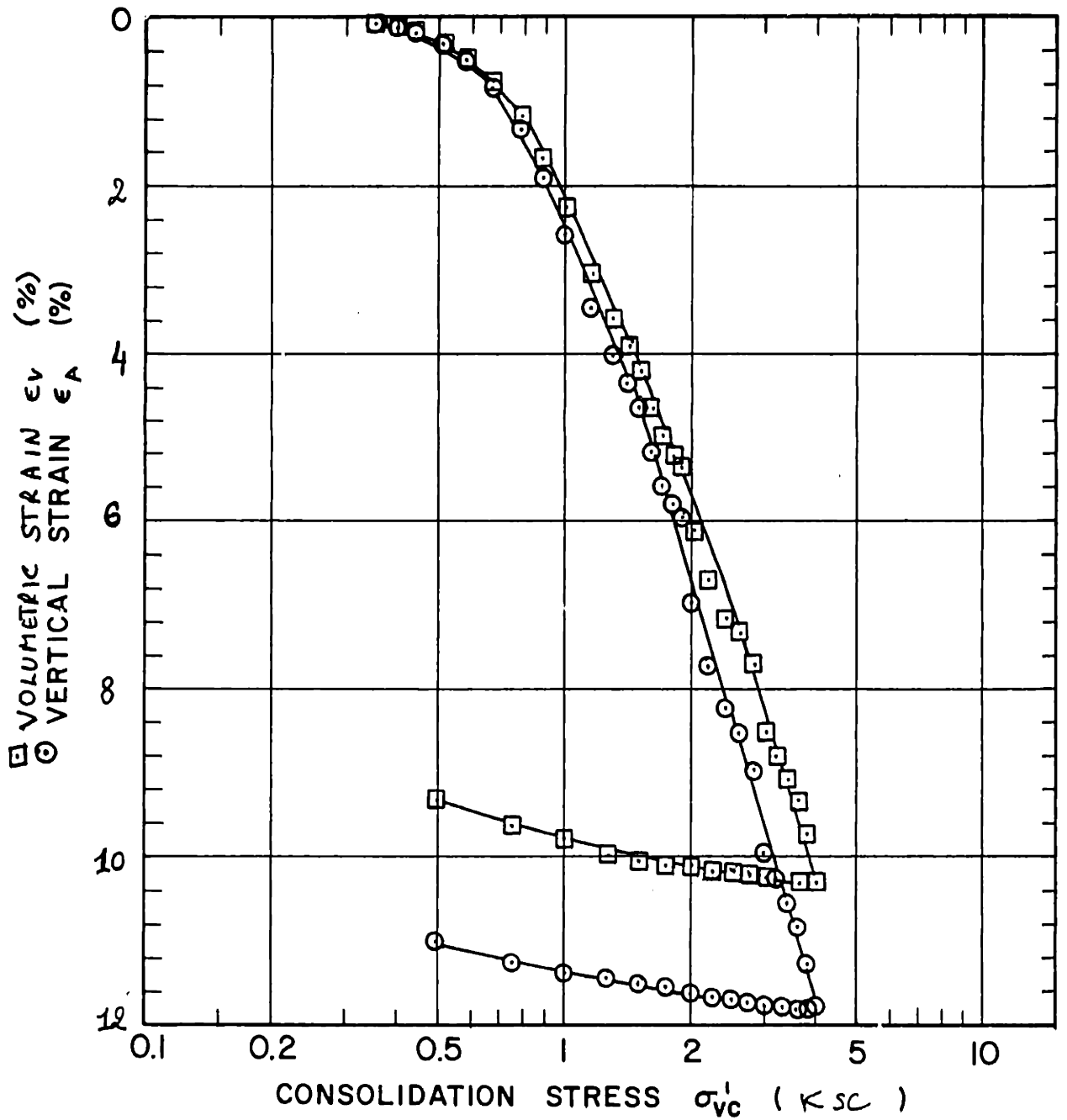
STEP	31	32	33	34	35	36	37	38	39	40
σ'_{vc}	3.00	2.74	2.50	2.25	2.00	1.75	1.49	1.26	0.99	0.75
σ'_{hc}	1.59	1.51	1.43	1.34	1.25	1.15	1.04	0.96	0.82	0.69
t_c (HRS)	10.75	7.5	6.5	10.0	14.5	14.0	10.5	9	13	13.5
E_o (%)	11.75	11.72	11.70	11.66	11.62	11.55	11.50	11.43	11.37	11.24
E_{vol} (%)	10.23	10.21	10.19	10.15	10.10	10.09	10.04	9.97	9.78	9.63
K_c	0.53	0.55	0.57	0.59	0.63	0.66	0.70	0.76	0.82	0.92

STEP	41	42	43	44	45	46	47	48	49	50
σ'_{vc}	0.49									
σ'_{hc}	0.53									
t_c (HRS)	24									
E_o (%)	10.99									
E_{vol} (%)	9.32									
K_c	1.07									

STEP	51	52	53	54	55	56	57	58	59	60
σ'_{vc}										
σ'_{hc}										
t_c (HRS)										
E_o (%)										
E_{vol} (%)										
K_c										

REMARKS

- VERTICAL AND VOLUMETRIC STRAINS ARE REFERENCED TO THE PRESHEAR DIMENSIONS.
- RATE OF UNLOADING WAS CHANGED TOWARD THE END BECAUSE, NEEDED THE TEST TO FINISH LATER DUE TO PRACTICAL PROBLEMS



Sample No.	w_N (%)	Estimated		
Depth	w_L (%)	σ'_{v0}	σ'_p	
Soil Type $\beta\beta C$	w_p (%)	CR 0.172	RR 0.012	
	I_p (%)	G_s	e_0	S (%)
○ At t_p or hr	Remarks			
● At () hr				

GEOTECHNICAL LABORATORY
DEPT. OF CIVIL ENGR.
M.I.T.

COMPRESSION CURVE
TEST NO. CK0VE8

FIGURE

Test CKoUC4
Batch 113

Sig'vm = 3.982 Kg/cm2
Sig'vc = .9966 Kg/cm2

Su = -.6229 Kg/c

v. strain %	q ----- sig'vc	p' ----- sig'vc	dU-dSIGh ----- sig'vc	sig'v ----- sig'h	Eu ----- Su	dQ ----- dQf
0.0003	0.0848	0.9151	-0.000	1.2043	193.22	-0.000
0.0008	0.0842	0.9164	-0.001	1.2024	292.92	0.0007
0.0010	0.0837	0.9175	-0.001	1.2008	407.27	0.0015
0.0011	0.0836	0.9183	-0.002	1.2003	378.16	0.0016
0.0014	0.0830	0.9198	-0.004	1.1985	429.07	0.0024
0.0015	0.0827	0.9206	-0.005	1.1974	486.19	0.0029
0.0023	0.0767	0.9121	-0.004	1.1836	1119.8	0.0113
0.0034	0.0665	0.9094	-0.012	1.1578	1737.0	0.0257
0.0057	0.0461	0.9049	-0.028	1.1073	2163.4	0.0545
0.0102	0.0240	0.9005	-0.046	1.0549	1911.2	0.0855
0.0160	0.0030	0.8959	-0.062	1.0068	1632.2	0.1151
0.0212	-0.010	0.8934	-0.073	0.9774	1431.5	0.1338
0.0284	-0.027	0.8894	-0.087	0.9397	1267.5	0.1584
0.0374	-0.043	0.8852	-0.099	0.9064	1098.6	0.1806
0.0469	-0.057	0.8812	-0.109	0.8777	971.44	0.2003
0.0542	-0.066	0.8793	-0.116	0.8599	892.11	0.2127
0.0678	-0.083	0.8753	-0.129	0.8263	793.94	0.2367
0.0858	-0.101	0.8718	-0.144	0.7917	694.59	0.2622
0.1005	-0.114	0.8703	-0.155	0.7666	636.38	0.2813
0.1237	-0.133	0.8723	-0.175	0.7343	565.36	0.3076
0.1513	-0.153	0.8771	-0.197	0.7027	503.55	0.3351
0.1995	-0.182	0.8878	-0.234	0.6595	428.57	0.3761
0.2448	-0.204	0.8893	-0.259	0.6263	378.20	0.4072
0.3038	-0.225	0.8895	-0.282	0.5956	326.96	0.4370
0.3833	-0.248	0.8900	-0.307	0.5640	278.10	0.4689
0.4907	-0.271	0.8884	-0.330	0.5313	232.75	0.5024
0.6001	-0.294	0.9010	-0.359	0.5073	202.35	0.5343
0.7088	-0.314	0.8932	-0.374	0.4794	180.26	0.5622
0.8018	-0.325	0.8872	-0.380	0.4636	163.65	0.5774
0.9049	-0.334	0.8828	-0.386	0.4508	148.22	0.5901
1.0079	-0.346	0.8896	-0.400	0.4398	136.86	0.6070
1.1089	-0.358	0.8880	-0.411	0.4243	128.10	0.6251
1.2462	-0.368	0.8774	-0.413	0.4090	116.31	0.6379
1.5077	-0.388	0.8771	-0.430	0.3862	100.46	0.6666
2.0181	-0.420	0.8687	-0.453	0.3481	80.081	0.7112
2.7533	-0.458	0.8588	-0.484	0.3043	63.117	0.7647
3.7724	-0.504	0.8664	-0.536	0.2639	50.019	0.8303
5.0041	-0.553	0.8911	-0.607	0.2341	40.800	0.8985
6.8195	-0.588	0.9410	-0.696	0.2303	31.612	0.9488
8.0018	-0.619	0.9910	-0.772	0.2308	28.167	0.9919
8.9941	-0.625	1.0365	-0.826	0.2476	25.262	1
12.752	-0.553	1.1449	-0.862	0.3481	16.025	0.8994
13.394	-0.558	1.1640	-0.880	0.3516	15.369	0.9060

CONSOLIDATED - UNDRAINED TRIAXIAL TEST

PROJECT BATCH 113
 SOIL TYPE BOSTON BLUE CLAY
 LOCATION Resedimented
 BORING NO. — SAMPLE NO. —
 DEPTH —

TEST NO. CKoU-Cyc-4
 TYPE OF TEST CKU cyclic
 APPARATUS NO. WFE-7
 TESTED BY PF
 DATE April 1986

WATER CONTENT

INITIAL, BASED ON TRIMMINGS 41.8 %
 INITIAL, BASED ON SAMPLE 43.6 %
 FINAL, BASED ON SAMPLE 35.2 %

ATTERBERG LIMITS

W_p _____ %
 W_L _____ %
 I_p _____ % I_L _____

PHASE RELATIONSHIPS

ρ_{WET} 1.812 g/cc ρ_{DRY} 1.262 g/cc
 e_i 1.209 e_f 0.994
 S_i 100.5 % $S_{precons}$ _____ %
 G_s 2.788

MISCELLANEOUS

B 94 %
 SATURATION ΔV -0.13 cc
 CONSOLIDATION ΔV 7.66 cc
 MEMBRANES 0 THICK 2 THIN
 CORRECTION FACTOR 1.942 = E
 FILTER STRIPS 5 x 1/4"
 CONFIGURATION Spiral
 CORRECTION FACTOR No
 AREA CORRECTION Right Cylinder

GRAIN SIZE

% -#200 _____
 % -2 μ _____
 C_u _____ C_c _____

SAMPLE APPEARANCE

				FINAL AREA
				()
				TOP
INITIAL, FRONT	FINAL, FRONT	FINAL, SIDE	FINAL, X-RAY	MIDDLE
				BOTTOM
				AVERAGE

COMMENTS After shearing was stopped,
the sample was very soft, Finger touch was enough
to change its appearance.
No measure of diameter was taken
because judged irrelevant. It was changing very much
depending on the position of the piston

CONSOLIDATED - UNDRAINED TRIAXIAL TEST

PROJECT Batch 113 TYPE OF TEST CK₀U cyclic TEST NO. _____ CK₀U-Cyc-4

STRESS HISTORY

IN SITU CONDITIONS

σ'_{vo} 0.25 kg/cm²
 σ'_p 1.0 kg/cm²
 OCR 4

TORVANE STRENGTH _____
 TORVANE w_c _____ %

TEST CONDITIONS

σ'_{vc} 0.35 kg/cm²
 σ'_p 4.00 kg/cm²
 OCR 4.00
 K_c 0.824 U_b 2 kg/cm²
 STRAIN RATE _____ %/HOUR
 FINAL ϵ_a _____ %

STRENGTH DATA

AT MAXIMUM q

ϵ_a _____ %
 q/σ'_{vc} _____
 p/σ'_{vc} _____
 $\Delta u - \Delta \sigma_h / \sigma'_{vc}$ _____
 ϕ' _____
 A_f _____
 TIME TO q_{max} _____

AT MAXIMUM OBLIQUITY

ϵ_a _____ %
 q/σ'_{vc} _____
 p/σ'_{vc} _____
 $\Delta u - \Delta \sigma_h / \sigma'_{vc}$ _____
 ϕ' _____
 $E_u(50\%) / q_f$ _____

TIME RECORD

SET UP 3/23/86
 START OF CONSOLIDATION 3/25/86
 START OF SHEAR 4/11/86
 END OF SHEAR 4/25/86
 REMOVAL 4/26/86
 TOTAL TIME IN APPARATUS 36 days
 CONSOLIDATION-SHEAR Δt 20 minutes

HYPERBOLIC STRESS-STRAIN PARAMETERS

G_i / σ'_{vc} _____
 R_f _____
 r^2 _____

RADIOGRAPHY

kV _____ mA _____
 EXPOSURE TIME _____

REMARKS

CONSOLIDATED - UNDRAINED TRIAXIAL TEST

PROJECT Batch 113 TYPE OF TEST CKoU cyclic TEST NO. CKoU-cyc-4

SAMPLE DIMENSIONS

	L (cm)	A (cm ²)	V (cm ³)	$\epsilon_o^{(D)}$ (%)	$\epsilon_{vol}^{(D)}$ (%)	W (gms)
INITIAL	8.00	9.834	78.669	0	0	142.6
PRECONSOLIDATION	7.996	9.834	78.635	0.04	0.04	
PRESHEAR	7.155	9.924	71.009	10.56	9.74	
POST SHEAR	6.664	-	-	16.70	-	
FINAL	6.616	-	-	17.30	-	
FINAL MEASURED						99.3

(a) Measured
(b) Based on initial dimensions

CONSOLIDATION DATA

STRESSES IN kg/cm²

STEP	1	2	3	4	5	6	7	8	9	10
σ'_{vc}	0.40	0.45	0.49	0.58	0.67	0.78	0.88	1.00	1.15	1.30
σ'_{hc}	0.37	0.40	0.37	0.41	0.44	0.47	0.51	0.57	0.62	0.65
t_c (HRS)	7	8	10	9	14	7	8	8.5	7.5	7.5
ϵ_o (%)	0.07	0.10	0.15	0.26	0.42	0.54	0.67	0.96	1.74	3.31
ϵ_{vol} (%)	0.08	0.11	0.13	0.26	0.43	0.58	0.73	1.09	1.86	3.11
K_c	0.94	0.90	0.76	0.70	0.65	0.6	0.58	0.57	0.54	0.50

STEP	11	12	13	14	15	16	17	18	19	20
σ'_{vc}	1.44	1.56	1.61	1.70	1.80	1.91	2.00	2.20	2.41	2.60
σ'_{hc}	0.71	0.75	0.76	0.80	0.85	0.90	0.94	1.03	1.13	1.22
t_c (HRS)	9.5	8.5	7	10	11.5	9.5	7.5	8	9.5	7.5
ϵ_o (%)	5.52	5.58	5.61	5.68	5.77	5.93	6.07	8.05	8.20	8.32
ϵ_{vol} (%)	4.84	4.94	4.99	5.08	5.20	5.37	5.55	7.21	7.43	7.53
K_c	0.49	0.48	0.48	0.47	0.47	0.47	0.47	0.47	0.47	0.47

STEP	21	22	23	24	25	26	27	28	29	30
σ'_{vc}	2.80	2.95	3.20	3.40	3.60	3.80	4.00	3.79	3.60	3.30
σ'_{hc}	1.31	1.41	1.50	1.61	1.70	1.80	1.89	1.83	1.77	1.69
t_c (HRS)	9.5	7.5	7.5	9.5	7	7	40	8.5	12	11
ϵ_o (%)	8.51	9.04	9.49	9.91	10.15	10.47	10.84	10.85	10.84	10.84
ϵ_{vol} (%)	7.73	8.34	8.77	9.20	9.43	9.76	10.22	10.23	10.20	10.18
K_c	0.47	0.48	0.47	0.47	0.47	0.47	0.47	0.48	0.49	0.51

GEOTECHNICAL LABORATORY
DEPT. OF CIVIL ENGR.
M.I.T.

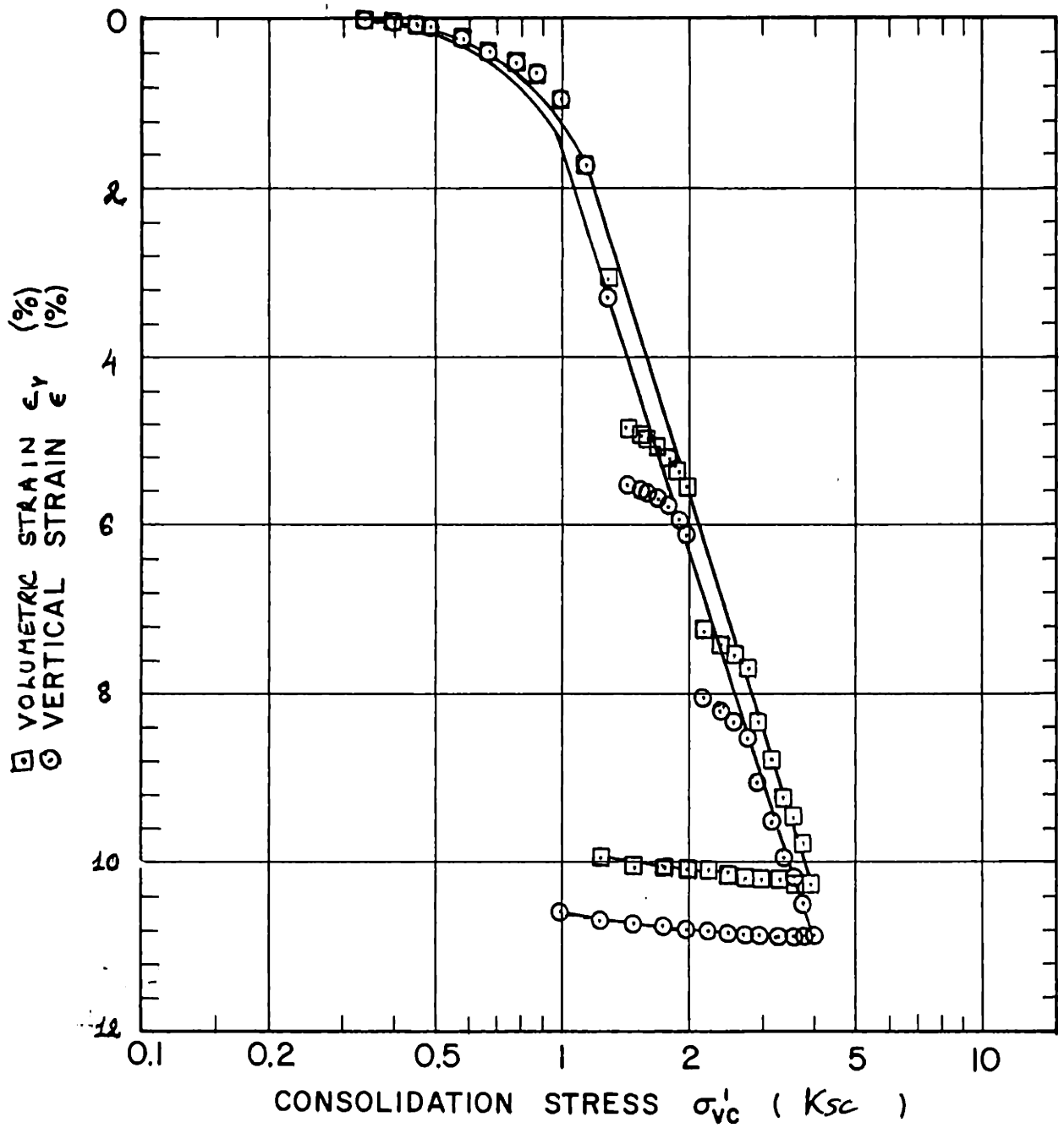
STEP	31	32	33	34	35	36	37	38	39	40
σ'_{vc}	2.99	2.75	2.50	2.24	2.00	1.75	1.49	1.25	1.00	
σ'_{hc}	1.59	1.51	1.43	1.33	1.25	1.16	1.05	0.94	0.82	
t_c (HRS)	10.5	7.5	6.5	10	8.5	7.5	9	7	4.8	
E_o (%)	10.83	10.82	10.81	10.78	10.76	10.73	10.70	10.65	10.56	
E_{vol} (%)	10.17	10.16	10.13	10.08	10.06	10.02	10.00	9.92	9.74	
K_c	0.53	0.55	0.57	0.59	0.63	0.66	0.70	0.75	0.82	

STEP	41	42	43	44	45	46	47	48	49	50
σ'_{vc}										
σ'_{hc}										
t_c (HRS)										
E_o (%)										
E_{vol} (%)										
K_c										

STEP	51	52	53	54	55	56	57	58	59	60
σ'_{vc}										
σ'_{hc}										
t_c (HRS)										
E_o (%)										
E_{vol} (%)										
K_c										

REMARKS

• VERTICAL and VOLUMETRIC STRAINS ARE REFERENCED TO THE PRESHEAR DIMENSIONS.



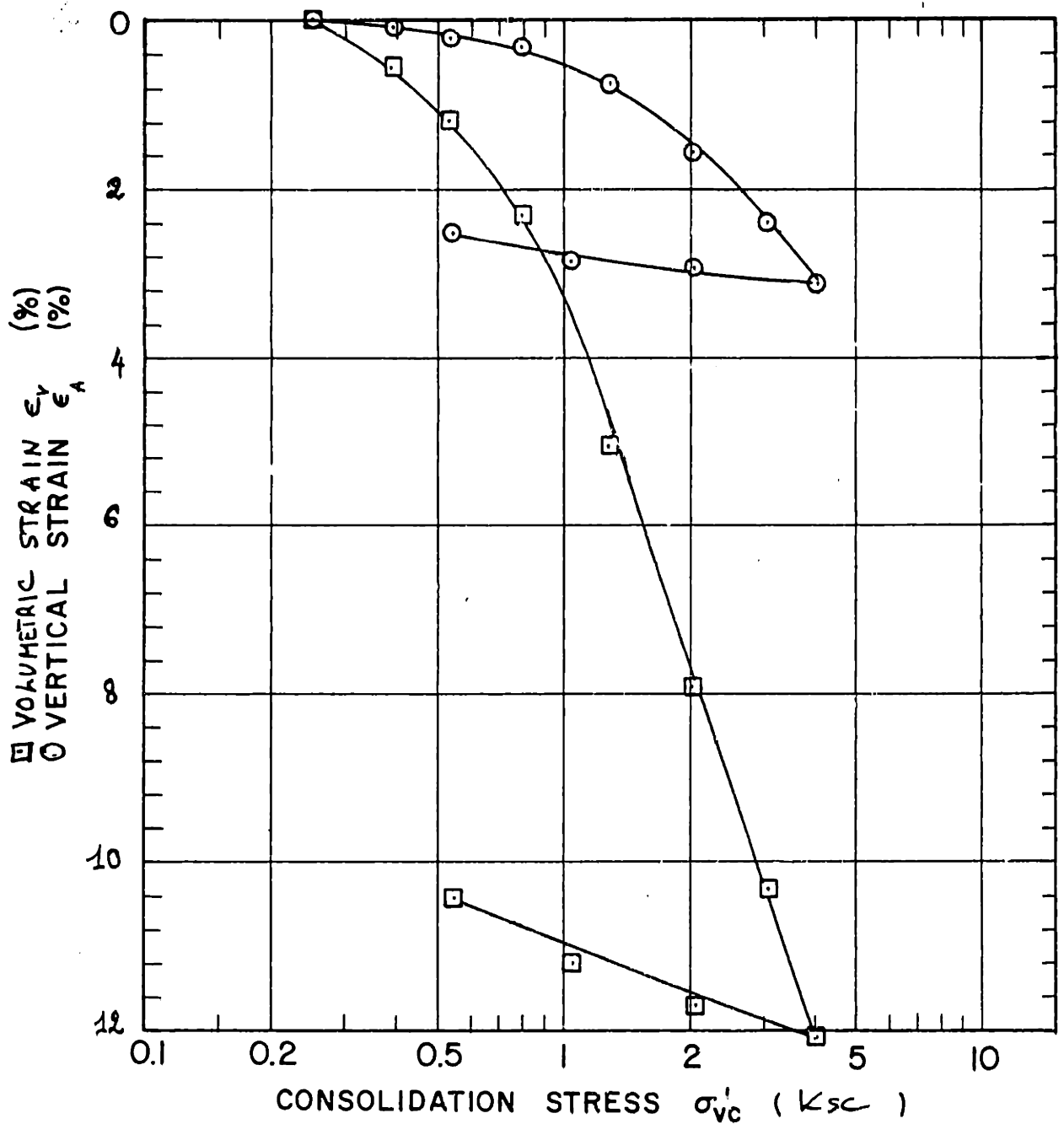
Sample No.	w_N (%)	Estimated		
Depth	w_L (%)	σ'_{v0}	σ'_p	
Soil Type BBC	w_p (%)	CR 0.157	RR 0.071	
	I_p (%)	G_s	e_0	S (%)

- At t_p or hr Remarks
- At () hr

GEOTECHNICAL LABORATORY
 DEPT. OF CIVIL ENGR.
 M.I.T.

COMPRESSION CURVE
 TEST NO. CK0V-Cyc-4

FIGURE



Sample No.	w_N (%)	Estimated		
Depth	w_L (%)	σ'_{v0}	σ'_p	
Soil Type <i>BC</i>	w_p (%)	CR 0.153	RR 0.02	
	I_p (%)	G_s	e_0	S (%)
○ At t_p or hr	Remarks			
● At () hr				

GEOTECHNICAL LABORATORY
DEPT. OF CIVIL ENGR.
M.I.T.

COMPRESSION CURVE
TEST NO. C10c8

FIGURE

Test CKoUEB
Batch 113

Sig'vm = 4.00 Kg/cm²
Sig'vc = .4848 Kg/cm²

Su = -.6697 Kg/cm²

v. strain %	q ----- sig'vc	p' ----- sig'vc	dU-dSIGh ----- sig'vc	sig'v ----- sig'h	Eu ----- Su	dQ ----- dQf
0.0031	-0.036	1.0288	-0.004	0.9314	175.63	0.0026
0.0037	-0.037	1.0329	-0.010	0.9307	171.84	0.0029
0.0026	-0.036	1.0388	-0.016	0.9315	231.16	0.0028
0.0063	-0.036	1.0412	-0.019	0.9318	94.107	0.0027
0.0063	-0.056	1.0511	-0.051	0.8972	584.69	0.0177
0.0095	-0.054	1.0499	-0.047	0.9020	343.94	0.0156
0.0138	-0.078	1.0551	-0.079	0.8622	507.39	0.0334
0.0133	-0.091	1.0550	-0.093	0.8405	684.60	0.0433
0.0175	-0.116	1.0529	-0.116	0.8008	740.81	0.0619
0.0223	-0.128	1.0546	-0.131	0.7821	668.57	0.0712
0.0244	-0.152	1.0563	-0.156	0.7477	760.01	0.0887
0.0308	-0.185	1.0605	-0.194	0.7019	770.64	0.1134
0.0335	-0.195	1.0620	-0.206	0.6887	756.39	0.1209
0.0420	-0.224	1.0694	-0.244	0.6532	708.94	0.1421
0.0446	-0.232	1.0731	-0.255	0.6432	696.72	0.1485
0.0542	-0.256	1.0811	-0.288	0.6164	641.32	0.1660
0.0670	-0.276	1.0905	-0.319	0.5955	565.10	0.1808
0.0744	-0.292	1.1008	-0.346	0.5801	542.33	0.1927
0.0851	-0.305	1.1083	-0.367	0.5682	497.71	0.2022
0.1000	-0.321	1.1221	-0.397	0.5549	448.50	0.2141
0.1601	-0.360	1.1668	-0.487	0.5282	318.07	0.2430
0.2080	-0.386	1.1992	-0.549	0.5124	264.57	0.2626
0.2590	-0.406	1.2189	-0.590	0.5002	224.18	0.2771
0.3027	-0.419	1.2025	-0.584	0.4828	198.68	0.2870
0.4032	-0.468	1.2817	-0.715	0.4643	168.22	0.3238
0.5054	-0.506	1.3395	-0.818	0.4514	145.73	0.3515
0.6043	-0.533	1.3792	-0.887	0.4424	128.82	0.3715
0.8076	-0.586	1.4247	-0.988	0.4166	106.70	0.4113
1.0033	-0.631	1.4972	-1.112	0.4066	92.843	0.4446
1.4119	-0.706	1.5892	-1.278	0.3842	74.304	0.5007
2.0001	-0.787	1.6793	-1.443	0.3615	58.708	0.5605
2.8329	-0.911	1.9424	-1.765	0.3611	48.282	0.6528
4.2683	-1.048	2.1553	-2.107	0.3453	37.037	0.7546
5.5362	-1.173	2.4552	-2.536	0.3533	32.059	0.8472
6.4229	-1.236	2.5873	-2.724	0.3533	29.159	0.8940
7.0152	-1.280	2.6986	-2.881	0.3563	27.684	0.9270
8.0359	-1.353	2.9260	-3.178	0.3673	25.583	0.9813
8.9345	-1.378	3.0979	-3.375	0.3842	23.431	0.9993
10.091	-1.381	3.2917	-3.569	0.4088	20.795	1.0017
11.505	-1.378	3.5048	-3.780	0.4353	18.202	0.9997
13.829	-1.359	3.7581	-4.007	0.4686	14.929	0.9856
15.412	-1.358	3.9126	-4.161	0.4846	13.382	0.9845

APPENDIX D

OEDOMETER TEST DATA

CONSOLIDATION TEST

Project OEDS Type of Test Standard No. 1.37 Tested by 1.37 Date Oct 1985
 Soil Type Residual Location Batch 113 Sample Height 2.089 cm
B3C Sample Diameter _____

Initial w(%) _____ G_s 2.78 w_N (%) _____ w_L (%) _____ Corrections _____
 Void Ratio e 1.215 S (%) _____ w_p (%) _____ I_p (%) _____ Units: σ'_{vc} kg/cm^2 $c_v \times 10^{-3}$ cm/sec

σ'_{vc}	Primary		Total			$C_{\alpha}(\%)$	Coef. of Consol.		Remarks
	t (hr)	$\epsilon_v(\%)$	e	t (hr)	$\epsilon_v(\%)$		e	\sqrt{t}	
0.125		0.295	1.208		0.30	1.208			
0.25		0.55	1.203		0.57	1.202		17.8	
0.5		1.68	1.178		1.70	1.177		10.4	
0.55					1.72	1.177		15.2	
1.0		3.16	1.145		3.32	1.141			
2.0		6.99	1.060		7.28	1.05		3.91	
4.0		11.00	0.971		11.38	0.963	0.057	4.31	
2.7					11.34	0.964		4.94	
2.0					11.28	0.965			
1.2					11.15	0.968			
0.8					10.98	0.972			
1.2					10.99	0.972			
1.8					11.04	0.970			
2.7					11.20	0.967			
4.0					11.47	0.961			
8.0		14.04	0.904		15.53	0.871			
16.0		19.09	0.792		19.98	0.773	0.443	8.19	
8.0					19.79	0.777		6.97	

GEOTECHNICAL LABORATORY Remarks
 DEPT. OF CIVIL ENGR.
 M.I.T.

CONSOLIDATION TEST

Project DED 27 Type of Test Standard No. 1.37 Tested by 1.37 Date Oct-1988
 Soil Type Resedimented Location Batch 113 Sample Height 1954
BBC Sample Diameter _____

Initial w(%) _____ G_s 2.28 w_N (%) _____ w_L (%) _____ Corrections _____

Void Ratio e 1.147 S (%) _____ w_p (%) _____ I_p (%) _____ Units: σ'_{vc} kg/cm² C_v 10⁻³ cm²/sec

σ'_{vc}	Primary		Total			C_u (%)	Coef. of Consol.		Remarks
	t (hr)	ϵ_v (%)	e	t (hr)	ϵ_v (%)		e	\sqrt{t}	
0.125					0.53	1.136			
0.25		1.09	1.124		1.10	1.123			
0.5		1.61	1.112		1.75	1.109			
1		3.38	1.074		3.39	1.074			
2		7.57	0.984		8.27	0.969			
4		12.39	0.881		12.59	0.877			
2					12.47	0.879			
0.8		12.06	0.888		12.04	0.889			
0.35					11.64	0.897			
0.15		11.21	0.906		11.12	0.908			
0.35					11.19	0.907			
0.8					11.25	0.905			
1.3					11.57	0.899			
2		12.02	0.889		12.09	0.887			
4		12.93	0.869		13.04	0.867			
8		16.53	0.792		16.94	0.783			
16		21.18	0.692		21.59	0.683			
8					21.43	0.687			

GEOTECHNICAL LABORATORY
 DEPT. OF CIVIL ENGR.
 M.I.T.
 Remarks

CONSOLIDATION TEST

Project 0ED 133 Type of Test Standard No. Tested by 1.37 Date Oct. 85

Soil Type Resedimented Location Batch 113 Sample Height 1.985 cm
BBC Sample Diameter

Initial w(%) G_s 2.28 w_N (%) w_L (%) Corrections

Void Ratio e 1.911 S (%) 98 w_p (%) I_p (%) Units: σ'_{vc} kg/cm² c_v 10⁻³ cm/sec

σ'_{vc}	Primary		Total		C_{α} (%)	Coef. of Consol.		Remarks
	t (hr)	ϵ_v (%)	e	t (hr)		ϵ_v (%)	e	
0.125								
0.25		0.72	1.195			1.20		8.86
0.5		1.18	1.185			1.183		13.2
1		2.49	1.156			1.151		
2		6.91	1.058			1.055		6.17
4		11.59	0.955			0.947		4.99
1.5						0.954		4.51
0.4		10.95	0.969			0.968		
0.125		10.41	0.981			0.979		
0.03						0.994		38.5
0.125						0.992		18.5
0.4						0.984		
1.5		11.08	0.966			0.966		7.5
4		11.94	0.947			0.935		3.6
8						0.855		
16		20.77	0.752			0.746		4.6
8						0.751		
4						0.761		

GEOTECHNICAL LABORATORY Remarks
 DEPT. OF CIVIL ENGR.
 M.I.T.

CONSOLIDATION TEST

Project OEDRI Type of Test Standard No. 153 Tested by 153 Date Feb 1986
 Soil Type Remolded Location Batch 108 Sample Height 2.401 cm
BBc Sample Diameter _____

Initial w(%) 34.2 G_s 2.78 w_N (%) _____ w_L (%) _____ Corrections _____
 Void Ratio e 1.149 S (%) 83 w_p (%) _____ l_p (%) _____ Units: σ'_{vc} kg/cm^2 c_v 10^{-3} cm^2/yr

σ'_{vc}	Primary		Total			$C_{\alpha}(\%)$	Coef. of Consol.		Remarks
	t (hr)	$\epsilon_v(\%)$	e	t (hr)	$\epsilon_v(\%)$		e	\sqrt{t}	
0.12					1.59	1.115			
0.22					2.33	1.099			
0.4		3.31	1.078		3.34	1.077			
0.78		5.23	1.037		5.38	1.033			
1.50		7.38	0.990		7.56	0.987			
3		10.09	0.932		10.29	0.928			
6		12.89	0.872		13.17	0.866			
10.5		15.43	0.817		15.61	0.814			
18		17.66	0.769		17.96	0.763			
30		20.08	0.717		20.27	0.713			
15		20.08	0.717		20.07	0.718			
8					19.67	0.726			
4		19.23	0.736		19.15	0.737			
2					18.44	0.753			
1					17.75	0.768			
0.5					16.94	0.785			